The Stability of Solitary Waves — **Source link** ⧉

Thomas Brooke Benjamin

Institutions: University of Essex

Related papers:

- On the stability theory of solitary waves

- Stability theory of solitary waves in the presence of symmetry, II☆

- Lyapunov stability of ground states of nonlinear dispersive evolution equations

- Stability and Instability of Solitary Waves of Korteweg-de Vries Type

- Asymptotic stability of solitary waves

Stabilité des ondes solitaires

Frédéric Chardard

THÈSE DE DOCTORAT
DE L'ÉCOLE NORMALE SUPÉRIEURE DE CACHAN

Présentée par
Monsieur Frédéric CHARDARD

pour obtenir le grade de

DOCTEUR DE L'ÉCOLE NORMALE SUPÉRIEURE DE CACHAN

Domaine : **MATHÉMATIQUES**

Sujet de la thèse :

STABILITÉ DES ONDES SOLITAIRES

Thèse présentée et soutenue à Cachan le 15 mai 2009 devant le jury composé de :

Thomas J. BRIDGES	Professeur	Surrey, Royaume-Uni	Examinateur
Frédéric DIAS	Professeur des Universités	ENS Cachan	Directeur de thèse
Christopher K.R.T. JONES	Professeur	UNC, États-Unis	Rapporteur
Juan-Pablo ORTEGA	Chargé de Recherches	CNRS	Examinateur
Jean-Claude SAUT	Professeur des Universités	Paris XI	Président
Nikolay TZVETKOV	Professeur des Universités	Lille I	Rapporteur

Centre de Mathématiques et de Leurs Applications
(ENS CACHAN/CNRS/UMR 8536)
61, avenue du Président Wilson, 94235 CACHAN CEDEX (France)

Remerciements

Résumé

Cette thèse porte sur la stabilité des ondes solitaires et plus précisément sur les applications de l'indice de Maslov au problème de la stabilité spectrale des ondes solitaires unidimensionnelles.

Dans le premier chapitre, nous montrons comment la stabilité peut être liée à l'étude d'une famille d'équations aux dérivées ordinaires linéaires hamiltoniennes. Il est alors possible de définir un indice de Maslov pour les ondes périodiques et les ondes solitaires. Nous calculons ensuite la limite de l'indice de Maslov d'une suite d'ondes périodiques approchant une onde solitaire et la comparons à l'indice de Maslov de l'onde solitaire.

Dans le second chapitre, nous décrivons un algorithme utilisant l'algèbre extérieure pour calculer l'indice de Maslov.

Dans le troisième chapitre, nous étudions l'indice de Maslov et la stabilité des ondes périodiques et des ondes solitaires de l'équation de Kawahara.

Le quatrième chapitre traite de l'indice de Maslov d'ondes solitaires apparaissant dans un modèle pour l'interaction entre ondes longues et ondes courtes.

Le sujet du dernier chapitre, un peu différent de celui du reste de la thèse, est la stabilité de solutions stationnaires apparaissant dans l'équation de Korteweg-de Vries avec forçage.

Mots clés : Stabilité, Équations aux Dérivées Partielles Hamiltoniennes, Indice de Maslov, Fonction d'Evans, Algèbre extérieure, Analyse numérique.

Abstract

This thesis is devoted to the stability of solitary waves, and more precisely to the applications of the Maslov index to the spectral stability problem.

In the first chapter, we show how the stability problem can be generically related to a family of linear Hamiltonian ODE. It is then possible to define a Maslov index for periodic waves and solitary waves. We compute the limit, when it exists, of the Maslov index of a sequence of periodic waves which converges to a solitary wave and compare the limit with the Maslov index of the solitary wave.

In the second chapter, we describe how exterior algebra can be used to compute the Maslov index, both in the periodic and solitary wave cases.

In the third chapter, we study the Maslov index and the stability of solitary waves and periodic waves arising in the Kawahara equation.

In the fourth chapter, we look at the Maslov index of solitary waves arising in a longwave-shortwave interaction system.

The last chapter deals with the stability of stationary solutions of a model for flows over a non-uniform bottom.

Keywords: Stability, Hamiltonian Partial Differential Equations, Maslov index, Evans function, Exterior Algebra, Numerical Analysis.

Contents

Introduction

When looking at linear waves in an homogeneous medium, Fourier analysis shows that there are two possible phenomena which are likely to destroy a wave packet:

- Dissipation: Fourier components are damped.

- Dispersion: Fourier components of the wave do not travel at the same speed.

It is also possible that the opposite phenomenon to dissipation occurs: Fourier components grow exponentially.

Because of these two effects, linear theory leads to the same conclusion as AIRY on water-waves: localized solutions travelling at a constant speed, called solitary waves, cannot exist in a dissipative or dispersive medium.

However, solitary waves occur in several areas such as an-harmonic nonlinear lattices, gas dynamics, hydromagnetic waves, ion-acoustic waves in cold plasma and hydrodynamics. But the most spectacular observation of solitary waves goes back to the nineteenth century, with the observation on horseback by Lord Scott Russell of a wave in a barge channel persisting for at least one hour.

BOUSSINESQ [18], KORTEWEG AND DE VRIES [83] derived from the full incompressible Euler equations with a free surface a one-dimensional model with third order derivatives, by making the shallow-water hypothesis (e.g. that the wavelength is much greater than the depth) and assuming a one-way propagation:

$$u_t = 6uu_x - u_{xxx}. \qquad (0.0.1)$$

This equation is *non-linear* and *dispersive*. The non-linearity can counteract the dispersion, and (0.0.1) admits a solitary wave solution $u(x) = -\frac{c}{2}\text{sech}^2(\frac{1}{2}\sqrt{c}(x - ct))$. This equation has later been used in the great variety of domains mentioned earlier.

In the wake of FERMI, PASTA, & ULAM studies on an-harmonic lattices, ZABUSKY AND KRUSKAL[130] performed numerical experiments which showed that, despite non-linearity, if solitary waves collide with each other, they emerge back again with the same shape and a phase shift. To emphasize the analogy of these waves with interacting particles, they coined the term soliton, often used as a synonym for solitary wave.

This caused an increasing interest for this equation. Theoretical advances using Sturm-Liouville theory and inverse scattering theory were made. One of the most striking results is the integrability of the Korteweg de Vries equation, proved by ZAKHAROV & FADEEV [131].

This is closely related to the existence of N-soliton solutions, which describe analytically the evolution of N colliding solitary waves observed in the numerical experiments.

However, if a Korteweg de Vries model is taken with a non-linearity which is not quadratic or cubic, the equation is no longer integrable and inverse scattering cannot be used. In that case there are still solitary wave solutions, often in the form $A\mathrm{sech}^p(b(x - ct))$.

In order to be observed, a solitary wave solution needs to be orbitally stable. Let E be a suitable Banach space of distributions over $\mathbb{R}$. Let $u(x, t) = \phi(x - ct)$ be a solitary wave solution, with $\phi \in E$. Then, u is said to be orbitally stable if and only if:

- The Cauchy problem admits a unique solution over $\mathbb{R}^+$ for any initial condition located in a neighborhood of ϕ.

- For any $\varepsilon > 0$, there exists a neighborhood U of $u(\cdot, 0)$ such that for any solution v with $v(\cdot, 0) \in U$, we have $\sup_{t \in \mathbb{R}^+} \inf_{\alpha \in \mathbb{R}} \|v(\cdot, t) - \phi(\alpha + .)\| \leq \varepsilon$.

Orbital stability is usually proved by finding a conserved quantity which traps neighboring solutions, for example $\mathcal{H} + c\mathcal{P}$, where $\mathcal{H}$ is the Hamiltonian of the solitary wave and $\mathcal{P}$ its momentum.

BONA & SOUGADINIS & STRAUSS [15] present a review of results of solitary waves of KdV-type equations.

While Korteweg-de Vries solitary waves and their stability are now well understood, this is not yet the case for other dispersive equations like Kawahara equation:

$$\frac{\partial u}{\partial t} - c\frac{\partial u}{\partial x} + \frac{\partial}{\partial x}\left(u^{q+1}\right) + P\frac{\partial^3 u}{\partial x^3} - \frac{\partial^5 u}{\partial x^5} = 0\,, \quad q \geq 1\,. \tag{0.0.2}$$

This equation is relevant when the cubic dispersion is low. It was introduced in [80] to take into account higher order dispersive terms. These additional terms can be relevant for water waves in presence of capillarity, since particular values of capillarity can annihilate the third order dispersive term.

Qualitatively, this equation is different from Korteweg-de Vries since it admits solitary wave solutions with *oscillating* tails and multi-pulse solutions. N-pulse solutions have N pulses which travel at the *same* speed. These solutions should not be confused with the N-soliton solution, where the N colliding solitons usually have a different velocity.

While one-pulse may be treated with much the same tools as for the Korteweg-de Vries equation (see [20, 89]), this is not the case for multi-pulse orbits whose existence has been proved by using bifurcation theory ([27, 34]) rather than minimization under constraint, which is the case for unimodal solution ([27, 70]). BURYAK & CHAMPNEYS [30] and later CHUGUNOVA & PELINOVSKY [42] applied the method of OSTROVSKY & GORSHKOV [67] to predict the stability of 2-pulse. The idea is to prove that when $P \to 2^-$, the two bumps behave approximately like a two-particle system with an interaction potential. In this framework, each 2-pulse solution corresponds to an equilibrium of the two particle system. It is then possible to get some information on the stability of the 2-pulse by looking at the stability of the corresponding equilibrium.

Another way to study the stability problem is to linearize the non-linear equation near the stationary solution $\widehat{\phi}$. Let $\widehat{\phi} + \phi$ be a solution of equation (0.0.2), with ϕ a small function. Then,

at the first order, ϕ is the solution of the following equation:

$$\frac{\partial}{\partial t}\phi = \mathbf{L}\phi \tag{0.0.3}$$

with $\mathbf{L}\phi = \frac{\mathrm{d}}{\mathrm{d}x}(\phi_{xxxx} - P\,\phi_{xx} + c\phi - (q+1)\widehat{\phi}(x)^q\,\phi)$. Of course, this can be generalized to other non-linear dispersive equations.

If we look for solutions $\phi(x,t) = f(x)g(t)$ with separation of variables of this equation, then $\phi(x,t) = e^{\widehat{\lambda}t}f(x)$ with $\mathbf{L}f = \widehat{\lambda}f$. Since only L^2 solutions are relevant, it enforces $f \in L^2(\mathbb{R})$.

Definition 1 *A solitary wave $\widehat{\phi}$ is said to be weakly spectrally stable if the spectral problem $\mathbf{L}u = \widehat{\lambda}u$ does not admit any solution such that $u \in L^2(\mathbb{R})$ and $\Re(\widehat{\lambda}) > 0$.*

Orbital stability implies weak spectral stability but the reverse is false.

The discrete spectrum of $\mathbf{L}$ can be computed by using the Evans function, studied in [1, 21, 62, 23, 101] for example. The spectral problem $\mathbf{L}u = \widehat{\lambda}$ can indeed be rewritten as a n-dimensional first-order differential system:

$$U_x = \mathbf{A}(x,\widehat{\lambda})U, \qquad \lim_{x\to\pm\infty}\mathbf{A}(x,\widehat{\lambda}) = \mathbf{A}_\infty(\widehat{\lambda}). \tag{0.0.4}$$

When $i\mathbb{R} \cap \mathrm{Sp}(\mathbf{A}_\infty(x,\widehat{\lambda})) = \emptyset$, a condition equivalent to $\widehat{\lambda} \notin \sigma_{ess}$ (where σ_{ess} denotes the essential spectrum), there exists $u_1(x,\widehat{\lambda}), \ldots, u_k(x,\widehat{\lambda})$ and $v_1(x,\widehat{\lambda}), \ldots, v_{n-k}(x,\widehat{\lambda})$ solutions of (0.0.4) such that:

- Let $u(x)$ be a solution of equation (0.0.4). Then $\lim_{x\to-\infty} u(x) = 0$ if and only if $u(x) \in \mathrm{Span}(u_1(x,\widehat{\lambda}), \ldots, u_k(x,\widehat{\lambda}))$. Otherwise, $\lim_{x\to-\infty} \|u(x)\| = +\infty$.

- Let $u(x)$ be a solution of equation (0.0.4). Then $\lim_{x\to+\infty} u(x) = 0$ if and only if $u(x) \in \mathrm{Span}(v_1(x,\widehat{\lambda}), \ldots, v_{n-k}(x,\widehat{\lambda}))$. Otherwise, $\lim_{x\to+\infty} \|u(x)\| = +\infty$.

.

$\mathrm{Span}(u_1(x,\widehat{\lambda}), \ldots, u_k(x,\widehat{\lambda}))$ and $\mathrm{Span}(v_1(x,\widehat{\lambda}), \ldots, v_{n-k}(x,\widehat{\lambda}))$ are called the unstable space and the stable space respectively.

Knowing this, it is evident that $\widehat{\lambda}$ is in the discrete spectrum, e.g. that there exists a solution in $L^2(\mathbb{R})$ of (0.0.4) if and only if:

$$\mathrm{Span}(u_1(x,\widehat{\lambda}), \ldots, u_k(x,\widehat{\lambda})) \cap \mathrm{Span}(v_1(x,\widehat{\lambda}), \ldots, v_{n-k}(x,\widehat{\lambda})) \neq \{0\}.$$

This condition is equivalent to:

$$D(\lambda) = 0$$

where $D(\lambda)$, called the Evans function is defined as:

$$D(\lambda) := e^{-\int_0^x \mathrm{trace}\,A(y,\lambda)\mathrm{d}y}(x,\lambda)\det(u_1(x,\widehat{\lambda}), \ldots, u_k(x,\widehat{\lambda}), v_1(x,\widehat{\lambda}), \ldots, v_{n-k}(x,\widehat{\lambda})).$$

It is possible to choose the vectors u_i and v_i analytically with respect to $\widehat{\lambda}$. If chosen this way, $D(\lambda)$ is an analytic function[1]. ALEXANDER, GARDNER & JONES [1] proved that the zeros of D

---

[1]Analytic continuation of the Evans function beyond the essential spectrum is often possible, as shown by GARDNER & ZUMBRUN [65]. Though this is often useful, we will not need it in this thesis.

with multiplicity are the eigenvalues of $\mathbf{L}$ with multiplicity, by using a topological object called the Chern complex. BRIDGES, DERKS & GOTTWALD [21] later provided an algorithm based on exterior algebra to compute numerically the Evans function. By using argument principle, they were able to count numerically eigenvalues inside a path.

Another approach developed in [42, 41, 82, 78] is to use the Hamiltonian structure of the Kawahara equation to link the number of negative eigenvalues of the Hessian of the Hamiltonian and the number of eigenvalues in the right-half plane.

This idea also applies to other Hamiltonian evolution equations in one space dimension, such as the nonlinear Schrödinger (NLS) equation and the longwave-shortwave resonance (LW-SW) equations but also to gradient flow-type system, like the Swift-Hohenberg equation or some reaction-diffusion systems. As explained in chapter 1, solitary wave solutions can be characterized as homoclinic orbits of a Hamiltonian ordinary differential equation (ODE). The spectral problem associated with the Hessian of the Hamiltonian (or the functional from which the gradient flow is derived) about a given homoclinic orbit, then leads to a parameter-dependent family of non-autonomous linear Hamiltonian systems. The advantage of these Hamiltonian structures is that the linear and nonlinear Hamiltonian systems have global geometric properties that aid in proving existence of the basic solitary wave and in understanding its stability as a solution of the time-dependent equation. Our interest in this thesis is in a particular geometric invariant – the Maslov index of homoclinic orbits.

The study of the stability of solitary waves using the Maslov index was pioneered in the papers by JONES [77] and BOSE & JONES [16]. The linear stability of steady standing wave solutions of a spatially-dependent NLS equation is studied in [77]. The linearization about a steady solution results in a linear $\lambda-$dependent Hamiltonian system of the form (0.0.6) (see below) with $n = 2$ and λ a spectral parameter. Geometric methods are then used to determine the Maslov index, and it is used to prove an instability result. Gradient parabolic partial differential equations (PDE) of the form

$$\begin{aligned} u_t &= d_1 u_{xx} + f_u(u,v) \\ v_t &= d_2 v_{xx} + f_v(u,v) \end{aligned} \tag{0.0.5}$$

are considered in [16], where d_1 and d_2 are positive parameters, $f(u,v)$ is a given smooth function with gradient (f_u, f_v). Linearizing about a steady solution $(\widehat{u}(x), \widehat{v}(x))$, and introducing a spectral parameter leads to a pair of linear second-order ODEs which can be put into the standard form (0.0.6) with $n = 2$, with the asymptotic property (0.0.9) and λ the spectral parameter. Since the PDE is a gradient system it is sufficient to restrict the spectral parameter to be real. Singular perturbation methods are then used to determine the Maslov index, which in turn is related to stability. A key feature of this work is the analysis of the induced system on the exterior algebra space $\bigwedge^2(\mathbb{R}^4)$.

Many of the most interesting solitary waves are only known numerically and therefore a numerical approach to the Maslov index is of interest. It is the aim of chapter 2 to develop a numerical framework for computing the Maslov index of homoclinic orbits. Once the solitary wave solution is known, analytically or numerically, it is the linearization about that solitary wave which encodes the Maslov index. Therefore, the starting point for developing the theory is

the following class of parameter-dependent Hamiltonian systems

$$\mathcal{J}\mathbf{u}_x = \mathbf{C}(x,\lambda)\mathbf{u}\,, \quad \mathbf{u} \in \mathbb{R}^{2n}\,, \quad x \in \mathbb{R}\,, \quad \lambda \in \mathbb{R}\,, \tag{0.0.6}$$

where $\mathcal{J}$ is the standard symplectic operator on $\mathbb{R}^{2n}$

$$\mathcal{J} = \begin{bmatrix} \mathbf{0} & -\mathbf{I} \\ \mathbf{I} & \mathbf{0} \end{bmatrix}\,, \tag{0.0.7}$$

and $\mathbf{B}(x,\lambda)$ is a symmetric matrix depending smoothly on x and λ. Let

$$\mathbf{B}(x,\lambda) = \mathcal{J}^{-1}\mathbf{C}(x,\lambda)\,. \tag{0.0.8}$$

The fact that $\mathbf{B}(x,\lambda)$ is obtained from the linearization about a solitary wave suggests the following asymptotic property:

$$\mathbf{B}_\infty(\lambda) = \lim_{x \to \pm\infty} \mathbf{B}(x,\lambda)\,, \tag{0.0.9}$$

and that $\mathbf{B}_\infty(\lambda)$ is strictly hyperbolic (e.g has no imaginary eigenvalue) for an open set of λ values that includes 0.

The Maslov index is a winding number associated with paths of solutions of (0.0.6), in particular paths of Lagrangian planes. A Lagrangian plane is an $n-$dimensional subspace of $\mathbb{R}^{2n}$, say span$\{\mathbf{z}_1, \ldots, \mathbf{z}_n\}$, satisfying

$$\langle \mathcal{J}\mathbf{z}_i, \mathbf{z}_j \rangle = 0\,, \quad \forall\ i, j = 1, \ldots, n\,,$$

where $\langle \cdot, \cdot \rangle$ is a standard inner product on $\mathbb{R}^{2n}$.

Suppose λ is fixed and on the interval $a \leq x \leq b$ consider a path of Lagrangian planes

$$[a, b] \mapsto \mathbf{Z}(x,\lambda) = [\mathbf{z}_1(x,\lambda)\,|\,\cdots\,|\,\mathbf{z}_n(x,\lambda)] \in \mathbb{R}^{2n \times n}\,,$$

satisfying $\mathbf{Z}_x = \mathbf{B}(x,\lambda)\mathbf{Z}$ for $a \leq x \leq b$. The Maslov index of this path is a count of the number of times this path of Lagrangian planes has a non-trivial intersection with a fixed reference Lagrangian plane. A precise definition is given in chapter 1. This index is of interest since it can count the solutions of the spectral problem for quite general systems. A proof based on comparison arguments is given in Appendix C. Hence, the Maslov index is directly related to stability.

We will first study the Maslov index of a sequence of periodic orbits which converges to a homoclinic orbit. The Maslov index for periodic orbits has indeed been widely developed because of its interest in semi-classical quantization (e.g. [71, 46, 90, 111, 104, 98] and references therein). Furthermore, any homoclinic orbit of Hamiltonian system can be approximated by such a sequence of periodic orbits (see [120]).

In section 1.3.1, we prove under suitable hypotheses that if the periodic orbit is asymptotic to a homoclinic orbit, the Maslov index converges to the Maslov index of the limiting homoclinic orbit.

We then compare this limit with the definition that is used by JONES [77] and BOSE & JONES [16] but also CHEN & HU [40], taking the Lagrangian path to be a path of unstable subspaces and taking the reference plane to be the stable subspace at infinity. We will extend

this definition by introducing an explicit and computable formula for the intersection index. This theory is developed in §1.1.2.

In chapter 2, we give an algorithm to compute the Maslov index both in the periodic and the homoclinic case. From the numerical point of view, the exterior algebra formulation is also advantageous. We give formulas for different representations of the Maslov index for Lagrangian planes on $\bigwedge^n(\mathbb{R}^{2n})$ for any n, and present a general algorithm that works – in principle – for any dimension n. However, the dimension of $\bigwedge^n(\mathbb{R}^{2n})$ increases rapidly with n and so the algorithm is most effective for low dimensional systems. The algorithm is constructed so that the manifold of Lagrangian planes is attracting. A tutorial example on $\mathbb{R}^2$ is available in Appendix E, where the details can be given explicitly. It is a scalar-reaction diffusion equation with an explicit localized solution.

In chapter 3, we apply the framework to the periodic waves and solitary waves of the afore-mentioned Kawahara equation. We also make some remarks on the behaviour of the Maslov index near bifurcation points: Consider a solitary-wave solution of (0.0.2). Then, if we change the parameter P, the homoclinic orbit may undergo a bifurcation. We observe that the value of the Maslov index changes at these points. Finally, we study directly the spectrum of $\mathbf{L}$ by computing its associated Evans function.

In chapter 4, the computational framework for the Maslov index is illustrated by an application to the LW-SW wave resonance equations, which has exact solitary-wave solutions. These equations arise in fluid mechanics and consist of a NLS equation coupled to a KdV equation. This example has two new interesting features: it is six-dimensional, and for appropriate parameter values has a Maslov index which is a non-monotone function of λ.

In the last chapter, we study the stability of stationary solutions of a model for a flow over a non-uniform bottom, the Korteweg-de Vries equation with a forcing term. In this case, space translational invariance is lost and therefore stationary solutions can be stable in the usual sense (u is said to be stable if the Cauchy problem admits a unique solution over $\mathbb{R}^+$ in a neighborhood of $u(\cdot, 0)$ and if for all $\varepsilon > 0$, there exists a neighborhood U of $u(\cdot, 0)$ such that if v is a solution and $v(\cdot, 0) \in U$, then $\sup_{t \in \mathbb{R}^+} \|v(\cdot, t) - u(\cdot, t)\| < \varepsilon$). Again, this study is based on the Hamiltonian structure of the PDE and the 2-dimensional version of the Maslov index theory, i.e. Sturm-Liouville theory.

Remarks:

- There is an index of definitions and notations in Appendix H.

- The work on the numerical computation of the Maslov index of periodic orbits has already been published in [37].

- The content of section 1.3.1 has been published in [35].

- The description on how to compute the Maslov index in dimension 4 has been published in [38]. It includes the longwave-shortwave example.

- The work on the Maslov index of multi-pulse solitary waves has been published in [39].

Chapter 1

The Maslov index for solitary waves

Contents

Introduction

Many physical models can be formulated as Hamiltonian systems or gradient flows.

Hamiltonian systems are problems consisting of finding $Z : [a,b] \to M$ such that

$$\forall t \in [a,b] \forall \delta v \quad \left\langle \left(\frac{\delta \mathcal{H}}{\delta u}\right)_{Z(t)}, \delta v \right\rangle = \omega_{Z(t)} \left(\frac{\mathrm{d}Z}{\mathrm{d}t}(t), \delta v\right) \tag{1.0.1}$$

where M is a manifold and ω is a non-degenerate antisymmetric bilinear form over the tangent space of M and $\mathcal{H} : M \times \mathbb{R} \to \mathbb{R}$ is a functional called the Hamiltonian. For example, the following systems can be put under an Hamiltonian form (in these cases, ω does not depend on Z, and therefore the Z-dependency is dropped out):

- N-body problem: $\mathcal{H}(p, q) = V(q) + \frac{p^2}{2m}$ and
  $\omega((q_1, p_1), (q_2, p_2)) = \langle p_1, q_2 \rangle - \langle q_1, p_2 \rangle$, where $\langle \cdot, \cdot \rangle$ is the standard scalar product on $\mathbb{R}^{3N}$.

- Korteweg-de Vries equation: $\mathcal{H}(u) = \int u_x^2 + \frac{\alpha}{q+2} u^{q+2}$ and $\omega(u, v) = \int_{\mathbb{R}} u(x)(\partial_x)^{-1} v(x) \mathrm{d}x$

- Kawahara equation: $\mathcal{H}(u) = \int_{\mathbb{R}} \left(\frac{1}{2} u_{xx}^2 + \frac{P}{2} u_x^2 - \frac{1}{q+2} u^{q+2} + \frac{c}{2} u^2 \right) \mathrm{d}x$

- Non-linear Schrödinger equations: $\mathcal{H}(\phi) = \int_{\mathbb{R}} \left(|\phi_x|^2 \pm |\phi|^4 \mathrm{d}x \right)$ and $\omega(\phi, \psi) = \int_{\mathbb{R}} \mathrm{Im}(\phi\bar{\psi}) \mathrm{d}x$

- Longwave-shortwave resonance equations:
  $\mathcal{H}(u, v, w) = \int \left(u_x^2 + v_x^2 + \frac{1}{2} w_x^2 - w(w^2 + u^2 + v^2) + \frac{1}{2} cw^2 + \nu(u^2 + v^2) \right) \mathrm{d}x$,
  $\omega((u_1, v_1, w_1), (u_2, v_2, w_2)) = \int_{\mathbb{R}} \left(u_1 v_2 - u_2 v_1 + w_1(\partial_x)^{-1} w_2 \right) \mathrm{d}x$.

If the functional $\mathcal{H}$ is time-independent, then $\mathcal{H}(Z(.))$ is a conserved quantity. Furthermore, an equilibrium of the system is then a critical point of $\mathcal{H}$.

Gradient-type[1] systems can be written as $u_t = \nabla F(u)$. They include for example:

- Reaction-diffusion systems (including the Fitzhugh-Nagumo equations): $F(u) = \int u_x^T A u_x + f(u)$ with $\langle u, v \rangle = \int uv$ as a scalar product.

- Swift-Hohenberg equation: $F(u) = \int u_{xx}^2 + P u_x^2 + \alpha u^2 + \beta u^3 + \gamma u^4$ with $\langle u, v \rangle = \int uv$ as a scalar product.

In this case, $F(u(t))$ is a decreasing function of time. As for Hamiltonian systems, stationary solutions are critical points of F. Besides, the linearization of a gradient-flow system near a stationary solution ϕ is $u_t = \nabla_\phi^2 F u$.

Hence, in these two cases, searching for a stationary solution is equivalent to look for a critical point of an action:

$$S(\phi) = \int_I l \left(\phi, \dots, \frac{\mathrm{d}^k \phi}{\mathrm{d}t^k}, t \right) \mathrm{d}t \tag{1.0.2}$$

where S is a Hamiltonian or the functional from which derives the gradient flow.

It is then possible to obtain *Euler-Lagrange* differential equations. Then, by making a change of variables, these equations can be put into an Hamiltonian form (see appendix B).

An interesting question concerning solutions of Euler-Lagrange equations is to determine what kind of critical points (e.g. minima, saddle, ...) of the functional S are obtained. The *Maslov* index, introduced in this chapter, can give the number of negative eigenvalues of the Hessian of S at the critical point.

The Maslov index is a generalization of the number of intersections of Sturm-Liouville's theory to systems with more than one degree of freedom. It is sometimes referred as the Conley-Zehnder index, which is defined for symplectic matrices (i.e. a matrix M such that $M^t \mathcal{J} M = \mathcal{J}$. More details on symplectic matrices are given in Appendix A), whereas the Maslov index is usually defined for Lagrangian planes. It is used in a wide range of physical applications: semi-classical quantization, quantum chaology, classical mechanics [6], etc.

---

[1] Hamiltonian systems can be seen as gradient-type systems. In that case the gradient is constructed from the symplectic form rather than from the scalar product.

The Maslov index has also been used in [77, 16] to determine the stability of travelling waves of Schrödinger or Fitzhugh-Nagumo equations. A Maslov index can be defined for one-dimensional solitary waves (but also periodic waves and fronts) when they are critical points of some functional S.

According to [82, 42, 78], the number of negative eigenvalues of the second variation $D^2\mathcal{H}$ of the Hamiltonian near ϕ is related to the number of unstable modes near the solitary wave ϕ. In the gradient-flow case, the Morse index of D^2F gives the exact number of unstable modes.

Suppose that we want to solve the following spectral problem:

$$\text{Find } \delta u \text{ such that } \forall v \quad \delta^2 S_\phi(\delta u, \delta v) = \lambda \int_I \delta u \delta v \tag{1.0.3}$$

Then, by using the set of coordinates introduced in appendix B, the above problem can be written as:

$$\forall \delta Z_2 \quad \int_I \left(\omega(\frac{\mathrm{d}\delta Z_1}{\mathrm{d}x}, \delta Z_2) - D^2 H(\delta Z_1, \delta Z_2) \right) \mathrm{d}x + \text{boundary terms} = \lambda \int_I \delta Z_1 \mathbf{D} \delta Z_2$$

with $\mathbf{D}$ a positive semi-definite matrix and ω the standard symplectic form ($\mathcal{J}$ is the matrix defined by equation (0.0.7).) on $\mathbb{R}^{2n}$:

$$\omega(x, y) = x^T \mathcal{J} y. \tag{1.0.4}$$

If we denote $\mathbf{C}(x, \lambda) = D^2 H_{\phi_x} + \lambda \mathbf{D}$, then $\partial_\lambda \mathbf{C}(x, \lambda) = \mathbf{D}$ is a positive semi-definite matrix and δZ_1 is a solution of the following linear Hamiltonian system:

$$\mathcal{J}\mathbf{z}_x = \mathbf{C}(x, \lambda)\mathbf{z} \tag{1.0.5}$$

However, not every solution $\mathbf{z}$ corresponds to an eigenvector of the spectral problem since u and therefore $\mathbf{z}$ must satisfy some boundary conditions.

In fact, the boundary conditions on $\mathbf{z}$ are often equivalent to the fact that $\mathbf{z}$ belongs simultaneously to two *Lagrangian* planes $R_1(x, \lambda)$ and $R_2(x, \lambda)$ of solutions. This is the case for the solitary wave problem and for the separated boundary conditions problem discussed in appendix G.

Definition 2 *A n-dimensional subspace G of $\mathbb{R}^{2n}$ is said to be a Lagrangian space if:*

$$\forall x, y \in G \quad \omega(x, y) = x^T \mathcal{J} y = 0$$

The great interest of Lagrangian planes lies in the following:

Proposition 1 *Let $V(t)$ be a space of solutions of the linear Hamiltonian system $\mathcal{J}x' = C(t)x$, where $C(t)$ is a symmetric matrix.*
If $V(t_0)$ is Lagrangian, then $V(t)$ is Lagrangian for any t.

Definition 3 *$\Lambda(n)$ is the set of all Lagrangian subspaces included in $\mathbb{R}^{2n}$.*

By looking at the paths made by $x \mapsto R_1(x, \lambda)$ and $x \mapsto R_2(x, \lambda)$, it is possible to count the eigenvalues of the problem (1.0.3).

In this chapter, we will first recall the definition of the Maslov index of paths. Then, we will define the Maslov index of hyperbolic periodic systems and study the convergence of the Maslov index when a sequence of periodic orbits is asymptotic to an homoclinic orbit and use it to define the Maslov index of homoclinic orbit. This limit is of interest, since VANDERBAUWHEDE & FIEDLER [120] proved that any homoclinic of an Hamiltonian system can be approximated by such a sequence of periodic orbits. Finally, we will compare this limit to the definitions of the Maslov index given by BOSE AND JONES [16] and CHEN AND HU [40].

1.1   The Maslov index of paths

In this section, we recall the definition of the Maslov index of paths with respect to a Lagrangian plane. Here, we use the identification of $\Lambda(n)$ with $U(n)/O(n)$ to define it.

Then, we define the Maslov index of a pair of elements of the universal covering $\widetilde{\Lambda(n)}$ with respect to a Lagrangian plane.

The latter definition will be useful to compare this work with [40, 16].

1.1.1   The Lagrangian manifold $\Lambda(n)$

Here, we describe the Lagrangian manifold $\Lambda(n)$ as a quotient space of two sets of matrices.

Definition 4 *The k-th Grassmannian $G_k(E)$ of a vector space is defined as the set of k-dimensional subspaces of E.*

$\Lambda(n)$ is a subset of $G_n(\mathbb{R}^{2n})$.

Let $\tau : \begin{cases} \{2n \times n\text{-matrices of rank } n\} \to G_n(\mathbb{R}^{2n}) \\ \begin{pmatrix} C_1 & \dots & C_n \end{pmatrix} \mapsto \text{Range}\left(\begin{pmatrix} C_1 & \dots & C_n \end{pmatrix} \right) = \text{span}(C_1, \dots, C_n) \end{cases}$.

τ is onto but not one-to-one. In fact:

$$\tau(A) = \tau(B) \Leftrightarrow \exists P \in GL_n(\mathbb{R}) \quad AP = B$$

Now, let us characterize matrices whose range is a Lagrangian space:

$$\text{Range}\left(\begin{pmatrix} X \\ Y \end{pmatrix}\right) \in \Lambda(n) \Leftrightarrow \begin{pmatrix} X \\ Y \end{pmatrix}^T \mathcal{J} \begin{pmatrix} X \\ Y \end{pmatrix} = 0 \Leftrightarrow X^T Y = Y^T X \qquad (1.1.6)$$

Definition 5 $X_n = \left\{ \begin{pmatrix} X \\ Y \end{pmatrix} \in M_{2n,n}(\mathbb{R}) \quad | \quad X^T Y = Y^T X \ \text{and} \ \begin{pmatrix} X \\ Y \end{pmatrix} \text{has rank } n \right\}$

Definition 6 *The train $\Lambda(U)$ of a Lagrangian plane U is defined as the set of Lagrangian planes not transverse to U.*

Range(A) and Range(B) are transverse if and only if $\det \begin{pmatrix} A & B \end{pmatrix} \neq 0$.

Let $Z = \begin{pmatrix} X \\ Y \end{pmatrix} \in X_n$.

Then $Z^t Z$ is a real symmetric positive definite matrix and $(X + iY)(Z^t Z)^{-\frac{1}{2}}$ is unitary. Therefore:

Proposition 2 $\theta : \begin{cases} U(n) \to \Lambda(n) \\ Z \mapsto \text{Range} \left(\begin{pmatrix} \text{Re}(Z) \\ \text{Im}(Z) \end{pmatrix} \right) \end{cases}$ *is a well-defined and onto mapping.*

Furthermore:

$$\theta(Z_1) = \theta(Z_2) \Leftrightarrow \exists P \in O(n) \quad Z_1 P = Z_2$$

Hence: $\Lambda(n) = U(n)/O(n)$ (and $\Lambda(n) = X_n/GL_n(\mathbb{R})$).

Furthermore, $\Lambda(n)$ is a differentiable manifold of dimension $\frac{n(n+1)}{2}$.

1.1.2 The Maslov index of paths

Here, we define the Maslov index by using the eigenvalues of a matrix.

Let $\psi : \begin{cases} (X_n)^2 \to GL_n(\mathbb{C}) \\ \left(\begin{pmatrix} W \\ Z \end{pmatrix}, \begin{pmatrix} X \\ Y \end{pmatrix} \right) \mapsto (X - iY)^{-1}(W - iZ)(W + iZ)^{-1}(X + iY) \end{cases}$.

The image of ψ is included in the set of symmetric (not Hermitian) matrices. $\psi(A, B)^*(A^t A)\psi(A, B) = A^t A$ and $A^t A$ is a real positive definite matrix. Therefore $\psi(A, B)$ is unitary with respect to the scalar product $(x, y) \to y^*(A^t A)x$. Consequently, $\psi(A, B)$ is similar to a diagonal matrix whose diagonal elements are of modulus one.

Besides, if Range(A) = Range(B) and Range(W) = Range(Z), then $\psi(A, W)$ and $\psi(B, Z)$ are *similar* and their eigenvalues are the same. The following mappings on $\Lambda(n)$ are therefore well defined:

Definition 7 *The Maslov determinant is defined as* $s : \begin{cases} \Lambda(n) \to \mathbb{U} \\ \text{Range}(A) \mapsto \det \psi(A, \begin{pmatrix} I \\ 0 \end{pmatrix}) \end{cases}$.

Definition 8 $K_{\text{Range}(Z)} : \begin{cases} \Lambda(n) \to \mathbb{U}^n/\sim \\ \text{Range}(A) \mapsto \textit{Eigenvalues of } \psi(A, Z) \end{cases}$ *where* $\sim$ *is the relation of equivalence defined by:*

$$(x_1, x_2, \ldots, x_n) \sim (y_1, y_2, \ldots, y_n) \Leftrightarrow \exists \sigma \textit{ one-to-one} \quad (x_1, x_2, \ldots, x_n) = (y_{\sigma(1)}, y_{\sigma(2)}, \ldots, y_{\sigma(n)})$$

Both s and $K_{\text{Range}(Z)}$ are continuous functions (this can be checked by taking a local set of coordinates in $\Lambda(n)$) which are dependent on the choice of a basis.

For convenience, we will not mention again the quotient for K.

Proposition 3 *The dimension of $U \cap W$ is equal to the number of elements of $K_U(W)$ equal to 1.*

Definition 9 *Let W be a Lagrangian space and $\gamma : [0,1] \to \Lambda(n)$ be a continuous path and let*
$\kappa : [0,1] \to \mathbb{R}$ be a continuous function such that $e^{i\kappa(x)} = s(\gamma(x))$.

Let $\alpha_1, \alpha_2, \ldots, \alpha_{n-a} \in]0, 2\pi[$, $\beta_1, \beta_2, \ldots, \beta_{n-b} \in]0, 2\pi[$ such that
$K_W(\gamma(0)) = (e^{i\alpha_1}, e^{i\alpha_2}, \ldots, e^{i\alpha_{n-a}}, 1, \ldots, 1)$ and $K_W(\gamma(1)) = (e^{i\beta_1}, e^{i\beta_2}, \ldots, e^{i\beta_{n-b}}, 1, \ldots, 1)$.

Then, the Maslov index $m_W(\gamma)$ of γ with respect to W is defined as:

$$m_W(\gamma) = \frac{\kappa(1) - \sum_{i=1}^{n-b} \beta_i}{2\pi} - \frac{\kappa(0) - \sum_{i=1}^{n-a} \alpha_i}{2\pi} + \frac{1}{2}(b - a)$$

Remark: Depending on the author, the term $\frac{1}{2}(b - a)$ might be replaced by $-a$ or b. The convention we use comes from ROBBIN & SALAMON [108].

Proposition 4

- *m is invariant by a symplectic change of coordinates, i.e. by a left multiplication of the Lagrangian planes by a symplectic matrix.*

- *Two paths γ, δ with the same endpoints are homotopy-equivalent if and only if there exists W s.t. $m_W(\gamma) = m_W(\delta)$.*

  In that case, for all $W \in \Lambda(n)$, we have $m_W(\gamma) = m_W(\delta)$.

- *If $\gamma : [0,1] \to \Lambda(n)$ is a closed path, e.g. $\gamma(0) = \gamma(1)$, and if κ is a continuous function such that $e^{i\kappa(x)} = s(\gamma(x))$, then $m_W(\gamma)$ is independent of the choice of W and:*

$$m_W(\gamma) = \frac{\kappa(1) - \kappa(0)}{2\pi}.$$

Definition 10 *If γ is a closed path in $\Lambda(n)$, its Maslov index $m(\gamma)$ is defined as $m(\gamma) = m_W(\gamma)$, where W is any element of $\Lambda(n)$.*

Definition 11 *Suppose that $\gamma = \text{Range} \circ A$ intersects non trivially $W = \text{Range}(U)$ at t_0 and that $\gamma(t_0)$ intersects W trivially in $[t_0 - \varepsilon, t_0 + \varepsilon] - \{t_0\}$. Let $r = \dim(\gamma(t_0))$.*

Let $\kappa_1, \kappa_2, \ldots, \kappa_n$ be continuous functions such that $e^{i\kappa_1(t)}, e^{i\kappa_2(t)}, \ldots, e^{i\kappa_n(t)}$ are the eigenvalues of $\psi(U, A(t))$ and $\kappa_i(t_0) = 0$ for $i \in \{1, \ldots, r\}$.

The sign of the intersection of γ with W at t_0 is defined as:

$$\text{sign}(\gamma, t_0, W) = \frac{1}{2}(\text{sign}^+(\gamma, t_0, W) + \text{sign}^-(\gamma, t_0, W))$$

with

- $$\begin{aligned} \text{sign}^+(\gamma, t_0, W) = \quad & \lim_{t \to t_0^+} \#\{i \in \{1, \ldots, r\} | \kappa_i(t) > 0\} \\ & - \lim_{t \to t_0^+} \#\{i \in \{1, \ldots, r\} | \kappa_i(t) < 0\} \end{aligned}$$

- $$\begin{aligned} \text{sign}^-(\gamma, t_0, W) = \quad & \lim_{t \to t_0^-} \#\{i \in \{1, \ldots, r\} | \kappa_i(t) < 0\} \\ & - \lim_{t \to t_0^-} \#\{i \in \{1, \ldots, r\} | \kappa_i(t) > 0\} \end{aligned}$$

Proposition 5 *Let $\gamma : [a, b] \to \Lambda(n)$.*

Suppose that $\gamma(t)$ intersects W non-trivially only a finite number of times. Then:

$$m_W(\gamma) = \frac{1}{2} \text{sign}^+(\gamma, a, W) + \sum_{a < t < b} \text{sign}(\gamma, t, W) + \frac{1}{2} \text{sign}^-(\gamma, b, W)$$

1.1.3 Intersection of Lagrangian planes in the differentiable case

Another interesting case is when the path is *differentiable*. When the derivative satisfies some non-degeneracy conditions, it is possible to compute the intersection sign from the derivative of the path.

Let $\gamma : t \mapsto \operatorname{Range}\left(\begin{pmatrix} X \\ Y \end{pmatrix}\right)$ a path in $\Lambda(n)$ and $\operatorname{Range}(W) \in \Lambda(n)$. Denote $U = \begin{pmatrix} X \\ Y \end{pmatrix}$.

Suppose that $\dim(\gamma(0) \cap \operatorname{Range}(W)) = k$.

Then there exists a $n \times k$ matrix G such that $\gamma(0)G$ spans $\operatorname{Range}(W) \cap \operatorname{Range} \circ \gamma(0)$. Then $Y(0)G = 0$.

Define:
$$\begin{aligned} q &= G^T U'(0)^T \mathcal{J} U(0) G + G^T U(0)^T \mathcal{J} U'(0) G \\ &= G^T (X'^T Y - Y'^T X) G + G^T (X^T Y' - Y^T X') G \end{aligned}$$

Let (r^+, r^-) be the signature[2] of q. (r^+, r^-) is independent of G.

Proposition 6 *The crossing of* $\operatorname{Range} \circ \gamma$ *with* $\operatorname{Range}(W)$ *at 0 is said to be* regular *if* $r^+ + r^- = k$.

In that case, we have:

$\operatorname{sign}^+(\gamma, t_0, \operatorname{Range}(W)) = \operatorname{sign}^-(\gamma, t_0, \operatorname{Range}(W)) = \operatorname{sign}(\gamma, t_0, \operatorname{Range}(W)) = r^+ - r^-$

Besides, there exists $\varepsilon > 0$ *such that if* $t \in]s - \varepsilon, s + \varepsilon[-\{s\}$, $\gamma(t) \cap W = \{0\}$.

The proof of this proposition can be found in [93]. The great advantage of this formula is that it uses an expression which only relies on the symplectic structure of $\mathbb{R}^{2n}$. Besides, this characterization is useful to prove that the Maslov index is an eigenvalue counter (see Appendix C).

1.1.4 The universal cover of $\Lambda(n)$

While we will mainly use the Maslov index of paths in the sequel, the Maslov index for elements of the universal cover is useful to compare with prior work. Now, let us construct a universal cover of $\Lambda(n)$.

Definition 12 $\widetilde{\Lambda(n)} = \{(\kappa, U) \in \mathbb{R} \times \Lambda(n) \text{ such that } e^{i\kappa} = s(U)\}$

$$p : \begin{cases} \widetilde{\Lambda(n)} \to \Lambda(n) \\ (\kappa, U) \mapsto U \end{cases}$$

Proposition 7 $\widetilde{\Lambda(n)}$ *is a universal cover[3] of* $\Lambda(n)$, *i.e.:*

- $\widetilde{\Lambda(n)}$ *is simply connected.*

- *If* $\tilde{U} \in \widetilde{\Lambda(n)}$, *there exists a neighborhood* Ω *of* $\tilde{U}$ *such that* $p_{|\Omega}$ *is an homeomorphism.*

For $U \in \Lambda(n)$, $p^{-1}(\Lambda(n) - \Lambda(U))$ is composed of an infinity of connected components. The Maslov index can label them.

---

[2]The signature of a real symmetric matrix q is defined as the pair of integers (r_+, r_-), where r_+ is the number of strictly positive eigenvalues of q and r_- is the number of strictly negative eigenvalues.

[3]The universal cover of a topological space is unique up to a homeomorphism.

Definition 13 *Let $(\alpha, A), (\beta, B) \in \widetilde{\Lambda(n)}$, $C \in \Lambda(n)$, and $r_A = \dim(A \cap C)$, $r_B = \dim(B \cap C)$. Let $\alpha_1, \alpha_2, \ldots, \alpha_{n-r_A} \in\ ]0, 2\pi[$, $\beta_1, \beta_2, \ldots, \beta_{n-r_B} \in\ ]0, 2\pi[$ such that $K_C(A) = (e^{i\alpha_1}, e^{i\alpha_2}, \ldots, e^{i\alpha_{n-r_A}}, 1, \ldots, 1)$ and $K_C(B) = (e^{i\beta_1}, e^{i\beta_2}, \ldots, e^{i\beta_{n-r_B}}, 1, \ldots, 1)$.*

Define

$$m_C((\alpha, A), (\beta, B)) = \frac{\beta - \sum_{i=0}^{n-r_B} \beta_i}{2\pi} - \frac{\alpha - \sum_{i=0}^{n-r_A} \alpha_i}{2\pi} + \frac{1}{2}(r_B - r_A)$$

There is an obvious link between the Maslov index for elements of the universal cover and the Maslov index for paths:

Proposition 8 *Let W be a Lagrangian space and $\gamma : [0, 1] \to \Lambda(n)$ be a continuous path and let $\kappa : [0, 1] \to \mathbb{R}$ be a continuous function such that $e^{i\kappa(x)} = s(\gamma(x))$. Then,*

$$m_W(\gamma) = m_W((\kappa(0), \gamma(0)), (\kappa(1), \gamma(1))).$$

Proposition 9 *Let $(\alpha, U), (\beta, V) \in \widetilde{\Lambda(n)}$ and $W \in \Lambda(n)$. Then:*

- $C_{i,(\alpha,U)} = \{\tilde{A} \in p^{-1}(\Lambda(n) - \Lambda(U)) \text{ s.t. } m_U((\alpha, U), \tilde{A}) = i\}$, with $i \in \frac{n}{2} + \mathbb{Z}$, are the connected components of $p^{-1}(\Lambda(n) - \Lambda(U))$,

- *If $\dim(U \cap V) = k$, then $(\beta, V) \in \bigcap_{j=1}^{k} \overline{C_{j+m_U((\alpha,U),(\beta,V)) - \frac{k+1}{2},(\alpha,U)}}$.*

m has a property of additivity:

Proposition 10 *Let $\tilde{U}, \tilde{V}, \tilde{W} \in \widetilde{\Lambda(n)}$ and $Z \in \Lambda(n)$. Then*

- $m_Z(\tilde{U}, \tilde{V}) \in \frac{1}{2}\mathbb{Z}$

- $m_Z(\tilde{U}, \tilde{W}) = m_Z(\tilde{U}, \tilde{V}) + m_Z(\tilde{V}, \tilde{W})$

- $m_Z(\tilde{U}, \tilde{U}) = 0$.

Finally, m has also a kind of continuity.

Proposition 11 *Suppose that $(\tilde{U}_r)_{r \in \mathbb{N}}, (\tilde{V}_r)_{r \in \mathbb{N}} \in \widetilde{\Lambda(n)}^{\mathbb{N}}$ and $(Z_r)_{r \in \mathbb{N}} \in \Lambda(n)^{\mathbb{N}}$ converge respectively to $\tilde{U}, \tilde{V}$ and Z and that:*

$$\begin{cases} \lim_{r \to \infty} \dim(p(\tilde{U}_r) \cap Z_r) = \dim p(U) \cap Z \\ \lim_{r \to \infty} \dim(p(\tilde{V}_r) \cap Z_r) = \dim p(V) \cap Z \end{cases}$$

Then:

$$\lim_{r \to \infty} m_{Z_r}(\tilde{U}_r, \tilde{V}_r) = m_Z(\tilde{U}, \tilde{V})$$

1.2 The Maslov index of periodic waves

We have now defined the Maslov index of paths and are therefore able to extend it to hyperbolic periodic waves. In section 1.3, we study the limit when the periodic wave converges to a solitary wave. In chapter 2, a numerical algorithm is given to compute this quantity and a numerical example is given in section 3.7.

Suppose that the 1D traveling L-periodic wave ϕ is a solution of an autonomous non-linear Hamiltonian system:

$$\mathcal{J}\mathbf{u}_x = \nabla_{\mathbf{u}} H \quad H : \mathbb{R}^{2n} \to \mathbb{R} \tag{1.2.7}$$

Suppose now that we look for the solutions of the following spectral problem:

$$\mathbf{z}_x = \mathbf{B}(x, \lambda)\mathbf{z}, \quad \mathbf{B}(x, \lambda) = -\mathcal{J}\mathbf{C}(x, \lambda), \, \mathcal{J} = \begin{pmatrix} \mathbf{0} & -\mathbf{I} \\ \mathbf{I} & \mathbf{0} \end{pmatrix}, \quad \mathbf{z} \in \mathbb{R}^{2n}$$
$$\mathbf{z} \text{ is bounded.} \tag{1.2.8}$$

where $\mathbf{C}(x, \lambda)$ is a symmetric matrix which usually satisfies:

$$\mathbf{C}(x, 0) = D^2 H_{\phi(x)}. \tag{1.2.9}$$

The latter formula means that, for $\lambda = 0$, system (1.2.8) is the linearization of system (1.2.7).

This spectral problem can also be reformulated in terms of Floquet multipliers. Consider the flow matrix $\mathbf{\Phi}(x_1, x_2, \lambda)$ defined by:

$$\mathbf{\Phi}(x_1, x_1, \lambda) = I_{2n}, \quad \frac{\partial \mathbf{\Phi}}{\partial x_1}(x_1, x_2, \lambda) = \mathbf{B}(x_1, \lambda)\mathbf{\Phi}(x_1, x_2, \lambda)$$

Define the monodromy matrix at 0 as:

$$\mathbf{M}(\lambda) = \mathbf{\Phi}(0, L, \lambda) \tag{1.2.10}$$

Taking for the monodromy matrix $\mathbf{\Phi}(x, x + L, \lambda)$ would lead to a similar matrix. The eigenvalues of $\mathbf{M}(\lambda)$ are therefore an invariant for the periodic system, they are called the Floquet multipliers of the system.

The set of λ such that the problem (1.2.8) has a non-trivial $\mathbf{z}$ solution is called the spectrum, which we denote by σ:

$$\sigma = \{\lambda \quad | \quad \mathbf{M}(\lambda) \text{ has at least an eigenvalue on the unit circle.}\}. \tag{1.2.11}$$

It is composed of closed intervals called bands and has no isolated points.

Definition 14 *The unstable space $\mathcal{U}(\cdot, \lambda)$ of system (1.2.8) is defined as the set of solutions of (1.2.8) which decay to 0 exponentially at $-\infty$ (Its dimension may vary with λ).*

Suppose that the studied wave is L-periodic. Then, $\mathbf{C}(x, \lambda)$ is L-periodic with respect to x. When $\dim(\mathcal{U}(\cdot, \lambda)) \in \{n - 1, n\}$, there are two cases when a Maslov index can be defined:

- The unstable space $\mathcal{U}(\cdot, \lambda)$ is a n-dimensional space. This is equivalent to $\lambda \notin \sigma$. The periodic system is said to be strictly hyperbolic.

Definition 15 *When $\mathcal{U}(\cdot, \lambda)$ is a n-dimensional space, it is also Lagrangian. The Maslov index at λ of system (1.2.8) is defined as $m(\mathcal{U}(\cdot, \lambda))$, where $\mathcal{U}(\cdot, \lambda)$ is taken over $[0, L]$.*

- The L-periodic travelling wave ϕ is a solution of (1.2.7) and the linear system (1.2.8) at $\lambda = 0$ is the linearization of system (1.2.7). ϕ_x is then a solution of the linear system at $\lambda = 0$ and therefore, $\mathcal{U}(\cdot, 0)$ is not n-dimensional. However, if it is $n - 1$-dimensional, the following definition can be used:

Definition 16 *If the dimension of the space $\mathcal{R}(x) = \mathcal{U}(x, 0)$ of solutions of $\mathcal{J}\mathbf{z}_x = D^2 H_\phi \mathbf{z}$ decaying to 0 at $-\infty$ is $n - 1$, then $(\mathbb{R}\phi_x \oplus \mathcal{R})_{|[0,L]}$ is a closed path over one period in the Lagrangian manifold and the Maslov index of ϕ at 0 is defined as $I_{per}(\phi) = m((\mathbb{R}\phi_x \oplus \mathcal{R})_{|[0,L]})$.*

When the system is not hyperbolic, there are alternative definitions [118, 104] of the Maslov index which include corrections for the case of Floquet multipliers on the unit circle.

1.3   The Maslov index of solitary waves

Consider now a solitary wave ϕ which decays exponentially at $\pm\infty$ which is a solution of an autonomous non-linear Hamiltonian system:

$$\mathcal{J}\mathbf{u}_x = \nabla_{\mathbf{u}} H \quad H : \mathbb{R}^{2n} \to \mathbb{R} \tag{1.3.12}$$

Suppose now that we look for the solutions of the following spectral problem:

$$\mathbf{z}_x = \mathbf{B}(x, \lambda)\mathbf{z}, \quad \mathbf{B}(x, \lambda) = -\mathcal{J}\mathbf{C}(x, \lambda), \, \mathcal{J} = \begin{pmatrix} \mathbf{0} & -\mathbf{I} \\ \mathbf{I} & \mathbf{0} \end{pmatrix}, \quad \mathbf{z} \in \mathbb{R}^{2n} \tag{1.3.13}$$
$$\lim_{|x|\to\infty} \mathbf{z}(x) = 0$$

where $\mathbf{C}(x, \lambda)$ is a symmetric matrix which usually satisfies:

$$\mathbf{C}(x, 0) = D^2 H_{\phi(x)}. \tag{1.3.14}$$

The latter formula means that, for $\lambda = 0$, system (1.3.13) is the linearization of system (1.2.7).

In this section, we first compute the limit of the Maslov index of a sequence of periodic orbits approximating an homoclinic one. This leads to an unambiguous definition of the Maslov index when λ is out of the spectrum.

The situation $\lambda = 0$ is also studied and we give the limit when it exists from the energy of the periodic solutions.

Unfortunately, the hypotheses for the $\lambda = 0$ case are too stringent as we shall see in section 3.7.

However, Bose & Jones [16] and later Chen & Hu [40] proved that it was possible to define a Maslov index with an intersection-based definition for the $\lambda = 0$ case.

1.3.1 The limit of the Maslov index of a sequence of periodic orbits approximating an homoclinic one

General hypotheses made on the homoclinic orbit

We suppose now that ϕ is a *solitary* wave and we consider a sequence ϕ^α approximating ϕ.

To determine the limits of $\alpha \to I_{per}(\phi^\alpha, \lambda)$ and $\alpha \to I_{per}(\phi^\alpha)$, some hypotheses will be needed. These two limits will in fact be handled separately.

However, the two cases share common hypotheses:

Hypothesis 1 • $\mathbf{B}(x, \lambda)$ *is a smooth function with respect to x and analytic with respect to λ.*

- *There exists $\mathbf{B}_\infty(\lambda)$, $\gamma > 0$ and $F > 0$ such that $\forall x, \lambda$ $\|\mathbf{B}(x, \lambda) - \mathbf{B}_\infty(\lambda)\| \leq Fe^{-\gamma|x|}$.*

- *The open set $\mathbb{X} = \mathbb{R} - \sigma_{ess}$ of real numbers is not empty, where the essential spectrum σ_{ess} is defined as:*

$$
\begin{aligned}
\sigma_{ess} &= \{\lambda \in \mathbb{C} \mid \mathbf{B}_\infty(\lambda) \text{ is not hyperbolic}\} \\
&= \{\lambda \in \mathbb{C} : \det[\mathbf{B}_\infty(\lambda) - i\kappa\mathbf{I}] = 0 \quad \text{for some } \kappa \in \mathbb{R}\}.
\end{aligned}
\tag{1.3.15}
$$

- *The discrete spectrum*

$$
\sigma_p = \{\lambda \in \mathbb{X} | \text{System (1.2.8) admits a non-trivial bounded solution}\}
\tag{1.3.16}
$$

is a strict subset of $\mathbb{X}$.

The discrete spectrum[4] only contains isolated points (see [64, 1]). $\sigma = \sigma_{ess} \cup \sigma_p$ is called the spectrum.

Define the stable and unstable subspaces of $\mathbf{B}_\infty(\lambda)$ by

$$
\mathrm{E}^s(\mathbf{B}_\infty(\lambda)) := \{\mathbf{u} \in \mathbb{R}^{2n} : \lim_{x \to +\infty} e^{\mathbf{B}_\infty(\lambda)x}\mathbf{u} = 0\}
$$

and

$$
\mathrm{E}^u(\mathbf{B}_\infty(\lambda)) := \{\mathbf{u} \in \mathbb{R}^{2n} : \lim_{x \to -\infty} e^{\mathbf{B}_\infty(\lambda)x}\mathbf{u} = 0\}
$$

$\mathrm{E}^s(\mathbf{B}_\infty(\lambda))$ ($\mathrm{E}^u(\mathbf{B}_\infty(\lambda))$) is also the direct sum of the generalized eigenspaces associated with the eigenvalues of $\mathbf{B}_\infty(\lambda)$ with negative (positive) real part.

Assume $\lambda \in \mathbb{X}$.

Since $\mathcal{J}\mathbf{B}_\infty(\lambda)$ is symmetric, $\dim E_u(\mathbf{B}_\infty(\lambda)) = \dim E_s(\mathbf{B}_\infty(\lambda))$. Therefore $E_u(\mathbf{B}_\infty(\lambda))$ and $E_s(\mathbf{B}_\infty(\lambda))$ have the same dimension: n.

Therefore, we can write: $\mathbb{R}^{2n} = E_u(\mathbf{B}_\infty(\lambda)) \oplus E_s(\mathbf{B}_\infty(\lambda))$.

Moreover, $\mathcal{U}(x, \lambda)$ has dimension n, is Lagrangian and $\lim_{x \to -\infty} \mathcal{U}(x, \lambda) = E_u(\mathbf{B}_\infty(\lambda))$. Symmetrically, the set of solutions that decay as $x \to +\infty$, which is called the stable space $\mathcal{S}(x, \lambda)$, is Lagrangian and $\lim_{x \to +\infty} \mathcal{S}(x, \lambda) = E_s(\mathbf{B}_\infty(\lambda))$.

---

[4]The fact that σ_p is only made of isolated points is a consequence of the analyticity of the Evans function, defined in section 2.4.1. In spectral theory, the discrete spectrum of an operator L is usually defined as the set of isolated points λ of the spectrum of the operator such that $L - \lambda$ has a finite-dimensional kernel. The complement in the spectrum is referred as the essential spectrum. Here, the two definitions match.

As we wish to define the Maslov index as a limit of the periodic case, we will also suppose that there is a family of periodic waves ϕ^α which approaches the solitary wave ϕ. More precisely, consider a family of systems parametrized by $\alpha \in [0, \alpha_0]$:

$$\mathcal{J}\mathbf{z}_x = \mathbf{C}^\alpha(x, \lambda)\mathbf{z} \tag{1.3.17}$$

We suppose that:

Hypothesis 2   • $\mathbf{C}^\alpha(x, \lambda)$ *is a smooth function with respect to x and α, and analytic with respect to λ and $\mathbf{C}^0(x, \lambda) = \mathbf{C}(x, \lambda)$.*

  • $\mathbf{C}^\alpha(\cdot, \lambda)$ *is L_α-periodic when $\alpha > 0$ and $\lim_{\alpha \to 0^+} L_\alpha = +\infty$.*

  • $\forall M > 0 \quad \lim_{\alpha \to 0} \sup_{x \in [-\frac{L_\alpha}{2}, \frac{L_\alpha}{2}], \lambda \in \mathbb{X}, |\lambda| < M} \|\mathbf{C}^\alpha(x, \lambda) - \mathbf{C}(x, \lambda)\| = 0.$

Maslov index for solitary waves when $\lambda \in \mathbb{X} - \sigma_p$

In this section, we will extend definition 15 and suppose that $\lambda \in \mathbb{X} - \sigma_p$.

By hypothesis, the space of solutions decaying both at $-\infty$ and $+\infty$ is reduced to $\{0\}$.

Then $\lim_{x \to +\infty} \mathcal{U}(x, \lambda) = E_u(\mathbf{B}_\infty(\lambda))$ (lemma 3.7 in [1]).

Therefore, $x \mapsto \mathcal{U}(x, \lambda)$ is a closed path in $\Lambda(n)$ over $\mathbb{R}$ for each $\lambda \in \mathbb{X} - \sigma_p$.

The quantity $m(\mathcal{U}(\cdot, \lambda))$ is therefore well defined. Let us now show that it is the limit[5] of $m(\mathcal{U}^\alpha(\cdot, \lambda))$ when $\alpha \to 0$.

Let $d(\cdot, \cdot)$ be a metric on $\Lambda(n)$ compatible with its compact manifold structure (It can be obtained by embedding $\Lambda(n)$ in $\mathbb{R}^N$).

Now, use lemma 2.11 p.172 of GARDNER [64]:

Theorem 1 (Gardner) *If hypotheses 1,2 are satisfied, let $\lambda \in \mathbb{X} - \sigma_p$. Then, for α small enough, the space $\mathcal{U}^\alpha(\cdot, \lambda)$ of solutions of (1.3.17) decaying at $-\infty$ is n-dimensional and converges x-uniformly to $\mathcal{U}(\cdot, \lambda)$:*

$$\lim_{\alpha \to 0} \sup_{x \in [-\frac{L_\alpha}{2}, \frac{L_\alpha}{2}]} d(\mathcal{U}^\alpha(x, \lambda), \mathcal{U}(x, \lambda)) = 0. \tag{1.3.18}$$

Corollary 1 *Let $\lambda \in \mathbb{X} - \sigma_p$. For α small, $I_{per}(\phi^\alpha, \lambda)$ is well-defined and equal to $m(\mathcal{U}^\alpha(\cdot, \lambda))$.*

Corollary 2 $\lim_{\alpha \to 0} \sup_{x \notin [-\frac{L_\alpha}{2}, \frac{L_\alpha}{2}]} d(\mathcal{U}^\alpha(\frac{L_\alpha}{2}, \lambda), \mathcal{U}(x, \lambda)) = 0.$

Proof.
By using the triangle inequality,
$d(\mathcal{U}^\alpha(\frac{L_\alpha}{2}, \lambda), \mathcal{U}(x, \lambda)) \leq d(\mathcal{U}^\alpha(\frac{L_\alpha}{2}, \lambda), \mathcal{U}(\frac{L_\alpha}{2}, \lambda)) + d(\mathcal{U}(\frac{L_\alpha}{2}, \lambda), E_u(\mathbf{B}_\infty(\lambda))) + d(E_u(\mathbf{B}_\infty(\lambda)), \mathcal{U}(x, \lambda)).$
Using $\lim_{|x| \to \infty} \mathcal{U}(x, \lambda) = E_u(\mathbf{B}_\infty(\lambda))$, corollary 2 is immediate.

Now define: $\mathcal{V}^\alpha(x, \lambda) = \begin{cases} \mathcal{U}^\alpha(x, \lambda) & \text{if} \quad x \in [-\frac{L_\alpha}{2}, \frac{L_\alpha}{2}] \\ \mathcal{U}^\alpha(\frac{L_\alpha}{2}, \lambda) & \text{if} \quad x \notin [-\frac{L_\alpha}{2}, \frac{L_\alpha}{2}] \end{cases}$.

From (1.3.18) and corollary 2, we get: $\lim_{\alpha \to 0} \sup_{x \in \mathbb{R}} d(\mathcal{V}^\alpha(x, \lambda), \mathcal{U}(x, \lambda)) = 0.$

---

[5]Of course, as m is an integer-valued function, it means that $m(\mathcal{U}^\alpha(\cdot, \lambda))$ is equal to $m(\mathcal{U}(\cdot, \lambda))$ for small enough α.

$\Lambda(n)$ is compact and therefore s is uniformly continuous over it. Consequently:

$$\lim_{\alpha \to 0} \sup_{x \in \mathbb{R}} |s(\mathcal{V}^\alpha(x, \lambda)) - s(\mathcal{U}(x, \lambda))| = 0.$$

Hence, if κ and κ^α are continuous such that $\mathcal{U} = e^{i\kappa}$ and $\mathcal{V}^\alpha = e^{i\kappa_\alpha}$, then

$$\lim_{\alpha \to 0} \sup_{x \in \mathbb{R}} |\kappa^\alpha(x, \lambda) - \kappa^\alpha(0) - \kappa(x, \lambda) + \kappa(0)| = 0.$$

Therefore:

$$\lim_{\alpha \to 0} |m(\mathcal{U}(\cdot, \lambda)) - m(\mathcal{V}^\alpha(\cdot, \lambda))| =$$

$$\lim_{\alpha \to 0} \left| \lim_{x \to \infty} \kappa(x, \lambda) - \lim_{x \to -\infty} \kappa(x, \lambda) - \lim_{x \to \infty} \kappa^\alpha(x, \lambda) + \lim_{x \to \infty} \kappa^\alpha(x, \lambda) \right| = 0.$$

This proves that the limit of $I_{per}(\phi^\alpha, \lambda) = m(\mathcal{V}^\alpha(\cdot, \lambda)) = m(\mathcal{U}^\alpha(\cdot, \lambda))$ as $\alpha \to 0$ exists. □

This limit is the basis for our definition of the Maslov index:

Definition 17 *The Maslov index of system (1.3.13) for $\lambda \in \mathbb{X} - \sigma_p$ is defined as $I_{hom}(\phi, \lambda) = m(\mathcal{U}(\cdot, \lambda))$.*

The limit of the Maslov index when the system is also the linearization of an autonomous system ($\lambda = 0$)

Using equations (1.2.7)-(1.2.9), it is easy to see that ϕ_x is a solution of system (1.3.13) at $\lambda = 0$ and therefore $0 \in \sigma_p$.

Let $\mathbf{M}^\alpha(\lambda)$ be the matrix such that $\mathbf{z}(L_\alpha) = \mathbf{M}^\alpha(\lambda)\mathbf{z}(0)$ for any $\mathbf{z}$ solution of $\mathcal{J}\mathbf{z}_x = \mathbf{C}^\alpha(x, \lambda)\mathbf{z}$. To determine $\lim_{\alpha \to 0} I_{per}(\phi^\alpha)$, make the following additional hypothesis:

Hypothesis 3   • *There is a unique family of L_α-periodic waves ϕ^α solutions of (1.2.7) such that ϕ^α converges to ϕ and $\mathbf{C}^\alpha(x, 0) = D^2 H_{\phi^\alpha(x)}$.*

   • *The functions $h(\alpha) = H(\phi^\alpha)$ and $l(\alpha) = L_\alpha$ are differentiable and in $]0, \alpha_0[$, we have $h' \neq 0$, $l' < 0$.*

   • *$\partial_\lambda \mathbf{C}^\alpha(\cdot, \lambda)$ is nonnegative-definite[6] in the sense of symmetric matrices.*

   • *$0 \in \mathbb{X}$ and the space of bounded solutions of the linear system (1.3.13) at $\lambda = 0$ is equal to $\mathbb{R}\phi_x$.*

   • *For small enough α, $\mathbf{M}^\alpha(0)$ has only two eigenvalues at $+1$, the others being off the unit circle.*

To determine the value of $I_{per}(\phi^\alpha)$, it is useful to study the behaviour of the two critical Floquet multipliers near $\lambda = 0$, which are equal to 1 when $\lambda = 0$. It turns out that this behaviour is governed by the sign of $h'(\alpha)$, as summarized in figure 1.1.

According to hypotheses 3, $\mathcal{R}^\alpha = \mathcal{U}^\alpha(\cdot, 0)$ has dimension $n - 1$ and $I_{per}(\phi^\alpha)$ is well-defined.

Let first assume that $h'(\alpha) > 0$. Then there exists a basis (x, y) of $E_1(\mathbf{M}^\alpha(0))$ and $\gamma > 0$ such that $^TyJx = 1$ and $\begin{pmatrix} 1 & \gamma \\ 0 & 1 \end{pmatrix}$ is the matrix of $\mathbf{M}^\alpha(0)_{|E_1(\mathbf{M}^\alpha(0))}$ in (x, y).

---

[6]The case $\partial_\lambda \mathbf{C}^\alpha(\cdot, \lambda)$ nonpositive-definite can be handled similarly, by replacing λ by $-\lambda$.
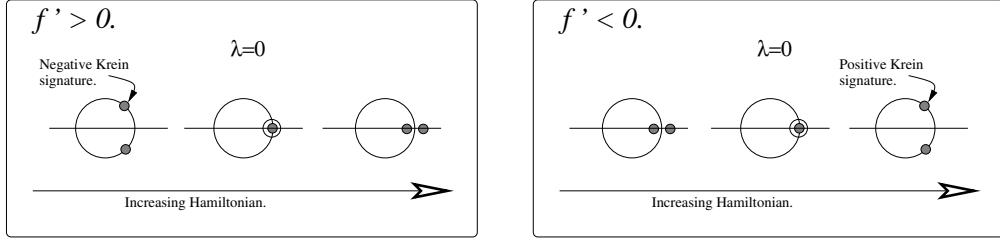
Figure 1.1: Position of the two critical eigenvalues of $\mathbf{M}^\alpha(\lambda)$ in the case where λ is close to 0 and $\partial_\lambda \mathbf{C}^\alpha(\cdot, \cdot)$ is positive semi-definite.

For λ near 0^+, there is one pair of eigenvalues of $\mathbf{M}^\alpha(\lambda)$ on the unit circle, the upper eigenvalue having a positive Krein signature[7].

For λ near 0^-, all the eigenvalues of $\mathbf{M}^\alpha(0)$ are off the unit circle, the unstable space $\mathcal{U}^\alpha(\cdot, \lambda)$ has dimension n and $\lim_{\lambda \to 0^-} \mathcal{U}^\alpha(\cdot, \lambda) = \mathbb{R}\phi_x^\alpha \oplus \mathcal{R}^\alpha$, x-uniformly.

If $h'(\alpha) < 0$, then the sign of γ and the Krein signature are reversed, and the two critical eigenvalues are on the unit circle when λ is close to 0^- and $\lim_{\lambda \to 0^+} \mathcal{U}^\alpha(\cdot, \lambda) = \mathbb{R}\phi_x^\alpha \oplus \mathcal{R}^\alpha$, x-uniformly.

Therefore, for small enough α, the Maslov index of ϕ^α is

$$I_{per}(\phi^\alpha) = \begin{cases} \lim_{\lambda \to 0^-} I_{per}(\phi^\alpha, \lambda) & \text{if } h'(\alpha) > 0 \\ \lim_{\lambda \to 0^+} I_{per}(\phi^\alpha, \lambda) & \text{if } h'(\alpha) < 0 \end{cases} .$$

Therefore, we *define* the Maslov index in the periodic limit of the solitary wave ϕ as:

$$I_{per \to hom}(\phi) = \begin{cases} \lim_{\lambda \to 0^-} I_{hom}(\phi, \lambda) & \text{if } h'_{]0,\alpha_0[} > 0 \\ \lim_{\lambda \to 0^+} I_{hom}(\phi, \lambda) & \text{if } h'_{]0,\alpha_0[} < 0 \end{cases} .$$

Unfortunately, this limit cannot be a basis for the Maslov index for all homoclinic orbits, because there are some cases where hypothesis 3 is not satisfied, like in section 3.4.

1.3.2 An intersection-based Maslov index when $\lambda \in \mathbb{X} - \sigma_{ess}$

In this section, we assume that hypothesis 1 holds.

Since the Maslov index is supposed to count the λ such that $\mathcal{S}(x, \lambda) \cap \mathcal{U}(x, \lambda) \neq \{0\}$, it is natural to look at the Maslov index of the path $\mathcal{U}(\cdot, \lambda)$ with respect to $\mathcal{S}_\infty(\lambda)$. When $\lambda \notin \sigma$, we have:

$$m_{\mathcal{S}_\infty(\lambda)}(\mathcal{U}(\cdot, \lambda)) = m(\mathcal{U}(\cdot, \lambda)) = I_{hom}(\phi, \lambda)$$

When $\lambda \in \sigma_p$, the situation is more subtle because $\lim_{x \to \infty} \mathcal{U}(x, \lambda)$ may no longer exist. BOSE & JONES defined in [16] the Maslov index by using ω-limit sets in $\widetilde{\Lambda(n)}$.

Definition 18 *The ω-limit set $\omega(f)$ of the mapping $f : \mathbb{R} \to E$ is defined as:*

$$\omega(f) = \{a \in E | \exists (x_n)_{n \in \mathbb{N}} \quad \lim_{n \to \infty} x_n = +\infty \ \& \ \lim_{n \to \infty} f(x_n) = a\}$$

---

[7]Suppose $e^{i\alpha}$, with $0 < \alpha < \pi$, is a simple eigenvalue of $\mathbf{M}^\alpha(\lambda)$ with eigenvector ξ, then the Krein signature of $e^{i\alpha}$ is

$$\text{sign}\left(-i\xi^* \mathcal{J}\xi\right),$$

where $*$ indicates complex conjugate transpose. More details about Krein signature are given in appendix A.

CHEN & HU later found a definition without using ω-limit sets in [40].

Definition 19 *Suppose $\lambda \notin \sigma_{ess}$. Let $\tilde{\mathcal{U}}(x,\lambda)$ be a lift of $\mathcal{U}(x,\lambda)$ in $\widetilde{\Lambda(n)}$. The Maslov index $I_{hom}(\phi,\lambda)$ is defined as:*

$$I_{hom}(\phi,\lambda) = m_{\mathcal{S}_\infty(\lambda)}(\lim_{x\to-\infty} \tilde{\mathcal{U}}(x,\lambda), \tilde{\mathcal{A}}) \text{ for } \tilde{\mathcal{A}} \in \omega(\tilde{\mathcal{U}}(\cdot,\lambda)) \quad \textit{(Bose and Jones)},$$

or equivalently as:

$$I_{hom}(\phi,\lambda) = \lim_{x_0\to+\infty} m_{\mathcal{S}(x_0,\lambda)}(\lim_{x\to-\infty} \tilde{\mathcal{U}}(x,\lambda), \tilde{\mathcal{U}}(x_0,\lambda)) \quad \textit{(Chen and Hu)}.$$

or:

$$\begin{aligned}I_{hom}(\phi,\lambda) = &\, m_{\mathcal{S}(x,\lambda)}(\tilde{\mathcal{S}}(x,\lambda), \tilde{\mathcal{U}}(x,\lambda)) \\ &- m_{\mathcal{S}_\infty(\lambda)}(\lim_{y\to-\infty} \tilde{\mathcal{U}}(y,\lambda), \lim_{y\to+\infty} \tilde{\mathcal{S}}(y,\lambda))\end{aligned} \quad \textit{(Chen and Hu modified)}.$$

Remark: This definition is dependent on the convention chosen for m.

Proof of well-definedness :

In the following paragraph, we prove that Chen-Hu's definition makes sense. Then we prove that Bose-Jones's definition is equivalent.

Let $\tilde{\mathcal{S}}(x,\lambda)$ be a lift of $\mathcal{S}(x,\lambda)$ in $\widetilde{\Lambda(n)}$.

We have $\mathcal{U}_\infty(\lambda) \cap S_\infty(\lambda) = \emptyset$. Therefore $\text{dist}(\mathcal{U}_\infty(\lambda), \Lambda(\mathcal{S}_\infty(\lambda))) > \varepsilon$.

For x_0 large enough, we have $\text{dist}(\mathcal{U}_\infty(\lambda), \Lambda(\mathcal{S}(x_0,\lambda))) > \frac{\varepsilon}{2}$.

Therefore, $m_{\mathcal{S}(x_0,\lambda)}(\lim_{x\to-\infty} \tilde{\mathcal{U}}(x,\lambda), \tilde{\mathcal{S}}(x_0,\lambda))$ is constant when x_0 is large enough.

Now, since $\mathcal{S}(x,\lambda)$ and $\mathcal{U}(x,\lambda)$ are the space of solutions of the same differential equation, $m_{\mathcal{S}(x,\lambda)}(\tilde{\mathcal{S}}(x,\lambda), \tilde{\mathcal{U}}(x,\lambda))$ is constant.

Therefore $\lim_{x_0\to+\infty} m_{\mathcal{S}(x_0,\lambda)}(\lim_{x\to-\infty} \tilde{\mathcal{U}}(x,\lambda), \tilde{\mathcal{U}}(x_0,\lambda))$ is well-defined since $m_{\mathcal{S}(x_0,\lambda)}(\lim_{x\to-\infty} \tilde{\mathcal{U}}(x,\lambda), \tilde{\mathcal{U}}(x_0,\lambda))$ is constant for x_0 large enough. This proves that Chen-Hu's definition makes sense.

Now, let us prove that Bose-Jones' definition is equivalent. Let us prove that:

$\forall \tilde{\mathcal{A}} \in \omega(\tilde{\mathcal{U}}(x,\lambda)) \quad m_{\mathcal{S}_\infty(\lambda)}(\lim_{x\to-\infty} \tilde{\mathcal{U}}(x,\lambda), \tilde{\mathcal{A}})$
$\qquad\qquad\qquad = \lim_{x_0\to+\infty} m_{\mathcal{S}(x_0,\lambda)}(\lim_{x\to-\infty} \tilde{\mathcal{U}}(x,\lambda), \tilde{\mathcal{U}}(x_0,\lambda)) = c$

Let $k = \dim(\mathcal{S}(x,\lambda) \cap \mathcal{U}(x,\lambda))$.

Let $\mathcal{W}(x)$ a Lagrangian plane such that:

- $\dim(\mathcal{W}(x) \cap \mathcal{U}(x,\lambda)) = n - k$

- $\mathcal{W}(x) \cap \mathcal{S}(\lambda,x) = \{0\}$

Then, $\lim_{x\to\infty} \mathcal{W}(x) = \mathcal{U}_\infty(\lambda)$.

Let $x_n \to \infty$ such that $\lim_{n\to\infty} \tilde{\mathcal{U}}(x_n,\lambda) = \tilde{\mathcal{A}}$.

Since $\dim W(x_n) \cap \mathcal{U}(x_n,\lambda) = n - k$, we have $\dim \mathcal{U}_\infty(\lambda) \cap \mathcal{A} \geq n - k$.

In the mean time $\dim \mathcal{S}_\infty(\lambda) \cap \mathcal{A} \geq k$ since $\dim(\mathcal{S}(x_n,\lambda) \cap \mathcal{U}(x,\lambda)) = k$.

Besides $\mathcal{U}_\infty(\lambda) \cap \mathcal{S}_\infty(\lambda) = \{0\}$ and $\dim(\mathcal{A}) = k + n - k$, therefore $\dim \mathcal{S}_\infty(\lambda) \cap \mathcal{A} = k$.

From proposition 11, we have:

$\lim_{n\to\infty} m_{\mathcal{S}(x_n,\lambda)}(\tilde{\mathcal{S}}(x_n,\lambda), \tilde{\mathcal{U}}(x_n,\lambda)) \quad = \lim_{x_0\to\infty} m_{\mathcal{S}(x_0,\lambda)}(\lim_{x\to-\infty} \tilde{\mathcal{U}}(x,\lambda), \tilde{\mathcal{U}}(x_0,\lambda))$
$\qquad\qquad\qquad\qquad\qquad\qquad = m_{\mathcal{S}_\infty(\lambda)}(\tilde{\mathcal{S}}_\infty(\lambda), \tilde{\mathcal{A}})$

$\square$

The following proposition is a nice characterization of definition 19, which is based on the s function and a suitable set of coordinates.

Proposition 12 *Suppose that the set of coordinates[8] is such that* $\mathrm{Range}(\begin{pmatrix} 0 \\ I \end{pmatrix}) = \mathcal{S}_\infty(\lambda)$ *and* $\mathrm{Range}(\begin{pmatrix} I \\ 0 \end{pmatrix}) = \mathcal{U}_\infty(\lambda)$.

Let $\kappa(x)$ *such that* $s(\mathcal{U}(x,\lambda)) = e^{i\kappa(x)}$. *Then:*

$$I_{hom}(\phi, \lambda) = \lim_{x \to \infty} \frac{\kappa(x) - \kappa(-x)}{2\pi}$$

Proof:

Let $(\kappa(x), \mathcal{U}(x,\lambda))$ be a lift of $\mathcal{U}(x,\lambda)$ in $\widetilde{\Lambda(n)}$.

Let $x_n \to \infty$. Then there exists $\phi : \mathbb{N} \to \mathbb{N}$ strictly increasing such that $(\kappa_{\phi(n)}, \mathcal{U}(x_{\phi(n)}, \lambda))$ converges to $(\beta, \mathcal{A})$, with $(\beta, \mathcal{A}) \in \widetilde{\Lambda(n)}$.

Now, $\dim(\mathcal{A}) \cap \dim(\mathcal{S}_\infty(\lambda)) = k$ and $\dim(\mathcal{A}) \cap \dim(\mathcal{U}_\infty(\lambda)) = n - k$. Therefore:

$K_{\mathcal{S}_{\infty(\lambda)}}(\mathcal{A}) = (1, \ldots, 1, -1, \ldots, -1)$

Therefore: $m_{\mathcal{S}_\infty(\lambda)}((0, \mathcal{S}_\infty(\lambda)), (\beta, \mathcal{A})) = \frac{\beta - (-(n-k)\pi)}{2\pi} - \frac{n}{2} + \frac{k}{2} = \frac{\beta}{2\pi}$

$K_{\mathcal{S}_{\infty(\lambda)}}(\mathcal{U}_\infty(\lambda))) = (-1, \ldots, -1, -1, \ldots, -1)$, therefore:

$m_{\mathcal{S}_\infty(\lambda)}((0, (\lim_{x \to -\infty} \kappa(x), \mathcal{U}_\infty(\lambda)))) = \frac{\lim_{x \to -\infty} \kappa(x) - (-n\pi)}{2\pi} - n\pi = \lim_{x \to -\infty} \kappa(x)$

As a consequence:

$\lim_{n \to \infty} \kappa_{x_{\phi(n)}} = I_{hom}(\phi, \lambda) + \lim_{x \to -\infty} \kappa(x)$

As a consequence, $\lim_{x \to \infty} \kappa(x)$ exists and:

$\lim_{x \to +\infty} \kappa(x) = 2\pi I_{hom}(\phi, \lambda) + \lim_{x \to -\infty} \kappa(x)$ $\square$

Using appendix C, it is easy to prove that $I_{hom}(\phi, b) - I_{hom}(\phi, a)$ counts the number of eigenvalues in the interval $[a, b]$ and the following proposition.

Proposition 13 *Assume that hypotheses 1,2,3 hold. Then:*

$$I_{per \to hom}(\phi) = I_{hom}(\phi, 0) + \frac{1}{2} \lim_{\alpha \to 0} \mathrm{sign}(h'(\alpha))$$

1.4 Conclusion

We constructed the Maslov index for solitary waves and showed that its definition is consistent with the limit Maslov index of periodic waves. Besides, from appendix C, we know that it counts eigenvalues as expected. It is now possible to apply the theory to partial differential equations (see appendix E for a simple example). However, to be able to do some numerical calculations, we will need to develop some numerical algorithms, which is done in the next chapter.

---

[8]Let U, V be two Lagrangian planes. There exists a symplectic change of coordinates such that $\mathrm{Range}(\begin{pmatrix} 0 \\ I \end{pmatrix}) = U$ and $\mathrm{Range}(\begin{pmatrix} I \\ 0 \end{pmatrix}) = V$

Chapter 2

Exterior algebra and computation on Lagrangian Grassmannians

Contents

Introduction

In the previous chapter, we have only used matrices to describe the Lagrangian manifold. This approach can sometimes be tedious. When integrating the equation $M' = AM$, all the columns of M can be attracted in the same direction. Hence, the other directions are lost unless orthogonalization (see [88, 25]) or high-precision arithmetic is used. To counterbalance this problem, exterior algebra has already been used to compute Lyapunov exponents and the Evans function (see ALLEN & BRIDGES [5, 4], BRIDGES, DERKS & GOTTWALD [21]).

Let E be a n-dimensional vector space and $(e_1, \ldots, e_n)$ be a basis of E.

The kth wedge product of E is denoted by $\bigwedge^k E$. The nonzero and distinct members of the set

$$\{e_{i_1} \wedge \ldots \wedge e_{i_k}, 1 \le i_1 < \ldots < i_k \le n\} \tag{2.0.1}$$

form a basis for the vector space $\bigwedge^k E$, with exactly $d = \frac{n!}{(n-k)!k!}$ distinct elements.

Choose an ordering such as a standard lexical ordering and label the nonzero distinct elements in the set (2.0.1) by $\mathbf{E}_1, \ldots, \mathbf{E}_d$. Then, any element $\mathbf{U} \in \bigwedge^k E$ can be represented as $\mathbf{U} = \sum_{j=1}^d U_j \, \mathbf{E}_j$.

In this basis, the wedge product of k elements of E can be written as:

$$\begin{cases} E^k \to \bigwedge^k E \\ (b_1, b_2, \ldots, b_k) = (\sum_{j=1}^n a_{1,j} e_j, \sum_{j=1}^n a_{2,j} e_j, \ldots, \sum_{j=1}^n a_{k,j} e_j) \\ \\ \mapsto b_1 \wedge b_2 \wedge \ldots \wedge b_k = \sum_{1 \le i_1 < \ldots < i_k \le n} \begin{vmatrix} a_{i_1,i_1} & a_{i_1,i_2} & \cdots & a_{i_1,i_k} \\ a_{i_2,i_1} & a_{i_2,i_2} & \cdots & a_{i_2,i_k} \\ \vdots & \vdots & \vdots & \vdots \\ a_{i_k,i_1} & a_{i_k,i_2} & \cdots & a_{i_k,i_k} \end{vmatrix} e_{i_1} \wedge \ldots \wedge e_{i_k} \end{cases}$$

The wedge product is not an onto mapping: $e_1 \wedge e_2 + e_3 \wedge e_4$ cannot be put into the form $a \wedge b$. k-linear forms which are equal to a wedge product $a_1 \wedge a_2 \wedge \ldots \wedge a_k$ of k vectors $a_1, \ldots, a_k$ are said to be purely decomposable.

Suppose that U is a k-dimensional subspace of E. Let $a_1, \ldots, a_k$ be a basis of U.

Then, we say that $\mathbf{U} = a_1 \wedge \ldots \wedge a_k$ represents the subspace U. This representation is unique up to a multiplicative constant, i.e. if $(b_1, b_2, \ldots b_k)$ is another basis of U, there exists a scalar such that $a_1 \wedge \ldots \wedge a_k = \alpha b_1 \wedge \ldots \wedge b_k$.

Stated differently, the following mapping is one-to-one (though not onto):

$$\begin{cases} G_k(E) \to \mathbb{P}(\bigwedge^k(E)) \\ \mathrm{Span}(b_1, \ldots, b_k) \mapsto \overline{b_1 \wedge \ldots \wedge b_n} \end{cases}$$

where $\mathbb{P}(\bigwedge^k(E))$ is the projectivization[1] of $\bigwedge^k E$.

In this chapter we first study the induced system on exterior algebra. We then give a characterization of the linear forms which represent Lagrangian planes and a way to compute the functions K, s sign$^\pm$ from the exterior algebra representation of Lagrangian planes.

Then, we give an algorithm for computing the Maslov index of periodic waves and solitary waves.

2.1   The multi-alternate product and induced system on $\bigwedge^k E$

Suppose that we want to find the k-dimensional subspace $V(t)$ of solutions of the following system:

$$x(0) \in V_0, \quad x' = B(t)x \tag{2.1.2}$$

---

[1]The projectivization of a vector space F is defined as the quotient of $F - \{0\}$ by the relation of equivalence $x \sim y \Leftrightarrow \exists \alpha \ne 0 \quad x = \alpha y$.

where V_0 is a k-dimensional subspace. Let $\Phi(t, u)$ be the flow associated to the system, e.g:

$$\Phi(u, u) = I, \quad \frac{\partial \Phi(t, u)}{\partial t} = B(t)\Phi(t, u)$$

If $a_1(t), a_2(t), \ldots a_k(t)$ is a basis of $V(t)$, then:

$$(a_1 \wedge a_2 \wedge \ldots \wedge a_k)' = \sum_{i=1}^{k} a_1 \wedge \ldots \wedge Ba_i \wedge \ldots \wedge a_k$$

$$(a_1 \wedge a_2 \wedge \ldots \wedge a_n)(t) = \Phi(t, u)a_1(u) \wedge \ldots \wedge \Phi(t, u)a_n(u)$$

The two previous equations can be interpreted as a *multi-alternate* product:

Definition 20 *Let $M_1, M_2, \ldots, M_k : F \rightarrow E$ be linear mappings.*

Then, the multi-alternate product $M_1 \odot M_2 \odot \ldots \odot M_k : \bigwedge^k F \rightarrow \bigwedge^k E$ of $M_1, M_2, \ldots, M_k$ is defined as the linear mapping such that:

$$M_1 \odot M_2 \odot \ldots \odot M_k(a_1 \wedge a_2 \wedge \ldots a_k)$$
$$= \frac{1}{k!} \sum_{\sigma \in \Sigma_k} M_{\sigma(1)}a_1 \wedge M_{\sigma(2)}a_2 \wedge \ldots \wedge M_{\sigma(k)}a_k$$

where Σ_k is the set of permutations of $\{1, \ldots, k\}$.

Definition 21 *Let $A : E \rightarrow E$ be a linear mapping.*

The mapping $A^{[k]}$ induced on $\bigwedge^k E$ by A is defined as:

$$A^{[k]} = A \odot A \odot \ldots \odot A$$

The compound mapping is defined as:

$$A^{(k)} = k(A \odot Id \ldots \odot Id)$$

In terms of multi-alternate product, we can rewrite the previous systems as:

$$(a_1 \wedge a_2 \wedge \ldots \wedge a_k)'(t) = B^{(k)}(t)(a_1 \wedge \ldots \wedge a_k)(t)$$

$$(a_1 \wedge a_2 \wedge \ldots \wedge a_n)(t) = \Phi^{[k]}(t, u)(a_1 \wedge \ldots \wedge a_n)(u)$$

Now, let us give the elements and eigenvalues of $A^{(k)}$ and $A^{[k]}$ as a function of elements and eigenvalues of A.

In the standard basis $\{e_{i_1} \wedge \ldots \wedge e_{i_k}, 1 \le i_1 < \ldots < i_k \le n\}$, the matrices[2] of these two mappings are:

$$(A^{[k]})_{\substack{1 \le i_1 < \ldots < i_k \le n, \\ 1 \le j_1 < \ldots < j_k \le n}} = \begin{vmatrix} a_{i_1,j_1} & a_{i_1,j_2} & \ldots & a_{i_1,j_k} \\ a_{i_2,j_1} & a_{i_2,j_2} & \ldots & a_{i_2,j_k} \\ \vdots & \vdots & \vdots & \vdots \\ a_{i_k,j_1} & a_{i_k,j_2} & \ldots & a_{i_k,j_k} \end{vmatrix} \qquad (2.1.3)$$

$$(A^{(k)})_{\substack{1 \le i_1 < \ldots < i_k \le n, \\ 1 \le j_1 < \ldots < j_k \le n}} = \begin{cases} 0 & \text{if } \#(\{i_1,\ldots,i_k\} \cup \{j_1,\ldots,j_k\}) > n+1 \\ (-1)^{r+s} a_{i_r,j_s} & \text{if } \{i_r,j_s\} = \{i_1,\ldots,i_k\}\Delta\{j_1,\ldots,j_k\} \\ \sum_{r=1}^{k} a_{i_r,i_r} & \text{if } \{i_1,\ldots,i_k\} = \{j_1,\ldots,j_k\} \end{cases} \qquad (2.1.4)$$

where Δ is defined as $V\Delta W = (V \cup W) - (V \cap W)$.

From (2.1.3) and (2.1.4), we deduce that (see [115]):

Proposition 14 *Let $A \in M_n(\mathbb{C})$ be a matrix.*

Let $P \in GL_n(\mathbb{C})$ such that $P^{-1}AP$ is an upper triangular matrix.

Let $\alpha_1, \ldots, \alpha_n$ be the diagonal elements of $P^{-1}AP$.

Then $(P^{[r]})^{-1}A^{(r)}P^{[r]} = (P^{-1}AP)^{(r)}$ and $(P^{[r]})^{-1}A^{[r]}P^{[r]} = (P^{-1}AP)^{[r]}$ are upper triangular matrices whose diagonal elements are respectively $(\sum_{k=1}^{r} \alpha_{i_k})_{1 \le i_1 < \ldots < i_r \le n}$ and $(\prod_{k=1}^{r} \alpha_{i_k})_{1 \le i_1 < \ldots < i_r \le n}$

2.2 Computing the Maslov index of paths on $\bigwedge^n(\mathbb{R}^{2n})$

In this section, we first make some comments on which n-forms are representative of Lagrangian space. Then we show how we can compute s, K from the exterior algebra representation.

2.2.1 The Lagrangian manifold $\Lambda(n)$ as a submanifold of $\mathbb{P}(\bigwedge^n(\mathbb{R}^{2n}))$

Case $n = 2$

Take $\mathbb{R}^4$ with its standard basis and symplectic and volume forms

$$\omega = \mathbf{e}_1^* \wedge \mathbf{e}_3^* + \mathbf{e}_2^* \wedge \mathbf{e}_4^*, \quad \bar{\omega} = \mathbf{e}_1 \wedge \mathbf{e}_3 + \mathbf{e}_2 \wedge \mathbf{e}_4, \quad \text{and} \quad \mathsf{vol} = \tfrac{1}{2}\omega \wedge \omega. \qquad (2.2.5)$$

The vector space $\bigwedge^2(\mathbb{R}^4)$ is six-dimensional, and the orthonormal basis induced from the basis of $\mathbb{R}^4$ is

$$\begin{aligned} \mathbf{E}_1 &= \mathbf{e}_1 \wedge \mathbf{e}_2, & \mathbf{E}_2 &= \mathbf{e}_1 \wedge \mathbf{e}_3, & \mathbf{E}_3 &= \mathbf{e}_1 \wedge \mathbf{e}_4, \\ \mathbf{E}_4 &= \mathbf{e}_2 \wedge \mathbf{e}_3, & \mathbf{E}_5 &= \mathbf{e}_2 \wedge \mathbf{e}_4, & \mathbf{E}_6 &= \mathbf{e}_3 \wedge \mathbf{e}_4. \end{aligned} \qquad (2.2.6)$$

---

[2]The matrix of the general multi-alternate product is $(M_1 \odot \ldots \odot M_k)_{\substack{1 \le i_1 < \ldots < i_k \le n, \\ 1 \le j_1 < \ldots < j_k \le n}} =$

$\frac{1}{k!}\sum_{\sigma \in \Sigma_n} \begin{vmatrix} (M_{\sigma(1)})_{i_1,j_1} & (M_{\sigma(1)})_{i_1,j_2} & \ldots & (M_{\sigma(1)})_{i_1,j_k} \\ (M_{\sigma(2)})_{i_2,j_1} & (M_{\sigma(2)})_{i_2,j_2} & \ldots & (M_{\sigma(2)})_{i_2,j_k} \\ \vdots & \vdots & \vdots & \vdots \\ (M_{\sigma(k)})_{i_k,j_1} & (M_{\sigma(k)})_{i_k,j_2} & \ldots & (M_{\sigma(k)})_{i_k,j_k} \end{vmatrix}.$

Any $\mathbf{U} \in \bigwedge^2(\mathbb{R}^4)$ can be represented in the form

$$\mathbf{U} = \sum_{j=1}^{6} U_j\, \mathbf{E}_j\,. \tag{2.2.7}$$

$\mathbf{U}$ represents an element of the Grassmannian $G_2(\mathbb{R}^4)$ if and only if:

$$0 = \mathbf{U} \wedge \mathbf{U} = I_1\, \mathsf{vol}\,, \quad I_1 := U_1 U_6 - U_2 U_5 + U_3 U_4\,. \tag{2.2.8}$$

In that case, the space represented by $\mathbf{U}$ is Lagrangian if and only if

$$0 = \bar{\omega} \wedge \mathbf{U} = I_2\, \mathsf{vol}\,, \quad I_2 := U_2 + U_5\,. \tag{2.2.9}$$

The Lagrangian-Grassmannian $\Lambda(2)$ is isomorphic to the three dimensional submanifold of $\mathbb{P}\left(\bigwedge^2(\mathbb{R}^4)\right)$ defined by $I_1 = I_2 = 0$.

Let $\mathbf{V} \in \bigwedge^2(\mathbb{R}^4)$ be a fixed Lagrangian plane. Then

$$\Lambda^1(2) = \{\ \mathbf{U} \in \bigwedge{}^2(\mathbb{R}^4) \cap \Lambda(2)\ :\ \mathbf{U} \wedge \mathbf{V} = 0\ \}\,,$$

is a codimension one submanifold of $\Lambda^2(2)$ [6]. We have a sequence of manifolds:

Manifold	$\bigwedge^2(\mathbb{R}^4)$	$\mathbb{P}\left(\bigwedge^2(\mathbb{R}^4)\right)$	$G_2(\mathbb{R}^4)$	$\Lambda(2)$	$\Lambda^1(2)$
Dimension	6	5	4	3	2

General case

In the general case, the decomposability of one k-form is more difficult to establish. However, we have:

Proposition 15 *Let* $\mathbf{U}$ *be a k-linear form and* $\rho_{\mathbf{U}}\ :\ \begin{cases} E \to \bigwedge^{k+1} E \\ x \to x \wedge \mathbf{U} \end{cases}$ *. Then* $\mathbf{U}$ *is purely-decomposable if and only if* $k \leq \dim(\ker \rho_{\mathbf{U}})$.

In that case, there are $u_1, \ldots, u_k$ *such that:*

$$\ker(\rho_{\mathbf{U}}) = \operatorname{span}(u_1, \ldots, u_k), \quad \mathbf{U} = u_1 \wedge \ldots \wedge u_k$$

If we look for an algebraic condition on the coordinates of $\mathbf{U}$, one may use the minors of the mapping $\rho_{\mathbf{U}}$ since:

$$\dim(\ker \rho_{\mathbf{U}}) \geq k \quad \Leftrightarrow \quad \dim(\operatorname{Range}(\rho_{\mathbf{U}})) \leq \dim(E) - k \quad \Leftrightarrow \quad (\rho_{\mathbf{U}})^{[\dim(E)-k+1]} = 0.$$

Now, consider $\mathbb{R}^{2n}$ with its standard basis and symplectic and volume forms

$$\bar{\omega} = \sum_{i=1}^{n} \mathbf{e}_i^* \wedge \mathbf{e}_{i+n}^*, \quad \bar{\omega} = \sum_{i=1}^{n} \mathbf{e}_i \wedge \mathbf{e}_{i+n} \quad \text{and} \quad \mathsf{vol} = \frac{1}{n!}\, \bar{\omega} \wedge \ldots \wedge \bar{\omega}\,. \tag{2.2.10}$$

Proposition 16 *Assume that* $\mathbf{U}$ *is a purely decomposable n-form. Then the space* $\ker \rho_{\mathbf{U}}$ *(e.g the space represented by* $\mathbf{U}$*) is Lagrangian if and only if:*

$$\bar{\omega} \wedge \mathbf{U} = 0 \qquad\qquad (2.2.11)$$

To prove this proposition, we will need the following lemma:

Lemma 1 *Let* U *be a n-dimensional subspace of* $\mathbb{R}^{2n}$. *There exists a basis* $(g_1, \ldots, g_n, f_1, \ldots, f_n)$ *of* $\mathbb{R}^{2n}$ *and* $k \in \{1, \ldots, \lfloor \frac{n}{2} \rfloor\}$ *such that:*

- $\bar{\omega} = \sum_{i=1}^{k}(g_i \wedge g_{i+k} + f_i \wedge f_{i+k}) + \sum_{i=2k}^{n} g_i \wedge f_i$,

- $\mathrm{span}(g_1, \ldots, g_n) = U$.

Proof: Let $U^{\perp} = \{u | \forall v \in U \ \ \omega(u,v) = 0\}$.

Let $k = \frac{n - \dim(U^{\perp} \cap U)}{2}$.

Let W such that $(U \cap U^{\perp}) \oplus W = U$.

$\omega_{|W \times W}$ has full rank. Therefore, there exists a basis $(g_1, \ldots, g_{2k})$ of W such that $\omega(g_i, g_{j+k}) = \delta_{ij}$ for $i, j \in \{1, \ldots, 2k\}$.

Let W' such that $U \cap U^{\perp} \oplus W' = U^{\perp}$.

$\omega_{|W' \times W'}$ has full rank. Therefore, there exists a basis $(f_1, \ldots, f_{2k})$ of W' such that $\omega(f_i, f_{j+k}) = \delta_{ij}$ for $i, j \in \{1, \ldots, 2k\}$.

Let $g_{2k+1}, \ldots, g_n$ be a basis of $U^{\perp} \cap U$ and $W'' \subset (W \oplus W')^{\perp}$ such that $W'' \oplus (U + U^{\perp}) = \mathbb{R}^{2n}$.

Let $\phi : \begin{cases} W'' \to (U \cap U^{\perp})^* \\ x \to (y \to \omega(x,y)) \end{cases}$. ϕ is a bijective mapping (Otherwise, we would have $\dim(U^{\perp} \cap U) + \dim((U^{\perp} \cap U)^{\perp}) \neq 2n$).

Let $(r_{2k+1}, \ldots, r_n)$ be the dual basis of $(g_{2k+1}, \ldots, g_n)$ in $U^{\perp} \cap U$. Now set $f_i = \phi^{-1}(r_i)$ for $2k + 1 \leq i \leq n$. $(f_{2k+1}, \ldots, f_n)$ is a basis of W''.

Then $(g_1, \ldots, g_n, f_1, \ldots, f_n)$ is a basis of $\mathbb{R}^{2n} = W \oplus (U \cap U^{\perp}) \oplus W' \oplus W''$ and we have:

- $\mathrm{span}(g_1, \ldots, g_n) = U$

- $\omega(g_i, g_{j+k}) = \delta_{ij}$ for $i, j \in \{1, \ldots, k\}$,

- $\omega(g_i, g_j) = 0$ if $j \in \{2k+1, \ldots, n\}$,

- $\omega(g_i, f_j) = 0$ if $i \in \{1, \ldots, 2k\}$,

- $\omega(g_i, f_j) = \delta_{ij}$ for $i, j \in \{2k+1, \ldots, n\}$,

- $\omega(f_i, f_{j+k}) = \delta_{ij}$ for $i, j \in \{1, \ldots, k\}$,

- $\omega(f_i, f_j) = 0$ if $j \in \{n - 2k + 1, \ldots, n\}$.

Otherwise stated, the matrix of ω in this basis is:

	$g_1 \cdots g_k$	$g_{k+1} \cdots g_{2k}$	$g_{2k+1} \cdots g_n$	$f_1 \cdots f_k$	$f_{k+1} \cdots f_{2k}$	$f_{2k+1} \cdots f_n$
g_1 ⋮ g_k	0	I	0	0	0	0
g_{k+1} ⋮ g_{2k}	$-I$	0	0	0	0	0
g_{2k+1} ⋮ g_n	0	0	0	0	0	I
f_1 ⋮ f_k	0	0	0	0	I	0
f_{k+1} ⋮ f_{2k}	0	0	0	$-I$	0	0
f_{2k+1} ⋮ f_n	0	0	$-I$	0	0	0

We have therefore $\bar{\omega} = \sum_{i=1}^{k}(g_i \wedge g_{i+k} + f_i \wedge f_{i+k}) + \sum_{i=2k}^{n} g_i \wedge f_i$. $\square$

Proof of proposition 16:

There exists a basis $(g_1, \ldots, g_n, f_1, \ldots, f_n)$ of $\mathbb{R}^{2n}$ and $k \in \{1, \ldots, \lfloor \frac{n}{2} \rfloor\}$ such that:

- $\bar{\omega} = \sum_{i=1}^{k}(g_i \wedge g_{i+k} + f_i \wedge f_{i+k}) + \sum_{i=2k}^{n} g_i \wedge f_i$,

- $\text{span}(g_1, \ldots, g_n) = \ker \rho_{\mathbf{U}}$

There exists α such that $\mathbf{U} = \alpha g_1 \wedge \ldots \wedge g_n$.

$$\bar{\omega} \wedge \mathbf{U} \quad = \alpha \left(\sum_{i=1}^{k}(g_i \wedge g_{i+k} + f_i \wedge f_{i+k}) + \sum_{i=2k+1}^{n} g_i \wedge f_i \right) \wedge g_1 \wedge \ldots \wedge g_n$$
$$= \alpha \sum_{i=1}^{k} f_i \wedge f_{i+k} \wedge g_1 \wedge \ldots \wedge g_n$$

Therefore $\bar{\omega} \wedge \mathbf{U} = 0$ if and only if $k = 0$, e.g. $\omega_{|U \times U} = 0$. $\square$

Even in the case $n = 3$, there is still much to understand. For example, we do not have useful representations of $G_3(\mathbb{R}^6)$ or $\Lambda(3)$ on $\bigwedge^3(\mathbb{R}^6)$. These would be useful for proving that $\Lambda(3)$ is an invariant manifold, and for understanding the numerical properties of the induced ODE (2.4.31) on $\Lambda(3)$. Some results about $\bigwedge^3(\mathbb{R}^6)$ and $\Lambda(3)$ can be found in Chapter 8 of the book [84]. Nevertheless, we can still compute the Maslov index in this case.

2.2.2   Computing s on $\bigwedge^n(\mathbb{R}^{2n})$

While the Maslov index is invariant with respect to a symplectic change of coordinates, this is not the case of s whose definition depends on the euclidean structure of $\mathbb{R}^{2n}$.

For this reason, we first introduce the induced inner product. Then we give a general formula for s in $\bigwedge^n(\mathbb{R}^{2n})$.

The induced inner product on $\bigwedge^k(\mathbb{R}^{2n})$

The inner product $\langle \cdot, \cdot \rangle$ on $\mathbb{R}^{2n}$ induces an inner product on each vector space $\bigwedge^k(\mathbb{R}^{2n})$ as follows. Let

$$\mathbf{U} = \mathbf{u}_1 \wedge \cdots \wedge \mathbf{u}_k \quad \text{and} \quad \mathbf{V} = \mathbf{v}_1 \wedge \cdots \wedge \mathbf{v}_k \,, \quad \mathbf{u}_i, \mathbf{v}_j \in \mathbb{R}^{2n} \,, \quad \forall \, i, j = 1, \ldots, k \,,$$

be any decomposable k-forms. A $k-$form is decomposable if it can be written as a pure form: a wedge product between k linearly independent vectors in $\mathbb{R}^{2n}$. The inner product of $\mathbf{U}$ and $\mathbf{V}$ is defined by

$$[\![\mathbf{U}, \mathbf{V}]\!]_k := \det \begin{bmatrix} \langle \mathbf{u}_1, \mathbf{v}_1 \rangle & \cdots & \langle \mathbf{u}_1, \mathbf{v}_k \rangle \\ \vdots & \ddots & \vdots \\ \langle \mathbf{u}_k, \mathbf{v}_1 \rangle & \cdots & \langle \mathbf{u}_k, \mathbf{v}_k \rangle \end{bmatrix} \,, \quad \mathbf{U}, \mathbf{V} \in \bigwedge^k(\mathbb{R}^{2n}) \,. \tag{2.2.12}$$

Since every element in $\bigwedge^k(\mathbb{R}^{2n})$ is a sum of decomposable elements, this definition extends by (multi)-linearity to any k-form. Using the orthonormality of the induced basis

$$[\![\mathbf{E}_i, \mathbf{E}_j]\!]_k = \begin{cases} 1 & \text{if } i = j \\ 0 & \text{if } i \neq j \end{cases} \,,$$

the inner product between two elements $\mathbf{U} = \sum_{i=1}^d U_i \mathbf{E}_i$ and $\mathbf{V} = \sum_{j=1}^d V_j \mathbf{E}_j$ is

$$\begin{aligned} [\![\mathbf{U}, \mathbf{V}]\!]_k &= \left[\!\!\left[\sum_{i=1}^d U_i \mathbf{E}_i, \sum_{k=1}^d V_j \mathbf{E}_j \right]\!\!\right]_k = \sum_{i=1}^d \sum_{j=1}^d U_i V_j [\![\mathbf{E}_i, \mathbf{E}_j]\!]_k \\ &= \sum_{i=1}^d U_i V_i := \langle \mathbf{U}, \mathbf{V} \rangle_d \,, \end{aligned}$$

yielding the equivalent representation

$$[\![\mathbf{U}, \mathbf{V}]\!]_k = \langle \mathbf{U}, \mathbf{V} \rangle_d \,, \quad \mathbf{U}, \mathbf{V} \in \bigwedge^k(\mathbb{R}^{2n}) \,. \tag{2.2.13}$$

Maslov angle – general formula on $\bigwedge^n(\mathbb{R}^{2n})$

In $\mathbb{R}^2$, the Maslov angle is just the angle associated with the polar representation of a vector in $\mathbb{R}^2$ as shown in §E.0.1. In higher dimension there is still a well-defined angle associated with any Lagrangian plane [93]. Consider the Lagrangian plane which is the range of a $2n \times n$ matrix $\mathbf{Z}$:

$$\mathbf{Z} = \begin{pmatrix} \mathbf{X} \\ \mathbf{Y} \end{pmatrix} = [\, \mathbf{z}_1 \mid \cdots \mid \mathbf{z}_n \,] \,, \quad \text{with} \quad \langle \mathcal{J} \mathbf{z}_i, \mathbf{z}_j \rangle = 0 \,, \quad \text{for} \quad i, j = 1, \ldots, n \,.$$

The exterior algebra representation of the Lagrangian plane is then just obtained by the mapping

$$(\mathbf{z}_1, \ldots, \mathbf{z}_n) \mapsto \mathbf{z}_1 \wedge \cdots \wedge \mathbf{z}_n \in \bigwedge^n(\mathbb{R}^{2n}) \,.$$

Denote the exterior algebra representation by

$$\mathbf{U} = \mathbf{z}_1 \wedge \cdots \wedge \mathbf{z}_n \,.$$

Proposition 17 *There exists a constant* $n-$*form* $\mathbf{C}$,

$$\mathbf{C} = \mathbf{C}_1 + \mathrm{i}\mathbf{C}_2 \,, \quad \textit{with} \quad \mathbf{C}_1, \mathbf{C}_2 \in \textstyle\bigwedge^n(\mathbb{R}^{2n}) \,,$$

such that

$$\det[\mathbf{X} - \mathrm{i}\mathbf{Y}]\mathsf{vol} = \mathbf{C} \wedge \mathbf{U} \,.$$

It follows from this proposition that there exists a scalar complex-valued function G such that $\mathbf{C} \wedge \mathbf{U} = G(\mathbf{U})\mathsf{vol}$. A formula for the Maslov angle is then immediate.

Proposition 18
$$\mathrm{e}^{\mathrm{i}\kappa} = G/\overline{G} \,.$$

It remains to prove Proposition 17. The proof is by explicit construction. Let

$$\mathbf{c}_j = \mathbf{e}_j - \mathrm{i}\mathcal{J}\mathbf{e}_j \,, \quad j = 1, \ldots, n \,.$$

Then

$$\mathbf{X} - \mathrm{i}\mathbf{Y} = \begin{pmatrix} \mathbf{I} \\ -\mathrm{i}\mathbf{I} \end{pmatrix}^T \begin{pmatrix} \mathbf{X} \\ \mathbf{Y} \end{pmatrix} = [\mathbf{c}_1 \mid \cdots \mid \mathbf{c}_n]^T [\mathbf{z}_1 \mid \cdots \mid \mathbf{z}_n] = \begin{pmatrix} \langle \mathbf{c}_1, \mathbf{z}_1 \rangle & \cdots & \langle \mathbf{c}_1, \mathbf{z}_n \rangle \\ \vdots & \ddots & \vdots \\ \langle \mathbf{c}_n, \mathbf{z}_1 \rangle & \cdots & \langle \mathbf{c}_n, \mathbf{z}_n \rangle \end{pmatrix} \,, \quad (2.2.14)$$

and so, using the induced inner product[3] on $\bigwedge^n(\mathbb{R}^{2n})$ (see section 2.2.2)

$$\det[\mathbf{X} - \mathrm{i}\mathbf{Y}]\mathsf{vol} = \det \begin{bmatrix} \langle \mathbf{c}_1, \mathbf{z}_1 \rangle & \cdots & \langle \mathbf{c}_1, \mathbf{z}_n \rangle \\ \vdots & \ddots & \vdots \\ \langle \mathbf{c}_n, \mathbf{z}_1 \rangle & \cdots & \langle \mathbf{c}_n, \mathbf{z}_n \rangle \end{bmatrix} \mathsf{vol} = [\![\mathbf{c}_1 \wedge \cdots \wedge \mathbf{c}_n, \mathbf{U}]\!]_n \mathsf{vol} \,.$$

This gives a formula for G,
$$G(\mathbf{U}) = [\![\mathbf{c}_1 \wedge \cdots \wedge \mathbf{c}_n, \mathbf{U}]\!]_n \,.$$

It is not necessary to give an expression for $\mathbf{C}$ since in the computations it is G that is needed. However, for completeness it is given. Let $\mathbf{C}$ be an $n-$form satisfying

$$\mathbf{c}_1 \wedge \cdots \wedge \mathbf{c}_n \wedge \overline{\mathbf{C}} = [\![\mathbf{c}_1 \wedge \cdots \wedge \mathbf{c}_n, \overline{\mathbf{c}_1 \wedge \cdots \wedge \mathbf{c}_n}]\!]_n \, \mathsf{vol} \,. \quad (2.2.15)$$

Then

$$G(\mathbf{U})\mathsf{vol} = \det[\mathbf{X} - \mathrm{i}\mathbf{Y}]\mathsf{vol} = \mathbf{C} \wedge \mathbf{U} \,.$$

The $n-$form $\mathbf{C}$ is in fact the Hodge star of $\mathbf{c}_1 \wedge \cdots \wedge \mathbf{c}_n$ although the details of that characterization are not needed.

---

[3]A real inner product is used throughout the paper. Complexification is used so rarely that a Hermitian inner product is not necessary. One just needs to keep track of the complex conjugations.

In standard coordinates, this can also be written as:

$$G(\mathbf{U}) = \det(\mathbf{X} - i\mathbf{Y}) = \sum_{\substack{(\{i_1\ldots i_n\},r) \\ i_1 < \ldots < i_n \\ \{i_1,\ldots,i_r,i_{r+1}-n,\ldots,i_n-n\}=\{1,\ldots,n\}}} i^{n-r}(-1)^{\sum_{j=1}^{r} i_j - j}\mathbf{U}_{i_1,\ldots,i_n}\,.$$

$$(2.2.16)$$

$$s(\text{Range}(\mathbf{Z})) = G(\mathbf{U})\overline{G(\mathbf{U})}^{-1} = \det(\mathbf{X} - i\mathbf{Y})^{-1}\overline{\det(\mathbf{X} - i\mathbf{Y})}.$$

The Maslov angle on $\bigwedge^2(\mathbb{R}^4)$

On $\mathbb{R}^4$ with the standard basis,

$$\begin{aligned}
\mathbf{c}_1 \wedge \mathbf{c}_2 &= (\mathbf{e}_1 - i\mathcal{J}\mathbf{e}_1) \wedge (\mathbf{e}_2 - i\mathcal{J}\mathbf{e}_2) \\
&= (\mathbf{e}_1 - i\mathbf{e}_3) \wedge (\mathbf{e}_2 - i\mathbf{e}_4) \\
&= \mathbf{e}_1 \wedge \mathbf{e}_2 - i\mathbf{e}_1 \wedge \mathbf{e}_4 + i\mathbf{e}_2 \wedge \mathbf{e}_3 - \mathbf{e}_3 \wedge \mathbf{e}_4\,.
\end{aligned}$$

Therefore, if $\mathbf{U} = \sum_{j=1}^{6} U_j\mathbf{E}_j$, with $\mathbf{E}_1,\ldots,\mathbf{E}_6$ the standard basis on $\bigwedge^2(\mathbb{R}^4)$, the expression for $G(\mathbf{U})$ and the Maslov angle are:

$$G(\mathbf{U}) = [\![\mathbf{c}_1 \wedge \mathbf{c}_2, \mathbf{U}]\!]_2 = U_1 - iU_3 + iU_4 - U_6\,,$$

$$e^{i\kappa} = \frac{U_1 - U_6 - iU_3 + iU_4}{U_1 - U_6 + iU_3 - iU_4}\,.$$

$$(2.2.17)$$

This expression is equivalent to the formula derived in equation (22) of [16].

A straightforward calculation shows that

$$\mathbf{C} = -\mathbf{e}_1 \wedge \mathbf{e}_2 + \mathbf{e}_3 \wedge \mathbf{e}_4 + i(\mathbf{e}_1 \wedge \mathbf{e}_4 - \mathbf{e}_2 \wedge \mathbf{e}_3)\,.$$

The Maslov angle on $\bigwedge^3(\mathbb{R}^6)$

On $\mathbb{R}^6$ with the standard basis

$$\begin{aligned}
\mathbf{c}_1 \wedge \mathbf{c}_2 \wedge \mathbf{c}_3 &= (\mathbf{e}_1 - i\mathcal{J}\mathbf{e}_1) \wedge (\mathbf{e}_2 - i\mathcal{J}\mathbf{e}_2) \wedge (\mathbf{e}_3 - i\mathcal{J}\mathbf{e}_3) \\
&= (\mathbf{e}_1 - i\mathbf{e}_4) \wedge (\mathbf{e}_2 - i\mathbf{e}_5) \wedge (\mathbf{e}_3 - i\mathbf{e}_6)\,,
\end{aligned}$$

or

$$\begin{aligned}
\mathbf{c}_1 \wedge \mathbf{c}_2 \wedge \mathbf{c}_3 = {}& \mathbf{e}_1 \wedge \mathbf{e}_2 \wedge \mathbf{e}_3 - \mathbf{e}_1 \wedge \mathbf{e}_5 \wedge \mathbf{e}_6 + \mathbf{e}_2 \wedge \mathbf{e}_4 \wedge \mathbf{e}_6 - \mathbf{e}_3 \wedge \mathbf{e}_4 \wedge \mathbf{e}_5 \\
& -i\mathbf{e}_1 \wedge \mathbf{e}_2 \wedge \mathbf{e}_6 + i\mathbf{e}_1 \wedge \mathbf{e}_3 \wedge \mathbf{e}_5 - i\mathbf{e}_2 \wedge \mathbf{e}_3 \wedge \mathbf{e}_4 + i\mathbf{e}_4 \wedge \mathbf{e}_5 \wedge \mathbf{e}_6\,.
\end{aligned}$$

Now take a standard lexical ordering for the $20-$dimensional basis

$$\bigwedge^3(\mathbb{R}^6) = \text{span}\{\mathbf{e}_1 \wedge \mathbf{e}_2 \wedge \mathbf{e}_3, \mathbf{e}_1 \wedge \mathbf{e}_2 \wedge \mathbf{e}_4,\ldots,\mathbf{e}_3 \wedge \mathbf{e}_5 \wedge \mathbf{e}_6, \mathbf{e}_4 \wedge \mathbf{e}_5 \wedge \mathbf{e}_6\}\,, \qquad (2.2.18)$$

and express an arbitrary element $\mathbf{U} \in \bigwedge^3(\mathbb{R}^6)$ in the form $\mathbf{U} = \sum_{i,j,k} P_{ijk}\mathbf{e}_i \wedge \mathbf{e}_j \wedge \mathbf{e}_k$. Then

$$\begin{aligned}
G &= [\![\mathbf{c}_1 \wedge \mathbf{c}_2 \wedge \mathbf{c}_3, \mathbf{U}]\!]_3 \\
&= P_{123} - P_{156} + P_{246} - P_{345} - iP_{126} + iP_{135} - iP_{234} + iP_{456}\,,
\end{aligned}$$

and so the expression for the Maslov angle is

$$\mathrm{e}^{i\kappa} = \frac{P_{123} - P_{156} + P_{246} - P_{345} - \mathrm{i}P_{126} + \mathrm{i}P_{135} - \mathrm{i}P_{234} + \mathrm{i}P_{456}}{P_{123} - P_{156} + P_{246} - P_{345} + \mathrm{i}P_{126} - \mathrm{i}P_{135} + \mathrm{i}P_{234} - \mathrm{i}P_{456}}. \tag{2.2.19}$$

In this case the definition (2.2.15) gives

$$
\begin{aligned}
\mathbf{C} \;=\;& \mathbf{e}_4 \wedge \mathbf{e}_5 \wedge \mathbf{e}_6 - \mathbf{e}_2 \wedge \mathbf{e}_3 \wedge \mathbf{e}_4 + \mathbf{e}_1 \wedge \mathbf{e}_3 \wedge \mathbf{e}_5 - \mathbf{e}_1 \wedge \mathbf{e}_2 \wedge \mathbf{e}_6 \\
&+\mathrm{i}(\mathbf{e}_3 \wedge \mathbf{e}_4 \wedge \mathbf{e}_5 - \mathbf{e}_2 \wedge \mathbf{e}_4 \wedge \mathbf{e}_6 + \mathbf{e}_1 \wedge \mathbf{e}_5 \wedge \mathbf{e}_6 - \mathbf{e}_1 \wedge \mathbf{e}_2 \wedge \mathbf{e}_3)\,.
\end{aligned}
$$

2.2.3 K function over $\bigwedge^n(\mathbb{R}^{2n})$

Let $\mathbf{Z} = \begin{pmatrix} \mathbf{X} \\ \mathbf{Y} \end{pmatrix} \in X_n$ be a Lagrangian frame on $\mathbb{R}^{2n}$. Then the matrix

$$\psi(\mathbf{Z}, \begin{pmatrix} I \\ 0 \end{pmatrix}) = \mathbf{Q} = (\mathbf{X} - \mathrm{i}\mathbf{Y})(\mathbf{X} + \mathrm{i}\mathbf{Y})^{-1}\,,$$

is a unitary and symmetric (but not Hermitian) matrix.

Let $\mathrm{e}^{i\kappa_j}$, $j = 1, \ldots, n$ with κ_j real, the n eigenvalues of $\mathbf{Q}$. These eigenvalues are the elements of $K_E(\mathbf{Z})$ (where $E = \mathrm{Range}(\begin{pmatrix} I \\ 0 \end{pmatrix})$))

Then:

$$s(\mathrm{Range}(\mathbf{Z})) = \mathrm{e}^{i\kappa_1}\,\mathrm{e}^{i\kappa_2}\ldots\mathrm{e}^{i\kappa_n}\,.$$

These angles can be computed in the exterior algebra framework: $e^{i\kappa_r}$ are the roots of the following polynomial:

$P(\lambda) = \det((\mathbf{X} - \mathrm{i}\mathbf{Y}) - \lambda(\mathbf{X} + \mathrm{i}\mathbf{Y}))$

The coefficients of P are antisymmetric n-linear functions of $\mathbf{Z}$. As a consequence, they can be expressed as a linear combination of the minors of $\mathbf{Z}$.

Thus, the angles associated to a Lagrangian space can be computed from any representation in $\Lambda^n(\mathbb{R}^{2n})$.

The case $n = 2$ is treated with much detail below.

Eigenvalues of the unitary matrix Q on $\bigwedge^2(\mathbb{R}^4)$

Let $\mathbf{Z} = \begin{pmatrix} \mathbf{X} \\ \mathbf{Y} \end{pmatrix} \in X_2$ be a Lagrangian frame on $\mathbb{R}^4$. Let $\mathbf{Q}$ be the matrix:

$$\mathbf{Q} = \psi(\mathbf{Z}, \begin{pmatrix} I \\ 0 \end{pmatrix}) = (\mathbf{X} - \mathrm{i}\mathbf{Y})(\mathbf{X} + \mathrm{i}\mathbf{Y})^{-1}\,,$$

In this section, we give an expression for the eigenvalues $\mathrm{e}^{i\kappa_j}$ $(j = 1, 2$ with κ_j real) of $\mathbf{Q}$.

Let $\mathbf{c}_1$ and $\mathbf{c}_2$ be as defined in §2.2.2. Then, as shown there,

$$\det[\mathbf{X} - \mathrm{i}\mathbf{Y}] = G(\mathbf{U}) := [\![\mathbf{c}_1 \wedge \mathbf{c}_2, \mathbf{U}]\!]_2 = U_1 - \mathrm{i}U_3 + \mathrm{i}U_4 - U_6\,,$$

for $\bigwedge^2(\mathbb{R}^4) \ni \mathbf{U} = \sum_{j=1}^6 U_j \mathbf{E}_j$. Hence

$$\det(\mathbf{Q}) = G/\overline{G}. \tag{2.2.20}$$

In this paragraph the following formula for $\text{Trace}(\mathbf{Q})$ is proved,

$$\text{Trace}(\mathbf{Q}) = \frac{2}{G}(U_1 + U_6). \tag{2.2.21}$$

Use (2.2.14) to relate the columns of $\mathbf{Z}$ to the $\mathbf{X} - \mathbf{Y}$ decomposition

$$\mathbf{X} + \mathrm{i}\mathbf{Y} = \begin{bmatrix} \langle \overline{\mathbf{c}_1}, \mathbf{z}_1 \rangle & \langle \overline{\mathbf{c}_1}, \mathbf{z}_2 \rangle \\ \langle \overline{\mathbf{c}_2}, \mathbf{z}_1 \rangle & \langle \overline{\mathbf{c}_2}, \mathbf{z}_2 \rangle \end{bmatrix}.$$

Hence

$$\mathbf{Q} = \frac{1}{\overline{G}} \begin{pmatrix} \langle \mathbf{c}_1, \mathbf{z}_1 \rangle & \langle \mathbf{c}_1, \mathbf{z}_2 \rangle \\ \langle \mathbf{c}_2, \mathbf{z}_1 \rangle & \langle \mathbf{c}_2, \mathbf{z}_2 \rangle \end{pmatrix} \begin{bmatrix} \langle \overline{\mathbf{c}_2}, \mathbf{z}_2 \rangle & -\langle \overline{\mathbf{c}_1}, \mathbf{z}_2 \rangle \\ -\langle \overline{\mathbf{c}_2}, \mathbf{z}_1 \rangle & \langle \overline{\mathbf{c}_1}, \mathbf{z}_1 \rangle \end{bmatrix},$$

and so

$$
\begin{aligned}
\text{Trace}(\mathbf{Q}) &= \tfrac{1}{\overline{G}} \left(\langle \mathbf{c}_1, \mathbf{z}_1 \rangle \langle \overline{\mathbf{c}_2}, \mathbf{z}_2 \rangle - \langle \mathbf{c}_1, \mathbf{z}_2 \rangle \langle \overline{\mathbf{c}_2}, \mathbf{z}_1 \rangle - \langle \mathbf{c}_2, \mathbf{z}_1 \rangle \langle \overline{\mathbf{c}_1}, \mathbf{z}_2 \rangle + \langle \mathbf{c}_2, \mathbf{z}_2 \rangle \langle \overline{\mathbf{c}_1}, \mathbf{z}_1 \rangle \right), \\
&= \tfrac{1}{\overline{G}} \left(\det \begin{bmatrix} \langle \mathbf{c}_1, \mathbf{z}_1 \rangle & \langle \mathbf{c}_1, \mathbf{z}_2 \rangle \\ \langle \overline{\mathbf{c}_2}, \mathbf{z}_1 \rangle & \langle \overline{\mathbf{c}_2}, \mathbf{z}_2 \rangle \end{bmatrix} + \det \begin{bmatrix} \langle \overline{\mathbf{c}_1}, \mathbf{z}_1 \rangle & \langle \overline{\mathbf{c}_1}, \mathbf{z}_2 \rangle \\ \langle \overline{\mathbf{c}_2}, \mathbf{z}_1 \rangle & \langle \overline{\mathbf{c}_2}, \mathbf{z}_2 \rangle \end{bmatrix} \right), \\
&= \tfrac{1}{\overline{G}} \left([\![\mathbf{c}_1 \wedge \overline{\mathbf{c}_2}, \mathbf{z}_1 \wedge \mathbf{z}_2]\!]_2 + [\![\overline{\mathbf{c}_1} \wedge \mathbf{c}_2, \mathbf{z}_1 \wedge \mathbf{z}_2]\!]_2 \right) \\
&= \tfrac{1}{\overline{G}} \left([\![\mathbf{c}_1 \wedge \overline{\mathbf{c}_2} + \overline{\mathbf{c}_1} \wedge \mathbf{c}_2, \mathbf{z}_1 \wedge \mathbf{z}_2]\!]_2 \right) \\
&= \tfrac{2}{\overline{G}} \left([\![\mathbf{e}_1 \wedge \mathbf{e}_2 + \mathbf{e}_3 \wedge \mathbf{e}_4, \mathbf{z}_1 \wedge \mathbf{z}_2]\!]_2 \right) \\
&= \tfrac{2}{\overline{G}} (U_1 + U_6),
\end{aligned}
$$

using

$$\text{Re}\,(\mathbf{c}_1 \wedge \overline{\mathbf{c}_2}) = \text{Re}\,((\mathbf{e}_1 - \mathrm{i}\mathbf{e}_3) \wedge (\mathbf{e}_2 + \mathrm{i}\mathbf{e}_4)) = \mathbf{e}_1 \wedge \mathbf{e}_2 + \mathbf{e}_3 \wedge \mathbf{e}_4,$$

proving (2.2.21).

Given a path $\mathbf{U} \in \bigwedge^2(\mathbb{R}^4)$ the eigenvalues of $\mathbf{Q}$ can be computed using (2.2.20) and (2.2.21),

$$\det(\mu\mathbf{I} - \mathbf{Q}) = \mu^2 - \text{Trace}(\mathbf{Q})\mu + \det(\mathbf{Q}),$$

where μ has unit modulus,

$$\mu_{1,2} := \mathrm{e}^{\mathrm{i}\kappa_{1,2}} = \frac{U_1 + U_6 \pm \sqrt{4U_1 U_6 + 2U_3 U_4 - U_3^2 - U_4^2}}{U_1 + \mathrm{i}U_3 - \mathrm{i}U_4 - U_6}.$$

Using the fact $U_2 + U_5 = 0$ and $U_1 U_6 - U_2 U_5 + U_3 U_4 = 0$, we can obtain

$$\mu_{1,2} := \mathrm{e}^{\mathrm{i}\kappa_{1,2}} = \frac{U_1 + U_6 \pm \mathrm{i}\sqrt{4U_5^2 + (U_3 + U_4)^2}}{U_1 + \mathrm{i}U_3 - \mathrm{i}U_4 - U_6}.$$

2.3 Computing the Maslov index for periodic orbits

In this section, we consider problem (1.2.8).

We provide an algorithm to compute:

- $I_{per}(\lambda, \phi)$ when λ is not in the spectrum,

- $I_{per}(\phi)$ when ϕ is an hyperbolic periodic orbit.

To obtain the unstable space, one generally computes Floquet multipliers and their associated eigenvectors. Here, we proceed differently, by integrating a random space over several periods to obtain the unstable space. As we shall see, this method is equivalent to a power method.

Computing $I_{per}(\phi, \lambda)$ on $\bigwedge^n(\mathbb{R}^{2n})$ when $\lambda \notin \sigma$

Assume that $\lambda \notin \sigma$.

There is an induced Floquet theory on the exterior algebra space. For a hyperbolic linear system (1.2.8) there are n Floquet multipliers with modulus greater than one, and n with modulus less than one.

If $\mu_1, \ldots, \mu_n$ are any n Floquet multipliers and $\zeta_1, \ldots, \zeta_n$ the corresponding eigenvectors of $\mathbf{M}(\lambda)$, then clearly:

$$\mathbf{M}^{[n]}(\lambda)(\zeta_1 \wedge \cdots \wedge \zeta_n) = \sigma\,(\zeta_1 \wedge \cdots \wedge \zeta_n)\,, \quad \text{with} \quad \sigma = \prod_{j=1}^n \mu_j\,.$$

Since the system is hyperbolic, there is a unique simple Floquet multiplier of largest modulus of $\mathbf{M}^{[n]}$ obtained by taking $\{\zeta_1, \ldots, \zeta_n\}$ to be a basis for the unstable subspace. Denote this Floquet multiplier by σ_+. It is always simple and real, even if some of the Floquet multipliers are complex.

Consider the induced system

$$\mathbf{U}_x = \mathbf{B}^{(n)}(x, \lambda)\mathbf{U}\,, \quad \mathbf{U}(0) = \zeta_1 \wedge \cdots \wedge \zeta_n\,,$$

with $\{\zeta_1, \ldots, \zeta_n\}$ a basis for the unstable subspace. Then

$$\mathbf{U}(L) = \sigma_+\,(\zeta_1 \wedge \cdots \wedge \zeta_n)\,;$$

that is, $\mathbf{U}(0)$ and $\mathbf{U}(L)$ are colinear. Hence, $\mathbf{U}(x + L) = \mathbf{U}(x)$ on $\mathbb{P}(\bigwedge^n(\mathbb{R}^{2n}))$. In practice, the numerical integration is performed on $\bigwedge^n(\mathbb{R}^{2n})$ and the formula for the Maslov angle automatically factors out the length.

In practice the unstable subspace, $\text{span}\{\zeta_1, \ldots, \zeta_n\}$, need not be computed explicitly. When the induced system on $\bigwedge^n(\mathbb{R}^{2n})$ is integrated in space, any randomly-chosen initial condition will be attracted to the most unstable direction. Hence, the Floquet multipliers or their eigenvectors do not need to be computed explicitly. It is sufficient to know that the linear system is hyperbolic. This strategy is equivalent to the *power method* for computing the eigenvalue of largest modulus of a matrix [74].

The rate of convergence of this version of the power method depends on the distance between the largest (in modulus) Floquet multiplier of $\mathbf{M}^{[n]}$ and the next largest Floquet multiplier.

Explicitly, let $\mu_1, \mu_2, \ldots, \mu_n$ be the unstable Floquet multipliers with multiplicities sorted so that $1 < |\mu_1| \leq |\mu_2| \leq \ldots \leq |\mu_n|$. Then the stable Floquet multipliers are $\frac{1}{\mu_1}, \ldots, \frac{1}{\mu_n}$. With these conditions, the two eigenvalues of largest modulus of $\mathbf{M}^{[n]}(\lambda)$ are $\mu_1 \mu_2 \cdots \mu_n$ and $\mu_1^{-1} \mu_2 \cdots \mu_n$. The ratio of the second largest to the largest (in modulus) is

$$\frac{\mu_1^{-1} \mu_2 \cdots \mu_n}{\mu_1 \mu_2 \cdots \mu_n} = \frac{1}{\mu_1^2},$$

and by construction this ratio has modulus strictly less than one. However the size of the ratio depends on the distance between μ_1 and the unit circle.

The Floquet multiplier of largest modulus $\mu_1 \mu_2 \ldots \mu_n$ is a simple and therefore real eigenvalue. Denote the right eigenvector by $\boldsymbol{\xi} \in \bigwedge^n(\mathbb{R}^{2n})$ and let $\boldsymbol{\eta}$ represent the left eigenvector, normalized so that $\langle \boldsymbol{\eta}, \boldsymbol{\xi} \rangle = 1$.

The solution of the initial-value problem for the induced system

$$\mathbf{U}_x = \mathbf{B}^{(n)}(x, \lambda) \mathbf{U}, \quad \mathbf{U} \in \bigwedge^n(\mathbb{R}^{2n}),$$

with a random initial condition $\mathbf{U}(x_0) = \mathbf{U}_0$ is of the form

$$\mathbf{U}(x) = \boldsymbol{\Phi}^{(n)}(x, 0, \lambda) \mathbf{U}_0.$$

But $\boldsymbol{\Phi}(L, t_0) = \mathbf{M}^{[n]}$ and so

$$\mathbf{U}(kL) = \left(\mathbf{M}^{[n]} \right)^k \mathbf{U}_0, \quad k = 0, 1, \ldots.$$

The effect of $\left(\mathbf{M}^{[n]} \right)^k$ on the randomly chosen initial condition can be computed by the power method.

Let $\mathbf{U}_0 := \boldsymbol{\zeta}_0$ be any randomly chosen vector such that $\langle \boldsymbol{\eta}, \boldsymbol{\zeta}_0 \rangle \neq 0$. Generically, almost every starting vector will satisfy this condition. Define the sequence $\{\boldsymbol{\zeta}_k\}$ by $\boldsymbol{\zeta}_{k+1} = \mathbf{M}^{[n]} \boldsymbol{\zeta}_k$. Then, from results on the power method, it follows that there exists a constant $C > 0$, for any $\varepsilon > 0$, such that

$$\left\| \frac{1}{\langle \boldsymbol{\eta}, \boldsymbol{\zeta}_k \rangle} \boldsymbol{\zeta}_k - \boldsymbol{\xi} \right\| \leq C(|\mu_1|^2 - \varepsilon)^{-k}, \quad k = 0, 1, 2, \ldots.$$

This result shows that the power method produces $\log_{10}(|\mu_1|^2 - \varepsilon)$ correct digits at each iteration. When $|\mu_1|$ is close to one, $\log_{10}(|\mu_1|^2 - \varepsilon) \sim \frac{2}{\log_e 10}(|\mu_1| - 1)$. The parameter ε can be set to 0 if the eigenvalue $\mu_1^{-1} \mu_2 \cdots \mu_n$ is semi-simple. This result ensures that a random initial condition will be globally attracted to the unstable subspace, when the linear system is hyperbolic. It also demonstrates the failure of convergence in the case where the periodic orbit is not hyperbolic, e.g. when $|\mu_1| = 1$.

If we now sum up the algorithm, we get:

- Choose a random n-form $\mathbf{U}_0 \in \bigwedge^n(\mathbb{R}^{2n})$.

- Integrate equation $\mathbf{U}_x = \mathbf{B}^{(n)}(x, \lambda) \mathbf{U}, \quad \mathbf{U}(0) = \mathbf{U}_0$ until:

  - Either $\boldsymbol{\zeta}_k = \mathbf{U}(kL)$ is nearly colinear to $\boldsymbol{\zeta}_{k+1} = \mathbf{U}((k+1)L)$, e.g. there exists α s.t. $\|\boldsymbol{\zeta}_k - \alpha \boldsymbol{\zeta}_{k+1}\| \leq \varepsilon \|\boldsymbol{\zeta}_k\|$ where ε is a small number.

– Or a maximal number of iterations is reached. In this case, the system is considered as non-hyperbolic and $I_{per}(\phi, \lambda)$ is not defined.

- Compute $e^{i\kappa(x)} = s(\mathcal{U}(x, \lambda)) = G(\mathbf{U}(x))$ using equation (2.2.16) over the interval $[kL, (k+1)L]$, assuming that $U(x)$ is representation of $\mathcal{U}(x, \lambda)$ over $[kL, (k+1)L]$

- Compute $\kappa(x)$ over $[kL, (k+1)L]$ such that $e^{i\kappa(x)} = s(\mathcal{U}(x, \lambda))$ and $|\kappa(x + \Delta x) - \kappa(x)| < \pi$, where Δx denotes the step-size.

- Return the Maslov index: $I_{per}(\phi, \lambda) = \frac{\kappa((k+1)L) - \kappa(kL)}{2\pi}$.

This algorithm was implemented with Matlab$^{\text{TM}}$. The code is given in Appendix I.3 in the case of the Kawahara equation.

Computing $I_{per}(\phi)$ when $\dim(\mathcal{U}(x, 0)) = n - 1$.

When ϕ is a $L-$periodic solution of an autonomous Hamiltonian system (e.g. equation (1.2.7)), the linearization of the Hamiltonian system about this periodic orbit can be cast into the standard form (1.2.8) where $\mathbf{C}(x, 0)$ is the Hessian of H evaluated at $\phi(x)$.

At $\lambda = 0$, the system will have two Floquet multipliers at $+1$ since $\phi_x(L) = \boldsymbol{M}(0)\phi_x(0) = \phi_x(0)$ and the orbit ϕ is supposed to be hyperbolic.

If we assume $\dim(\mathcal{U}(x, 0)) = n - 1$, then there are $n - 1$ Floquet multipliers with modulus strictly greater than one. Therefore, there are exactly two Floquet multipliers on the unit circle. $E_1(\mathbf{M}(0))$ is two-dimensional and contains the vector $\phi_x(0)$.

If we ignore the fact that the linearized system is not hyperbolic and apply the same algorithm as in the previous section, there are two cases:

- $\mathbf{M}(0)\big|_{E_1(\mathbf{M}(0))}$ is the identity and then taking a random starting point will not lead to convergence to a form representing $\mathcal{U}(x, 0) \oplus \phi_x(x)$ in general.

- $\mathbf{M}(0)\big|_{E_1(\mathbf{M}(0))}$ is not the identity and then it will generally converge to $\mathcal{U}(x, 0) \oplus \phi_x(x)$ with the difference between $\mathcal{U}(x, 0) \oplus \phi_x(x)$ and the kth approximation behaving like $\frac{1}{1+k}$.

Hence, if there is convergence, it is very slow. Instead of using an n-dimensional random Lagrangian space for initial data, we can take advantage of the fact that we generally know what ϕ_x is and:

- choose a n-dimensional Lagrangian space which already contains the ϕ_x vector.

- choose an $(n - 1)$-dimensional subspace.

These two approaches have the same rate of convergence, namely $C\frac{1}{(|\mu_2| - \varepsilon)^r}$ at the rth iteration. For the first one, the setup is nearly identical to what has been done in the previous sections: we just pick ϕ_x and $n - 1$ other random vectors $\boldsymbol{\xi}_1, \ldots, \boldsymbol{\xi}_{n-1}$ and compute $\phi_x(0) \wedge \boldsymbol{\xi}_1 \wedge \cdots \wedge \boldsymbol{\xi}_{n-1}$ for initial data.

For the second approach, we integrate until we get $\mathcal{U}(x, 0)$. Knowing $\phi_x(x)$, it is then possible to compute $s(\mathcal{U}(x, 0) \oplus \phi_x(x))$. Moreover, the dimension of the space to integrate is smaller.

Another approach is to add an external parameter that perturbs the $+1$ Floquet multipliers off the unit circle. In the application to stability of waves in §3.7.1 and §3.7.1 the spectral parameter λ plays precisely this role (see Figures 3.19 and 3.23).

2.4   Computing the Maslov index in the homoclinic case.

In this section, we assume that hypothesis 1 of chapter 1 holds.

We first give the definition of the *Evans* function which is an analytic function of the spectral parameter λ whose zeros with multiplicities are the eigenvalues of the spectral problem with multiplicity.

Then we give an algorithm to compute $I_{hom}(x, \lambda)$ when $\lambda \notin \sigma$. This formulation enables to give a condition for the Maslov index to tend to 0 when $|\lambda| \to 0$.

Finally we discuss how to compute $I_{hom}(x, \lambda)$ when $\lambda \in \sigma_p$.

2.4.1   The Evans function of the self-adjoint system

In order to compare the number of eigenvalues of (1.3.13) with the Maslov index, we will use the Evans function to determine eigenvalues using the setup in ALEXANDER, GARDNER & JONES [1], adapted to the symplectic setting in BRIDGES & DERKS [23].

Consider the linear system of ODEs,

$$\mathbf{u}_x = \mathbf{B}(x, \lambda)\mathbf{u}, \quad \mathbf{u} \in \mathbb{R}^{2n}, \tag{2.4.22}$$

where $\mathbf{B}(x, \lambda) = \mathcal{J}^{-1}\mathbf{C}(x, \lambda)$ and $\mathbf{C}(x, \lambda)$ is symmetric and depends smoothly on x and λ. In general λ can be complex but here it will be restricted to be real. Assume that $\mathbf{B}(x, \lambda)$ tends exponentially fast to a matrix $\mathbf{B}_\infty(\lambda)$ when $x \to \pm\infty$.

We will assume throughout that σ_{ess} is real and $\lambda \notin \sigma_{ess}$.

Let $\bigwedge^n(\mathbb{R}^{2n})$ be the vector space of $n-$vectors in $\mathbb{R}^{2n}$. There is an induced system from (2.4.22)

$$\mathbf{U}_x = \mathbf{B}^{(n)}(x, \lambda)\mathbf{U}, \quad \mathbf{U} \in \bigwedge^n(\mathbb{R}^{2n}). \tag{2.4.23}$$

Let $u_1(x, \lambda), u_2(x, \lambda), \dots, u_n(x, \lambda)$ and $s_1(x, \lambda), s_2(x, \lambda), \dots, s_n(x, \lambda)$ such that:

$$\mathcal{U}(x, \lambda) = \text{span}(u_1(x, \lambda), \dots, u_n(x, \lambda))$$
$$\mathcal{S}(x, \lambda) = \text{span}(s_1(x, \lambda), \dots \wedge s_n(x, \lambda))$$

Now, define:

$$\mathbf{U}(x, \lambda) = u_1(x, \lambda) \wedge \dots \wedge u_n(x, \lambda),$$
$$\mathbf{S}(x, \lambda) = s_1(x, \lambda) \wedge \dots \wedge s_n(x, \lambda).$$

Let $\sigma_+(\lambda)$ be the sum of the eigenvalues of $\mathbf{B}_\infty(\lambda)$ with positive real part, and let $\sigma_-(\lambda)$ be the sum of the eigenvalues with negative real part. $\sigma_+(\lambda)$ (resp. $\sigma_-(\lambda)$) is also the eigenvalue of $\mathbf{B}_\infty^{(n)}(\lambda)$ with greatest (resp. smallest) real part of $\mathbf{B}_\infty(\lambda)$.

Then $\mathbf{U}(x, \lambda)$ and $\mathbf{S}(x, \lambda)$ are solutions of (2.4.23) with maximal decay as x goes to $-\infty$ and $+\infty$ respectively satisfying

$$\lim_{x \to -\infty} e^{-\sigma_+(\lambda)x} \mathbf{U}(x, \lambda) = \zeta^+(\lambda) \in \bigwedge^n(\mathbb{R}^{2n}), \tag{2.4.24}$$

and

$$\lim_{x \to +\infty} e^{-\sigma_-(\lambda)x} \mathbf{S}(x, \lambda) = \zeta^-(\lambda) \in \bigwedge^n(\mathbb{R}^{2n}), \tag{2.4.25}$$

where $\zeta^\pm(\lambda)$ are eigenvectors

$$\mathbf{B}_\infty^{(n)}(\lambda)\zeta^\pm(\lambda) = \sigma_\pm(\lambda)\zeta^\pm(\lambda)\,. \tag{2.4.26}$$

A value $\lambda \in \mathbb{R}\setminus\sigma_{ess}$ is called an eigenvalue if the stable $\mathcal{S}(x,\lambda)$ and unstable solutions $\mathcal{U}(x,\lambda)$ have nontrivial intersection. Eigenvalues are detected by the *Evans function* [1] which is defined by

$$D(\lambda)\,\mathsf{vol} = \mathbf{S}(x,\lambda) \wedge \mathbf{U}(x,\lambda) \in \bigwedge\nolimits^{2n}(\mathbb{R}^{2n})\,. \tag{2.4.27}$$

To obtain a unequivocally defined function, a normalisation condition is needed. Here, since the systems at $-\infty$ and at $+\infty$ are the same, we have $\zeta^+(\lambda)\wedge\zeta^-(\lambda) \neq 0$. A convenient normalization that we will use from now on is:

$$\zeta^+(\lambda) \wedge \zeta^-(\lambda) = \mathsf{vol} \tag{2.4.28}$$

The Evans function is independent of x and is an analytic function of λ [1]. Analyticity assures that the zeros of $D(\lambda)$ are isolated. In the definition (2.4.27) the fact that $\text{trace}(\mathbf{B}(x,\lambda)) = 0$ has been used.

Furthermore, the Evans function is invariant under exponential scaling of the following form:

$$\begin{aligned}
\widehat{\mathbf{U}}(x,\lambda) &= e^{-\sigma_+(\lambda)x}\mathbf{U}(x,\lambda)\,, \\
\widehat{\mathbf{S}}(x,\lambda) &= e^{-\sigma_-(\lambda)x}\mathbf{S}(x,\lambda)\,.
\end{aligned}$$

Then the scaled functions satisfy

$$\begin{aligned}
\widehat{\mathbf{U}}_x &= [\mathbf{B}^{(n)}(x,\lambda) - \sigma_+(\lambda)\mathbf{I}]\widehat{\mathbf{U}}\,, \\
\widehat{\mathbf{S}}_x &= [\mathbf{B}^{(n)}(x,\lambda) - \sigma_-(\lambda)\mathbf{I}]\widehat{\mathbf{S}}\,,
\end{aligned}$$

but the Evans function becomes

$$D(\lambda)\,\mathsf{vol} = e^{(\sigma_-(\lambda)+\sigma_+(\lambda))x}\widehat{\mathbf{S}}(x,\lambda) \wedge \widehat{\mathbf{U}}(x,\lambda) = \widehat{\mathbf{S}}(x,\lambda) \wedge \widehat{\mathbf{U}}(x,\lambda)\,,$$

since $\sigma_-(\lambda) + \sigma_+(\lambda) = \text{Trace}(\mathbf{B}_\infty(\lambda)) = 0$.

Proposition 19 *Let $\lambda \notin \sigma$ and assume that (2.4.28) holds, then:*

$$\text{sign}(D(\lambda)) = (-1)^{I_{hom}(\phi,\lambda)}$$

Proof:

Let $\lambda \notin \sigma$.

Let κ be such that $e^{i\frac{\kappa(x)}{2}} = \frac{G(\mathbf{U})}{|G(\mathbf{U})|}$. Then $(\kappa(x),\mathcal{U}(x,\lambda))$ is a lift of $\mathcal{U}(x,\lambda)$.

We have $\lim_{x\to+\infty} G(\widehat{\mathbf{U}}(x,\lambda)) = D(\lambda)\lim_{x\to-\infty} G(\widehat{\mathbf{U}}(x,\lambda))$.

Therefore $e^{i\frac{\lim_{x\to+\infty}\kappa(x)}{2}} = \text{sign}(D(\lambda))e^{i\frac{\lim_{x\to-\infty}\kappa(x)}{2}}$.

Therefore $(-1)^{I_{hom}(\lambda,\phi)} = e^{i\pi\frac{\lim_{x\to+\infty}\kappa(x)-\lim_{x\to+\infty}\kappa(x)}{2\pi}} = \text{sign}(D(\lambda))$.

$\square$

2.4.2   Computation of $I_{hom}(\phi, \lambda)$ when $\lambda \notin \sigma$.

Fix λ and a basic periodic solution, which is an approximation to a solitary wave. The steps in the algorithm are as follows.

1. Choose a large enough interval $[-L, L]$.

2. Compute the eigenvalue with largest real part of $\mathbf{B}_\infty^{(n)}(\lambda)$, denoted by $\sigma_+(\lambda)$, and its associated eigenvector $\zeta^+(\lambda)$.

3. Integrate equation
$$\widehat{\mathbf{U}} = [\mathbf{B}^{(n)}(x, \lambda) - \sigma_+(\lambda)\mathbf{I}]\widehat{\mathbf{U}}, \tag{2.4.29}$$
on $[-L, L]$, taking $\zeta^+(\lambda)$ as initial condition at $x = -L$, using any standard numerical integration scheme. The justification for the arbitrariness in choice of numerical scheme is given below in this section.

4. $\widehat{\mathbf{U}}(L, \lambda)$ and $\widehat{\mathbf{U}}(-L, \lambda)$ are nearly colinear, and an approximation to the Evans function is determined from their ratio $\frac{\widehat{\mathbf{U}}(L,\lambda)}{\widehat{\mathbf{U}}(-L,\lambda)}$. (The error is smaller than machine precision.)

5. Compute $\mathrm{e}^{\mathrm{i}\kappa(x)} = s(\mathcal{U}(x, \lambda)) = G(\widehat{\mathbf{U}}(x, \lambda))\overline{G(\widehat{\mathbf{U}}(x, \lambda))}^{-1}$ using equation (2.2.16) or an analogous representation.

6. Compute a lift of $\kappa(x)$ and assume that $|\kappa(x + \Delta x) - \kappa(x)| < \pi$ where Δx is the step-size.

7. Return the Maslov index $I_{hom}(\phi, \lambda) = \frac{\kappa(L) - \kappa(-L)}{2\pi}$.

There are several sources of error in the algorithm. Two parameters have to be chosen: L and the step size Δx. The choice of the step size is a familiar source of error. The consistency error of the numerical integration scheme will be of the form $C\,\Delta x^p$, for some natural number p, at each step, where C is a constant depending on the derivatives of $\mathbf{B}$. The choice of the numerical scheme will also impose some stability condition.

By choosing a finite value of L there will be some error introduced in the initial condition at $x = -L$. Choosing ζ^+ as an approximation of $\mathbf{U}(-L, \lambda)$ will induce a relative error of

$$2Z \int_{-\infty}^{L/2} \|\mathbf{B}^{(n)}(x, \lambda) - \mathbf{B}_\infty^{(n)}(\lambda)\|\mathrm{d}x,$$

where

$$Z = \sup_{x \in \mathbb{R}^+} \|\mathrm{e}^{x(\mathbf{B}_\infty^{(n)} - \sigma_+ \mathbf{I})}\|.$$

An initial perturbation will be multiplied by at most:

$$Z\,\mathrm{e}^{Z \int_{\mathbb{R}} \|\mathbf{B}^{(n)}(x,\lambda) - \mathbf{B}_\infty(\lambda)\|\mathrm{d}x}.$$

Since the Maslov index is an integer, the proposed scheme will give the Maslov index if the relative error on $\mathbf{U}(\cdot, \lambda)$ is small enough. However, if $\sup_{\mathbb{R}} \|\widehat{\mathbf{U}}(\cdot, \lambda)\|$ is very small (for example when the Evans function is small), the relative error may be too big and lead to a miscomputed Maslov index. This is the case when λ is an eigenvalue or near an eigenvalue.

Attractivity of the Lagrangian Grassmannian $\Lambda(2)$

One of the advantages of subtracting off the growth rate at infinity in the equations on $\bigwedge^2(\mathbb{R}^4)$, as in (2.4.31), is that the Lagrangian Grassmannian becomes an attracting invariant manifold. When $\Lambda(2)$ is attractive, one has greater freedom in choosing the numerical integration scheme.

To prove attractivity, consider the integration of the $2-$form representing the unstable subspace $\mathbf{U}(x, \lambda)$

$$\frac{d}{dx}\mathbf{U} = \mathbf{B}^{(2)}(x, \lambda)\mathbf{U} \quad \mathbf{U} \in \bigwedge^2(\mathbb{R}^4) \quad -L < x < +L\,.$$

Introduce the transformation

$$\mathbf{U}(x, \lambda) = \mathrm{e}^{\sigma_+(\lambda)x}\,\widehat{\mathbf{U}}(x, \lambda)$$

where $\sigma_+(\lambda)$ is the sum of the eigenvalues of $\mathbf{B}_\infty(\lambda)$ with positive real part. Then $\widehat{\mathbf{U}}$ satisfies

$$\frac{d}{dx}\widehat{\mathbf{U}} = [\mathbf{B}^{(2)}(x, \lambda) - \sigma_+(\lambda)\mathbf{I}]\widehat{\mathbf{U}} \qquad -L < x < +L \tag{2.4.30}$$

The Lagrangian Grassmannian is the set

$$\widehat{\mathbf{U}} \wedge \widehat{\mathbf{U}} = 0 \quad \text{and} \quad \omega \wedge \widehat{\mathbf{U}} = 0\,.$$

When evaluated on the differential equation (2.4.30) these invariants satisfy

$$\begin{aligned}
\frac{d}{dx}\widehat{\mathbf{U}} \wedge \widehat{\mathbf{U}} &= \frac{d}{dx}\widehat{\mathbf{U}} \wedge \widehat{\mathbf{U}} + \widehat{\mathbf{U}} \wedge \frac{d}{dx}\widehat{\mathbf{U}} \\
&= \mathbf{B}^{(2)}\widehat{\mathbf{U}} \wedge \widehat{\mathbf{U}} + \widehat{\mathbf{U}} \wedge \mathbf{B}^{(2)}\widehat{\mathbf{U}} - 2\sigma_+\,\widehat{\mathbf{U}} \wedge \widehat{\mathbf{U}} \\
&= \mathrm{Trace}(\mathbf{B})\,\widehat{\mathbf{U}} \wedge \widehat{\mathbf{U}} - 2\sigma_+\,\widehat{\mathbf{U}} \wedge \widehat{\mathbf{U}} \\
&= -2\sigma_+\,\widehat{\mathbf{U}} \wedge \widehat{\mathbf{U}}\,,
\end{aligned}$$

since $\mathrm{Trace}(\mathbf{B}) = 0$. A similar calculation with $\omega \wedge \widehat{\mathbf{U}}$ yields

$$\frac{d}{dx}\omega \wedge \widehat{\mathbf{U}} = \omega \wedge (\mathbf{B}^{(2)} - \sigma_+\mathbf{I})\mathbf{U} = -\mathbf{B}^{(2)}\omega \wedge \mathbf{U} - \sigma_+\,\omega \wedge \widehat{\mathbf{U}} = -\sigma_+\,\omega \wedge \widehat{\mathbf{U}}\,,$$

using the fact that $\mathbf{B}^{(2)}\omega = 0$, which is proved in Appendix D. This proves that

$$\widehat{\mathbf{U}} \wedge \widehat{\mathbf{U}}(x) = \mathrm{e}^{-2\sigma_+x}\widehat{\mathbf{U}} \wedge \widehat{\mathbf{U}}\bigg|_{x=-L} \quad \text{and} \quad \omega \wedge \widehat{\mathbf{U}}(x) = \mathrm{e}^{-\sigma_+x}\omega \wedge \widehat{\mathbf{U}}\bigg|_{x=-L}\,, \quad \text{for} \quad x > -L\,.$$

The eigenvalue σ_+ is real and positive. Hence when integrating the unstable subspace $\mathbf{U}$ along the Lagrangian Grassmannian, both $\widehat{\mathbf{U}} \wedge \widehat{\mathbf{U}}$ and $\omega \wedge \widehat{\mathbf{U}}(x)$ are exponentially attracted to the zero set. Therefore a special integrator is not required for maintaining the constraints; a standard Runge-Kutta algorithm is quite satisfactory.

This proof holds only in the case $n = 2$. The difficulty with proving it in higher dimensions is that we do not have a nice characterization of the Lagrangian Grassmannian. However, numerical results for the case $n = 3$ show similar stabilizing behaviour in the integration.

The Maslov index when λ is large

When $\lambda \to +\infty$ (or $\lambda \to -\infty$ if the essential spectrum extends to minus infinity) we expect the Maslov index to stabilize. This property is similar to the property of the Evans function for large λ. The hypotheses are based on the analogous result of [103], adapted to the setting of the Maslov index.

Hypothesis 4　　• *Suppose there exists $\lambda_0 \in \mathbb{R}$ such that σ_{ess} is empty for all $\lambda > \lambda_0$*

- *For large enough λ, $\mathbf{B}_\infty(\lambda)$ has no pure imaginary eigenvalue.*

- *Let $\mathbf{V}(\lambda)$ be a symplectic $2n \times 2n$ matrix depending analytically on λ whose first n columns are a basis for $\mathrm{E}^u(\mathbf{B}(x, \lambda))$ and whose last n columns are a basis for $\mathrm{E}^s(\mathbf{B}(x, \lambda))$ Define*

$$\mathbf{F}(x, \lambda) = \mathbf{V}^{-1}(\lambda)(\mathbf{B}(x, \lambda) - \mathbf{B}_\infty(\lambda))\mathbf{V}(\lambda).$$

- *Suppose that, for large enough λ:*

$$\int_{\mathbb{R}} |\mathbf{F}(x, \lambda)| \mathrm{d}x \quad \text{is bounded, uniformly in } \lambda$$
$$\int_{|x| > x_0} |\mathbf{F}(x, \lambda)| \mathrm{d}x \quad \text{tends to 0 when } x_0 \to \infty, \text{ uniformly in } \lambda$$
$$\int_{\mathbb{R}} |\mathbf{F}^{(n)}(x, \lambda)\mathbf{e}_1| \mathrm{d}x \quad \text{tends to 0}.$$

If there exists λ_0 such that σ_{ess} is empty for all $\lambda < \lambda_0$ the above hypotheses can be modified accordingly.

Proposition 20 *Assume that hypothesis 4 is met by $\mathbf{B}(x, \lambda)$, then*

$$\lim_{\lambda \to -\infty} D(\lambda) = 1, \quad \text{and} \quad \lim_{\lambda \to -\infty} I_{hom}(\phi, \lambda) = 0.$$

Following the argument in Proposition 1.17 in PEGO & WEINSTEIN [103] and the Appendix of BRIDGES & DERKS [23], we can prove $(V^{[n]}(\lambda))^{-1}Y(\cdot, \lambda)$ converges, uniformly in x, to the constant vector $\mathbf{e}_1$ when $\lambda \to -\infty$. Then, for large enough λ, $(V^{[n]}(\lambda))^{-1}Y(\cdot, \lambda)$ has a null Maslov index and so does $Y(\cdot, \lambda)$. In appendix F.2, we describe how to apply this proposition to the Kawahara equation.

2.4.3　Computing $I_{hom}(\phi, \lambda)$ when $\lambda \in \sigma_p$

When $\lambda \in \sigma_p$, $D(\lambda) = 0$. As a consequence $\sup_{x \in \mathbb{R}} \|\widehat{\mathbf{U}}(x, \lambda)\| = 0$.

Therefore, the algorithm of section 2.4.2 will fail to converge.

If $\dim(\mathcal{U}(x, \lambda) \cap \mathcal{S}(x, \lambda))$ is known and $\partial_\lambda \mathbf{C}(x, \lambda)$ is positive, then we can use proposition 3 to compute $I_{hom}(x, \lambda)$ and we have:

$$I_{hom}(\phi, \lambda) = \frac{I_{hom}(\phi, \lambda + \varepsilon) + I_{hom}(\phi, \lambda - \varepsilon)}{2}$$

whenever

$$I_{hom}(\phi, \lambda + \varepsilon) - I_{hom}(\phi, \lambda - \varepsilon) = \dim(\mathcal{U}(x, \lambda) \cap \mathcal{S}(x, \lambda)).$$

So here is how $I_{hom}(\phi, \lambda)$ can be computed

1. Choose a $\varepsilon > 0$.

2. Compute $I_{hom}(\phi, \lambda + \varepsilon) - I_{hom}(\phi, \lambda - \varepsilon)$, choosing suitably the step size and L.

3. If $I_{hom}(\phi, \lambda + \varepsilon) - I_{hom}(\phi, \lambda - \varepsilon) = k$, then return $\frac{I_{hom}(\phi,\lambda+\varepsilon)+I_{hom}(\phi,\lambda-\varepsilon)}{2}$. Otherwise set $\varepsilon := \frac{\varepsilon}{2}$ and go to Step 2.

2.4.4 Tracking intersections of $\mathcal{U}(x, \lambda)$ with $\mathcal{S}_\infty(\lambda)$

The algorithm in §2.4.2 gives little information about where intersections of $\mathcal{U}(x, \lambda)$ with $\mathcal{S}_\infty(\lambda)$ occur.

Besides, the path made by the unstable space in the case of a dark solitary wave or a front is not generically closed. To extend the definition of the Maslov index to these cases, tracking the intersections would be mandatory.

The algorithm of this section is quite similar except that the computation of the angle $\kappa(x)$ is replaced by the computation of the angles $\kappa_1, \ldots, \kappa_n$.

The initial algorithm can be modified as follows:

1. Choose a large interval $-L \leq x \leq L$. Initialize Maslov (the counter used to determine $I_{hom}(\phi, \lambda)$) to 0.

2. Find a symplectic matrix $\mathbf{R}(\lambda)$ such that $\mathbf{R}(\lambda)\begin{pmatrix} I \\ 0 \end{pmatrix}$ and $\mathbf{R}(\lambda)\begin{pmatrix} 0 \\ I \end{pmatrix}$ represent the stable and unstable spaces of $\mathbf{B}_\infty(\lambda)$.

   $\mathbf{R}(\lambda)$ define a symplectic change of coordinates in which the coordinates of stable and unstable spaces in the exterior algebra are respectively $S_0 = \begin{pmatrix} 1 \\ 0 \\ \vdots \\ 0 \end{pmatrix}$ and $V_0 = \begin{pmatrix} 0 \\ \vdots \\ 0 \\ 1 \end{pmatrix}$.

3. Compute the eigenvalue with largest real part, $\sigma_+(\lambda)$, of $\mathbf{B}_\infty^{(n)}(\lambda)$.

4. Integrate the equation

$$\mathbf{R}^{[n]}(\lambda)^{-1}\mathbf{U}_x = \mathbf{R}^{[n]}(\lambda)^{-1}([\mathbf{B}^{(n)}(x, \lambda) - \sigma_+(\lambda)\mathbf{I}])\mathbf{R}^{[n]}(\lambda)\mathbf{R}^{[n]}(\lambda)^{-1}\mathbf{U}, \qquad (2.4.31)$$

   in the new system of coordinates on $[-L, L]$, taking U_0 as initial condition for $\mathbf{R}^{[n]}(\lambda)^{-1}\mathbf{U}$ at $x = -L$ and using any standard numerical integration scheme.

5. Compute the angles $(\kappa_1, \kappa_2, \ldots, \kappa_n)$ corresponding to the eigenvalues of $\psi(\mathbf{R}(\lambda)^{-1}\mathbf{U}, \begin{pmatrix} I \\ 0 \end{pmatrix})$ over $[-L, L]$. If a κ_i crosses $2\pi\mathbb{Z}$ between x and $x + \Delta x$, update the value of the Maslov index to:

$$\mathsf{Maslov} \mapsto \mathsf{Maslov} + \mathrm{sign}\left(\kappa_i(x + \Delta x) - \kappa_i(x)\right).$$

$$\mathsf{Intersection\_list} = \mathsf{Intersection\_list} \cup \{(x, \mathrm{sign}\left(\kappa_i(x + \Delta x) - \kappa_i(x)\right))\}$$

6. Return $\mathbf{R}^{[n]}(\lambda)^{-1}\mathbf{U}(L,\lambda) \wedge S_0$ as an approximation to the Evans function.

7. At $x = +L$, return $I_{hom}(\phi,\lambda) = \mathsf{Maslov}$ and $\mathsf{Intersection\_list}$.

This algorithm was implemented with Matlab$^{\mathrm{TM}}$. The code is given in Appendix I.4 in the case of the Kawahara equation.

2.5   Conclusion

We have obtained numerical algorithms to compute the Maslov index of periodic waves and of solitary waves. We are now going to apply these algorithms to waves arising in several partial differential equation models.

Chapter 3

The Kawahara equation

Contents

Introduction

In this chapter, we first recall the physical context in which the Kawahara equation arises. Then we make some comments on the structure of the ODE satisfied by travelling waves. Then, we discuss the Maslov index of the solitary waves and the implication for their stability and what occurs at bifurcation points, e.g. points where several branches of solutions merge. Finally, we look at the Maslov index of some periodic waves which converge to a solitary wave.

Figure 3.1: Water-strider (Gerrida) taking advantage of surface tension to counterbalance gravity.

3.1   Physical context

We consider a two-dimensional inviscid, incompressible, irrotational fluid, subject to capillarity and gravity.

Let

- x be the horizontal variable and z the vertical one.

- $(x, B(x))$ be the bottom of the fluid.

- $(x, \eta(x,t))$ be the free surface of the fluid.

- $\phi(x, z, t)$ be the velocity potential. ϕ is a function such that $\nabla \phi$ is the velocity of the fluid.

- g be the acceleration due to gravity.

Then, the two-dimensional Euler equations can be written as:

$$
\begin{aligned}
\frac{\partial^2 \phi}{\partial x^2} + \frac{\partial^2 \phi}{\partial z^2} &= 0 && \text{when } B(x) < z < \eta(x,t) \\
\frac{\partial \phi}{\partial z} &= \frac{\partial B}{\partial x} \frac{\partial \phi}{\partial x} && \text{at } z = B(x) \\
\frac{\partial \phi}{\partial z} &= \frac{\partial \eta}{\partial x} \frac{\partial \phi}{\partial x} + \frac{\partial \eta}{\partial t} && \text{at } z = \eta(x,t) \\
\frac{\partial \phi}{\partial t} + \frac{1}{2}\left(\left(\frac{\partial \phi}{\partial x}\right)^2 + \left(\frac{\partial \phi}{\partial z}\right)^2 \right) + g\eta &= \frac{\sigma}{\rho} \frac{\frac{\partial^2 \eta}{\partial x^2}}{(\frac{\partial \eta}{\partial x}^2 + 1)^{\frac{3}{2}}} && \text{at } z = \eta(x,t)
\end{aligned}
\tag{3.1.1}
$$

Now, we assume that the bottom of the fluid is flat, e.g. $B(x) = -H$.

The dispersion relation for the linearized equations near the constant state $\phi = 0$ and $\eta = 0$ is (see [123]):

$$
\omega^2 = gk(1 + \frac{\sigma H^2}{\rho}k^2)\tanh(kH) \tag{3.1.2}
$$

The phase and group velocity are therefore:

$$
c(k) = \frac{\omega}{k} = \pm\sqrt{\left(\frac{g}{k} + \frac{\sigma H^2}{\rho}k\right)\tanh(kH)} \tag{3.1.3}
$$

$$c_g(k) = \frac{\mathrm{d}\omega}{\mathrm{d}k} = \pm\frac{1}{2}c(k)\left(\frac{\rho g + 3\sigma k^2}{\rho g + \sigma k^2} + \frac{2kH}{\sinh(2kH)}\right) \tag{3.1.4}$$

If we make the Taylor expansion of ω^2, then one gets:

$$\omega^2 = Hgk^2 + \frac{\left(3H^3 g\sigma - H^3 g\rho\right)k^4}{3\rho} - \frac{\left(5H^5 g\sigma - 2H^5 g\rho\right)k^6}{15\rho} + 0(k^8)$$

While the Korteweg-de Vries approximation only recovers the first terms of the dispersion relation, the Kawahara equation takes in account the next term.

Let

- $c_0 = \sqrt{gH}$ be the speed of long-waves,

- η_0 be the characteristic height of the wave,

- L be the characteristic length of the wave.

Let us introduce the following dimensionless quantities

- $B = \frac{\sigma}{\rho g H^2}$ the Bond number,

- $\varepsilon = \frac{\eta_0}{H}$ the non-linearity parameter,

- $\mu = \frac{H}{L}$ the long-wave parameter.

ε and μ are assumed to be small quantities.

The Euler equations can be put into an non-dimensional form by choosing the following set of variables:

$$\mu x = H\tilde{x}, \quad z = H\tilde{z}, \quad \mu t = H(gH)^{-\frac{1}{2}}\tilde{t},$$
$$\mu\phi = \varepsilon H(gH)^{\frac{1}{2}}\tilde{\phi}, \quad \eta = \varepsilon H\tilde{\eta}.$$

Assume that $\varepsilon = \mu^4$ and that the wave under consideration is propagating to the right. Let $\alpha = \frac{B - \frac{1}{3}}{\mu^2}$. Then, at order ε^2, $\tilde{\eta}$ is a solution of the Kawahara equation [80, 82, 52, 34, 20, 53, 21]:

$$\tilde{\eta}_{\tilde{t}} - \tilde{\eta}_{\tilde{x}} + \varepsilon\left(\frac{\alpha}{2}\tilde{\eta}_{\tilde{x}\tilde{x}\tilde{x}} - \frac{1}{90}\tilde{\eta}_{\tilde{x}\tilde{x}\tilde{x}\tilde{x}\tilde{x}} - \frac{3}{2}\tilde{\eta}\tilde{\eta}_{\tilde{x}}\right) = 0$$

Via another change of the variables, it is possible to put the previous equation into the form:

$$\frac{\partial u}{\partial t} - c\frac{\partial u}{\partial x} + \frac{\partial}{\partial x}\left(u^{q+1}\right) + P\frac{\partial^3 u}{\partial x^3} - \frac{\partial^5 u}{\partial x^5} = 0, \quad q = 1. \tag{3.1.5}$$

A further scaling can be introduced so that $c = 1$, but including c is useful for comparing with results in the literature on the Kawahara equation. In fact, q is a third parameter, which can be useful to set to other values than 1 in some applications of the Kawahara equation, e.g. plasmas physics. Here, we will restrict to integer values of q.

SAUT AND TZVETKOV [114] proved the well-posedness of a Kawahara-KP model in L^2 for a torus and $\mathbb{R}^2$, which is the natural extension of the Kawahara equation to the three-dimensional water-wave problem.

The Kawahara equation can be put into a Hamiltonian form by taking:

$$\omega(u, v) = \int_{\mathbb{R}} u(x)(\partial_x)^{-1} v(x) \mathrm{d}x \tag{3.1.6}$$

$$\mathcal{H}(u) = \int_{\mathbb{R}} \left(\frac{1}{2} u_{xx}^2 + \frac{P}{2} u_x^2 - \frac{1}{q+2} u^{q+2} + \frac{c}{2} u^2 \right) \mathrm{d}x \tag{3.1.7}$$

as symplectic form and Hamiltonian.

3.2 The steady problem

The steady part of the Kawahara equation can be written as:

$$u_{xxxx} - P u_{xx} + cu - u^{q+1} = 0. \tag{3.2.8}$$

This ODE also arises in a number of physical examples. For instance, it is also the steady part of the one-dimensional Swift-Hohenberg equation

$$\phi_t = -\phi_{xxxx} + P\phi_{xx} - \phi + \phi^{1+q} \tag{3.2.9}$$

The same equation arises in the study of beam buckling. A history with references is given by CHAMPNEYS [34].

The ODE (3.2.8) has been extensively studied and many solitary wave solutions have been found; a classification is given in [27].

The linearization of $u_{xxxx} - P u_{xx} + cu - u^{q+1} = 0$ near $\phi = 0$ is $u_{xxxx} - P u_{xx} + cu = 0$. If $\phi = e^{kx}$ is a solution to the linear equation, then k must satisfy the equation $k^4 - Pk^2 + c = 0$. Solutions of this polynomial equation are:

1. Imaginary if $Pc^{-\frac{1}{2}} < -2$. There cannot be solitary wave solutions to the non-linear ODE with exponentially decaying tails.

2. Complex and non-real, not imaginary if $-2 < Pc^{-\frac{1}{2}} < 2$. Solitary waves with oscillating tails have been found.

3. Real if $2 < Pc^{-\frac{1}{2}}$. Solitary waves with non-oscillating tails can be found.

There are some special cases where explicit solitary wave solutions have been found. An example is the explicit solution $\widehat{\phi}(x) = \left(\frac{(q+4)(3q+4)}{8(q+2)} \right)^{1/q} \mathrm{sech}^{4/q} \left(xq\sqrt{\frac{1}{8(q+2)}} \right)$ which exists when $q \geq 1$ and $P = \frac{q^2+4q+8}{2(q+2)}$. However, the interesting solutions of (3.2.8) need to be computed numerically. They can be computed using a spectral method (approximate the solitary wave by a periodic function of large wavelength and then use Fourier series to represent it), or in the case of symmetric solitary waves a shooting algorithm can be used. We used both methods to compute solitary waves. Symmetric solutions are computed numerically using a shooting method: the starting point is an element of the tangent space of the unstable manifold and the ending point is a symmetric point. We chose the fourth order Runge-Kutta method as integrator and a space step equal to $\frac{1}{1000}$. With this space step, the error was close to the machine error
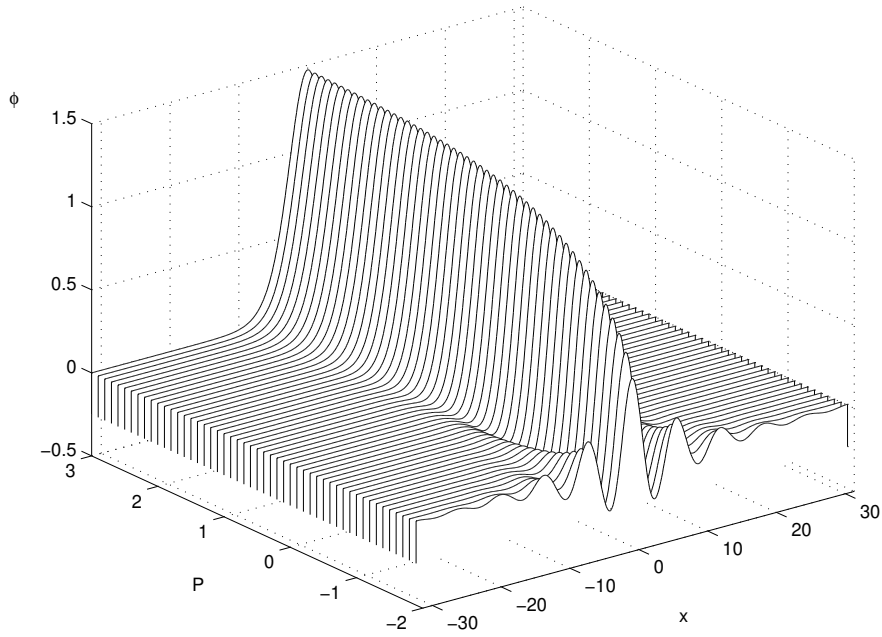
Figure 3.2: Numerically computed unimodal solitary waves for the Kawahara equation for the case $q = 1$, $c = 1$ and $-2 < P < 3$.

precision. More details about the spectral and the shooting methods, as well as a Matlab$^{\text{TM}}$code, are given in Appendix I.1 and Appendix I.2 respectively. An example of the family of unimodal solitary waves as a function of P, computed using a spectral method, is shown in Figure 3.2.

Although these solitary waves are solutions of the model ODE, they are representative of solutions of the full water-wave problem. Dias, Menasce & Vanden-Broeck [55] have found large-amplitude branches of these solutions in the full water-wave equations.

Stationary wave solutions u are critical points of the Hamiltonian of the Kawahara equation. Therefore, equation (3.2.8) can be put into a spatial Hamiltonian system. Here, we choose the following set of coordinates:

$$\begin{cases} q_1 = u \\ q_2 = u_{xx} \\ p_1 = u_{xxx} - Pu_x \\ p_2 = u_x \end{cases}.$$

In this set of coordinates, the reversibility of (3.2.8) can be expressed as:

$$\begin{pmatrix} q_1(t) \\ q_2(t) \\ p_1(t) \\ p_2(t) \end{pmatrix} \text{ is a solution } \Leftrightarrow R \begin{pmatrix} q_1(-t) \\ q_2(-t) \\ p_1(-t) \\ p_2(-t) \end{pmatrix} \text{ is a solution,}$$

$$\text{with } R = \begin{pmatrix} 1 & 0 & 0 & 0 \\ 0 & 1 & 0 & 0 \\ 0 & 0 & -1 & 0 \\ 0 & 0 & 0 & -1 \end{pmatrix} \qquad (3.2.10)$$

The spatial Hamiltonian in the original coordinates is:

$$E(u) = \tfrac{1}{2}u_{xx}^2 + \tfrac{1}{2}Pu_x^2 - \tfrac{1}{2}cu^2 + \frac{1}{q+2}u^{q+2} - u_x u_{xxx}\,.$$

It satisfies $\frac{dE}{dx} = 0$ along solutions of (3.2.8). Physically, for the Kawahara equation, this quantity is associated with the momentum flux.

The system (3.1.5), linearized about a solitary wave $\widehat{\phi}(x)$ solution of (3.2.8), takes the form

$$\frac{\partial \phi}{\partial t} = \frac{\partial}{\partial x}\left(\mathscr{L}\phi\right),$$

with

$$\mathscr{L}\phi := \phi_{xxxx} - P\,\phi_{xx} + c\phi - (q+1)\widehat{\phi}(x)^q\,\phi\,. \qquad (3.2.11)$$

There are two spectral problems:

$$\mathscr{L}\phi = \lambda\phi \quad \text{and} \quad \mathbf{L}\phi = \widehat{\lambda}\phi\,, \quad \mathbf{L}\phi := \frac{d}{dx}\mathscr{L}\,. \qquad (3.2.12)$$

The operator $\mathscr{L}$ is self-adjoint (in a suitable Hilbert space) and so $\lambda \in \mathbb{R}$. On the other hand, $\mathbf{L}$ is not self-adjoint, and $\widehat{\lambda}$ which is the stability exponent, can in general be complex. The relationship between these two eigenvalue problems is discussed in §3.5.1. First, we study the Maslov index of the spectral problem $\mathscr{L}\phi = \lambda\phi$, which can be put in the form (1.2.8,1.3.13):

$$\mathcal{J}\mathbf{z}_x = \mathbf{C}(x,\lambda)\mathbf{z}\,, \quad \mathbf{z} := \begin{pmatrix} w \\ w_{xx} \\ w_{xxx} - Pw_x \\ w_x \end{pmatrix}\,,$$

with $\mathcal{J}$ in the standard form (A.0.1) and

$$\mathbf{C}(x,\lambda) = \begin{pmatrix} a(x) - \lambda & 0 & 0 & 0 \\ 0 & -1 & 0 & 0 \\ 0 & 0 & 0 & 1 \\ 0 & 0 & 1 & P \end{pmatrix}\,, \quad a(x) = 1 - (p+1)\,\widehat{\phi}(x)^q\,. \qquad (3.2.13)$$

3.3 The Maslov index of solitary waves of the Kawahara equation

In this section we study the Maslov index as a function of λ for the ODE eigenvalue problem

$$\phi_{xxxx} - P\phi_{xx} + a(x)\phi = \lambda\phi\,, \tag{3.3.14}$$

where $\phi(x)$ is scalar valued, P is a real parameter and $a(x)$ is a localized function which satisfies $a(x) \to a_\infty$ as $x \to \pm\infty$, with exponential decay of $a(x)$ at infinity. For definiteness it is assumed that $a_\infty > 0$. The ODE (3.3.14) can be put in the form (1.2.8). The spectrum of the system at infinity $\mathbf{B}_\infty(\lambda) = \mathcal{J}^{-1}\mathbf{C}_\infty(\lambda)$ has the characteristic polynomial

$$\det[\mathbf{B}_\infty(\lambda) - \mu\mathbf{I}] = \mu^4 - P\mu^2 + a_\infty - \lambda\,. \tag{3.3.15}$$

With $a_\infty > 0$ and $\lambda = 0$ the four roots are hyperbolic for all P such that

$$P + 2\sqrt{a_\infty} > 0\,,$$

which is assumed to be satisfied henceforth. When $\lambda \neq 0$ the essential spectrum will form the boundary of the hyperbolic region. The essential spectrum is

$$\sigma_{\text{ess}} = \{\lambda \in \mathbb{R} \ : \ \lambda = a_\infty + Pk^2 + k^4\,,\ k \in \mathbb{R}\}\,.$$

When

$$\lambda < \lambda^{\text{edge}} = a_\infty - \frac{1}{8}P(P - |P|)\,,$$

the spectrum of $\mathbf{B}_\infty(\lambda)$ is hyperbolic. Hence, all the hypotheses for the existence of the Evans function and the Maslov index are satisfied. We will apply this theory to determine the Maslov index of a class of multi-pulse homoclinic orbits.

Furthermore, using Proposition 20 and the proof in Appendix F.2, it follows that the Kawahara system satisfies hypothesis 4 and therefore $D(\lambda) \to 1$ and the Maslov index tends to 0 as $\lambda \to -\infty$.

Spectral problems of the form (3.3.14) also arise in the physical examples mentioned above in section 3.2. In the case of the one-dimensional Swift-Hohenberg equation, $\frac{\partial\phi}{\partial t} = -\mathscr{L}\phi$ is the linearization about the localized solutions. $-\lambda$ in (1.3.13) is then the spectral parameter for the stability of localized solutions.

3.4 The Maslov index of unimodal solitary waves

First consider the case $P = \frac{13}{6}$, $q = 1$ and $c = 1$ where the unimodal solitary wave is given explicitly. The lifts $\kappa(x)$ of the Maslov angle for this system are plotted as a function of x in Figure 3.3 for various values of λ. In Figure 3.4, the corresponding Maslov indices have been plotted as a function of λ. The Evans function shows that $\mathscr{L}$ has exactly three eigenvalues in this case. Denote these eigenvalues by

$$\lambda_1 < \lambda_2 = 0 < \lambda_3\,.$$
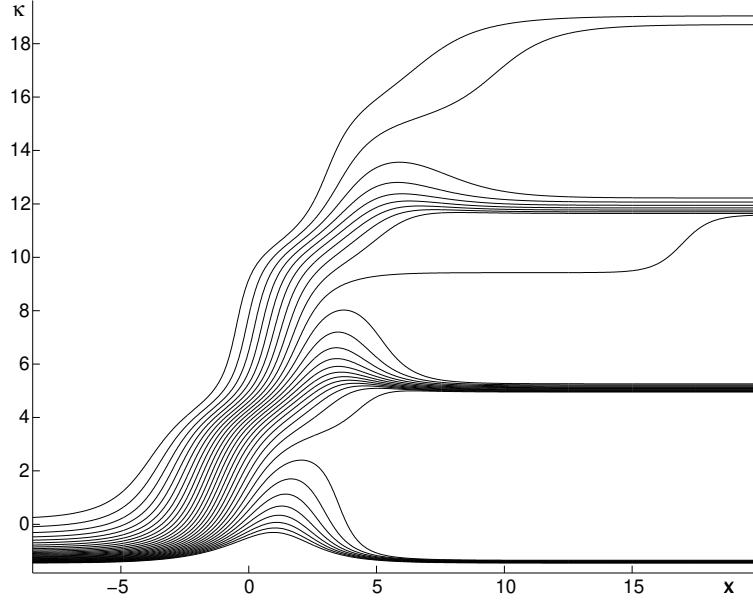
Figure 3.3: κ as a function of x for the following values of λ:$-2, -1.9, \ldots, 0.9$. κ is λ-growing. The parameter values are $P = \frac{13}{6}$, $c = 1$ and $q = 1$.

The qualitative behaviour of the Maslov index in this case is similar to the example on $\mathbb{R}^2$ in Appendix E. The values of the Maslov are shown in the table below. The Maslov index in this case is computed using the Maslov angle, and this Maslov index is denoted by $I_{hom}(\phi, \lambda)$.

λ	$\lambda < \lambda_1$	$\lambda_1 < \lambda < \lambda_2$	$\lambda_2 < \lambda < \lambda_3$	$\lambda > \lambda_3$
$I_{hom}(\phi, \lambda)$	0	1	2	3

Note that the Maslov index in each region predicts the number of eigenvalues of $\mathscr{L}$ in each λ interval.

λ region	$\lambda < \lambda_1$	$\lambda < \lambda_2$	$\lambda < \lambda_3$	$\lambda < \lambda^{\text{edge}}$
# Eigs($\mathscr{L}$)	0	1	2	3

It is immediate from this table that

$$I_{hom}(\phi, 0) = \frac{\lim_{\lambda \to 0^+} I_{hom}(\phi, \lambda) + \lim_{\lambda \to 0^+} I_{hom}(\phi, \lambda)}{2} = 1 + \frac{1}{2}.$$

The operator $\mathscr{L}$ has exactly one negative eigenvalue in this case. Our calculations indicate that this is the case for all the unimodal homoclinic orbits. It is easy to show analytically that the
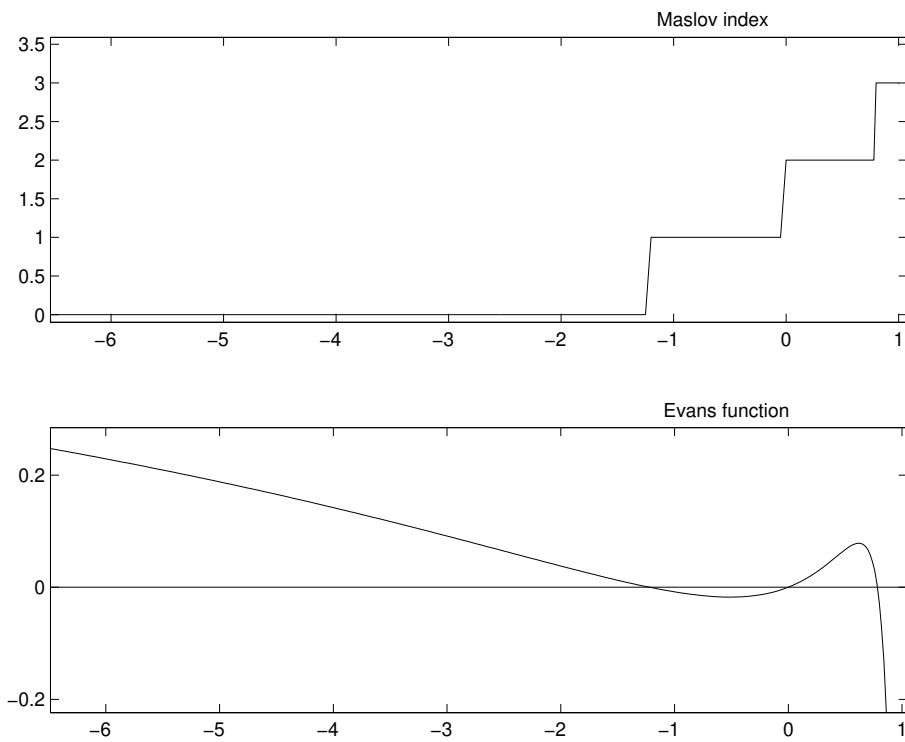
Figure 3.4: Evans function and Maslov index as a function of λ for the explicit unimodal solitary wave solution when $P = \frac{13}{6}$, $c = 1$ and $q = 1$
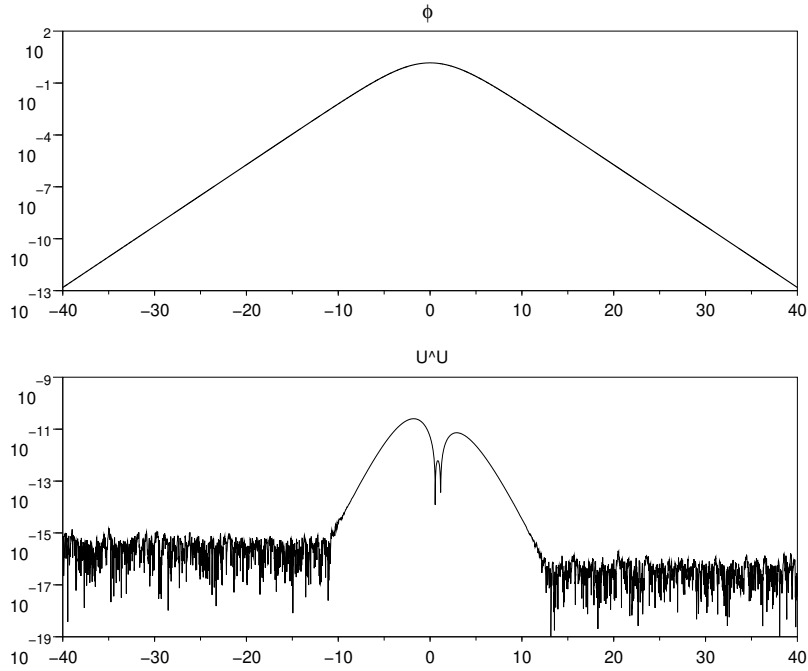
Figure 3.5:   The decomposability of a 2-form is equivalent to $I_1 = 0$ where I_1 is defined in (3.4.16). The upper figure shows the logarithm of the difference between $a(x)$ and its limit a_∞, and the lower figure shows the logarithm of the value of I_1 when $q = 1$, $P = \frac{13}{6}$, $\lambda = -10$ and when the space step in the algorithm to compute the Maslov index is equal to $dx = .01$. The fast oscillations are associated with round-off errors.

Maslov index of a unimodal homoclinic orbit is greater than or equal to $1 + \frac{1}{2}$. An elementary proof is given in Appendix F.1. The fact that $\#\mathscr{L}^- = 1$ is proved in [42, 70]. This result has implications for the stability of the solitary waves as solutions of the Kawahara equation and it is discussed in §3.5.1.

3.4.1   Numerical tests on the accuracy of the algorithm

To test how accurately the Lagrangian Grassmannian is preserved by the numerical scheme, the values of

$$I_1 = \mathbf{U} \wedge \mathbf{U} \quad \text{and} \quad I_2 = \omega \wedge \mathbf{U}, \tag{3.4.16}$$

are computed as a function of x. In these calculations the standard explicit fourth-order Runge-Kutta algorithm is used. The value of I_1 is shown in Figure 3.5 and shows that the error is of order of the machine accuracy, except for a small region around zero, but the error there is still exceptionally small. Concerning I_2, it is in fact exactly preserved, even numerically: if the value of $\mathbf{U}_2 + \mathbf{U}_5$ is the machine zero, it remains at the machine zero.
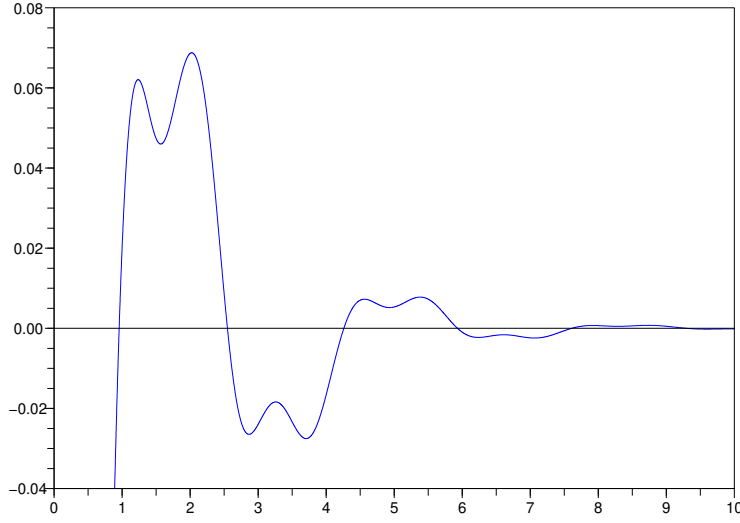
Figure 3.6: Value of $\frac{\kappa_1}{2\pi}$ when $q = 1$, $P = -1.5$, and $\lambda = 0$ as defined in section 2.4.4. Each intersection of κ_1 with 0 corresponds to a non-trivial intersection of $\mathcal{U}(x, \lambda)$ with $\mathcal{S}_\infty(\lambda)$.

3.5 Multi-pulse solutions

The ODE (3.2.8) has a family of solutions ϕ_P defined for $P \in [-2, \infty[$ with a symmetric point at $x = 0$ (i.e. $\phi'_P(0) = \phi'''_P(0) = 0$) which is the unique maximum when $P > 2$. For any $\varepsilon \in [-2 + \varepsilon, 2[$, it can be proved that there is an infinity of families of homoclinic solutions made of copies of the unimodal solutions. See [27] and references therein for a classification of these solutions.

These families can be classified in the following manner by looking at their behaviour near $P = 2^-$. A family ψ_P of solutions is said to have a mode at s_P if

$$\lim_{P \to 2^+} (\psi_P(s_P), \psi'_P(s_P), \psi''_P(s_P), \psi'''_P(s_P)) = (\phi_2(0), \phi'_2(0), \phi''_2(0), \phi'''_2(0)).$$

A multi-pulse homoclinic family orbit is said to have type $\mathbf{n}(\ell_1, \ell_2, \ldots, \ell_n)$ if it has n modes at the points $s_{1,P}, s_{2,P}, \ldots, s_{n,P}$, and

$$\lim_{P \to 2^+} s_{i+1,P} - s_{i,P} = \infty,$$

and the number of zeros of $\frac{1}{2}\psi''^2_P - \frac{1}{2}\psi^2_P + \frac{1}{3}\psi^3_P$ in $[s_{i,P}, s_{i+1,P}]$ is equal to $2k_i$. It has been conjectured that there is a unique family of each type, up to a space translation. This classification has been introduced in [27]. These solutions can be computed using shooting, or by approximating them by periodic solutions and using a spectral method. Examples of bimodal solutions are shown in Figure 3.7. An example of asymmetric solutions, of type $\mathbf{3}(3, 1)$ is shown in Figure 3.8.

Figure 3.7: Bimodal solutions when $q = 1$, $c = 1$ and $P = -1.5$.

Figure 3.8: Trimodal solution $\mathbf{3}(3, 1)$ when $q = 1$, $c = 1$ and $P = -1.5$.

These multi-modal orbits occur only for P satisfying $-2 < P < +2$ and therefore they have oscillatory tails.

The value of the Maslov index for solitary waves of various families when $\lambda = 0$ is given in the following table.

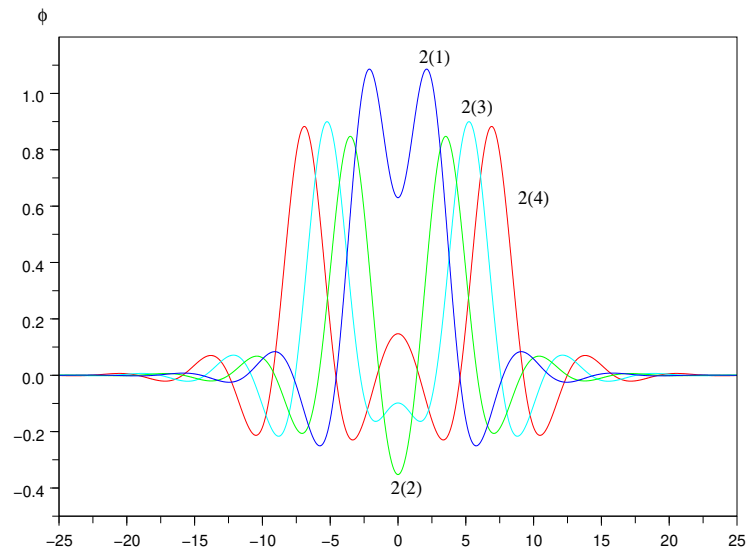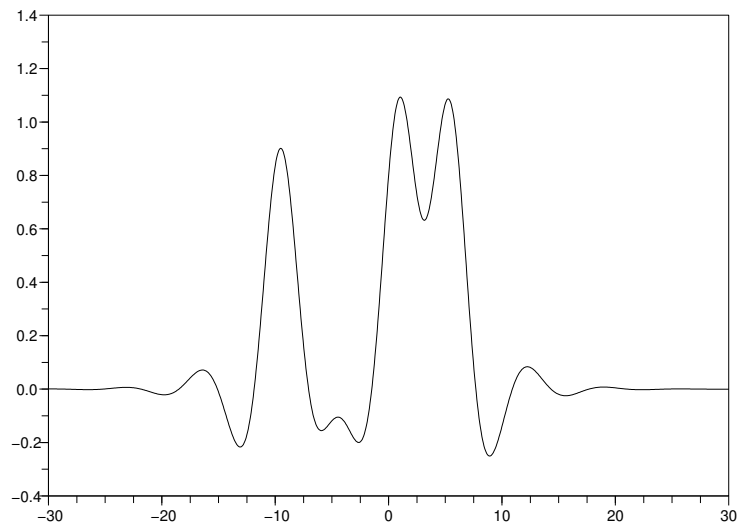| Family		Family		Family	
1	1	**3**$(2,1)$	4	**4**$(3,4,3)$	6
2(1)	3	**3**$(3,1)$	5	**4**$(3,5,3)$	7
2(2)	2	**3**$(1,1)$	5	**4**$(3,6,3)$	6
2(3)	3	**3**$(2,2)$	3	**5**$(3,1,1,3)$	9
2(4)	2	**3**$(3,3)$	5	**5**$(3,2,2,3)$	7
2(5)	3	**3**$(4,4)$	3	**5**$(3,3,3,3)$	9
2(6)	2	**3**$(5,5)$	5	**6**$(3,2,1,2,3)$	9
2(7)	3	**3**$(6,6)$	3	**6**$(3,2,2,2,3)$	8
2(8)	2	**4**$(3,1,3)$	7	**6**$(3,2,3,2,3)$	9
2(9)	3	**4**$(3,2,3)$	6		
2(10)	2	**4**$(3,3,3)$	7		

Value of $I_{hom}(\phi, 0) - \frac{1}{2}$ for the different families of solitary waves.

From this table, we see that there is a pattern between the type $\mathbf{n}(\ell_1, \ell_2, \ldots, \ell_{n-1})$ and the Maslov index. We find the remarkable conjecture that the value of the Maslov index is predicted by the type, determined by the following formula

$$I_{hom}(\phi, 0) - \frac{1}{2} = n_{even} + 2n_{odd} + 1 \qquad (3.5.17)$$

where n_{even} is the number of even indices among $(\ell_1, \ell_2, \ldots, \ell_{n-1})$ and n_{odd} the number of odd ones.

Computing the Evans function for multi-pulse orbits

To see the connection between the number of eigenvalues of $\mathscr{L}$ and the Maslov index for multi-pulse, the Evans function for multi-pulse orbits is computed for an example. Consider the multi-pulse orbit of type $\mathbf{5}(3,1,1,3)$ at $P = -1.5$, $c = 1$ and $q = 1$. It is shown in Figure 3.9. The computed Maslov index and Evans function for this case as a function of λ are shown in Figure 3.10. From this result and the previous calculations it appears that the number of negative eigenvalues of $\mathscr{L}$ is predicted by the Maslov index with the formula

$$\#\mathscr{L}^- = I_{hom}(\phi, 0) - \frac{1}{2}. \qquad (3.5.18)$$

This formula is of interest when we consider the relation between the spectrum of $\mathbf{L}$, which determines the stability of solutions of the Kawahara equations and the spectrum of $\mathscr{L}$.

Then, it appears that (3.5.17) is consistent with PELINOVSKY & CHUGUNOVA [42] results in the case of a $\mathbf{2}(i)$ pulse since they found that $\#\mathscr{L}^- = 3$ if i is odd and $\#\mathscr{L}^- = 2$ is even.
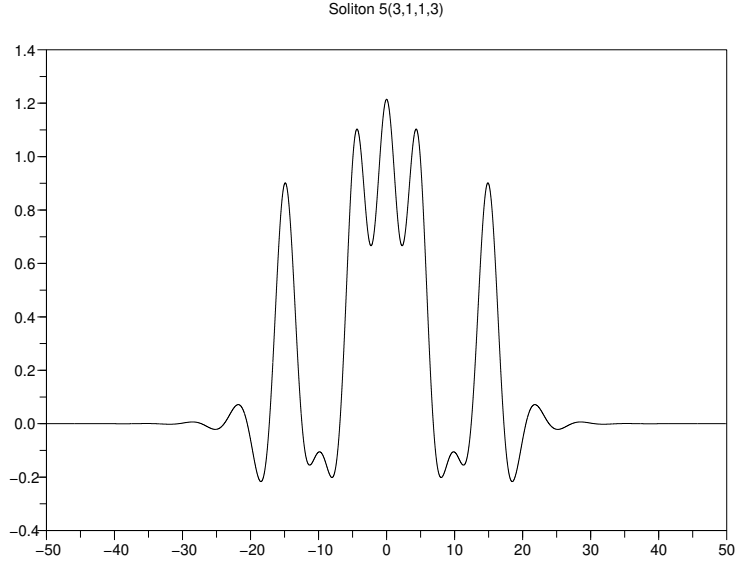
Figure 3.9: A multi-pulse solitary wave of type $\mathbf{5}(3, 1, 1, 3)$ at $P = -1.5$ and $q = 1$.

3.5.1   Spectrum of $\mathscr{L}$ and the stability of solitary waves for the Kawahara equation

One of the intriguing properties of the Maslov index is its connection with the number of eigenvalues in subsets of the λ space, and subsequently the relationship with the stability of waves.

For the Swift-Hohenberg equation (3.2.9), the connection between the spectrum of $\mathscr{L}$ and unstable eigenvalues is exact: $\#\mathscr{L}^-$, the number of negative eigenvalues of $\mathscr{L}$, is equal to the number of unstable eigenvalues associated with the basic steady solution of (3.2.9).

On the other hand, the connection between stability and $\#\mathscr{L}^-$ for the Kawahara equation is not as direct. For unimodal solitary-wave solutions of Kawahara, KODAMA & PELINOVSKY [82] have studied this connection. Suppose the following integral exists

$$N(P, c) = \int_{\mathbb{R}} \widehat{\phi}(x, c, P)^2 \mathrm{d}x\,,$$

and is a differentiable function of c. Define

$$r = \begin{cases} 0 & \text{if } \frac{\partial N}{\partial c}(1, P) < 0 \\ 1 & \text{if } \frac{\partial N}{\partial c}(1, P) > 0 \end{cases}\,.$$

The functional $N(P, c)$ is sometimes called the *momentum of the solitary wave*. In [82] it is argued (see proposition 3.8 there) that a unimodal solitary wave is stable if $r = +1$ and $\#\mathscr{L}^- = 1$. This result assumes that there are no pure imaginary eigenvalues of $\mathbf{L}$. Hence, in this case the stability of the solitary wave is determined by the sign of $\frac{dN}{dc}$. This observation
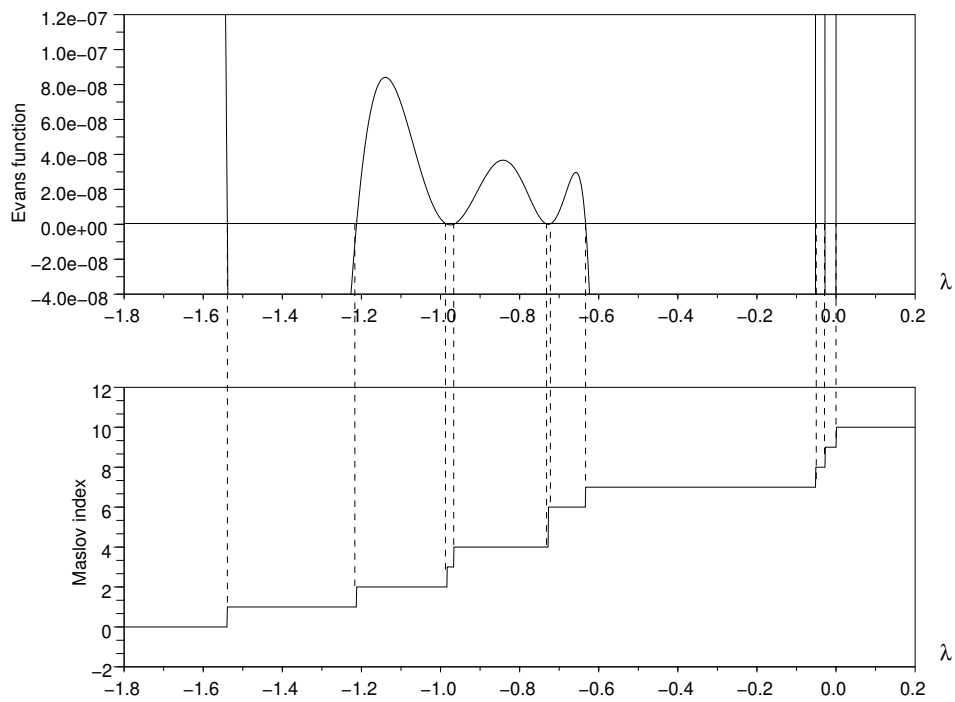
Figure 3.10: The computed Evans function and Maslov index associated with the multi-pulse solitary wave in Figure 3.9.

is consistent with the theory of [20] where instability results for a class of unimodal solitary waves were obtained. Some later results about values of $\frac{\partial N}{\partial c}$, which have been published by LEWANDOSKY [89], can be seen on figure 3.11.

More refined results on stability of two-pulse solitary waves were obtained by PELINOVSKY & CHUGUNOVA [42]. They relate $\#\mathscr{L}^-$ with the complex eigenvalues of $\mathbf{L}$, where $\mathbf{L}$ is defined in (3.2.12). Consider a symmetric solitary wave and suppose that $\mathbf{L}$ has only simple eigenvalues except a double eigenvalue at 0 and suppose $\frac{\partial N}{\partial c}(1, P) \neq 0$. In [42], it is proved that

$$N_{unst} = \#\mathscr{L}^- - r - N_{imag}^-, \qquad (3.5.19)$$

where N_{unst} is the number of eigenvalues with strictly positive real part of $\mathbf{L}$ and N_{imag}^- is the number of pure imaginary eigenvalues of $\mathbf{L}$ with negative Krein signature[1]. Combining with (3.5.18) gives

$$N_{unst} = I_{hom}(\phi, 0) - \frac{1}{2} - r - N_{imag}^-.$$

It is immediate from this formula that if $N_{imag}^- = 0$ and $I_{hom}(\phi, \lambda) - \frac{1}{2} = 1$ then the basic state is stable if $\frac{dN}{dc} > 0$ and unstable if $\frac{dN}{dc} < 0$.

These observations are consistent with the results of BURYAK & CHAMPNEYS [30]. They consider the stability of $2-$pulse solutions of the form $\mathbf{2}(\ell)$, $\ell = 1, \ldots, 9$. They find that the solutions of the type $\mathbf{2}(\ell)$ with ℓ odd are stable and those with ℓ even are unstable.

Using the formula (3.5.17) and the fact that N_{imag}^- is even, we conclude that any solution such that $I_{hom}(\phi, \lambda) - \frac{1}{2} - r$ is odd is unstable.

3.5.2 Evolution of the Maslov index near bifurcation points

IOOSS & PÉROUÈME [76] proved the existence of two even solutions near $P = -2^+$ and there is numerical evidence that these two solutions correspond to $\mathbf{1}$ and $\mathbf{2}(2)$ (see also DIAS & IOOSS [52]).

Due to the existence of an horseshoe map (proved by DEVANEY [50]), there exists an infinity of homoclinic orbits for any $P \in]-2, 2[$. However, BUFFONI, CHAMPNEYS & TOLAND [27, 34] presented numerical evidence that each multi-pulse $\mathbf{n}(i_1, i_2, \ldots, i_{n-1})$ orbit which is not $\mathbf{2}(2)$ ceases to exist at a point $P_{\mathbf{n}(m_{i_1}, m_{i_2}, \ldots, m_{i_{n-1}})}$.

It turns out that branches of multipulse orbits connect to each other at $P = P_{crit}$ in two different manners:

- Coalescence (corresponding to figure 3.14):

  When $P < P_{crit}$, no orbit exists.

  When $P = P_{crit}$, there is one non-transverse homoclinic orbit, e.g. an orbit for which $\dim(\mathcal{U}(x, 0) \cap \mathcal{S}(x, 0)) > 1$.

  When $P > P_{crit}$, there are two homoclinic orbits converging to the non-transverse orbit when $P \to P_{crit}^+$.

---

[1]Let u be the eigenfunction associated to the purely imaginary simple eigenvalue $i\theta$. Then, the Krein signature of $i\theta$ is defined as the sign of $\langle u, \mathcal{L}u \rangle$. More details about the Krein signature in finite dimension is given in Appendix C.
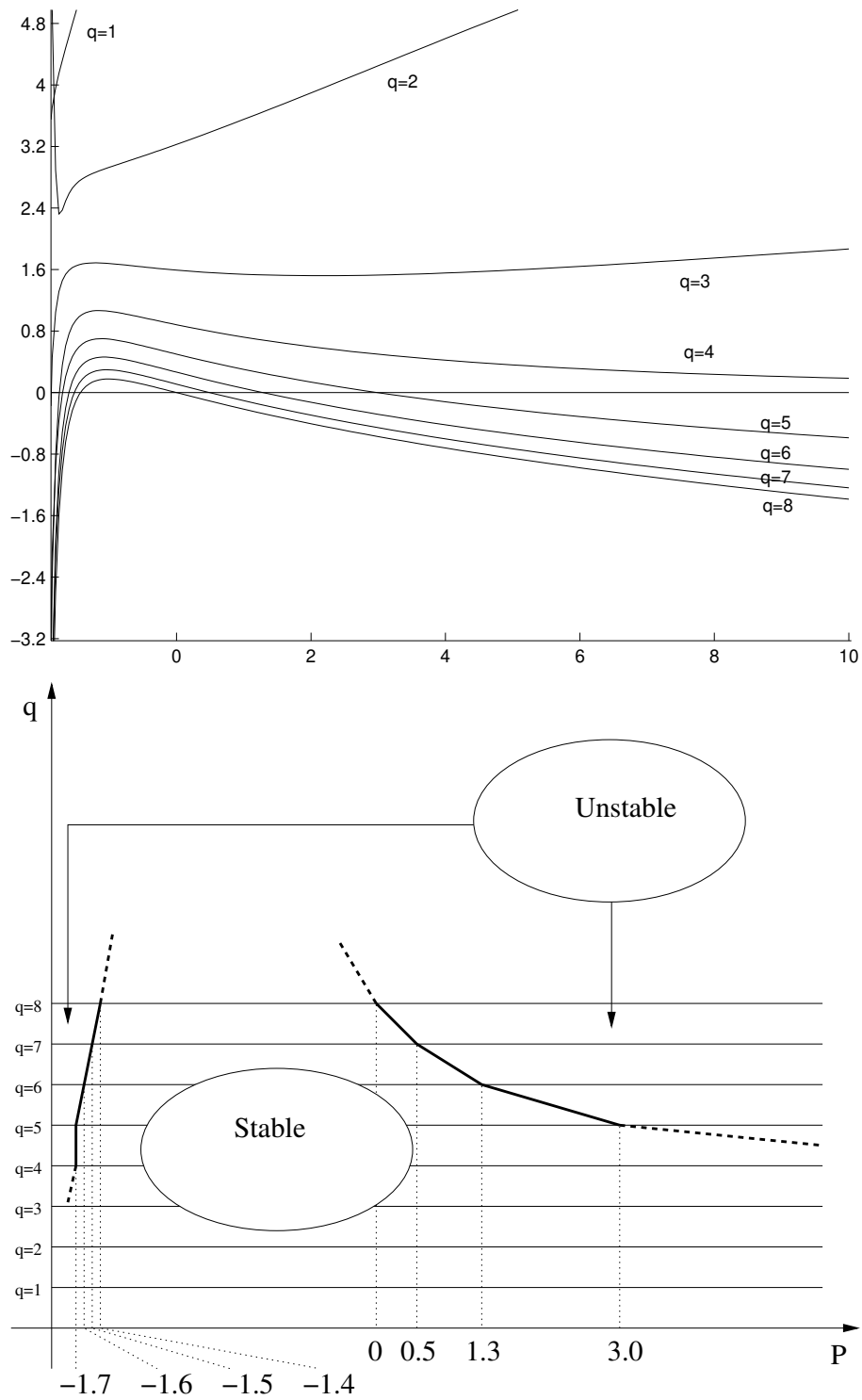
Figure 3.11: Unimodal case. Top, values of $\frac{\mathrm{d}N}{\mathrm{d}c}$ as a function of P for several values of q. Bottom, stability domain of the unimodal solution in the (P, q)-plane.
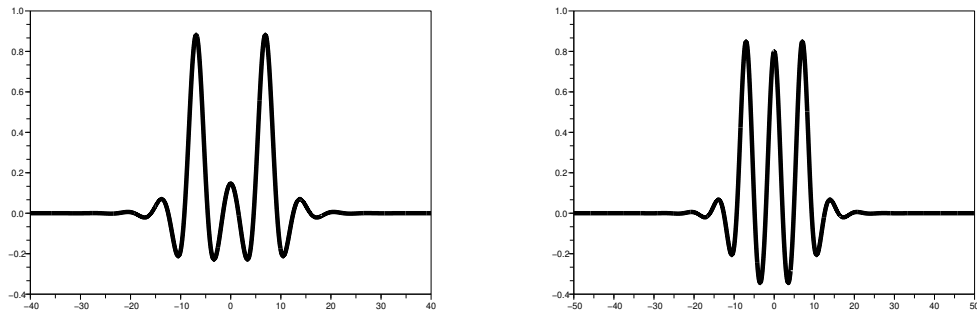
Figure 3.12: Orbits **2**(4) and **3**(2, 2) when $P = -1.5$. These two orbits coalesce when $P = -1.79047$. The difference in the Maslov index between these two orbits is one.
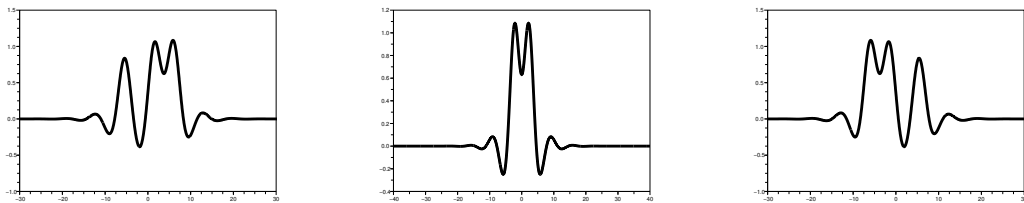
Figure 3.13: Orbits **3**(2, 1), **2**(1), **3**(1, 2) when $P = -1.5$. **3**(2, 1) and **3**(1, 2) bifurcates from **2**(1) at $P = 1.83817$.
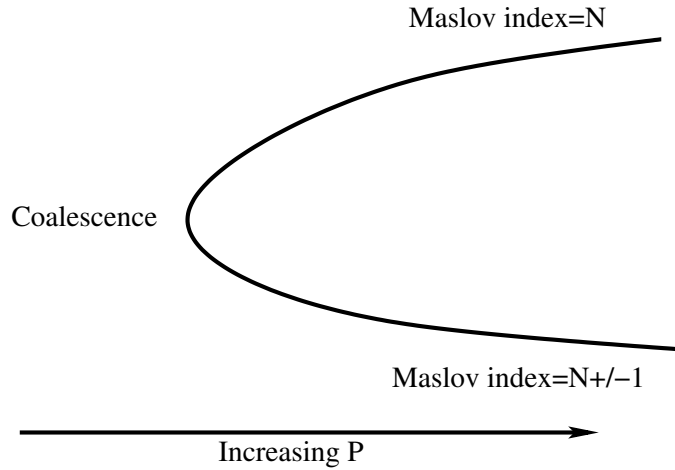
Figure 3.14: The bifurcation diagram near a coalescence. At the coalescence, the Maslov index jumps by one.

- Pitchfork bifurcation (corresponding to figure 3.15):

  When $P < P_{crit}$, there is one symmetric orbit.

  When $P = P_{crit}$, there is one symmetric non-transverse orbit.

  When $P > P_{crit}$, there are one symmetric orbit and two asymmetric orbits. The two asymmetric orbits are image of one another by a reflection (e.g if ϕ^l is one of the asymmetric orbits, the other is $\phi^r(x) = \mathcal{R}\phi^l(-x)$).

Several immediate remarks can be made:

- The Maslov index can jump by at most one. Otherwise, the intersection of the stable space and of the unstable space would be strictly greater than 2 for the orbit corresponding to jump.

- If $\phi^l(x) = \mathcal{R}\phi^r(-x)$, then ϕ^l and ϕ^r have the same Maslov index.

We observed that:

- The Maslov index of the homoclinic orbit jumps by one when changing of branch in the coalescence case.

- Let us now study the pitchfork bifurcation case:

  Let $P_1 < P_{crit} < P_2$.

  Let $\phi^{sym,1}$ be the symmetric orbit when $P = P_1$.

  Let $\phi^{sym,2}$ be the symmetric orbit when $P = P_2$ and let ϕ^l and ϕ^r be the two asymmetric orbits when $P = P_2$.

  Then the Maslov index has the following behaviour:
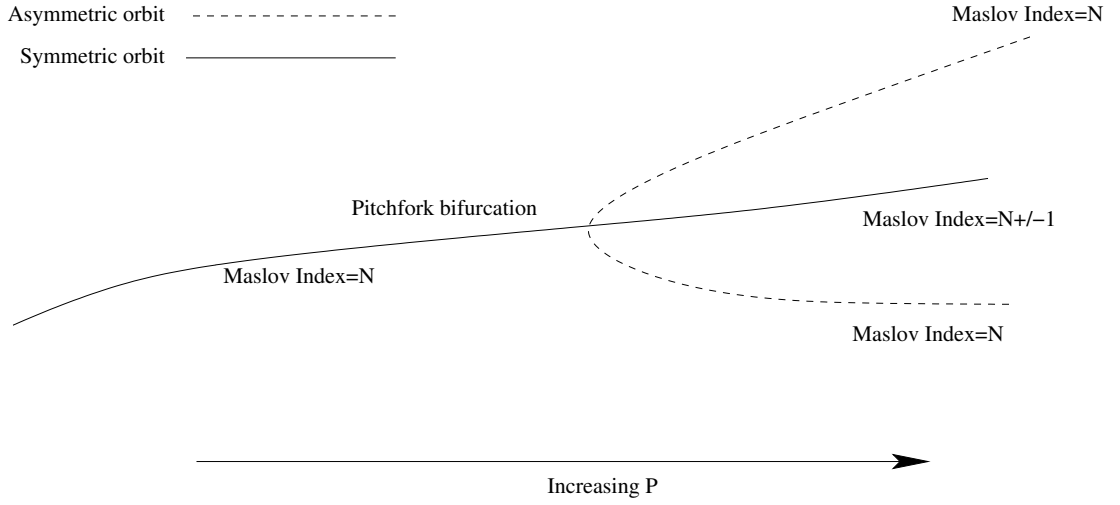
Figure 3.15: The bifurcation diagram near a pitchfork bifurcation and the Maslov index

$$I_{hom}(0, \phi^{sym,1}) = I_{hom}(0, \phi^l) = I_{hom}(0, \phi^r),$$

and

$$|I_{hom}(0, \phi^{sym,1}) - I_{hom}(0, \phi^{sym,2})| = 1.$$

That means that a bifurcation point may be the place of an exchange of stability. Besides, taking into account formula (3.5.17), the Maslov index can be useful to determine which orbits connect each other.

3.6   Direct study of the spectrum of $\mathbf{L} = \partial_x \mathscr{L}$

In this section, we use the algorithm presented by BRIDGES, DERKS & GOTTWALD [21] to look at the spectrum of $\mathbf{L}$.

The spectral problem $\mathbf{L}u = \lambda u$ can be put into a first-order system:

$$u_x = \mathbf{A}(x, \lambda)u,$$

$$\mathbf{A}(x, \lambda) = \begin{pmatrix} 0 & 1 & 0 & 0 & 0 \\ 0 & 0 & 1 & 0 & 0 \\ 0 & 0 & 0 & 1 & 0 \\ -a(x) & 0 & P & 0 & 1 \\ \lambda & 0 & 0 & 0 & 0 \end{pmatrix}, \quad a(x) = 1 - (p+1)\,\widehat{\phi}(x)^q \qquad (3.6.20)$$

The essential spectrum of $\mathbf{L}$ is:

$$\sigma_{ess} = \{\lambda \quad | \quad \exists \kappa \in \mathbb{R} \quad \det(\mathbf{A}_\infty(\lambda) - i\kappa) = 0\} = i\mathbb{R}$$

Therefore σ_{ess} splits $\mathbb{C}$ into two parts.

Then, it is possible to construct an Evans function for $\mathbf{L}$ on $\{\lambda \in \mathbb{C} | \operatorname{Re}(\lambda) > 0\}$ like in section 2.4.1:

Let $\mathbf{U}(x, \lambda)$ and $\mathbf{S}(x, \lambda)$ be solutions of $\mathbf{U}_x(x, \lambda) = \mathbf{A}^{(2)}(x, \lambda)\mathbf{U}(x, \lambda)$ and $\mathbf{S}_x(x, \lambda) = \mathbf{A}^{(3)}(x, \lambda)\mathbf{S}(x, \lambda)$ with maximal decay as x goes to $-\infty$ and $+\infty$ respectively satisfying

$$\lim_{x \to -\infty} e^{-\sigma_+(\lambda)x}\mathbf{U}(x, \lambda) = \zeta^+(\lambda) \in \bigwedge\nolimits^2(\mathbb{C}^5), \tag{3.6.21}$$

and

$$\lim_{x \to +\infty} e^{-\sigma_-(\lambda)x}\mathbf{S}(x, \lambda) = \zeta^-(\lambda) \in \bigwedge\nolimits^3(\mathbb{C}^5), \tag{3.6.22}$$

where $\zeta^\pm(\lambda)$ are eigenvectors

$$\mathbf{A}_\infty^{(\frac{5}{2} \pm \frac{1}{2})}(\lambda)\zeta^\pm(\lambda) = \sigma_\pm(\lambda)\zeta^\pm(\lambda). \tag{3.6.23}$$

A value $\lambda \in \mathbb{C} \setminus \sigma_{ess}$ is called an eigenvalue if the stable and unstable solutions have nontrivial intersection. Eigenvalues are detected by the following Evans function:

$$E(\lambda)\,\mathsf{vol} = \mathbf{S}(x, \lambda) \wedge \mathbf{U}(x, \lambda) \in \bigwedge\nolimits^5(\mathbb{C}^5). \tag{3.6.24}$$

where vol is the standard volume form over $\mathbb{R}^5$. As in section 2.4.1, we use the fact that $\operatorname{trace}(\mathbf{A}(x, \lambda)) = 0$. Again, the following normalization is chosen:

$$\zeta^+(\lambda) \wedge \zeta^-(\lambda) = \mathsf{vol} \tag{3.6.25}$$

The numerical computation of the Evans function works as follow:

- Initialize $\widehat{\mathbf{U}}(-L, \lambda)$ to $\zeta^+(\lambda)$ and $\widehat{\mathbf{S}}(-L, \lambda)$ to $\zeta^-(\lambda)$ with $\zeta^+(\lambda) \wedge \zeta^-(\lambda) = \mathsf{vol}$.

- Integrate $\mathbf{U}_x(x, \lambda) = (\mathbf{A}^{(2)}(x, \lambda) - \sigma_+(\lambda)\mathbf{I})\mathbf{U}(x, \lambda)$ and $\mathbf{S}_x(x, \lambda) = (\mathbf{A}^{(3)} - \sigma_-(\lambda)\mathbf{I})\mathbf{S}(x, \lambda)$ over $[-L, 0]$ and $[0, L]$ using any standard integrator[2].

- Return $E(\lambda)$ such that $\widehat{\mathbf{S}}(0, \lambda) \wedge \widehat{\mathbf{U}}(0, \lambda) = E(\lambda)\,\mathsf{vol}$.

Once the Evans function is computable, one can:

- Compute the Evans function over $\alpha + i\mathbb{R}$. Then the number of eigenvalues with a real part greater than α is the number of loops made by $t \to E(\alpha + it)$ around 0.

- Use the secant method to locate eigenvalues.

BURYAK & CHAMPNEYS theory predicts that two-pulse solutions with an odd index have an unstable real eigenvalue. Now consider the $\mathbf{n}(i_1, i_2, \ldots, i_{n-1})$ pulse. One could conjecture that each odd index i_α should be associated to a real eigenvalue, i.e. $n_{even} = N_{real}$ when $r = 1$. This prediction is consistent with the Evans computations we performed.

However, we find for most cases that there is a pair of complex eigenvalues with a small real part associated to each even index. Dividing by two the step and multiplying by two the length of the interval did not shift significantly the eigenvalue. Hence, this suggests $N_{imag}^- \neq 2n_{odd}$.

---

[2]Here, the fourth-order Runge-Kutta method was used.
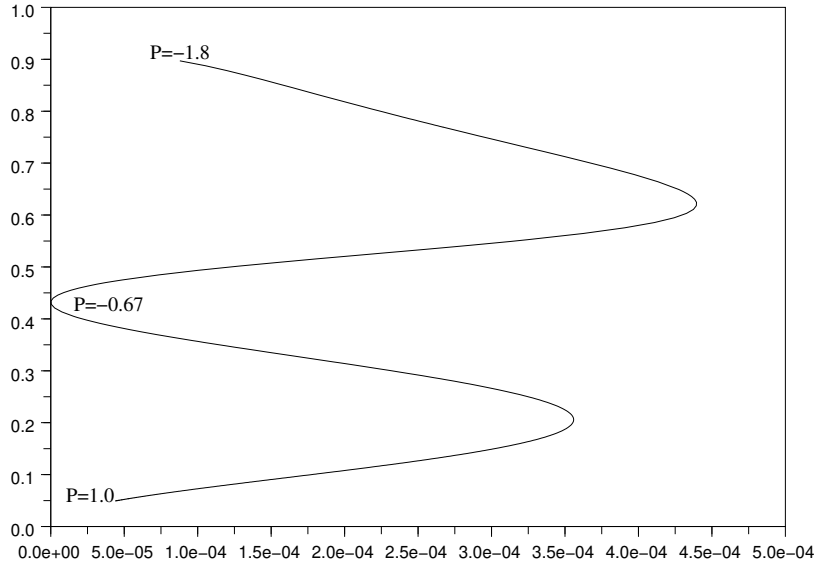
Figure 3.16: Eigenvalue of $\mathbf{L} = \partial_x \mathscr{L}$ in the case of the bimodal solitary wave $\mathbf{2}(1)$, when $P \in [-1.8, 1]$. The real part of this eigenvalue seems to vanish for a value of P close to -0.666.

This means that a lot of multi-pulse solutions with only odd indices might be unstable. We also tried to track these eigenvalues when P is varied. Some of the results are presented in figure 3.16 and 3.17.

According to the estimates of CHUGUNOVA & PELINOVSKY [42], when P is close to 2, these eigenvalues should tend to 0, their real part tending to zero much faster than their imaginary part. While we were not able to confirm this prediction for the solitary wave $\mathbf{2}(1)$ (it would be needed to go further than $P = 1$ to observe this convergence), this seems to be confirmed for $\mathbf{2}(3)$. The difference in the speed of convergence may be due to:

- the fact that the real part of the eigenvalue of $\mathbf{2}(1)$ is already small,

- the fact that the two pulses of $\mathbf{2}(1)$ remain close to each other much longer that the two pulses of $\mathbf{2}(3)$.

An intriguing phenomenon is that in the case of the solitary wave $\mathbf{2}(1)$, there is a value of P (i.e. $P \approx -0.666$) for which the real part of the complex eigenvalue seems to vanish (the smallest real part observed was 10^{-12}, which is quite close to the machine error). For this value of P, the solitary wave would be stable. A similar pattern was also observed for other solitary waves with a 1 in their classifying sequence.
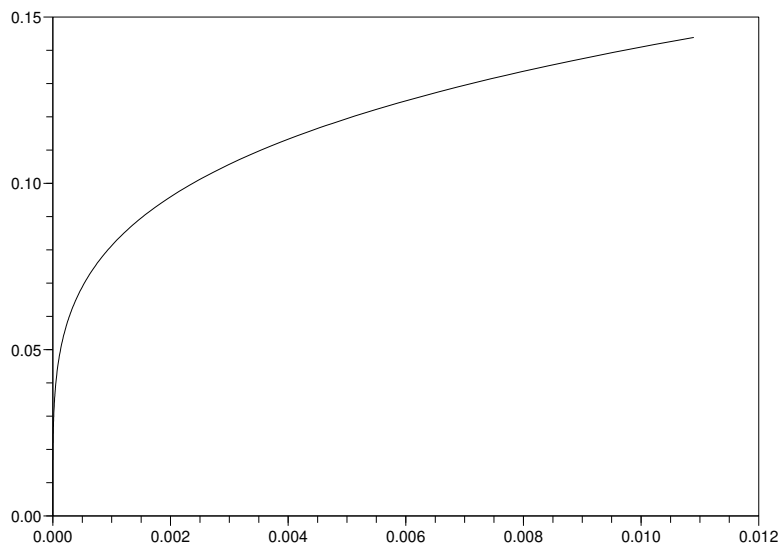
Figure 3.17: Eigenvalue of $\mathbf{L} = \partial_x \mathscr{L}$ in the case of the bimodal solitary wave $\mathbf{2}(3)$, when P is in $[-1.5, 0.65]$. The eigenvalue tends to 0 when $P \to 2$.

3.7 The Maslov index of periodic waves of the Kawahara equation

In this section, we study the Maslov index of *spatially*-periodic waves approximating the unimodal homoclinic orbit. The existence of such periodic orbits have been proved by VANDERBAUWHEDE & FIEDLER [120]. Two cases emerge:

- The homoclinic orbit has non-oscillating tails, e.g. $P \in [2, \infty[$.

- The homoclinic orbit has oscillating tails, e.g. $P \in]-2, 2[$.

The goal of this study was to test the numerical algorithm presented in section 2.3 on a concrete example and to try to give an intrinsic definition of the Maslov index of homoclinic orbits at $\lambda = 0$. As we shall see for the case where $P \in]-2, 2[$, this attempt failed, since the energy of these periodic orbits can oscillate.

Finally, we make some remarks on the stability of these periodic orbits.

3.7.1 Periodic solutions when $P > 2$

In this section, we study numerically the periodic solutions for $P \in]2, \infty[$. They approximate the unimodal solution, which has in this case non-oscillating tails.

In Figure 3.18 examples of periodic solutions of (3.2.8) are shown for the case of $q = 1$ and $P = \frac{13}{6}$. These solutions have been computed numerically.
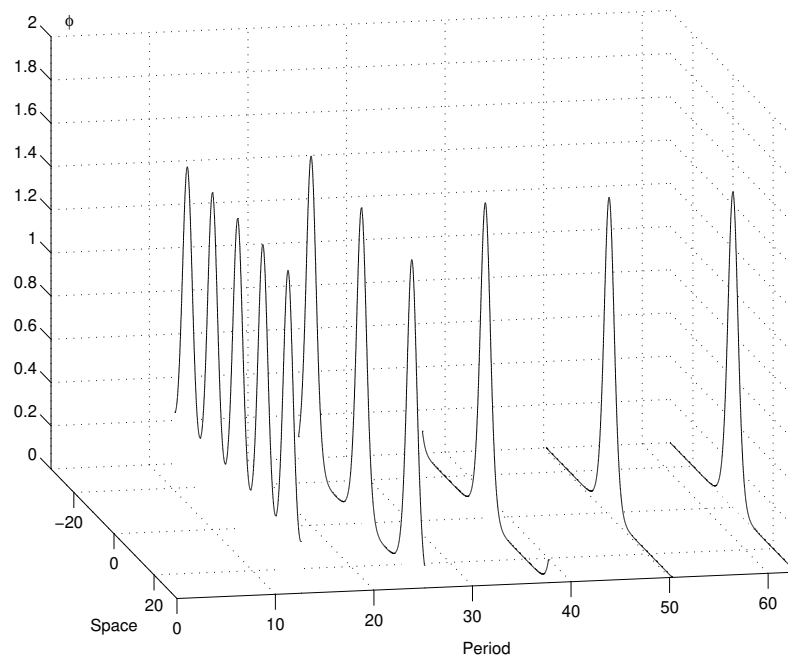
Figure 3.18: Periodic solutions of the steady Kawahara equation for $q = 1$, $P = \frac{13}{6}$ and periods $4\pi, 8\pi, 12\pi, 16\pi, 20\pi$.

Elements λ in the spectrum of $\mathscr{L}$ satisfy $\mathscr{L}w = \lambda w$ with w bounded for $x \in \mathbb{R}$ and, since $\mathscr{L}$ is self-adjoint as a mapping from $\mathscr{D}(\mathscr{L}) \to L^2(\mathbb{R})$, the spectrum is real[3]. For operators with periodic coefficients, the discrete spectrum is empty, and the spectrum consists of a sequence of bands [128].

When $\lambda = 0$ and $\phi(x)$ is periodic, this system is not hyperbolic because it is the linearization about an autonomous ODE. But when λ is perturbed away from zero the two Floquet multipliers at $+1$ move, becoming either elliptic[4] or hyperbolic[5]. At other values of λ, there can be bifurcations of Floquet multipliers as well; indeed, such bifurcations can be expected due to the band structure of the spectrum of $\mathscr{L}$. These issues will appear in the numerics.

In the following figures, the results of our calculations of the Maslov index are shown, for periodic solutions of (3.2.8) with periods $L = 4\pi, 8\pi, 16\pi, 20\pi$. For each of the four cases, two figures are shown. The first figure shows the number of iterations for the algorithm of section 2.3 to converge (an iteration is an integration from $x = (r-1)L$ to $x = rL$ for some integer r). When the system is hyperbolic, the Maslov index converges fast, and in the spectral bands the algorithm generally fails to converge. However, as shown in the second plot for each case, the Maslov index at bifurcation points is easily determined by computing in a left or right neighborhood of the bifurcation points. The Maslov index shows its expected behavior for values of λ less than ≈ 1.

The fluctuations in the region λ greater than ≈ 1 are due to the appearance of spectral bands. When entering a band, as λ is varied, at least two Floquet multipliers (one inside the circle and the other outside) collide on the unit circle. Then they move along the unit circle. When leaving the band, Floquet multipliers collide again and leave the circle. When λ is in a band, there are Floquet multipliers on the unit circle and hyperbolicity is lost. Hence when λ is in a band the algorithm should not (and does not) in general converge.

The bands can be observed in the numerical results: the non-convergence can be used as an indication of the presence of spectrum. If the number of iterations necessary for convergence exceeded 100, it was considered an indication that the value λ was in a spectrum band or close to it. Another indication of a band, where some Floquet multipliers are on the unit circle, is the change in the value of the Maslov index: between two real numbers where the Maslov index is different, there is at least a band.

A lower bound for all the bands can be computed which is valid for all finite wavelengths. If λ is in a band, then there exists w and γ such that $\mathscr{L}w = \lambda w, \forall x \quad w(x+L) = \gamma w(x)$ and $|\gamma| = 1$. Multiply $\mathscr{L}w - \lambda w$ by $\overline{w}(x)$ and integrate over a period:

$$\int_0^L |w_{xx}|^2 \, \mathrm{d}x + P \int_0^L |w_x|^2 \, \mathrm{d}x - 2 \int_0^L |\phi(x)|^2 |w|^2 \, \mathrm{d}x + \int_0^L |w|^2 \, \mathrm{d}x = \lambda \int_0^L |w|^2 \, \mathrm{d}x \, .$$

Now use the fact that $P > 0$ and $|\phi(x)| \leq \phi^{\mathrm{max}}$ for all $x \in \mathbb{R}$ to obtain

$$\lambda \geq 1 - 2|\phi^{\mathrm{max}}|^2 \, .$$

With $|\phi^{\mathrm{max}}| \approx 1.4$ (from Figure (3.18)), we obtain a lower bound of approximately -3. This is

---

[3] $\mathscr{D}(\mathscr{L})$ is the domain of the operator $\mathscr{L}$ and can be taken to be the Hilbert space $H^4(\mathbb{R})$ in this case.

[4] An eigenvalue of a symplectic matrix is said to be elliptic if it is on the unit circle. See Appendix A.

[5] An eigenvalue of a symplectic matrix is said to be hyperbolic if it is a real strictly positive number. See Appendix A.
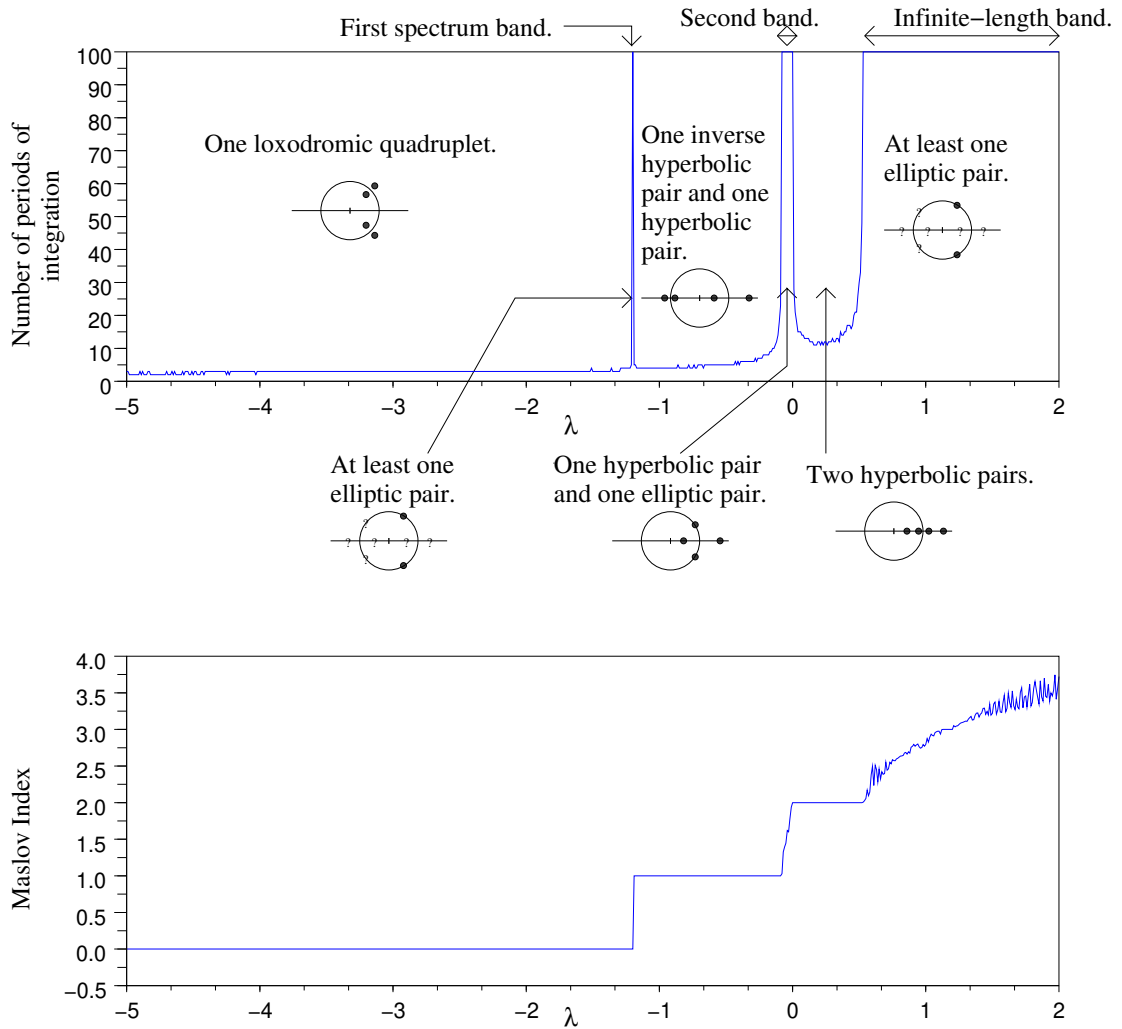
Figure 3.19: Maslov index $I_{per}(\phi, \lambda)$ of the 4π-periodic solution as a function of λ and position of the Floquet multipliers of the system. The classification of the Floquet multipliers is explained in definition 26 of Appendix A.1.
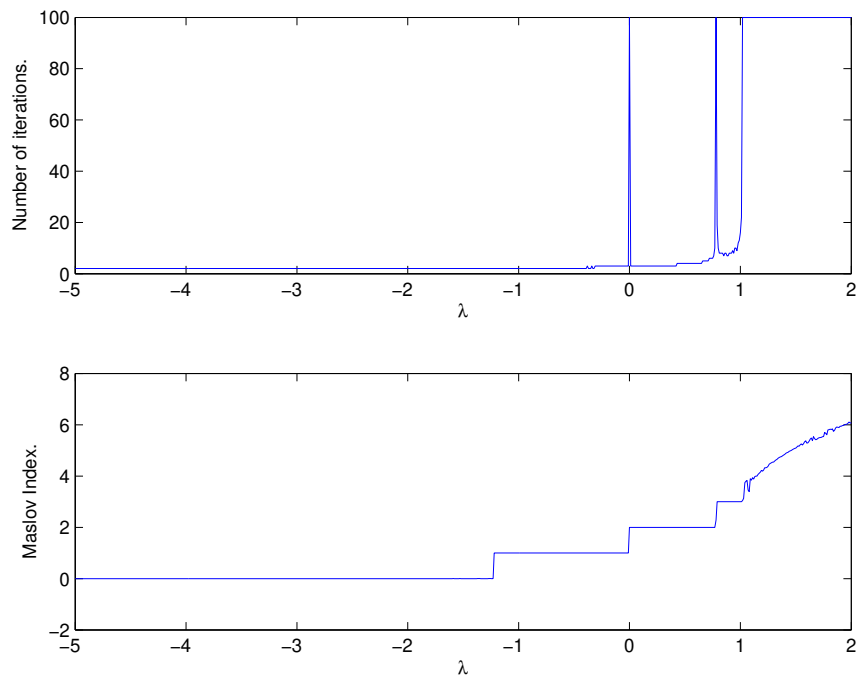
Figure 3.20: Maslov index of the 8π-periodic solution as a function of λ.
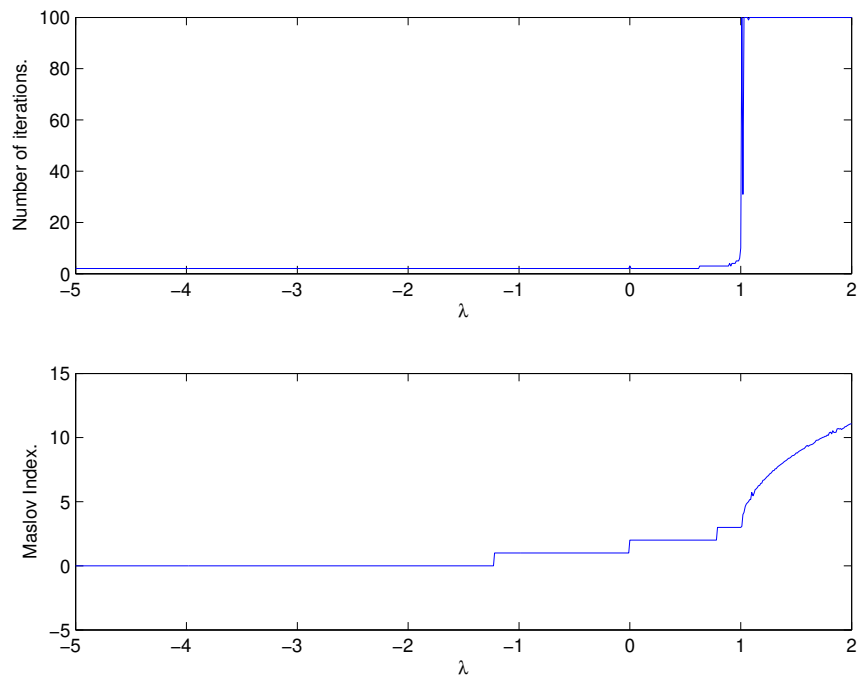
Figure 3.21: Maslov index of the 16π-periodic solution as a function of λ.
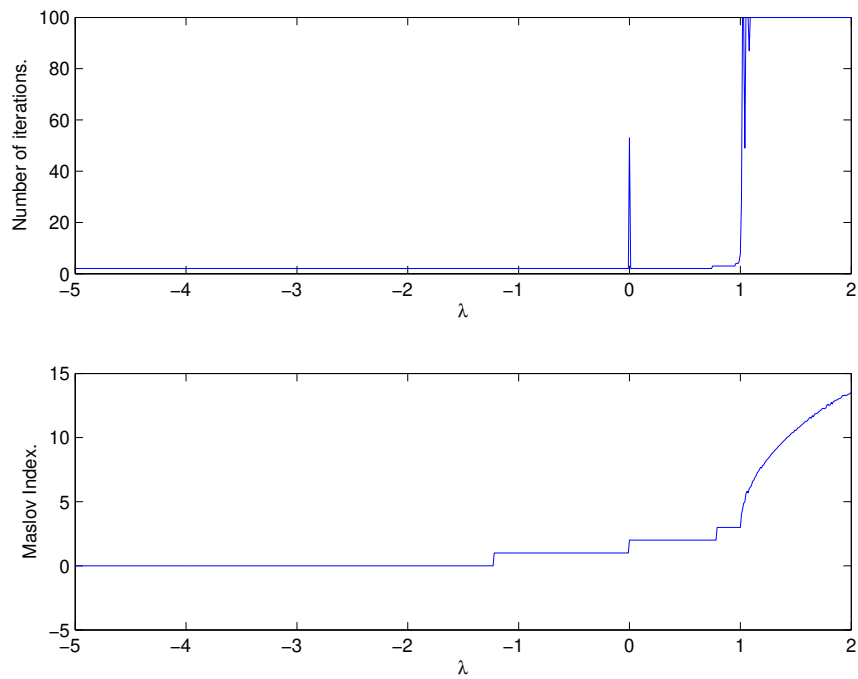
Figure 3.22: Maslov index of the 20π-periodic solution as a function of λ.
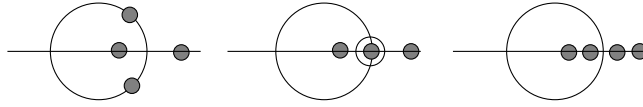
Figure 3.23: Position of the Floquet multipliers when going from $\lambda < 0$ to $\lambda > 0$ when $q = 1$ and $P = \frac{13}{6}$

consistent with the numerical computations which indicate that the lowest band is at approximately -1.25.

When the period of the periodic state $\phi(x)$ tends to ∞, the width of the bands contracts, and in the limit the continuous spectrum is limited to the one band $\lambda \in [1, \infty)$, of infinite length, and the band near zero contracts to the point $\lambda = 0$.

Consider now the case when λ is near zero. In this case the system is hyperbolic on only one side of $\lambda = 0$. When $\lambda = 0$ there are two Floquet multipliers at $+1$ and two hyperbolic Floquet multipliers as shown schematically in the middle figure in Figure 3.23.

It is clear from Figure 3.19 that there is a band for $\lambda = 0^-$ and for $\lambda = 0^+$ the system is hyperbolic, as shown schematically in Figure 3.23. Our theory applies for $\lambda = 0^+$ which gives a Maslov index of $I_{per}(\phi) = 2$. The energy of the periodic waves is plotted as a function of k on figure 3.24. In this case the energy is a monotone function of wave number and the convergence $k \to 0$ is rapid. According to section 1.3.1, there should be a band on the left if $E'(k) > 0$ and on the right if $E'(k) < 0$. The fact that $E'(k) > 0$ is consistent with the fact that the spectrum band is on the left.

$I_{per \to hom}(\phi)$, introduced in section 1.3.1, seems therefore to be well-defined. Its value would be 2.

3.7.2   Periodic solutions when $-2 < P < 2$

Keeping $q = 1$ but decreasing P to $P = -1$, then the energy of the periodic solutions as function of the wave number k begins to show oscillations indicative of a Shilnikov-type bifurcation as shown in Figure 3.25. Decreasing P further to $P = -1.9$ shows more dramatically the Shilnikov-type oscillations. Each point on this diagram where $E'(k) = 0$ corresponds to a saddle-centre bifurcation of Floquet multipliers. There are always two Floquet multipliers at $+1$ due to the fact that (3.2.8) is autonomous. When $E'(k) = 0$, two additional Floquet multipliers coalesce at $+1$. Therefore, for some orbits on the branch, the spectrum band extends on both sides of 0. Each one of these saddle-centre bifurcations of the branch of periodic orbits leads to a secondary homoclinic bifurcation [24]. So, in addition to the limiting homoclinic orbit that we are principally interested in, there is a countable number of other orbits generated along the branch, which are homoclinic to the branch of periodic orbits. Although there is an infinite number of bifurcations along the branch we will see that the Maslov index of the limiting homoclinic orbit is finite.

It follows that when $-2 < P < 2$, $I_{per \to hom}(\phi)$ is ill-defined.

It is also possible to compute periodic approximations to multi-modal solutions. The same phenomenon as for uni-modal solutions takes place: families of periodic orbits approaching mul-
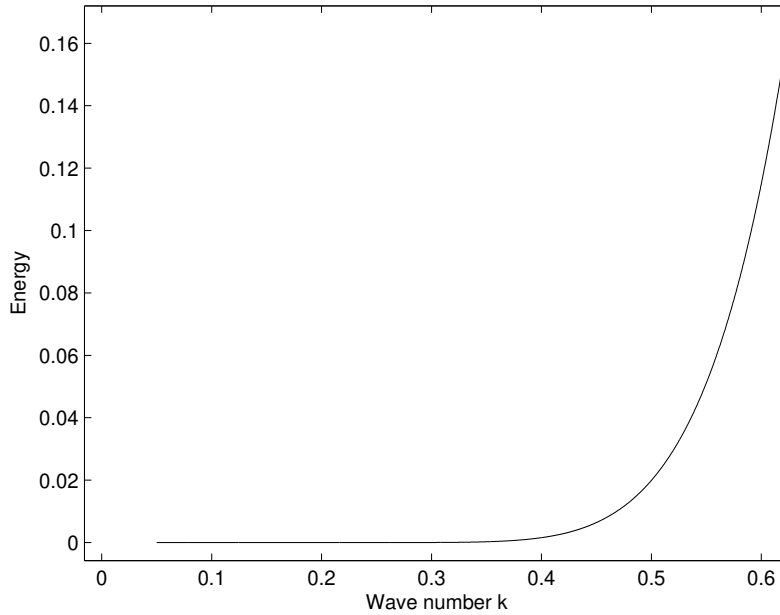
Figure 3.24: Energy of the $\frac{2\pi}{k}$-periodic solutions as function of k for $q = 1$ and $P = \frac{13}{6}$.

timodal solutions have an oscillating Hamiltonian with respect to the period as shown in Figures 3.25 and 3.26.

3.7.3 Remarks concerning the stability of the periodic waves

Define the unbounded operators $\mathscr{L}_\theta$ and $\mathbf{L}_\theta$ over $L^2_{per}([0, L])$ as:

$$\mathbf{L}_\theta \phi := (\partial_x + i\frac{\theta}{L})\mathscr{L}_\theta \phi \tag{3.7.26}$$

$$\mathscr{L}_\theta \phi := (\partial_x + i\frac{\theta}{L})^4 \phi - P(\partial_x + i\frac{\theta}{L})^2 \phi + c\phi - (q+1)\widehat{\phi}(x)^q \phi. \tag{3.7.27}$$

$\mathscr{L}_\theta$ and $\mathbf{L}_\theta$ have only point spectrum.

According to Bloch wave decomposition, we have:

$$\operatorname{spec} \mathbf{L} = \bigcup_{\theta \in [0, 2\pi[} \operatorname{spec} \mathbf{L}_\theta$$

$$\operatorname{spec} \mathscr{L} = \bigcup_{\theta \in [0, 2\pi[} \operatorname{spec} \mathscr{L}_\theta$$

If $0 \notin \operatorname{spec} \mathscr{L}_\theta$, then, according to results of [42, 41, 75] we have:

$$N_{unst}(\theta) + N^-_{imag}(\theta) = n_-(\theta)$$
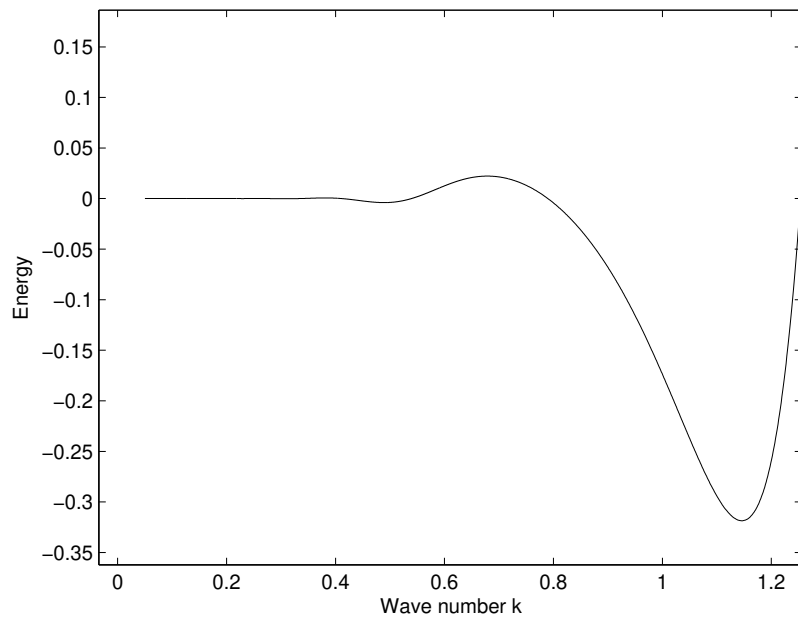
Figure 3.25: Energy of the $\frac{2\pi}{k}$-periodic solutions as function of k for $q = 1$ and $P = -1$.
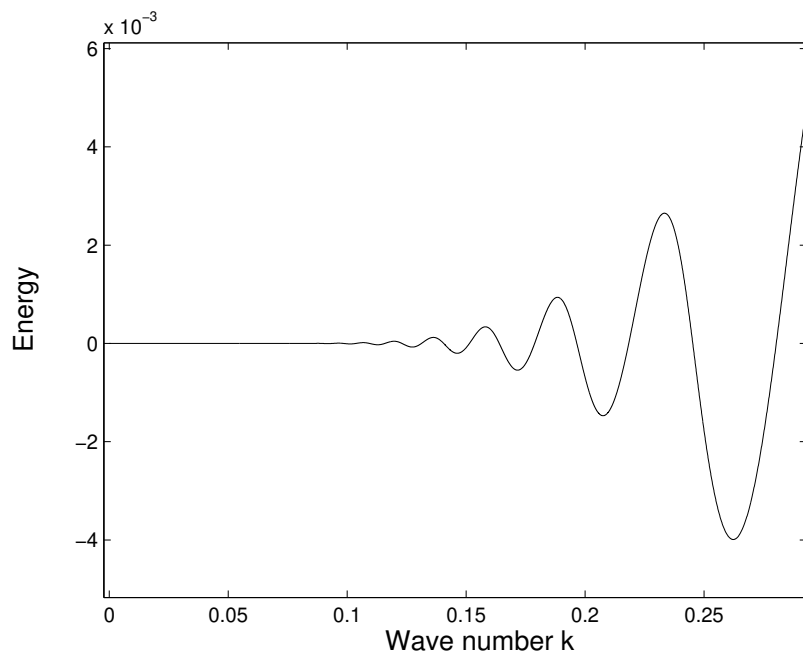
Figure 3.26: Enlargement of the low wavenumber region of the Energy-wavenumber plot for the parameter values $q = 1$ and $P = -1.9$.

with:

- $N_{unst}(\theta)$ the number of unstable modes of $\mathbf{L}_\theta$,

- $N^-_{imag}(\theta)$ the number of oscillatory modes of $\mathbf{L}_\theta$ with negative energy, e.g. $\langle u, \mathscr{L}_\theta u \rangle < 0$,

- $n_-(\theta)$ the number of strictly negative eigenvalues of $\mathscr{L}_\theta$.

$N^-_{imag}(\theta)$ is an even number, and except for isolated values of θ, we will have $0 \notin \operatorname{spec} \mathscr{L}_\theta$. Assume that we are in one of the following two cases:

- the periodic orbit is not hyperbolic and there exists $\theta \neq 0[\pi]$ such that $0 \in \operatorname{spec}(\mathscr{L}_\theta)$.

- the periodic orbits have an odd Maslov index (1 in this case).

For each $P \in]-2, 2[$, there exists an infinity of periodic solutions in this situation.

Then there exists θ such that $0 \notin \operatorname{spec} \mathscr{L}_\theta$ and $n_-(\theta)$ is odd. Therefore, $N_{unst}(\theta)$ is odd and there will be at least a real unstable eigenvalue for $\mathbf{L}_\theta$. As a consequence, these solutions are not spectrally stable.

That means that a lot of periodic orbits in the oscillating case are spectrally unstable.

When $P \in]2, +\infty[$, the periodic orbits are hyperbolic and their Maslov index is two. Hence we have:

- $n_-(\theta) = 2$ and $0 \notin \operatorname{spec} \mathscr{L}_\theta$ if $\theta \neq 0[2\pi]$,

- $n_-(0) = 1$.

As a consequence, we have:

$$\forall \theta \neq 0[2\pi] \quad N_{unst}(\theta) + N^-_{imag}(\theta) = 2.$$

Hence, this does not give enough information to conclude on stability. However, taking into account that the limiting homoclinic orbit is stable, these orbits are likely to be stable.

3.8 Conclusion

We found an interesting relationship (3.5.17) between the classification of multi-pulse solitary waves and their Maslov index. The Maslov index provides valuable information on the stability of Kawahara solitary waves: when $I_{hom}(\phi, 0) - \frac{1}{2}$ is even (assuming that $r = 1$), the solitary wave is unstable. This is sufficient to recover the instability results in [30, 42] concerning the two-pulse solitary waves, e.g. that the solutions $\mathbf{2}(2i)$ are unstable. Besides, it gives the maximal number of unstable eigenmodes.

In the periodic case, we make the observation that a non-hyperbolic orbit and hyperbolic orbits with an odd Maslov index cannot be stable with respect to localized perturbations. From this observation, we are able to conclude on the instability of some periodic waves, when $P \in]-2, 2[$.

The numerical computation of the Evans function revealed an unexpected behaviour: it seems that all multi-pulse solitary waves are unstable, including those of type $\mathbf{2}(2i+1)$. This new kind of instability is however very weak, especially when $P \to 2^-$, and these multi-pulse solutions might be observed in a transitional manner.

Chapter 4

The Maslov index of solitary waves arising in the long wave-short wave resonance equation

Contents

Introduction

In this chapter, we study the Maslov index of solitary waves arising in a model PDE for the long-wave short-wave resonance. It serves as a test case for the computation of the Maslov index in 6-dimensional case. Secondly, we study an operator, which has been inspired by the long-wave short-wave equations, with a non-monotone Maslov index. It highlights the importance of the semi-definiteness $\partial_\lambda \mathbf{C}(x, \lambda)$, which is not automatic for spectral problems which do not come from the Hessian of a functional.

4.1   A model PDE for long-wave short-wave resonance

In this section the Maslov index is computed numerically for a class of solitary waves which arise in a model PDE for long-wave short-wave (LW-SW) resonance (cf. KAWAHARA ET AL. [81], MA [91], BENILOV & BURTSEV [12], LATIFI & LEON [86]). The LW-SW equations are a coupled system with one equation of nonlinear Schrödinger type and the other of KdV type. A typical form is

$$\begin{aligned}
E_t &= \mathrm{i}(E_{xx} + \rho E - \nu E) \\
\rho_t &= \partial_x(\rho_{xx} - c\rho + 3\rho^2 + |E|^2)\,,
\end{aligned} \tag{4.1.1}$$

were $\rho(x,t)$ is real valued, $E(x,t)$ is complex valued, and c, ν are considered to be positive real parameters. In real coordinates, $E = u + \mathrm{i}v$ and $\rho = w$, the above equations can be written:

$$\begin{aligned}
u_t &= -v_{xx} - vw + \nu v \\
v_t &= u_{xx} + uw - \nu u \\
w_t &= w_{xxx} - cw_x + 6ww_x + 2uu_x + 2vv_x\,.
\end{aligned} \tag{4.1.2}$$

This system can be expressed as a Hamiltonian system in time.

Let:

$$\omega((u_1, v_1, w_1), (u_2, v_2, w_2)) = \int_{\mathbb{R}} \left(2(u_1 v_2 - u_2 v_1) + w_1(\partial_x)^{-1} w_2\right) \mathrm{d}x$$

$$\mathcal{H}(Z) = \int_{-\infty}^{+\infty} \left(u_x^2 + v_x^2 + \frac{1}{2}w_x^2 - w(w^2 + u^2 + v^2) + \frac{1}{2}cw^2 + \nu(u^2 + v^2)\right) \mathrm{d}x,$$

with $Z = (u, v, w)$.

Then the previous system is equivalent to a Hamiltonian system, with ω as the symplectic form and H as the Hamiltonian.

If we set:

$$\mathbf{K} = \begin{bmatrix} 0 & \frac{1}{2} & 0 \\ -\frac{1}{2} & 0 & 0 \\ 0 & 0 & -\partial_x \end{bmatrix},$$

then the system becomes

$$Z_t = \mathbf{K}\nabla\mathcal{H}(Z)\,,$$

$$\nabla\mathcal{H}(Z) = \begin{pmatrix} \mathcal{H}_u \\ \mathcal{H}_v \\ \mathcal{H}_w \end{pmatrix} = \begin{pmatrix} -2u_{xx} - 2uw + 2\nu u \\ -2v_{xx} - 2vw + 2\nu v \\ -w_{xx} + cw - 3w^2 - u^2 - v^2 \end{pmatrix}.$$

If we look for solitary wave solutions, the Euler-Lagrange equations give:

$$\begin{aligned}
-2u_{xx} - 2uw + 2\nu u &= 0 \\
-2v_{xx} - 2vw + 2\nu v &= 0 \\
-w_{xx} + cw - 3w^2 - u^2 - v^2 &= \mathtt{constant}\,.
\end{aligned} \tag{4.1.3}$$

Using equation (B.2.3), one can cast this system into an Hamiltonian form, by choosing the following set of coordinates:

$$
\begin{pmatrix} u \\ v \\ w \\ \frac{\partial l}{\partial u_x} \\ \frac{\partial l}{\partial v_x} \\ \frac{\partial l}{\partial w_x} \end{pmatrix} = \begin{pmatrix} u \\ v \\ w \\ 2u_x \\ 2v_x \\ w_x \end{pmatrix} \tag{4.1.4}
$$

where $l(u, v, w, u_x, v_x, w_x) = u_x^2 + v_x^2 + \frac{1}{2}w_x^2 - w(w^2 + u^2 + v^2) + \frac{1}{2}cw^2 + \nu(u^2 + v^2)$.

Solitary waves satisfy the steady equations where the signs and coefficients are modified to ensure that they are the Euler-Lagrange equation associated with the Hamiltonian function $\mathcal{H}(Z)$. Exact solutions of this problem are known [91]; for example,

$$
u(x) = A \operatorname{sech}(\sqrt{\nu}\, x), \quad v(x) = 0 \quad \text{and} \quad w(x) = 2\nu \operatorname{sech}^2(\sqrt{\nu}\, x), \tag{4.1.5}
$$

with $\mathsf{constant} = 0$ and $A^2 = 2\nu\,(c - 4\nu)$, and the existence condition $c - 4\nu > 0$.

To study the Maslov index of these solutions, linearize the steady equations about the basic solitary wave and introduce a spectral parameter: $\mathbf{L}Z = \lambda Z$ with $\mathbf{L} = D^2\mathcal{H}(\widehat{Z})$. Written out, this equation is

$$
\begin{aligned}
-2u_{xx} - 2\widehat{w}u - 2\widehat{u}w + 2\nu u &= \lambda u \\
-2v_{xx} - 2\widehat{w}v - 2\widehat{v}w + 2\nu v &= \lambda v \\
-w_{xx} + cw - 6\widehat{w}w - 2\widehat{u}u - 2\widehat{v}v &= \lambda w.
\end{aligned} \tag{4.1.6}
$$

When $\widehat{v} = 0$ this system decouples into a second order equation for v, and a fourth order coupled system for u, w,

$$
\begin{aligned}
-2u_{xx} - 2\widehat{w}u - 2\widehat{u}w + 2\nu u &= \lambda u \\
-w_{xx} + cw - 6\widehat{w}w - 2\widehat{u}u &= \lambda w.
\end{aligned} \tag{4.1.7}
$$

The decoupled equation for v is then

$$
-2v_{xx} - 2\widehat{w}v + 2\nu v = \lambda v. \tag{4.1.8}
$$

This latter system can be analyzed completely and the result in given in section 4.1.1.

Using coordinates (4.1.4), the fourth-order system for u, w (4.1.7) can be written as a standard Hamiltonian ODE in the form (1.3.13) with $n = 2$ by taking

$$
\mathbf{u}(x, \lambda) = \begin{pmatrix} u \\ w \\ 2u_x \\ w_x \end{pmatrix}, \quad \mathbf{B}(x, \lambda) = \begin{pmatrix} \lambda - 2\nu + 2\widehat{w}(x) & 2\widehat{u}(x) & 0 & 0 \\ 2\widehat{u} & \lambda - c + 6\widehat{w}(x) & 0 & 0 \\ 0 & 0 & \frac{1}{2} & 0 \\ 0 & 0 & 0 & 1 \end{pmatrix}.
$$

The essential spectrum for this equation is

$$
\sigma_{ess} = \{\, \lambda \in \mathbb{R} \ : \ \lambda \geq 2\nu \text{ and } \lambda \geq c \,\}.
$$
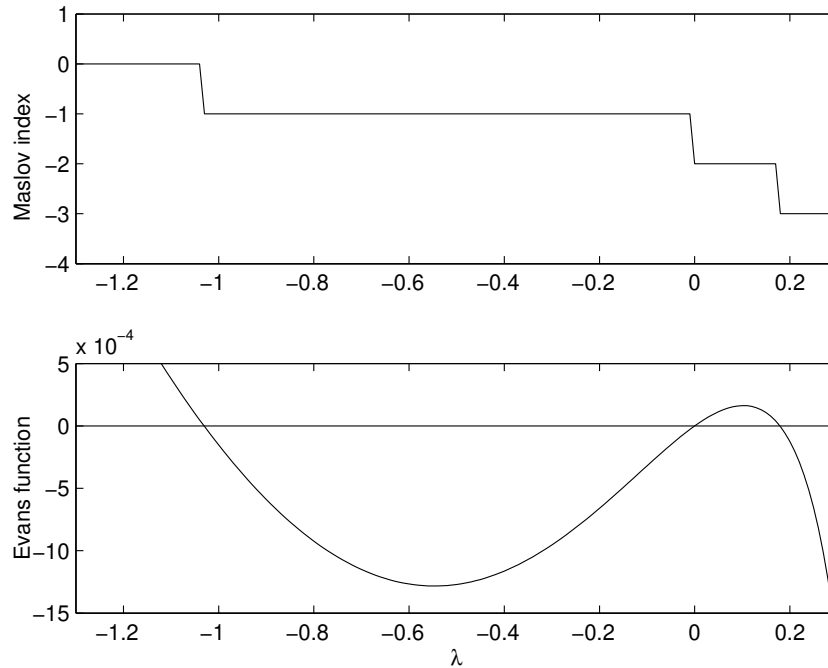
Figure 4.1: Longwave-Shortwave problem for the following parameters $c = 1$, $\nu = 0.2$. Top, the Maslov index as a function of λ. Bottom: the Evans function as a function of λ.

Adding the condition that $c > 4\nu$, the system at infinity is hyperbolic for all $\lambda \in \mathbb{R}$ such that $\lambda < 2\nu$.

The Maslov index is computed for the case $c = 1$ and $\nu = 0.2$ and the results are shown, along with the Evans function, in Figure 4.1 and tabulated in the table below, where $\lambda_1 < \lambda_2 = 0 < \lambda_3$ are the three roots of the Evans function.

λ	$\lambda < \lambda_1$	$\lambda_1 < \lambda < \lambda_2$	$\lambda_2 < \lambda < \lambda_3$	$\lambda > \lambda_3$
$I_{hom}((u,w),\lambda)$	0	-1	-2	-3

4.1.1   The reduced 2×2 eigenvalue problem associated with LW-SW equations

The two-dimensional ODE (4.1.8) that arises in the reduced problem for LW-SW resonance can be written in the form

$$v_{xx} + 2\nu \operatorname{sech}^2(\sqrt{\nu}x)\, v - \nu v + \frac{1}{2}\lambda v = 0\,.$$

ODEs of this type – with sech^2 potential – can be solved explicitly. The essential spectrum related to this problem is the semi-infinite interval $\sigma_{ess}(L) = [2\nu, +\infty[$. Now suppose that $\lambda < 2\nu$. Then the system at infinity is hyperbolic and one can explicitly construct the solutions (v^+, v^-) which give the solutions for the stable and unstable subspaces

$$v^{\pm}(x; \lambda) = e^{\pm\mu\sqrt{\nu}x}(\mp\mu + \tanh(\sqrt{\nu}x)), \quad \mu = \sqrt{1 - \frac{\lambda}{2\nu}} \,.$$

The Evans function can be obtained from

$$D(\lambda) = \frac{\lim_{x\to\infty} e^{-\mu\sqrt{\nu}x}e^{+\mu\sqrt{\nu}x}(-\mu + \tanh(\sqrt{\nu}x))}{\lim_{x\to-\infty} e^{-\mu\sqrt{\nu}x}e^{+\mu\sqrt{\nu}x}(-\mu + \tanh(\sqrt{\nu}x))} \,,$$

from which we obtain

$$D(\lambda) = \frac{-\mu + 1}{-\mu - 1} = \frac{\sqrt{1 - \frac{\lambda}{2\nu}} - 1}{\sqrt{1 - \frac{\lambda}{2\nu}} + 1} \,.$$

The Maslov index can be obtained from

$$\frac{v_x(x; \lambda)}{v(x; \lambda)} = -\mu\sqrt{\nu} + \frac{1 - \tanh(\sqrt{\nu}x)^2}{\mu + \tanh(\sqrt{\nu}x)} \,.$$

From this quotient we can get:

$$\mathsf{Maslov}(\lambda) = \begin{cases} 0 \text{ if } \mu > 1 \\ -1 \text{ if } \mu < 1 \end{cases} = \begin{cases} 0 \text{ if } \lambda < 0 \\ -1 \text{ if } \lambda > 0 \end{cases} \,.$$

4.1.2 Computing the Maslov index in the case $n = 3$.

In the case of the longwave-shortwave resonance equation, the system (4.1.6) can be reformulated as a coupled system on $\mathbb{R}^6$. Define $\mathbf{u} = (u, v, w, 2u_x, 2v_x, w_x)$, and

$$\mathbf{B}(x, \lambda) = \begin{pmatrix} -2\nu + \lambda + 2\hat{w} & 0 & 2\hat{u} & 0 & 0 & 0 \\ 0 & -2\nu + \lambda + 2\hat{w} & 2\hat{v} & 0 & 0 & 0 \\ 2\hat{u} & 2\hat{v} & \lambda - c + 6\hat{w} & 0 & 0 & 0 \\ 0 & 0 & 0 & \frac{1}{2} & 0 & 0 \\ 0 & 0 & 0 & 0 & \frac{1}{2} & 0 \\ 0 & 0 & 0 & 0 & 0 & 1 \end{pmatrix}$$

Then (4.1.6) is in the standard form (0.0.6) on $\mathbb{R}^6$.

When $\hat{v} = 0$ the system decouples into two subsystems as noted in §4.1. In this section, the full system will be integrated on $\bigwedge^3(\mathbb{R}^6)$ for the decoupled case. This way the calculation can be checked against the previous calculation on $\mathbb{R}^4$. The reduced two-dimensional system (4.1.7) can be solved explicitly and the calculation is given in Appendix 4.1.1.

When a system decouples into two subsystems, the Evans function of the full system is the product of two subsystems and the Maslov index of the full system is the sum of the Maslov indexes of the two subsystems

$$I^{2D} \oplus I^{4D} = I^{6D} \,.$$
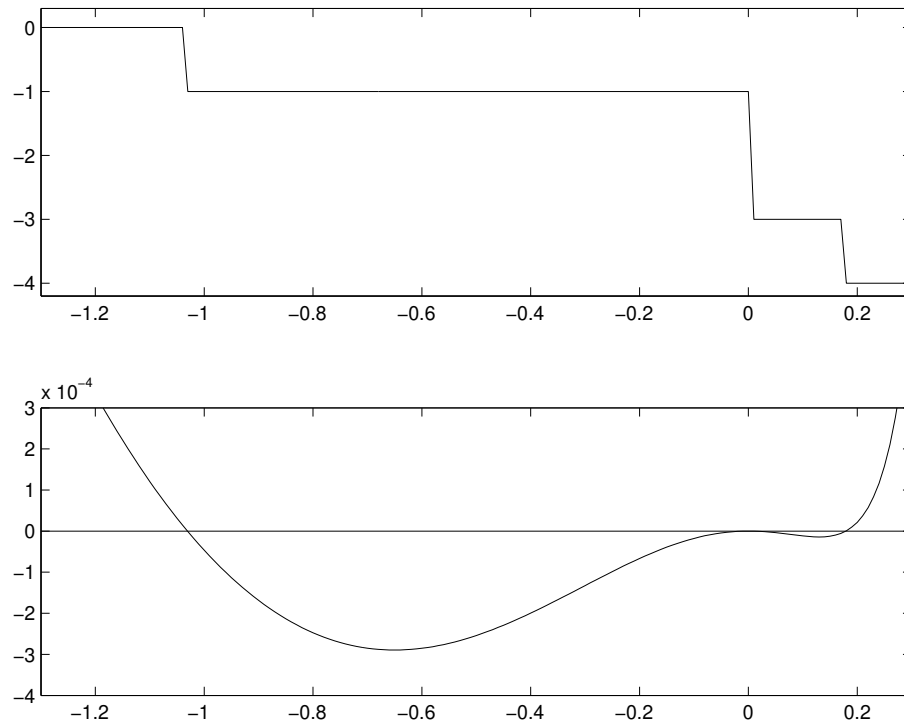
Figure 4.2: Maslov index and Evans function as functions of λ associated to the 6×6 system (4.1.6) when $q = 1$, $\nu = 0.2$ and $c = 1$.

λ	$\lambda < -1$	$-1 < \lambda < 0$	$0 < \lambda <\approx 0.19$	$\lambda >\approx 0.19$
$I^{2D}_{hom}(v, \lambda)$	0	0	-1	-1
$I^{4D}_{hom}((u, w), \lambda)$	0	-1	-2	-3
$I^{6D}_{hom}((u, v, w), \lambda)$	0	-1	-3	-4

The induced system $\mathbf{B}^{(3)}$ can be constructed using the general formula in § 2.1. An explicit formula is given in the Appendix of [5]. In the calculations reported here, the Maslov angle and the algorithm in §2.4.2 are used.

Numerical results are presented in Figure 4.2. The results are in complete agreement with the product of the Evans function of the subsystems and the sum of the Maslov indices of the subsystems.

As noted in Appendix 4.1.1 the Maslov index for the reduced system is 0 if $\lambda < 0$ and -1 if $\lambda > 0$. Adding these values to the Maslov indices in Figure 4.1 agrees with the Maslov indices in Figure 4.2. Note also that the Evans function has a double zero at $\lambda = 0$ as expected.

4.2 A non-monotone Maslov index

In the case of systems coming from the second variation of a functional, the Maslov index is a monotone function of λ (Note however that $\kappa(x)$ and $m_{\mathcal{S}_\infty(\lambda)}(\lim_{y\to\infty}\tilde{\mathcal{U}}(y,\lambda),\tilde{\mathcal{U}}(x,\lambda))$ are not monotone functions of x.). However, the Maslov index can also be defined for other self-adjoint operators. Here we show an example where the Maslov index is not a monotone function of λ. It is a slight modification of the LW-SW resonance equations. In this case the correlation between the number of roots of the Evans function and the value of the Maslov index is no longer apparent. Look at the eigenvalue problem

$$\mathbf{L}\begin{pmatrix} u \\ w \end{pmatrix} = \lambda \begin{pmatrix} u \\ w \end{pmatrix}, \quad \text{with} \quad \mathbf{L}\begin{pmatrix} u \\ w \end{pmatrix} := \begin{pmatrix} -2u_{xx} - 2\widehat{w}(x)u + 2\widehat{u}(x)w + 2\nu u \\ w_{xx} - cw + 6\widehat{w}(x)w + 2\widehat{u}(x)u \end{pmatrix}, \quad (4.2.9)$$

with $c > 4\nu > 0$,

$$\widehat{u}(x) = A\mathrm{sech}(\sqrt{\nu}\,x) \quad \text{and} \quad \widehat{w}(x) = 2\nu\,\mathrm{sech}^2(\sqrt{\nu}\,x)$$

with $A^2 = 2\nu(c - 4\nu)$, and the requirement $c > 4\nu > 0$.

The spectral problem associated to this operator can be expressed in the form (0.0.6) with $n = 2$,

$$\mathbf{u}(x) = \begin{pmatrix} u \\ w \\ 2u_x \\ w_x \end{pmatrix}, \quad \text{and} \quad \mathbf{B}(x,\lambda) = \begin{pmatrix} \lambda - 2\nu + 2\hat{w}(x) & 2\hat{u}(x) & 0 & 0 \\ 2\hat{u}(x) & -\lambda - c + 6\hat{w}(x) & 0 & 0 \\ 0 & 0 & \frac{1}{2} & 0 \\ 0 & 0 & 0 & 1 \end{pmatrix}.$$

The essential spectrum consists of

$$\{\,\lambda \ : \ -\infty < \lambda < -c \ \cup \ 2\nu < \lambda < +\infty\,\}.$$

The essential spectrum is unbounded from above and below, hence a *Morse index* cannot be defined for $\mathbf{L}$. However, we will still be able to compute a Maslov index. The key property that leads to non-monotonicity is that the matrix $\partial_\lambda\mathbf{B}(x,\lambda)$ is *not monotone* with respect to λ.

Results for the case $c = 1$ and $\nu = 0.21$ are tabulated below and shown in Figure 4.3. In this case there are 5 eigenvalues, but there is no longer a correlation between the Maslov index and the number of eigenvalues in a subset of λ.

λ	$-c$				0				2ν
$D(\lambda)$	$+\infty$	$+$	$-$	$+$	0	$-$	$+$	$-$	$-\infty$
Maslov(λ)		-4	-3	-2		-1	-2	-3	

4.3 Conclusion

We computed numerically the Maslov index for 6×6 system and we could observe that it was consistent with the results obtained for the two subsystems. From the Maslov index of these solutions, one should expect that there is at most one unstable mode. To conclude on stability,
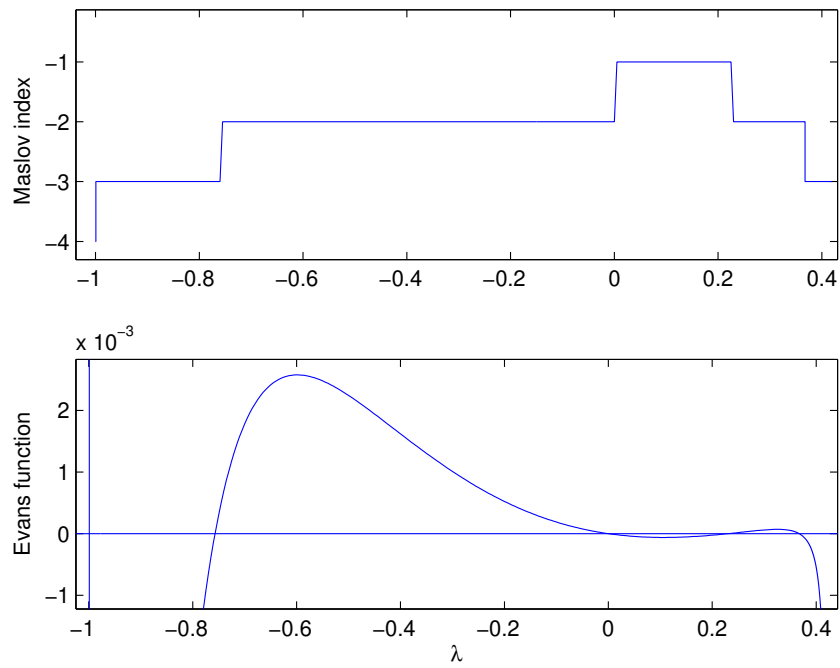
Figure 4.3: Plot of the Maslov index for the non-monotone example (4.2.9) for the case $c = 1$ and $\nu = 0.21$. The upper figure shows the Maslov index and the lower figure the Evans function.

it would be necessary to study the matrix $(\langle u_i, \mathbf{L} u_j \rangle)_{1 \leq i \leq k, 1 \leq j \leq k}$, where $u_1, \ldots, u_k$ is a basis of the generalized kernel of $\mathbf{KL}$.

Concerning the second system, we have exhibited an operator unbounded from both above and below for which it was possible to compute numerically a Maslov index. This shows that if one wants to count the eigenvalues of an operator with Maslov index, one has to be careful about the semidefiniteness of $\partial_\lambda \mathbf{C}(x, \lambda)$.

Chapter 5

Table-top solutions arising in the forced Korteweg-de Vries model

Contents

Introduction

The topic of this chapter is slightly different of the rest of this thesis since it is not about solitary waves but stationary solutions in a non-homogeneous medium. It uses a special case of the Maslov index theory: the classical Sturm-Liouville theory.

A forcing disturbance moving steadily in a channel can generate all kinds of interesting flows. There are two points of view to study this problem: either one considers an obstacle moving at constant velocity U in a uniform layer of water initially at rest, or one considers an obstacle fixed in a uniform stream of velocity U. Suppose now that a second obstacle is placed downstream of the first. Then several flows are possible.

[56] showed that in the presence of an obstacle one can construct mathematically solutions with a uniform level downstream but waves upstream. We call such solutions generalized hydraulic falls. Such solutions are not physical in the sense that the radiation condition is not satisfied. [54] computed new solutions for the flow past two obstacles of arbitrary shape. These solutions are characterised by a train of waves 'trapped' between the obstacles. It was shown that the generalised hydraulic falls describe locally the flow over one of the two obstacles when the distance between the two obstacles is large.

Here, we study the stability of one family of solutions arising past two obstacles. A weakly nonlinear analysis is used. A forced Korteweg–de Vries equation is integrated numerically.

5.1   The forced Korteweg–de Vries (fKdV) model

The classical KdV equation can be extended to admit arbitrary forcing functions if the forcing disturbances are limited to unidirectional motion, say

$$B^* = B^*(x^* + Ut^*), \tag{5.1.1}$$

representing a left-going (or right-going) bathymetry when U is positive (or negative). These forcing functions are supposed to be sufficiently smooth, localized and to vanish identically for $t^* < 0$. In the derivation of KdV type equations, it is also assumed that the velocity U is close to critical so that $F - 1 = O(\epsilon)$. The small number ϵ is usually defined as the square of the ratio between the undisturbed water depth H and a typical wavelength λ. Then stretched coordinates are introduced and asymptotic expansions are assumed. After a few substitutions and integrations, one obtains the following forced KdV equation as a model for open-channel flow past an obstruction:

$$\eta_t = \frac{1}{6}\eta_{xxx} + \frac{3}{4}(\eta^2)_x - (F-1)\eta_x + \frac{1}{2}B_x, \tag{5.1.2}$$

where F is the Froude number and B is the forcing term. Let us summarize the link between the physical variables and the variables appearing in the fKdV model ($*$ are used for the physical quantities).

$$x = \frac{x^* + Ut^*}{H}, \quad \eta = \frac{\eta^*}{H}, \quad B = \frac{B^*}{H}, \quad t = \frac{c_0 t^*}{H}.$$

The speed c_0 is the long wave speed

$$c_0 = (gH)^{\frac{1}{2}}$$

and the Froude number is defined by

$$F = \frac{U}{c_0}.$$

Only supercritical flows with $F > 1$ are considered here. The stability of solutions is considered. But first exact steady solutions are constructed by considering the inverse problem where we look for bottom shapes providing explicit solutions.

While the stability of solutions arising past single-humped obstacle like

$$\eta = A \operatorname{sech}^2 \alpha x, \tag{5.1.3}$$

has been studied in [32, 31], this is not the case for solutions arising past double-humped obstacle. Here, we study a family of table-top solutions generated by a double humped obstacle.

5.2   Hamiltonian structure of the partial differential equation

The forced Korteweg-de Vries has an Hamiltonian structure which is useful to determine stability. It can indeed be written as:

$$\eta_t = \mathbf{J}\frac{\delta \mathcal{H}}{\delta \eta} \qquad (5.2.4)$$

where $\mathbf{J}$ is the following operator:

$$\mathbf{J} = \frac{\partial}{\partial x} \qquad (5.2.5)$$

and $\mathcal{H}$ a functional called the Hamiltonian:

$$\mathcal{H}(\tilde{\eta}) = \frac{1}{6}\int_{\mathbb{R}} \left(-\frac{1}{2}\tilde{\eta}_x^2 + \frac{3}{2}\tilde{\eta}^3 - 3(F-1)\tilde{\eta}^2 + 3B\tilde{\eta} \right) \mathrm{d}x. \qquad (5.2.6)$$

If we linearize near a stationary solution $\boldsymbol{\eta}$ equation (5.2.4), one gets:

$$\tilde{\eta}_t = \frac{\partial}{\partial x}\mathcal{L}\tilde{\eta}$$

where $\mathcal{L}$ is the Hessian of the functional $\mathcal{H}$:

$$\mathcal{L}\tilde{\eta} = \left[\frac{\delta^2 \mathcal{H}}{\delta \eta^2}\right]_{\eta=\boldsymbol{\eta}}(\tilde{\eta}) = \frac{1}{6}(\tilde{\eta}_{xx} + 9(\boldsymbol{\eta})\tilde{\eta} - 6(F-1)\tilde{\eta}).$$

As we shall see in the sequel, the spectrum of $\mathcal{L}$ is related to the spectrum of $\partial_x\mathcal{L}$, and this relationship is sometimes sufficient to conclude on stability.

5.3   Two obstacles: exact table-top solutions

Assume now that the solitary wave at the surface of the channel is of the form (depicted on figure 5.1):

$$\eta_{\alpha,L} = A\tanh\alpha(x+L) - A\tanh\alpha(x-L), \quad A = \frac{2}{3}(F-1). \qquad (5.3.7)$$

In other words, it is the superposition of two fronts centred at $x = L$ (rising front) and at $x = -L$ (falling front), where α and L are positive parameters. We look for a corresponding double hump at the bottom. In order to do this, we substitute (5.3.7) into (5.1.2):

$$B_{\alpha,L} = \frac{1}{3}\left(6(F-1)\eta_{\alpha,L} - \frac{9}{2}(\eta_{\alpha,L})^2 - (\eta_{\alpha,L})_{xx} \right).$$

Now, we are going to study the stability of these solutions. First we study the spectrum of the Hessian of the Hamiltonian (via Sturm-Liouville theory). Then, we will deduce some cases of stability and instability.
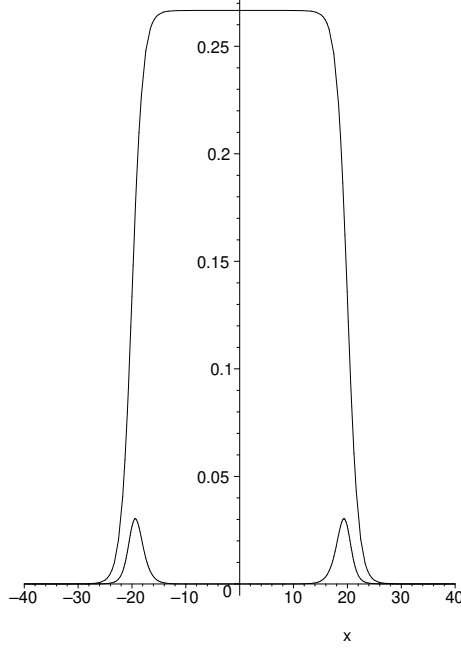
Figure 5.1: Table-top solution past two obstacles when $L = 20$, $F = 1.2$ and $\alpha = -.5$.

Spectrum of the Hessian of the Hamiltonian

In this paragraph, we assume that $\alpha < 0$ and $L > 0$ and we are interested in the eigenvalues of the Hessian of the Hamiltonian near $\eta = \eta_{\alpha,L}$ when $B = B_{\alpha,L}$.

The Hamiltonian can then be written as:

$$\mathcal{H}_{\alpha,L}(\tilde{\eta}) = \frac{1}{6} \int_{\mathbb{R}} \left(-\frac{1}{2}\tilde{\eta}_x^2 + \frac{3}{2}\tilde{\eta}^3 - 3(F-1)\tilde{\eta}^2 + 3B_{\alpha,L}\tilde{\eta} \right) \mathrm{d}x$$

The Hessian of the Hamiltonian is (by taking $(u,v) \to \int_{\mathbb{R}} uv$ as a scalar product):

$$\mathcal{L}_{\alpha,L}(\tilde{\eta}) = \frac{1}{6}(\tilde{\eta}_{xx} + 9(\eta_{\alpha,L})\tilde{\eta} - 6(F-1)\tilde{\eta})$$

The spectral problem $\mathcal{L}$ can be written as a first-order linear system:

$$\mathcal{J}U_x(x) = \mathbf{C}_{\alpha,L}(x,\lambda)U(x), \quad U(x) = \begin{pmatrix} \tilde{\eta} \\ \tilde{\eta}_x \end{pmatrix}, \quad \mathcal{J} = \begin{pmatrix} 0 & -1 \\ 1 & 0 \end{pmatrix}$$

$$\mathbf{C}_{\alpha,L}(x,\lambda) = \begin{pmatrix} 6(F-1) - 9\eta_{\alpha,L} + 6\lambda & 0 \\ 0 & -1 \end{pmatrix}. \tag{5.3.8}$$

The essential spectrum of $\mathcal{L}_{\alpha,L}$ is $\sigma_{ess}(\mathcal{L}_{\alpha,L}) = [2(F-1), +\infty[$ and 0 does not belong to it.

Let $n_+(\alpha, L)$ be the number of strictly positive eigenvalues of $\mathcal{L}_{\alpha,L}$.

$n_+(\alpha, L)$ can jump by at most one e.g., if (α_m, L_m) converges to (α, L), then there exists m_0 such that $\forall m \geq m_0 \quad |n_+(\alpha, L) - n_+(\alpha_m, L_m)| \leq 1$. (Assume that it is not the case near (α, L). Then 0 would be a multiple eigenvalue of $\mathcal{L}_{\alpha,L}$, which is impossible.)

If α and x are fixed, then $\eta_{\alpha,L}(x)$ is an increasing function of L and

$$L_1 < L_2 \Rightarrow \forall u \quad \langle u, \mathcal{L}_{\alpha,L_1} u \rangle \leq \langle u, \mathcal{L}_{\alpha,L_2} u \rangle.$$

As a consequence, $n_+(\alpha, L)$ is an increasing function of L when α is fixed.

When $L = 0$, $\eta = 0$ and therefore $n_+(\alpha, 0) = 0$. Therefore, there exists $0 < L_1(\alpha) < L_2(\alpha) < \ldots$ such that $n_+(\alpha, L) = i$ if and only if $x \in]L_i(\alpha), L_{i+1}(\alpha)]$, e.g.

$$n_+(\alpha, L) = \sum_{i=1}^{+\infty} \mathbb{1}_{]L_i(\alpha), +\infty[}(L).$$

Here are some estimates of $L_i(\alpha)$ when $F = 1.2$ and $\alpha = -0.3$:

$L_1(-0.3)$	2.36823	$L_6(-0.3)$	9.32896
$L_2(-0.3)$	3.65133	$L_7(-0.3)$	10.7628
$L_3(-0.3)$	5.04097	$L_8(-0.3)$	12.1967
$L_4(-0.3)$	6.46378	$L_9(-0.3)$	13.6306
$L_5(-0.3)$	7.89555	$L_{10}(-0.3)$	15.0646

Let us now give an estimate of $L_{i+1}(\alpha) - L_i(\alpha)$.

Let $\zeta_{\alpha,L}$ be a solution of system (5.3.8) when $\lambda = 0$ such that $\lim_{x \to -\infty} \zeta_{\alpha,L}(x) = 0$. $n_+(\alpha, L)$ is equal to twice the number of rotations of $\zeta_{\alpha,L}$ around zero. If we set $\eta_{\alpha,\infty} = \frac{4}{3}(F - 1)$, then

$\mathbf{C}_{\alpha,\infty}(\lambda) = \begin{pmatrix} -6(F-1) + 6\lambda & 0 \\ 0 & -1 \end{pmatrix}$, which is approximately the value of $\mathbf{C}_{\alpha,L}(x, \lambda)$ when x is close to 0. When $\lambda = 0$, the period of the associated system is $\frac{2\pi}{\sqrt{6(F-1)}}$ (0 is then in the essential spectrum). Therefore, when $2L$ increases by T, the flat zone on which $\mathbf{C}_{\alpha,L}(x, \lambda) \simeq \mathbf{C}_{\alpha,\infty}(\lambda)$ also increases by T. $n_+(\alpha, L)$ should increase by approximately $\frac{T2\sqrt{6(F-1)}}{\pi}$. So one could expect that $L_{i+1}(\alpha) - L_i(\alpha) \sim_{i \to \infty} \frac{\pi}{2\sqrt{6(F-1)}}$ (if $F = 1.2$, $\frac{\pi}{2\sqrt{6(F-1)}} = 1.4339$, which is consistent with the preceding table).

Stability and instability of some table-top solutions.

Assume that $0 \notin \sigma(\mathcal{L}_{\alpha,L})$, then according to [41], we have the following relationship[1] between the eigenmodes of $\mathcal{L}_{\alpha,L}$ and those of $\partial_x \mathcal{L}_{\alpha,L}$:

$$n_+(\alpha, L) = N_{unst} + N_{imag}^+$$

where N_{unst} is the number of unstable modes of $\partial_x \mathcal{L}_{\alpha,L}$ and N_{imag}^+ is the number of oscillatory modes u of $\partial_x \mathcal{L}_{\alpha,L}$ such that $\langle u, \mathcal{L}_{\alpha,L} u \rangle > 0$.

If $N_{unst} \neq 0$, the stationary solution is unstable. Otherwise, it is said to be spectrally stable.

Using the previous paragraph, there are two cases for which it is possible to conclude on the stability of the table-top solutions:

- $L \in [0, L_1(\alpha)[$. Then the table-top solution is stable.

---

[1] CHUGUNOVA & PELINOVSKY [41] only mentioned the solitary wave case. Since the stationary solution is symmetric, one can do the same proof. Contrary to the solitary wave case, the kernel of $\partial_x \mathcal{L}$ is empty, and there is no need to take in account the generalized kernel of $\partial_x \mathcal{L}_{\alpha,L}$.

- $L \in \cup_{i \in \mathbb{N}}]L_{2i+1}(\alpha), L_{2i+2}(\alpha)[$. Then the table-top solution is unstable.

In the first case, the lowest eigenvalue of $\mathcal{L}_{\alpha,L}$ is strictly positive. We have therefore $N_{unst} = 0$. From section 5 of CAMASSA AND WU [31], this also implies the non-linear stability of the stationary solution.

In the second-case, $n_+(\alpha, L)$ is an odd number and there is no zero eigenvalue. Since N_{imag}^- is even, N_{unst} is odd and hence non-zero. Therefore, the solution is unstable.

If $L \in \cup_{i \in \mathbb{N}}[L_{2i+2}(\alpha), L_{2i+3}(\alpha)]$, none of the previous arguments works. However, numerical simulations seem to indicate that these solutions are unstable (see figure 5.4).

Numerical simulations

We tried to determine the stability of table-top solutions by integrating the fKdV system. Except for $L \in [0, L_1(\alpha)[$, all the table-top solutions we observed were unstable, although some instabilities were slower to appear than others. In fact, there were two kinds of leading instabilities:

- Some oscillations increased alternatively in the left and in the right of the table-top. This seems to indicate a leading pair of complex eigenvalues.

- Some oscillations grew rather uniformly on the table-top solution, which seem to indicate a leading real eigenvalue.

We observed that the period of the oscillations appearing in the table-top could be accurately predicted by the relation of dispersion of the system when $\eta = \eta_{\alpha,\infty} = \frac{2}{3}(F - 1)$.

The relation of dispersion for $\eta = \eta_{\alpha,\infty} = \frac{2}{3}(F - 1)$ is indeed:

$$\mathrm{i}\omega = \mathrm{i}k(-\frac{k^2}{6} + \frac{6}{4}\frac{4}{3}(F - 1) - (F - 1))$$

or

$$\omega = k(-\frac{k^2}{6} + (F - 1)).$$

If we look for stationary oscillations, then $\omega = 0$. This implies $k = 0$ or $k = \sqrt{6(F - 1)}$, and the period of the oscillation should be $\frac{2\pi}{\sqrt{6(F-1)}}$.

As a consequence, one could expect roughly $\frac{L\sqrt{6(F-1)}}{\pi}$ oscillations developing between the obstacles and these oscillations were indeed observed.

5.4 Details about the numerical simulations

Suppose that x takes values in the interval $[-L \; L]$. In order to work in the interval $[-\pi \; \pi]$, we use the scaling coefficient $S = \pi/L$. In other words

$$Sx = x_{\mathrm{new}}, \quad x_{\mathrm{new}} \in [-\pi \; \pi]$$

Without changing notation, the equation (5.1.2) becomes

$$\eta_t = \frac{1}{6}S^3\eta_{xxx} + \frac{3}{4}S(\eta^2)_x - (F - 1)S\eta_x + \frac{1}{2}SB_x. \tag{5.4.9}$$
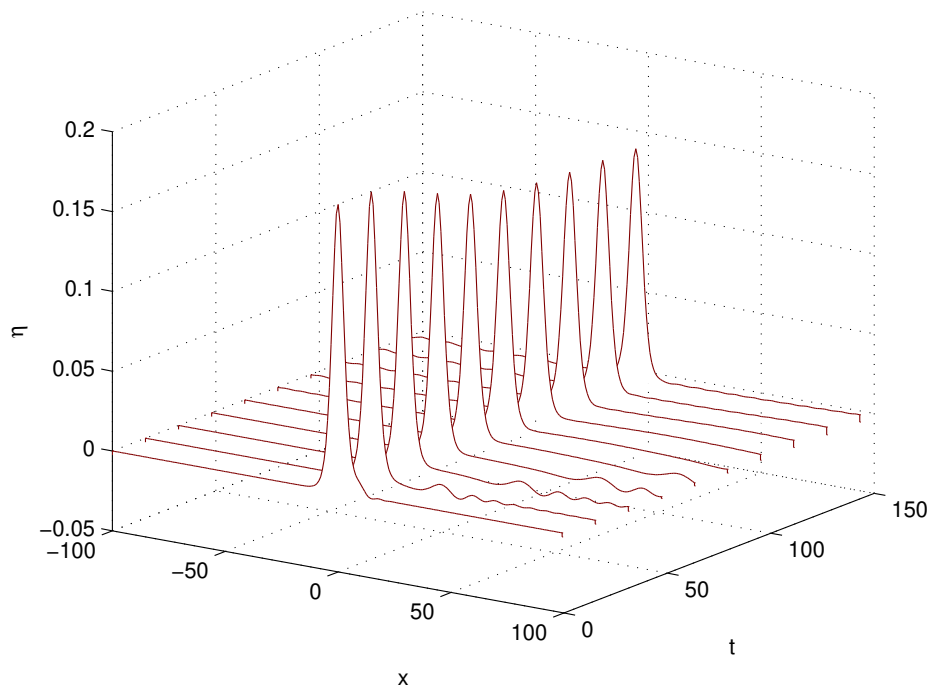
Figure 5.2: Stable solution when $L = 2$, $\alpha = -0.3$ and $F = 1.2$ (In that case $n_+(-0.3, 2) = 0$). The initial condition was a perturbation of the stable solution.
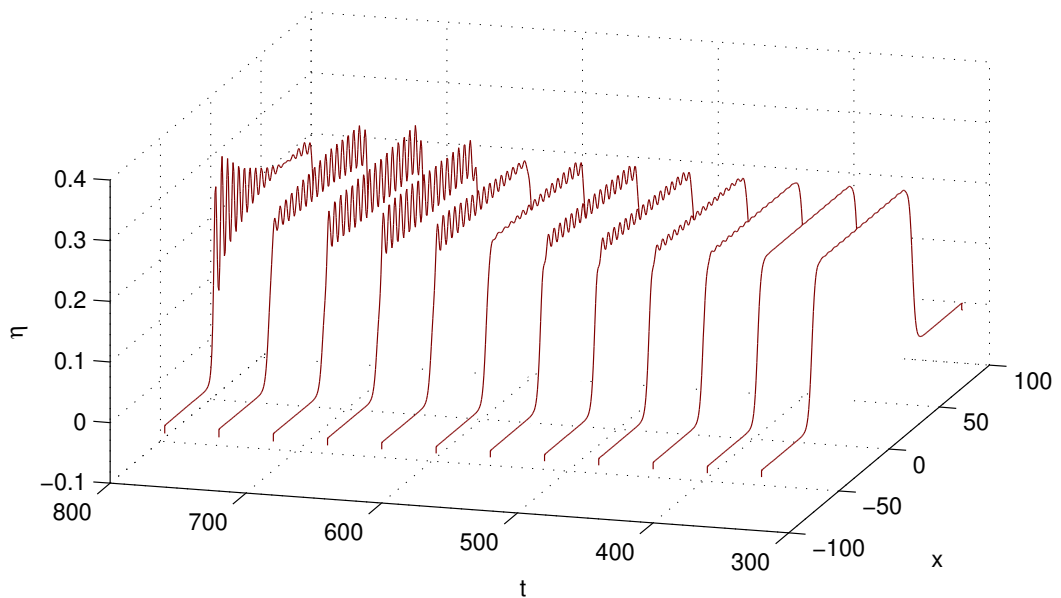
Figure 5.3: Instability developing on the table-top solution when $L = 50$, $\alpha = -0.3$ and $F = 1.2$ (In that case $n_+(-0.3, 50) = 34$). The leading instability seems to be associated to a complex eigenvalue, since the instability has not a uniform growth rate (the instability appears alternatively on the right and the left of the table-top solution). There are 16 oscillations developing between the two edges of the solution, which is quite close of the 17 expected oscillations.
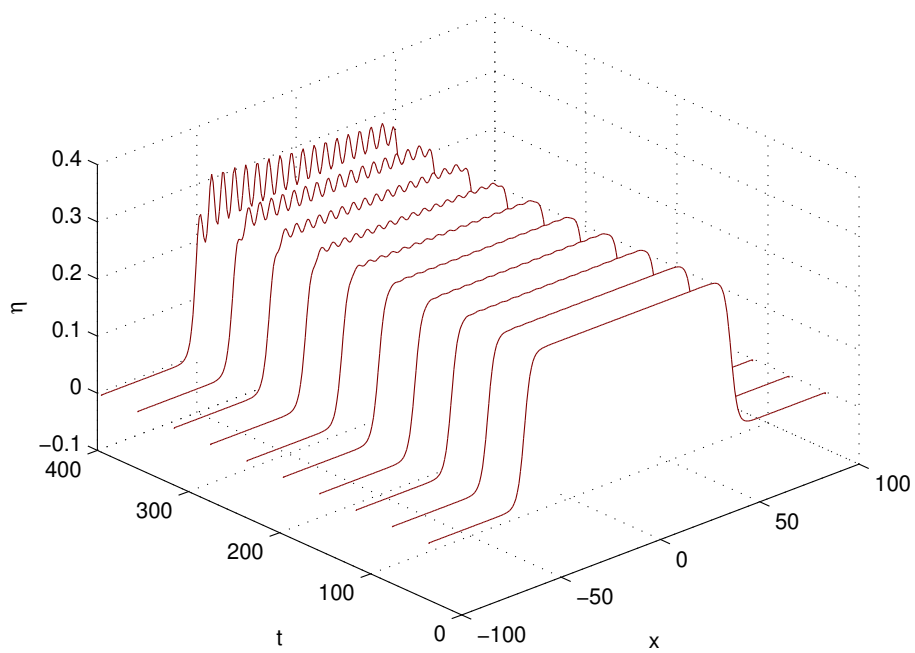
Figure 5.4: Instability developing on the table-top solution when $L = 52$, $\alpha = -0.3$ and $F = 1.2$ (In that case $n_+(-0.3, 52) = 35$). Here, the leading instability seems to be associated to a real eigenvalue, since it grows rather uniformly. There are 17 oscillations developing between the two edges of the solution, which is quite close of the 18 expected oscillations.

The numerical results are produced by using a Fourier spectral method. The forced KdV equation is solved by converting it into an ordinary differential equation and then discretising via a fourth order Runge–Kutta scheme.

5.5   Conclusion

It seems that except for low values of L, table-top solutions are unstable. The conclusion is the same if the two obstacles have a different shape. One should not expect to observe these solutions except in a transitional manner.

Conclusion

The Maslov index provides a fast way to count the number of unstable modes added to the number of neutral modes with negative energy. If its value is low enough, it can be possible to reach a conclusion on spectral stability. Besides, its parity can be enough to prove instability. In addition to the orientation index (see [3, 2]) and the Chern number (see [1]), the Maslov index is another tool linking the stationary part of a PDE to its stability. Finally, it can be used to detect bifurcation points.

However, the dimension of $\bigwedge^n(\mathbb{R}^{2n})$ is C_{2n}^n and it grows rapidly (for example $C_{16}^8 = 12870$) and therefore the practical application of working on exterior algebra spaces is limited to low dimension. For higher dimension, *orthosymplectic integration* becomes appealing. In orthosymplectic integration, continuous orthogonalization is used and the symplectic structure is retained. For example, the algorithm proposed in [88] could be adapted to the computation of the Maslov index. In principle, if the periodic system is hyperbolic, then random orthosymplectic initial conditions can be used. However, special integrators, such as implicit Gauss-Legendre Runge-Kutta methods, are required in order to preserve symplecticity and orthonormality to high accuracy, and the ODE is highly nonlinear. On the other hand, orthosymplectic integrators will be essential for systems of high dimension since the dimension grows only like $2n^2$ for linear systems of dimension $2n$.

A sketch of how orthosymplectic integration can be used is as follows. Let $\mathbf{\Phi}(x, \lambda)$ be a path of symplectic matrices such that the n first columns of $\mathbf{\Phi}(x, \lambda)$ span the unstable subspace and $\mathbf{J}\mathbf{\Phi}_x(x, \lambda) = \mathbf{B}(x, \lambda)\mathbf{\Phi}(\mathbf{x}, \lambda)$. Decompose $\mathbf{\Phi}(t)$ following [88],

$$\mathbf{\Phi}(x, \lambda) = \mathbf{Q}(x, \lambda)\mathbf{X}(x, \lambda), \quad \text{with} \quad \mathbf{X}(x, \lambda) = \begin{pmatrix} X_{11}(x, \lambda) & X_{12}(x, \lambda) \\ 0 & X_{22}(x, \lambda) \end{pmatrix}. \tag{5.5.10}$$

The path of matrices $\mathbf{Q}(x, \lambda)$ is symplectic and orthogonal and $X_{11}(x, \lambda)$ is an $n \times n$ upper triangular matrix and X_{22} is an $n \times n$ lower triangular matrix.

Since $\mathbf{Q}$ is both orthogonal and symplectic, it can be expressed in the form

$$\mathbf{Q} = \begin{pmatrix} \mathbf{Q}_1 & -\mathbf{Q}_2 \\ \mathbf{Q}_2 & \mathbf{Q}_1 \end{pmatrix}, \quad \text{with} \quad \mathbf{Q}_1 + \mathrm{i}\mathbf{Q}_2 \quad \text{unitary}.$$

If $k \leq n$, the k first columns of $\mathbf{Q}$ span the space spanned by the first k columns of $\mathbf{\Phi}$ and therefore when $k = n$ the columns of $\begin{pmatrix} \mathbf{Q}_1 \\ \mathbf{Q}_2 \end{pmatrix}$ span the unstable space. Define κ by $e^{\mathrm{i}\kappa(x, \lambda)} = \frac{\det(\mathbf{Q}_1(x, \lambda) - \mathrm{i}\mathbf{Q}_2(x, \lambda))}{\det(\mathbf{Q}_1(x, \lambda) + \mathrm{i}\mathbf{Q}_2(x, \lambda))}$, then the Maslov index is again $\frac{\kappa(0, \lambda) - \kappa(L, \lambda)}{2\pi}$ in the periodic case and

$\frac{\lim_{x \to +\infty} \kappa(x,\lambda) - \lim_{x \to -\infty} \kappa(x,\lambda)}{2\pi}$ in the solitary wave case. One still needs to prove that $\frac{\kappa(T) - \kappa(0)}{2\pi}$ is an integer, even though $\mathbf{\Phi}(t)$ is not necessarily periodic.

Concerning multi-pulse solutions, it seems that a lot of them are spectrally unstable. However that does not mean that these solutions are not interesting. First, the instability exponent is quite low and is even lower when the distance between the pulses is greater, and if they appear, they can last for quite a long time, as numerical simulations have revealed. Second, collisions are likely to produce them in a transitional manner.

It would also be interesting to extend the result on the Hessian of the Hamiltonian to the LW-SW equations. This would produce concluding evidence on the stability of sech^2-type solutions.

Appendix A

Modes of finite-dimensional linear Hamiltonian systems

In this appendix, we describe the eigenmodes of linear Hamiltonian systems.

Let $E = \mathbb{R}^{2n}$. Suppose that there is a symplectic form:

$$\omega : (x, y) \mapsto x^T \mathcal{J} y \quad \text{with} \quad \mathcal{J} = \begin{pmatrix} 0_n & -I_n \\ I_n & 0_n \end{pmatrix} \tag{A.0.1}$$

Consider the following linear system:

$$u' = Au \tag{A.0.2}$$

This system is Hamiltonian if and only if:

$$\mathcal{J}A = (\mathcal{J}A)^T$$

The associated Hamiltonian is then $H(x) = \frac{1}{2}x^T(\mathcal{J}A)x$. This leads to the following definition:

Definition 22 *A matrix is said to be Hamiltonian if and only if $A^T\mathcal{J} + \mathcal{J}A = 0$, i.e. $\mathcal{J}A = (\mathcal{J}A)^T$.*

Now, consider the flow of system (A.0.2), i.e. $\Phi : I^2 \to GL_n(\mathbb{R})$ such that:

$$\Phi(a, a) = I_{2n}, \quad \frac{\partial \Phi}{\partial t_1}(t_1, t_2) = A(t_1)\Phi(t_1, t_2) \tag{A.0.3}$$

Then $\Phi(t, u)$ is a symplectic matrix:

Definition 23 *A matrix C is said to be symplectic if and only if $\forall x, y \quad \omega(Cx, Cy) = \omega(x, y)$, or equivalently if and only if $C^T\mathcal{J}C = \mathcal{J}$.*

Definition 24 *The set of symplectic matrices is a Lie group called the symplectic group. It is denoted as $Sp(2n)$. Its Lie algebra is the space of Hamiltonian matrices. Its dimension is therefore $n(2n + 1)$.*

$Sp(2n)$ is connected and therefore any symplectic matrix is the flow of a Hamiltonian system.

Now, to understand the spectral stability of Hamiltonian systems, the eigenvalues of these matrices are studied. To this end, the notion of Krein signature is introduced.

The theory is then applied to the particular case of *orthosymplectic* matrices, which will be useful for the definition of the Maslov Index.

Then these results are transposed to Hamiltonian matrices.

Proposition 32 is of great importance, since it gives a bound on the number of eigenvalues which are not on the imaginary axis. Hence, the local shape of the Hamiltonian is therefore linked to the number of unstable modes.

It has been generalized in the infinite-dimensional case by SANDSTEDE & AL. [78] and then by CHUGUNOVA & PELINOVSKY [41] for symplectic forms like the ones involved in Korteweg-de Vries and Kawahara equations.

A.1 Eigenvalues of symplectic matrices.

Definition 25 *Two spaces E and F are said to be ω-orthogonal if and only if for all $x \in E$ and $y \in F$, $\omega(x, y) = 0$.*

Proposition 21 *If λ is an eigenvalue of A, then $\bar{\lambda}$, $\frac{1}{\lambda}$, $\frac{1}{\bar{\lambda}}$ are also eigenvalues.*
Besides $\dim E_\lambda = \dim E_{\bar{\lambda}} = \dim E_{\frac{1}{\lambda}} = \dim E_{\frac{1}{\bar{\lambda}}}$

Let λ is an eigenvalue of A, and u an associated (generalized) eigenvector. Then:

- $u^T \mathcal{J}^{-1}$ is a (generalized) left eigenvector of A associated to $\frac{1}{\lambda}$.

- $\bar{u}$ is a (generalized) right eigenvector of A associated to $\bar{\lambda}$.

- $\bar{u}^T \mathcal{J}^{-1}$ is a (generalized) left eigenvector of A associated to $\frac{1}{\bar{\lambda}}$.

This property leads to classification of the eigenvalues of symplectic matrices:

Definition 26 *Let λ be an eigenvalue different from ± 1.*

- *If $|\lambda| = 1$, $\{\lambda, \frac{1}{\lambda}\}$ is said to be an elliptic pair.*

- *If λ is real positive, $\{\lambda, \frac{1}{\lambda}\}$ is said to be an hyperbolic pair.*

- *If λ is real negative, $\{\lambda, \frac{1}{\lambda}\}$ is said to be an inverse hyperbolic pair.*

- *If $\lambda \neq 1$ $|\lambda| \neq 1$, $\{\lambda, \frac{1}{\lambda}, \frac{1}{\bar{\lambda}}, \bar{\lambda}\}$ is said to be a loxodromic quadruplet.*

Let now define $S = \{\lambda \in \mathbb{C} \text{ s.t. } |\lambda| \geq 1 \text{ and } \operatorname{Im} \lambda > 0\}$.
For any $\lambda \in S$, let $F_\lambda = E_\lambda + E_{\frac{1}{\lambda}} + E_{\bar{\lambda}} + E_{\frac{1}{\bar{\lambda}}}$. Then:

Proposition 22

$$\mathbb{R}^{2n} = \bigoplus_{\lambda \in S} F_\lambda.$$

This decomposition is ω-orthogonal.

The direct sum is obvious. ω-orthogonality can be proved by recurrence:

Let us prove by recurrence over k that $\forall k \quad \ker(A - \lambda)^k \perp_\omega \ker(A - \mu)$:

- For $k = 1$:

  Let $x \in \ker(A - \lambda)$ and $y \in \ker(A - \mu)$ with $\mu\lambda \neq 1$ Then:

  $\omega(x, y) = \omega(Ax, Ay) = \lambda\mu\omega(x, y)$

- If $\ker(A - \lambda)^k \perp_\omega \ker(A - \mu)$, then, for $x \in \ker(A - \lambda)^{k+1}$ and $y \in \ker(A - \mu)$:

  $\omega(x, y) = \omega(Ax, Ay)$

  $\omega(x, y) = \omega((A - \lambda)x + \lambda x, \mu y)$

  $\omega(x, y) = \omega((A - \lambda)x, Ay) + \lambda\mu\omega(x, y)$ Therefore: $(1 - \lambda\mu)\omega(x, y) = 0$.

  That concludes the recurrence argument.

From above, we have $E_\lambda \perp_\omega \ker(A - \mu) = 0$

Let us prove by recurrence over l that $\forall l \quad E_\lambda \perp_\omega \ker(A - \mu)^l$:

- Proved for $l = 1$

- Suppose that $E_\lambda \perp_\omega \ker(A - \mu)^l$. Let $x \in E_\lambda$ and $y \in \ker(A - \mu)^{l+1}$:

  $\omega(x, y) = \omega(Ax, Ay)$

  $\omega(x, y) = \omega((A - \lambda)x, (A - \mu)y) + \lambda\omega(x, (A - \mu)y) + \mu\omega((A - \lambda)x, y) + \lambda\mu\omega(x, y)$

  By using the recurrence hypothesis:

  $\omega((A - \lambda)x, (A - \mu)y) = \omega((A - \lambda)x, y) = \omega((A - \lambda)x, y) = 0$

  That concludes the recurrence argument.

Therefore, $E_\lambda \perp_\omega E_\mu$ if $\lambda\mu \neq 1$.

This way, we can prove that if $\lambda, \mu \in S$ and $\lambda \neq \mu$ then $F_\lambda \perp_\omega F_\mu$. $\qquad\square$

Proposition 23 *The dimension of F_λ is even.*

When $\lambda \neq 1$ and $\lambda \neq -1$, $\dim F_\lambda$ is obviously even and $\det A_{|F_\lambda} = 1$.

Since ω is preserved by A, $\det = \bigwedge_{k=1}^n \omega$ is also preserved by A.

Therefore $\det A = \det A_{|F_{-1}} = 1$.

So $\dim F_{-1}$ is even. Therefore $\dim F_1$ is even too.

A.2 Krein signature

For $A \in Sp(2n)$, let Q be the following symmetric bilinear form:

$Q : \begin{cases} (\mathbb{R}^{2n})^2 \to \mathbb{R} \\ (x, y) \mapsto \frac{1}{2}\omega(x, Ay) + \frac{1}{2}\omega(y, Ax) \end{cases}$. Its matrix is $\frac{1}{2}\mathcal{J}A + \frac{1}{2}(\mathcal{J}A)^T = \frac{1}{2}\mathcal{J}A + \frac{1}{2}(\mathcal{J}A)^{-1}$.

Proposition 24 *Let $\lambda, \mu \in S$ such that $\lambda \neq \mu$. Then F_λ and F_μ are Q-orthogonal.*

Let $x \in F_\lambda$ and $y \in F_\mu$. Then $Ax \in F_\lambda$ and $Ay \in F_\mu$.

$Q(x, y) = \frac{1}{2}\omega(x, Ay) + \frac{1}{2}\omega(y, Ax) = 0$ (by using ω-orthogonality)

Definition 27 *Let R be a quadratic form. The signature of R is the couple (p, q) where p is the number of positive eigenvalues of R and q the number of negative eigenvalues of R.*

Proposition 25 *Let $\lambda \in S$ such that $|\lambda| > 1$ and $2m$ be the dimension of F_λ. Then the signature of $Q_{|F_\lambda}$ is (m, m).*

Proposition 26 *Let $\lambda \in S$ such that $|\lambda| = 1, \lambda^2 \neq 1$ and $2m$ be the dimension of F_λ. Then there exists r such that $(2r, 2(m - r))$ is the signature of $Q_{|F_\lambda}$.*

Definition 28 *The Krein signature of an eigenvalue $\lambda \in S$ such that $|\lambda| = 1, \lambda^2 \neq 1$ is defined as the pair $(r_\lambda^-, r_\lambda^+)$ such that $(2r_\lambda^-, 2r_\lambda^+)$ is the signature of $Q_{|F_\lambda}$.*

When λ is a simple eigenvalue, its Krein signature is either $(1, 0)$ or $(0, 1)$. Then, the eigenvalue is said to have a negative or positive Krein signature.

Proposition 27 *Let (α, β) be the signature of $Q_{|F_1 + F_{-1}}$.*
Let (a, b) be the signature of Q and $a + b = 2n$. Then:
$a = \sum_{\lambda \in S, |\lambda| > 1} \dim F_\lambda + 2 \sum_{\lambda \in S, |\lambda| = 1} r_\lambda^- + \alpha$
$b = \sum_{\lambda \in S, |\lambda| > 1} \dim F_\lambda + 2 \sum_{\lambda \in S, |\lambda| = 1} r_\lambda^+ + \beta$

A.3 Krein signature and orthosymplectic matrices

$\mathbf{\Phi}$ is an orthosymplectic matrix (i.e both orthogonal and symplectic) if and only if it can be written under the form $\mathbf{\Phi} = \begin{pmatrix} \mathbf{X} & -\mathbf{Y} \\ \mathbf{Y} & \mathbf{X} \end{pmatrix}$ such that $\mathbf{X} - i\mathbf{Y}$ is a unitary matrix.

Let $u_1, u_2 \ldots, u_n$ be an orthonormal basis of eigenvectors of $\mathbf{X} - i\mathbf{Y}$ associated to the eigenvalues $\mu_1, \mu_2, \ldots, \mu_n$, which are all of modulus one.

The eigenvalues of $\begin{pmatrix} \mathbf{X} & -\mathbf{Y} \\ \mathbf{Y} & \mathbf{X} \end{pmatrix}$ are $\mu_1, \mu_2, \ldots, \mu_n, \overline{\mu_1}, \overline{\mu_2}, \ldots, \overline{\mu_n}$ and the associated eigenvectors are $\begin{pmatrix} u_1 \\ iu_1 \end{pmatrix}, \begin{pmatrix} u_2 \\ iu_2 \end{pmatrix}, \ldots, \begin{pmatrix} u_n \\ iu_n \end{pmatrix}, \begin{pmatrix} \overline{u_1} \\ -i\overline{u_1} \end{pmatrix}, \begin{pmatrix} \overline{u_2} \\ -i\overline{u_2} \end{pmatrix}, \ldots, \begin{pmatrix} \overline{u_n} \\ -i\overline{u_n} \end{pmatrix}$.

The previous family of vectors is a basis, and can be turned into an orthosymplectic basis:
$\begin{pmatrix} \operatorname{Re} u_1 \\ -\operatorname{Im} u_1 \end{pmatrix}, \begin{pmatrix} \operatorname{Re} u_2 \\ -\operatorname{Im} u_2 \end{pmatrix}, \ldots, \begin{pmatrix} \operatorname{Re} u_n \\ -\operatorname{Im} u_n \end{pmatrix}, \begin{pmatrix} \operatorname{Im} u_1 \\ \operatorname{Re} u_1 \end{pmatrix}, \begin{pmatrix} \operatorname{Im} u_2 \\ \operatorname{Re} u_2 \end{pmatrix}, \ldots, \begin{pmatrix} \operatorname{Im} u_n \\ \operatorname{Re} u_n \end{pmatrix}$.

Let $k \in \{1, \ldots, n\}$.
Suppose $\lambda_k \neq \pm 1$.

$\omega\left(\begin{pmatrix} \operatorname{Re} u_k \\ -\operatorname{Im} u_k \end{pmatrix}, \mathbf{\Phi}\begin{pmatrix} \operatorname{Re} u_k \\ -\operatorname{Im} u_k \end{pmatrix}\right) = \omega\left(\begin{pmatrix} \operatorname{Re} u_k \\ -\operatorname{Im} u_k \end{pmatrix}, \begin{pmatrix} \operatorname{Re} \lambda_k \operatorname{Re} u_k - \operatorname{Im} \lambda_k \operatorname{Im} u_k \\ \operatorname{Im} \lambda_k \operatorname{Re} u_k + \operatorname{Re} \lambda_k \operatorname{Im} u_k \end{pmatrix}\right)$

$\omega\left(\begin{pmatrix} \operatorname{Re} u_k \\ -\operatorname{Im} u_k \end{pmatrix}, \mathbf{\Phi}\begin{pmatrix} \operatorname{Re} u_k \\ -\operatorname{Im} u_k \end{pmatrix}\right) = \operatorname{Im} \lambda_k(\operatorname{Re} u_k^T \operatorname{Re} u_k + \operatorname{Im} u_k^T \operatorname{Im} u_k) = \operatorname{Im} \lambda_k$

From this and the symplecticity of the previous basis, we deduce that the Krein signature of the eigenvalue $\lambda \in S$ will be $(\#\{k | \overline{\mu_k} = \lambda\}, \#\{k | \mu_k = \lambda\})$.

A.4 Krein signature for Hamiltonian matrices

The eigenvalues of Hamiltonian matrices can be treated in much the same way as symplectic matrices:

Let M be an Hamiltonian matrix and: $Q(x,y) = \frac{1}{2}\omega(x, My) + \frac{1}{2}\omega(y, Mx)$

(Note: $x \mapsto Q(x,x)$ is the Hamiltonian of the system)

Proposition 28 *If λ be an eigenvalue of A, then λ, $-\lambda$, $-\bar{\lambda}$ are also eigenvalues.*

Besides $\dim E_\lambda = \dim E_{\bar{\lambda}} = \dim E_{-\lambda} = \dim E_{-\bar{\lambda}}$

Let $\mathcal{S} = \{\lambda \mid \operatorname{Re}\lambda \geq 0 \ \& \ \operatorname{Im}\lambda \geq 0\}$.

For any $\lambda \in \mathcal{S}$, let $f_\lambda = E_\lambda + E_{\bar{\lambda}} + E_{-\lambda} + E_{-\bar{\lambda}}$.

Then:

Proposition 29

$$\mathbb{R}^{2n} = \bigoplus_{\lambda \in \mathcal{S}} f_\lambda.$$

This decomposition is ω-orthogonal (and also Q-orthogonal).

Proposition 30 *The dimension of f_λ is even.*

Proposition 31 *Let $\lambda \in \mathcal{S}$ such that $\operatorname{Re}\lambda = 0, \lambda \neq 0$ and $2m$ be the dimension of f_λ. Then there exists r such that $(2r, 2(m-r))$ is the signature of $Q_{|f_\lambda}$.*

Definition 29 *The Krein signature of an eigenvalue $\lambda \in \mathcal{S}$ such that $\operatorname{Re}\lambda = 0, \lambda \neq 0$ is defined as the pair $(r_\lambda^-, r_\lambda^+)$ such that $(2r_\lambda^-, 2r_\lambda^+)$ is the signature of $Q_{|f_\lambda}$.*

Proposition 32 *Let (α, β) be the signature of $Q_{|f_0}$. Let (a, b) be the signature of Q and $a + b = 2n$. Then:*

$a = \sum_{\lambda \in \mathcal{S}, \operatorname{Re}\lambda > 0} \dim F_\lambda + \sum_{\lambda \in \mathcal{S}, \operatorname{Re}\lambda = 0} r_\lambda^- + \alpha$

$b = \sum_{\lambda \in \mathcal{S}, \operatorname{Re}\lambda > 0} \dim F_\lambda + \sum_{\lambda \in \mathcal{S}, \operatorname{Re}\lambda = 0} r_\lambda^+ + \beta$

Appendix B

Euler-Lagrange equations

In this appendix, we show how to transform a variational problem, (like finding a stationary solution), into an Hamiltonian differential equation. We closely follow the standard procedure. The interest of this part lies in the fact that this is rarely done for derivatives greater than one.

First, we determine the differential equation satisfied by the critical point as well as the Lagrange multipliers associated with the boundary conditions.

Second, we give an Hamiltonian formulation of the differential equation and a formula for the second derivative of the action.

B.1 Differential equation version

Let $C(\phi, a, b) = \begin{pmatrix} a \\ \phi(a) \\ \phi'(a) \\ \vdots \\ \phi^{(n-1)}(a) \\ b \\ \phi(b) \\ \phi'(b) \\ \vdots \\ \phi^{(n-1)}(b) \end{pmatrix}$ and $S(\phi, a, b) = \int_a^b L(\phi, \phi', \phi^{(2)}, \ldots, \phi^{(n)}, t)\mathrm{d}t$.

To find the critical point (ϕ, a, b) of the action S under the constraint $C(\phi, a, b) = C_0 = \begin{pmatrix} \alpha_0 \\ \alpha_1 \\ \vdots \\ \alpha_n \\ \beta_0 \\ \beta_1 \\ \vdots \\ \beta_n \end{pmatrix}$,

let us compute $\mathrm{d}S$ and $\mathrm{d}C$.

The differential of S near the point (ϕ, a, b) is:

$$\mathrm{d}S(\delta\phi, \mathrm{d}a, \mathrm{d}b) = \int_a^b \sum_{k=0}^n \frac{\partial L}{\partial \phi^{(k)}} \delta\phi^{(k)} \mathrm{d}t + L(b)\mathrm{d}b - L(a)\mathrm{d}a$$

Integrating by parts yields:

$$\begin{aligned}
\mathrm{d}S(\delta\phi, \mathrm{d}a, \mathrm{d}b) = \ & \int_a^b \delta\phi \sum_{k=0}^n (-1)^k \frac{\mathrm{d}^k}{\mathrm{d}t^k}\left(\frac{\partial L}{\partial \phi^{(k)}}\right) \mathrm{d}t \\
& + \left[\sum_{k=0}^{n-1} \delta\phi^{(k)} \sum_{r=k+1}^n (-1)^{r-k+1} \frac{\mathrm{d}^{r-k}}{\mathrm{d}t^{r-k}}\left(\frac{\partial L}{\partial \phi^{(r)}}\right)\right]_a^b \\
& + L(b)\mathrm{d}b - L(a)\mathrm{d}a
\end{aligned} \tag{B.1.1}$$

The differential of C is

$$\mathrm{d}C(\delta\phi, \mathrm{d}a, \mathrm{d}b) = \begin{pmatrix} \mathrm{d}a \\ \delta\phi(a) + \phi'(a)\mathrm{d}a \\ \delta\phi'(a) + \phi^{(2)}(a)\mathrm{d}a \\ \vdots \\ \delta\phi^{(n-1)}(a) + \phi^{(n)}(a)\mathrm{d}a \\ \mathrm{d}b \\ \delta\phi(b) + \phi'(b)\mathrm{d}b \\ \delta\phi'(b) + \phi^{(2)}(b)\mathrm{d}b \\ \vdots \\ \delta\phi^{(n-1)}(b) + \phi^{(n)}(b)\mathrm{d}b \end{pmatrix}.$$

Then, if (ϕ, a, b) is a critical point of S under the constraint $C(\phi, a, b) = C_0$, there exists $\Lambda = \begin{pmatrix} \lambda_0 & -\lambda_1 & \dots & -\lambda_n & -\mu_0 & \mu_1 & \dots & \mu_n \end{pmatrix}$ such that:

$$\mathrm{d}S = \Lambda \cdot \mathrm{d}C$$

From this equality, one obtains the Euler-Lagrange equations:

$$\sum_{k=0}^n (-1)^k \frac{\mathrm{d}^k}{\mathrm{d}t^k}\left(\frac{\partial L}{\partial \phi^{(k)}}\right) = 0 \tag{B.1.2}$$

Besides, the Lagrange multipliers are equal to:

$$\begin{aligned}
\lambda_0 &= \sum_{i=1}^n \lambda_i \phi^{(i)}(a) - L(a) \\
\mu_0 &= \sum_{i=1}^n \mu_i \phi^{(i)}(b) - L(b) \\
\lambda_i &= \sum_{r=k+1}^n (-1)^{r-k+1} \frac{\mathrm{d}^{r-k}}{\mathrm{d}t^{r-k}}\left(\frac{\partial L}{\partial \phi^{(r)}}\right)(a) \quad \text{for } 1 \leq i \leq n \\
\mu_i &= \sum_{r=k+1}^n (-1)^{r-k+1} \frac{\mathrm{d}^{r-k}}{\mathrm{d}t^{r-k}}\left(\frac{\partial L}{\partial \phi^{(r)}}\right)(b) \quad \text{for } 1 \leq i \leq n
\end{aligned}$$

B.2 Hamiltonian formulation

Let:

$$
\begin{cases}
q_k = \phi^{(k-1)} \\
p_k = \sum_{r=k}^n (-1)^{r-k+1} \frac{\mathrm{d}^{r-k}}{\mathrm{d}t^{r-k}}\left(\frac{\partial L}{\partial \phi^{(r)}}\right) \\
H = \sum_{i=1}^n p_i \frac{\mathrm{d}}{\mathrm{d}t} q_i - L
\end{cases} \quad .
\tag{B.2.3}
$$

If $Z = (Q, P) = (q_1, q_2, \ldots, q_n, p_1, \ldots, p_n)$ expressed as a function of $(\phi, \phi', \ldots, \phi^{(2n-1)})$ is a diffeomorphism, then:

$$
S(Z, a, b) = \int_a^b \left(P \frac{\mathrm{d}Q}{\mathrm{d}t} - H \right) \mathrm{d}t
\tag{B.2.4}
$$

Define the symplectic form ω as: $\omega((Q_1, P_1), (Q_2, P_2)) = P_2 Q_1 - P_1 Q_2$. Then:

$$
\mathrm{d}S(\delta Z, \delta a, \delta b) = \int_a^b \left(\omega\left(\frac{\mathrm{d}Z}{\mathrm{d}t}, \delta Z\right) - \mathrm{d}H(\delta Z) \right) \mathrm{d}t + [P\delta Q]_a^b + [(P\frac{\mathrm{d}Q}{\mathrm{d}t} - H)\delta t]_{t=a}^{t=b}
\tag{B.2.5}
$$

Suppose that Z is a critical point of S under the constraint $C(\phi, a, b) = C_0$, then the Euler-Lagrange equations can be written as:

$$
\forall v \quad \mathrm{d}H_Z(v) = \omega(\frac{\mathrm{d}Z}{\mathrm{d}t}, v)
\tag{B.2.6}
$$

In (Q, P) coordinates, this can be written as:

$$
\frac{\mathrm{d}}{\mathrm{d}t} P = \frac{\partial H}{\partial Q}, \quad \frac{\mathrm{d}}{\mathrm{d}t} Q = -\frac{\partial H}{\partial P}.
\tag{B.2.7}
$$

If we compute the second variation $\delta^2 S$ near a critical point Z, then:

$$
\begin{aligned}
\delta^2 S(\delta Z_1, 0, 0, \delta Z_2, 0, 0) &= \int_a^b \omega(\frac{\mathrm{d}\delta Z_1}{\mathrm{d}t}, \delta Z_2) - D^2 H(\delta Z_1, \delta Z_2)\mathrm{d}t \\
&\quad + [\delta Q_1 \delta P_2]_a^b.
\end{aligned}
\tag{B.2.8}
$$

Appendix C

Theorems linking the Maslov index and the number of eigenvalues

In this appendix, we give a proof of that if λ and μ are not eigenvalues, then $I(\lambda) - I(\mu)$ counts the number of eigenvalues with multiplicities in $[\lambda, \mu]$.

Proofs of the link between the Maslov index and the number of eigenvalues can be found in the case of a finite length interval in [7, 17, 60]

The existence of eigenvalues is shown by using the change of topology of the path made by the unstable space. BOSE AND JONES [16] were the first to exhibit such an argument which relied on the fact that $\kappa(x, \lambda)$ was increasing with respect to λ.

CHEN AND HU [40] proved under some assumptions that the Morse index of an operator is equal to the Maslov index.

However, proving the monotony of κ is not an easy thing to prove and CHEN AND HU [40] proof is not formulated for the problems we are considering. On the contrary, verifying that $\partial_\lambda \mathbf{C}(x, \lambda)$ is semi-definite is usually straightforward. For example, as mentioned in the introduction of chapter 1, it is possible to put the spectral problem associated to the Hessian of a functional into such a form. Furthermore, this property is true for all systems discussed in this thesis, at the exception of the purposefully crafted example of section 4.2.

The *exact* count of eigenvalues requires the additional hypothesis that the Hamiltonian is increasing with λ. To achieve this, we need perturbative arguments and the comparison principle.

C.1   The comparison principle

Proposition 33 *For $i = 1, 2$, let γ_i be a lift in $\widetilde{\Lambda(n)}$ of a Lagrangian plane of solutions of the system $x' = \mathcal{J} H_i x$ with H_i symmetric. Let α be a Lagrangian plane of solutions of $x' = \mathcal{J} H_1 x$.*

Suppose that $H_1 < H_2$, then the set $I = \{\, t \,|\gamma_2(t) \cap \alpha(t) \neq \{0\}\}$ is discrete and for $a < b$, we

have:

$$m_{\alpha(b)}(\gamma_1(b), \gamma_2(b)) - m_{\alpha(a)}(\gamma_1(a), \gamma_2(a))$$

$$= \tfrac{1}{2}\dim(\alpha(a) \cap \gamma_2(a)) + \sum_{t \in]a,b[\cap I} \dim(\alpha(t) \cap \gamma_2(t)) + \frac{1}{2}\dim(\alpha(b) \cap \gamma_2(b))$$

$$\geq 0$$

This comparison theorem can be found in [7] but not the equality. While it is not difficult to obtain it, we reproduce it here for completeness.

This proposition can be proved by taking a set of coordinates which moves with $x' = \mathcal{J}H_1 x$.

Let $\Phi_1(t)$ be a symplectic matrix such that: $\Phi'_1(t) = \mathcal{J}H_1\Phi_1(t)$ and $\alpha(s) = \mathrm{Range}(\Phi_1(s)\begin{pmatrix} I \\ 0 \end{pmatrix})$.

Let now ξ be a $2n \times n$-matrix such that: $\xi' = \mathcal{J}H_2\xi$ and $\mathrm{Range}(\xi) = p \circ \gamma_2$.

Now, let $Z = \Phi_1^{-1}\xi$ and $E = \mathrm{Range}\left(\begin{pmatrix} I \\ 0 \end{pmatrix}\right)$. Then:

$$m_E(\mathrm{Range}(Z_{|[a,b]})) = m_{\alpha(b)}(\alpha(b), \gamma_2(b)) - m_{\alpha(a)}(\alpha(a), \gamma_2(a))$$

$$\dim(E \cap \mathrm{Range}(Z(t))) = \dim(\alpha(t) \cap \gamma_2(t))$$

$Z' = \Phi_1^{-1}\mathcal{J}(H_2 - H_1)\Phi_1 Z$
$Z' = \mathcal{J}(\Phi_1^T)(H_2 - H_1)\Phi_1 Z$
Let $t \in [a, b]$.
If $k = \dim(E \cap \mathrm{Range}\, Z(t)) > 0$, let G be a $k \times n$-matrix of rank k such that $\mathrm{Range}(Z(t)G) = E \cap Z(t)$.
As $H_1 - H_2 > 0$, $(\Phi_1^T)(H_2 - H_1)\Phi_1 > 0$.
Therefore $G^T(Z'(t)^T \mathcal{J} Z(t) + Z(t)^T \mathcal{J} Z'(t))G = G^T(Z^T(\Phi_1^T)(H_2 - H_1)\Phi_1 Z)G > 0$.
As a consequence, the crossing at t is regular and:

$$\mathrm{sign}^{\pm}(\mathrm{Range}(Z), t, E) = \dim(E \cap \mathrm{Range}(Z(t))) = \dim(\gamma_2(t) \cap \alpha(t)).$$

Therefore, since the crossing points are regular, they are isolated. As a consequence $I = \{\, t \,|\, \gamma_2(t) \cap \alpha(t) \neq \{0\}\}$ is discrete. Since $[a, b]$ is also a closed bounded set, there is only a finite number of crossings in $[a, b]$.

Therefore:

$$m_E(\mathrm{Range}(Z_{|[a,b]})) = \quad \tfrac{1}{2}\dim(\gamma_2(a) \cap \alpha(a)) + \sum_{t \in]a,b[\cap I} \dim(\gamma_2(t) \cap \alpha(t))$$
$$+ \tfrac{1}{2}\dim(\gamma_2(b) \cap \alpha(b)).$$

Since $\Phi_1^{-1}(t)\alpha(t)$ and $\Phi^{-1}(t)\gamma_1(t)$ are constant in moving frames, $m_{\alpha(t)}(\alpha(t), \gamma_1(t))$ is constant. Therefore:

$$\begin{aligned}
m_E(\mathrm{Range}(Z_{|[a,b]})) &= m_{\alpha(b)}(\alpha(b), \gamma_2(b)) - m_{\alpha(b)}(\alpha(b), \gamma_1(b)) \\
&\quad + m_{\alpha(a)}(\alpha(a), \gamma_1(a)) - m_{\alpha(a)}(\alpha(a), \gamma_2(a)) \\
&= m_{\alpha(b)}(\gamma_1(b), \gamma_2(b)) - m_{\alpha(a)}(\gamma_1(a), \gamma_2(a))
\end{aligned}$$

$\square$.

C.2 The Maslov index and the number of eigenvalues

Lemma 2 *Let $\mu \in \sigma_p$ and $a, b \notin \sigma$ such that $[a, b] \cap \sigma = \{\mu\}$. Then the multiplicity of μ is at least $|I_{hom}(\phi, b) - I_{hom}(\phi, a)|$.*

Let $a, b \notin \sigma$ be such that $\sigma \cap [a, b] = \{\mu\}$.

Let $\varepsilon = \frac{1}{2} \min \left(\text{dist}(\mathcal{S}_\infty(\mu), \Lambda(\mathcal{U}_\infty(\mu))), \text{dist}(\mathcal{U}_\infty(\mu), \Lambda(\mathcal{S}_\infty(\mu))) \right)$.

ε is different of zero because $\Lambda(\mathcal{U}_\infty(\mu))$ and $\Lambda(\mathcal{S}_\infty(\mu))$ are closed sets and $\mathcal{U}_\infty(\mu) \cap \mathcal{S}_\infty(\mu) = \{0\}$.

Now, let $\lambda_1 \in [a, \mu[$ and $\lambda_2 \in]\mu, b]$ such that:

$$\forall \lambda \in [\lambda_1, \lambda_2] \quad \text{dist}(\mathcal{U}_\infty(\lambda), \mathcal{U}_\infty(\mu)) < \varepsilon \quad \text{and} \quad \text{dist}(\mathcal{S}_\infty(\lambda), \mathcal{S}_\infty(\mu)) < \varepsilon. \tag{C.2.1}$$

Let x_0 be such that:

$$\forall \lambda \in [\lambda_1, \lambda_2], \forall x > x_0 \quad \text{dist}(\mathcal{S}(x, \lambda), \mathcal{S}_\infty(\lambda)) < \varepsilon$$
$$\forall x > x_0 \quad \text{dist}(\mathcal{U}(x, \lambda_1), \mathcal{U}_\infty(\lambda)) < \varepsilon \text{ and } \text{dist}(\mathcal{U}(x, \lambda_2), \mathcal{U}_\infty(\lambda)) < \varepsilon. \tag{C.2.2}$$

$\mathcal{U} : [\lambda_1, \lambda_2] \times [-\infty, +\infty[\to \Lambda(n)$ and $\mathcal{S} : [\lambda_1, \lambda_2] \times] - \infty, +\infty] \to \Lambda(n)$ are continuous functions over simply connected domains. Therefore, they can be lifted in $\widehat{\Lambda(n)}$. Let $\tilde{\mathcal{U}}$ and $\tilde{\mathcal{S}}$ be their respective lifts.

By definition, we have $I_{hom}(\phi, \lambda_i) = m_{\mathcal{S}_\infty(\lambda_i)}(\tilde{\mathcal{U}}(-\infty, \lambda_i), \tilde{\mathcal{U}}(+\infty, \lambda_i))$ for $i = 1, 2$.

Using the previous hypotheses:

$I_{hom}(\phi, \lambda_i) = m_{\mathcal{S}(x_0, \lambda_i)}(\tilde{\mathcal{U}}(-\infty, \mu), \tilde{\mathcal{U}}(x_0, \lambda_i)))$

$\begin{aligned} I_{hom}(\phi, \lambda_2) - I_{hom}(\phi, \lambda_1) = & \quad m_{\mathcal{S}(x_0, \lambda_2)}(\tilde{\mathcal{U}}(-\infty, \mu), \tilde{\mathcal{U}}(x_0, \lambda_2))) \\ & -m_{\mathcal{S}(x_0, \lambda_1)}(\tilde{\mathcal{U}}(-\infty, \mu), \tilde{\mathcal{U}}(x_0, \lambda_1))) \end{aligned}$

Since $m_{\mathcal{S}(x_0, \lambda_1)}(\tilde{\mathcal{U}}(-\infty, \mu), \tilde{\mathcal{S}}(x_0, \lambda_1)) = m_{\mathcal{S}(x_0, \lambda_2)}(\tilde{\mathcal{U}}(-\infty, \mu), \tilde{\mathcal{S}}(x_0, \lambda_2)))$:

$\begin{aligned} I_{hom}(\phi, \lambda_2) - I_{hom}(\phi, \lambda_1) = & \quad m_{\mathcal{S}(x_0, \lambda_2)}(\tilde{\mathcal{S}}(x_0, \lambda_2), \tilde{\mathcal{U}}(x_0, \lambda_2))) \\ & -m_{\mathcal{S}(x_0, \lambda_1)}(\tilde{\mathcal{S}}(x_0, \lambda_1), \tilde{\mathcal{U}}(x_0, \lambda_1))) \end{aligned}$

Except at $\lambda = \mu$, $\mathcal{S}(x_0, \lambda) \cap \mathcal{U}(x_0, \lambda) = \{0\}$ and therefore $m_{\mathcal{S}(x_0, \lambda)}(\tilde{\mathcal{S}}(x_0, \lambda), \tilde{\mathcal{U}}(x_0, \lambda))$ is constant over $[\lambda_1, \mu[$ and $]\mu, \lambda_2]$ and the jump at μ is equal to $I_{hom}(\phi, \lambda_2) - I_{hom}(\phi, \lambda_1)$.

Since

$\begin{aligned} \dim(\mathcal{S}(x_0, \mu) \cap \mathcal{U}(x_0, \mu)) \geq & \quad \lim_{\lambda \to \mu^+} m_{\mathcal{S}(x_0, \lambda)}(\tilde{\mathcal{S}}(x_0, \lambda), \tilde{\mathcal{U}}(x_0, \lambda))) \\ & - \lim_{\lambda \to \mu^-} m_{\mathcal{S}(x_0, \lambda)}(\tilde{\mathcal{S}}(x_0, \lambda), \tilde{\mathcal{U}}(x_0, \lambda))) \end{aligned}$,

we have $\dim(\mathcal{S}(x_0, \mu) \cap \mathcal{U}(x_0, \mu)) \geq I_{hom}(\phi, \lambda_2) - I_{hom}(\phi, \lambda_1)$.

Therefore, μ is an eigenvalue of multiplicity of at least $|I_{hom}(\phi, \lambda_2) - I_{hom}(\phi, \lambda_1)|$.

Since I is constant over $[a, \lambda_1]$ and $[\lambda_2, b]$, we have $I_{hom}(\phi, \lambda_2) - I_{hom}(\phi, \lambda_1) = I_{hom}(\phi, b) - I_{hom}(\phi, a)$.

$\square$

Lemma 3 *Suppose that $\partial_\lambda \mathcal{J} A(x, \lambda)$ is positive.*

Let $\mu \in \sigma$ and $a, b \notin \sigma$ such that $[a, b] \cap \sigma = \{\mu\}$ and $a < b$. Then, the multiplicity of μ is $I_{hom}(\phi, b) - I_{hom}(\phi, a)$.

Furthermore, for x_0 large enough: $m_{\mathcal{S}(x_0, \mu)}(\tilde{\mathcal{U}}(-\infty, \mu), \tilde{\mathcal{U}}(x_0, \mu)) = \frac{I_{hom}(\phi, a) + I_{hom}(\phi, b)}{2}$.

Denote by r the multiplicity of the eigenvalue μ. Then $r = \dim(\mathcal{U}(x, \mu) \cap \mathcal{S}(x, \mu))$.

As for the previous lemma, let us introduce the quantities $\varepsilon, \lambda_1, \lambda_2, x_0$.

We know from lemma 2 that $|I_{hom}(\phi, \lambda_1) - I_{hom}(\phi, \lambda_2)| \leq r$. It remains to prove that $r \leq I_{hom}(\phi, \lambda_2) - I_{hom}(\phi, \lambda_2)$.

Now, consider the slightly perturbed problem:

$$u_x = (A(x, \lambda) + \theta(\lambda - \mu)\mathcal{J})u. \tag{C.2.3}$$

Since λ_1, λ_2 are not elements of the spectrum, we have $\lim_{\theta \to 0^+} \tilde{\mathcal{U}}^\theta(x_0, \lambda_i) = \tilde{\mathcal{U}}(x_0, \lambda_i)$.

For θ small enough, we have:

$m_{\mathcal{S}(x_0, \mu)}(\tilde{\mathcal{S}}(x_0, \mu), \tilde{\mathcal{U}}^\theta(x_0, \lambda_i)) = m_{\mathcal{S}(x_0, \mu)}(\tilde{\mathcal{S}}(x_0, \mu), \tilde{\mathcal{U}}^\theta(x_0, \lambda_i))$.

Now, let consider $\tilde{\mathcal{U}}^{\theta, L}$ such that:

- $\tilde{\mathcal{U}}^{\theta, L}(-L, \lambda) = \tilde{\mathcal{U}}(-L, \mu)$

- $\mathcal{U}^{\theta, L}$ is a Lagrangian space of solutions of $u_x = (A(x, \lambda) + \theta(\lambda - \mu)\mathcal{J})u$.

From proposition 33 we have:

- $m_{\mathcal{S}(x, \mu)}(\tilde{\mathcal{U}}(x, \mu), \tilde{\mathcal{U}}^{\theta, L}(x, \lambda)) \geq \frac{k}{2}$ if $x > -L$ and $\lambda > \mu$,

- $m_{\mathcal{S}(x, \mu)}(\tilde{\mathcal{U}}(x, \mu), \tilde{\mathcal{U}}^{\theta, L}(x, \lambda)) \leq -\frac{k}{2}$ if $x > -L$ and $\lambda < \mu$.

Besides, $\lim_{L \to \infty} \text{dist}(\tilde{\mathcal{U}}^{\theta, L}(x_0, \lambda), \tilde{\mathcal{U}}^\theta(x_0, \lambda)) = 0$ and $\mathcal{U}^\theta(x_0, \lambda) \cap \mathcal{S}(x_0, \mu) = \{0\}$.

Therefore, for L large enough:

$m_{\mathcal{S}(x_0, \mu)}(\tilde{\mathcal{U}}(x_0, \mu), \tilde{\mathcal{U}}^{\theta, L}(x_0, \lambda_i)) = m_{\mathcal{S}(x_0, \mu)}(\tilde{\mathcal{U}}(x_0, \mu), \tilde{\mathcal{U}}^\theta(x_0, \lambda_i))$.

From this, we conclude that:

- $m_{\mathcal{S}(x_0, \mu)}(\tilde{\mathcal{U}}(x_0, \mu), \tilde{\mathcal{U}}(x_0, \lambda_1)) \leq -\frac{k}{2}$,

- $m_{\mathcal{S}(x_0, \mu)}(\tilde{\mathcal{U}}(x_0, \mu), \tilde{\mathcal{U}}(x_0, \lambda_2)) \geq \frac{k}{2}$.

Therefore, we have $m_{\mathcal{S}(x_0, \mu)}(\tilde{\mathcal{U}}(x_0, \lambda_1), \tilde{\mathcal{U}}(x_0, \lambda_2)) \geq k$.

We have $I_{hom}(\phi, \lambda_i) = m_{\mathcal{S}(x_0, \mu)}(\tilde{\mathcal{U}}(-\infty, \lambda_i), \tilde{\mathcal{U}}(+\infty, \lambda_i))$ and $m_{\mathcal{S}(x_0, \mu)}(\tilde{\mathcal{U}}(-\infty, \lambda_i), \tilde{\mathcal{U}}(-\infty, \lambda_{3-i})) = m_{\mathcal{S}(x_0, \mu)}(\tilde{\mathcal{U}}(-\infty, \lambda_i), \tilde{\mathcal{U}}(x_0, \lambda_i)) = 0$, so

$$I_{hom}(\phi, \lambda_2) - I_{hom}(\phi, \lambda_1) \geq k.$$

Using the previous lemma, $I_{hom}(\phi, \lambda_2) - I_{hom}(\phi, \lambda_1) = k$.

Furthermore, $m_{\mathcal{S}(x_0, \mu)}(\tilde{\mathcal{U}}(-\infty, \mu), \tilde{\mathcal{U}}(x_0, \mu)) = \frac{I_{hom}(\phi, \lambda_1) + I_{hom}(\phi, \lambda_2)}{2}$.

□

Proposition 34 *Let $a, b \notin \sigma$ such that $[a, b] \cap \sigma_{ess} = \emptyset$. The number of eigenvalues with multiplicity in $[a, b]$ is at least $|I_{hom}(\phi, b) - I_{hom}(\phi, a)|$.*

The number of eigenvalues is finite in $[a, b]$. Otherwise there would be an accumulation point of eigenvalues and hence an element of the essential spectrum.

So we can find $a = \lambda_1, \ldots, \lambda_n = b$ such that $\{\sigma \cap [\lambda_i, \lambda_{i+1}]\} = \{\mu_i\}$.

Therefore $|I_{hom}(\phi, \lambda_n) - I_{hom}(\phi, \lambda_1)| \leq \sum_{k=1}^{n-1} |I_{hom}(\phi, \lambda_{k+1}) - I_{hom}(\phi, \lambda_k)| \leq \sum_{k=1}^{n-1}$ multiplicity of μ_i.

□

Proposition 35 *Suppose that $\partial_\lambda \mathcal{J} A(x, \lambda)$ is positive.*

Let $\lambda_1, \lambda_2 \notin \sigma$ such that $[\lambda_1, \lambda_2] \cap \sigma_{ess} = \emptyset$. The number of eigenvalues with multiplicity in $[\lambda_1, \lambda_2]$ is $I_{hom}(\phi, \lambda_2) - I_{hom}(\phi, \lambda_1)$.

The demonstration is the same as the previous lemma, except that inequalities can be replaced by equalities and absolute values removed.

Appendix D

Properties of $\mathbf{B}^{(2)}$ on $\bigwedge^n(\mathbb{R}^{2n})$

Proposition 36 *The induced matrix* $\mathbf{B}^{(2)}$ *satisfies* $\omega\mathbf{B}^{(2)} = 0$, *where* ω *is defined in (2.2.5), if and only if* $\mathbf{JB}$ *is symmetric.*

Proof.
$$
\begin{aligned}
\omega\mathbf{B}^{(2)} = 0 \quad &\Leftrightarrow \forall x, y \in \mathbb{R}^{2n} \quad \omega\mathbf{B}^{(2)}(x \wedge y) = 0 \\
&\Leftrightarrow \forall x, y \quad < \omega, (\mathbf{B}x) \wedge y + x \wedge (\mathbf{B}y) >_{\bigwedge^2(\mathbb{R}^{2n})} = 0 \\
&\Leftrightarrow \forall x, y \quad \omega(\mathbf{B}x, y) + \omega(x, \mathbf{B}y) = 0 \\
&\Leftrightarrow \forall x, y \quad (\mathbf{B}x)^t \mathbf{J}y + y^t \mathbf{J}(\mathbf{B}x) = 0 \\
&\Leftrightarrow \forall x, y \quad y^t(-(\mathbf{JB})^t + \mathbf{JB})y = 0 \\
&\Leftrightarrow (\mathbf{JB})^t = \mathbf{JB}
\end{aligned}
$$

$\square$

Let $\mathbf{B}$ be an arbitrary 4×4 matrix with entries b_{ij}. Then, with respect to the standard basis (2.2.6) on $\bigwedge^2(\mathbb{R}^4)$ the induced matrix is

$$
\mathbf{B}^{(2)} = \begin{bmatrix}
b_{11} + b_{22} & b_{23} & b_{24} & -b_{13} & -b_{14} & 0 \\
b_{32} & b_{11} + b_{33} & b_{34} & b_{12} & 0 & -b_{14} \\
b_{42} & b_{43} & b_{11} + b_{44} & 0 & b_{12} & b_{13} \\
-b_{31} & b_{21} & 0 & b_{22} + b_{33} & b_{34} & -b_{24} \\
-b_{41} & 0 & b_{21} & b_{43} & b_{22} + b_{44} & b_{23} \\
0 & -b_{41} & b_{31} & -b_{42} & b_{32} & b_{33} + b_{44}
\end{bmatrix}, \qquad \text{(D.0.1)}
$$

A constructive proof is given in §2 of [4].

Appendix E

Maslov index theory for a simple dissipative equation

In this appendix, we consider a simple, exactly computable model which shows how the Maslov index of homoclinic orbits works and how it can be used to determine the stability of dissipative structures.

It is a simplified version of the class of nonlinear parabolic PDEs studied in [16].

Consider the nonlinear parabolic PDE

$$\frac{\partial \phi}{\partial t} = \frac{\partial^2 \phi}{\partial x^2} - \phi + \phi^2 \,, \quad x \in \mathbb{R} \,, \tag{E.0.1}$$

for the scalar-valued function $\phi(x, t)$. There is a basic steady solitary wave solution

$$\widehat{\phi}(x) = \tfrac{3}{2} \operatorname{sech}^2 \left(\tfrac{1}{2} x \right) \,, \tag{E.0.2}$$

which satisfies $\widehat{\phi}_{xx} - \widehat{\phi} + \widehat{\phi}^2 = 0$. Linearizing (E.0.1) about the basic state $\widehat{\phi}$ and looking for solutions proportional to $\mathrm{e}^{\lambda t}$ leads to the spectral problem

$$\mathscr{L}\phi = \lambda \phi \,, \quad \text{with} \quad \mathscr{L}\phi := \frac{d^2 \phi}{dx^2} - \phi + 2\widehat{\phi}(x)\phi \,. \tag{E.0.3}$$

The basic state (E.0.2) is said to be (spectrally) unstable if any part of the spectrum of $\mathscr{L}$ is positive. The spectrum of $\mathscr{L}$ can be explicitly constructed. It consists of a branch of essential spectra and a point spectrum

$$\sigma(\mathscr{L}) = \sigma_{ess}(\mathscr{L}) \cup \sigma_p(\mathscr{L}) \,,$$

with $\sigma_{ess}(\mathscr{L}) = \{\lambda \in \mathbb{R} \; : \; \lambda \leq -1\}$ and $\sigma_p(\mathscr{L}) = \left\{ -\tfrac{3}{4}, \, 0, \, \tfrac{5}{4} \right\}$. The spectrum is illustrated in Figure E.1.

The point spectrum can be verified by constructing the Evans function. First reformulate (E.0.3) as a first-order system. Let

$$\mathbf{u}(x, \lambda) = \begin{pmatrix} \phi(x, \lambda) \\ \phi_x(x, \lambda) \end{pmatrix} \,,$$
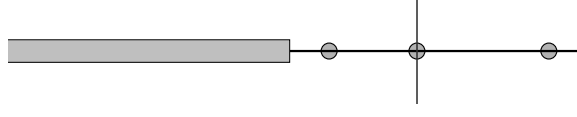
Figure E.1: Plot of the spectrum of $\mathscr{L}$.

then

$$\mathcal{J}\mathbf{u}_x = \mathbf{C}(x, \lambda)\mathbf{u}, \quad \mathbf{u} \in \mathbb{R}^2, \quad \lambda \in \mathbb{R}, \tag{E.0.4}$$

with

$$\mathbf{C}(x, \lambda) = \begin{bmatrix} \lambda + 1 - 3\mathrm{sech}^2(\frac{1}{2}x) & 0 \\ 0 & 1 \end{bmatrix}.$$

The eigenvalues of $\mathbf{B}_\infty(\lambda)$ are real and hyperbolic when $\lambda + 1 > 0$. In this formulation the stable ($\mathbf{u}^-$) and unstable ($\mathbf{u}^+$) subspaces are represented by

$$\mathbf{u}^\pm(x, \lambda) = \mathrm{e}^{\pm\gamma s} \begin{pmatrix} h^\pm \\ \frac{1}{2}(h_s^\pm \pm \gamma h^\pm) \end{pmatrix},$$

where $s = \frac{1}{2}x$, $\gamma = 2\sqrt{\lambda + 1}$,

$$h^\pm(s, \lambda) = \pm a_0 + a_1\mathrm{tanh}(s) \pm a_2\mathrm{tanh}^2(s) + a_3\,\mathrm{tanh}^3(s),$$

and

$$a_0 = \frac{\gamma}{15}(4 - \gamma^2)\,a_3, \quad a_1 = \frac{1}{5}(2\gamma^2 - 3)\,a_3, \quad a_2 = -\gamma\,a_3, \tag{E.0.5}$$

and a_3 is an arbitrary nonzero real number. The Evans function is then

$$D(\lambda) = \mathbf{u}^-(x, \lambda) \wedge \mathbf{u}^+(x, \lambda).$$

Evaluating at $x = 0$, a straightforward calculation leads to

$$D(\lambda) = -2\sqrt{\lambda + 1}\left(\frac{2a_3}{15}\right)^2 \lambda\,(4\lambda + 3)(4\lambda - 5).$$

Details of calculations of this type can be found in the Appendix of [22].

For linear Hamiltonian systems on $\mathbb{R}^2$ Lagrangian subspaces are just one-dimensional subspaces. The path of unstable subspaces $\mathbf{u}^+(x, \lambda)$ is used to define the Maslov index. The natural one-dimensional subspace to choose for the reference space is $\mathrm{E}^s(\mathbf{B}_\infty(\lambda))$,

$$\mathrm{E}^s(\mathbf{B}_\infty(\lambda)) = \mathrm{span}\left\{\begin{pmatrix} 2 \\ -\gamma \end{pmatrix}\right\}.$$

Then, assume simple intersections between $\mathrm{E}_\infty^s(\lambda)$ and $\mathbf{u}^+(x, \lambda)$ – which can be confirmed a posteriori for the example (E.0.4) – and assume that

$$\lim_{x \to \pm\infty} \mathrm{span}(\mathbf{u}^+(x, \lambda)) \bigcap \mathrm{E}^s(\mathbf{B}_\infty(\lambda)) = \{0\}.$$

This latter assumption is equivalent to assuming that λ is not an eigenvalue. The Maslov index for this case is

$$m_{\mathrm{E}^s(\mathbf{B}_\infty(\lambda))}(\mathbf{u}^+) = \sum_{x_0} \mathrm{sign}\,\langle \mathbf{J}\mathbf{u}_x^+, \mathbf{u}^+ \rangle\,,$$

with x_0 the points at which $\mathbf{u}^+(x,\lambda) \cap \mathrm{E}^s(\mathbf{B}_\infty(\lambda))$ is non-trivial.

The path of unstable subspaces is

$$\mathbf{u}^+(x,\lambda) = \tfrac{1}{2}\mathrm{e}^{\gamma s} \begin{pmatrix} 2h^+ \\ h_s^+ + \gamma h^+ \end{pmatrix}\,. \tag{E.0.6}$$

The intersection form in this case is

$$\begin{aligned}
\mathrm{sign}(\mathbf{u}^+, \mathrm{E}^s(\mathbf{B}_\infty(\lambda)), x_0) &= \mathrm{sign}\left(\langle \mathbf{J}\mathbf{u}_x^+, \mathbf{u}^+ \rangle \Big|_{x=x_0} \right)\,, \\
&= \mathrm{sign}\left((-u_1^+ \dot{u}_2^+ + u_2^+ \dot{u}_1^+) \Big|_{x=x_0} \right) \\
&= \mathrm{sign}\left(\left[((u_2^+)^2 - \lambda - 1 + 12\,\mathrm{sech}^2 s)(u_1^+)^2 \right] \Big|_{x=x_0} \right)\,.
\end{aligned}$$

However, at a point x_0 where $\mathbf{u}^+$ intersects E_λ^s, $u_2^+ = -\tfrac{1}{2}\gamma u_1^+$ and so

$$\mathrm{sign}(\mathbf{u}^+, \mathrm{E}^s(\mathbf{B}_\infty), x_0) = \mathrm{sign}(12\,\mathrm{sech}^2 \tfrac{1}{2}x_0\,(u_1^+)^2)\,.$$

Hence $\Gamma(\mathbf{u}^+, \mathrm{E}^s) > 0$ at each intersection, and the Maslov index is just the sum of the intersections. An intersection occurs when

$$\xi^s \wedge \mathbf{u}^+ = 0\,, \quad \text{where} \quad \xi^s = \begin{pmatrix} 2 \\ -\gamma \end{pmatrix}\,.$$

Now

$$\xi^s \wedge \mathbf{u}^+ = (2u_2^+ + \gamma u_1^+)\mathsf{vol}\,.$$

The factor $\mathrm{e}^{\gamma s}$ is not important and so can be divided out, giving

$$\xi^s \wedge \mathbf{u}^+ \sim (\frac{dh^+}{ds} + 2\gamma h^+)\mathsf{vol}\,.$$

This function has $0, 1, 2$ or 3 zeros depending on the value of λ. Each zero corresponds to an intersection between the unstable subspace with $\mathrm{E}^s(\mathbf{B}_\infty(\lambda))$. The function $\xi^s \wedge \mathbf{u}^+$ is illustrated in Figure E.2 for the case $\lambda = -0.8$ where $\xi^s \wedge \mathbf{u}^+$ has three zeros indicating three intersections. A summary of the Maslov index in each region is tabulated below.

λ	$-1 < \lambda < -\frac{3}{4}$	$-\frac{3}{4} < \lambda < 0$	$0 < \lambda < \frac{5}{4}$	$\lambda > \frac{5}{4}$
$m_{\mathrm{E}^s(\mathbf{B}_\infty(\lambda))}(\mathbf{u}^+)$	3	2	1	0

We make the following observation about the connection between the Maslov index and the number of eigenvalues as a function of λ. Let λ_0 be any fixed real value of λ such that $\lambda_0 > -1$ and λ_0 is not an eigenvalue, then the value of the Maslov index equals the number of eigenvalues of $\mathscr{L}$ in the set $\lambda > \lambda_0$.
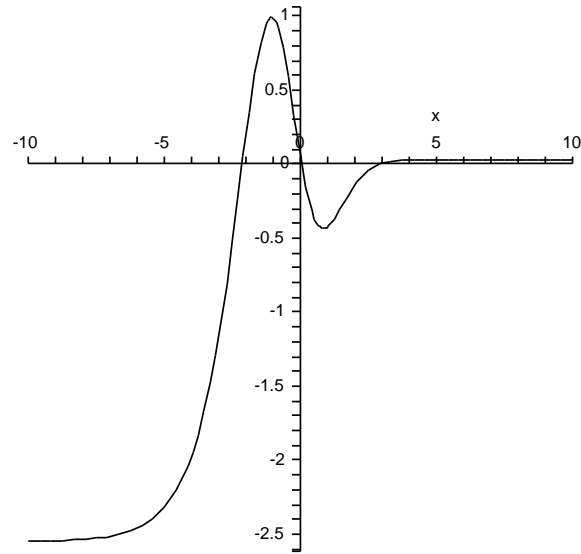
Figure E.2: Plot of $\xi^s \wedge \mathbf{u}^+(x, \lambda)$ for the case $\lambda = -0.8$.

E.0.1 The Maslov angle in $\bigwedge^1(\mathbb{R}^2)$

Another way to count intersections between the path $\mathbf{u}^+$ and some reference plane is to use s. In this case the angle $\kappa(x, \lambda)$ is just the angle determined by a polar representation of $\mathbf{u}^+$

$$s(\mathbf{u}^+(x, \lambda)\mathbb{R}) = \mathrm{e}^{\mathrm{i}\kappa(x,\lambda)} := \frac{u_1^+(x, \lambda) - \mathrm{i}u_2^+(x, \lambda)}{u_1^+(x, \lambda) + \mathrm{i}u_2^+(x, \lambda)}.$$

As $x \to \pm\infty$

$$\lim_{x \to \pm\infty} \mathrm{e}^{\mathrm{i}\kappa(x,\lambda)} = \frac{2 - \mathrm{i}\gamma}{2 + \mathrm{i}\gamma}.$$

The Maslov index is then the count of the number of times that κ crosses some reference angle as x varies, such as the angle associated with the stable subspace.

Appendix F

Technical issues concerning the Kawahara equation

In this appendix, we prove that:

- $\mathscr{L}$, introduced in (3.3.14), has at least one strictly negative eigenvalue.

- the Maslov index of Kawahara solitary waves $I_{hom}(\phi, \lambda)$ converges to zero when $\lambda \to -\infty$.

F.1   The existence of at least one negative eigenvalue

Consider the linear operator

$$\mathscr{L}\phi := \phi_{xxxx} - P\phi_{xx} + a(x)\phi\,, \tag{F.1.1}$$

introduced in (3.3.14) with $a(x) = c - (q+1)\widehat{\phi}(x)^q$ and $\widehat{\phi}(x)$ satisfying (3.2.8). Assume

$$P + 2c \geq 0 \quad \text{and} \quad 0 < c \leq 1 \quad \text{or} \quad P > 0 \quad \text{and} \quad c > 0\,. \tag{F.1.2}$$

The essential spectrum for this problem is non-negative. Here it is proved that $\mathscr{L}$ has at least one negative eigenvalue in the point spectrum.

Multiply (3.2.8) by the basic state $\widehat{\phi}(x)$,

$$
\begin{aligned}
\widehat{\phi}^{q+2} &= c\widehat{\phi}^2 - P\widehat{\phi}\widehat{\phi}_{xx} + \widehat{\phi}\widehat{\phi}_{xxxx} \\
&= c\widehat{\phi}^2 - (P+2c)\widehat{\phi}\widehat{\phi}_{xx} + 2c\widehat{\phi}\widehat{\phi}_{xx} + \widehat{\phi}\widehat{\phi}_{xxxx} \\
&= c(\widehat{\phi} + \widehat{\phi}_{xx})^2 - (P+2c)\widehat{\phi}\widehat{\phi}_{xx} - c\widehat{\phi}_{xx}^2 + \widehat{\phi}\widehat{\phi}_{xxxx}\,.
\end{aligned}
$$

Hence integrating, using the fact that $\widehat{\phi}$ and its derivatives decay exponentially as $x \to \pm\infty$, and the hypotheses (F.1.2) yields

$$\int_{-\infty}^{\infty} \widehat{\phi}^{q+2}\mathrm{d}x = \int_{-\infty}^{\infty} c(\widehat{\phi} + \widehat{\phi}_{xx})^2\mathrm{d}x + (P+2c)\int_{-\infty}^{\infty} \widehat{\phi}_x^2\mathrm{d}x + (1-c)\int_{-\infty}^{+\infty} \widehat{\phi}_{xx}^2\,\mathrm{d}x > 0\,, \tag{F.1.3}$$

or if $P > 0$ and $c > 0$,

$$\int_{-\infty}^{\infty} \widehat{\phi}^{q+2} \mathrm{d}x = \int_{-\infty}^{\infty} (c\widehat{\phi}^2 + P\widehat{\phi}_x^2 + \widehat{\phi}_{xx}^2) \, \mathrm{d}x > 0 \,. \tag{F.1.4}$$

To prove that (F.1.1) has a negative eigenvalue, we will show that the quadratic form $\langle u, \mathscr{L}u \rangle$ is negative when $u = \widehat{\phi}$ where $\langle u, \mathscr{L}u \rangle := \int_{-\infty}^{\infty} u \, \mathscr{L}u \, \mathrm{d}x$. Now

$$
\begin{aligned}
\langle u, \mathscr{L}u \rangle \big|_{u=\widehat{\phi}} &= \int_{-\infty}^{\infty} (\widehat{\phi}(\widehat{\phi}_{xxxx} - P\widehat{\phi}_{xx} + a(x)\widehat{\phi})) \, \mathrm{d}x \\
&= \int_{-\infty}^{\infty} (\widehat{\phi}_{xx}^2 + P\,\widehat{\phi}_x^2 + c\widehat{\phi}^2) \, \mathrm{d}x - (q+1) \int_{-\infty}^{\infty} \widehat{\phi}^{q+2} \mathrm{d}x \\
&= -q \int_{-\infty}^{\infty} \widehat{\phi}^{q+2} \mathrm{d}x \,,
\end{aligned}
$$

using (F.1.4) in the last line. It follows from (F.1.3) or (F.1.4) that $\langle \widehat{\phi}, \mathscr{L}\widehat{\phi} \rangle < 0$.

F.2   Proof that $\lim_{\lambda \to -\infty} I_{hom}(\phi, \lambda) = 0$ for the Kawahara system

Here, we give the details of the proof that $\mathbf{B}(x, \lambda) = \mathcal{J}^{-1}\mathbf{C}(x, \lambda)$ for the Kawahara equation, with $\mathbf{C}(x, \lambda)$ defined in (3.2.13), satisfies Hypothesis 4. Then we can apply proposition 20 and prove that $\lim_{\lambda \to -\infty} I_{hom}(\phi, \lambda) = 0$.

First set

$$s = \frac{1}{(1-\lambda)^{\frac{1}{4}}} \,.$$

When λ is large and negative, s is a small parameter. This parameter will be used to obtain series expansions of the eigenvectors and of the eigenvalues.

The characteristic polynomial of $\mathbf{B}_\infty(\lambda)$ is

$$0 = \det[X\mathbf{I} - \mathbf{B}_\infty(\lambda)] = X^4 - PX^2 + \frac{1}{s^4} \,.$$

This polynomial is a biquadratic and for s small it has four complex roots, one in each quadrant. Let $\theta(s)$ be the eigenvalue in the right-upper quadrant. Its Taylor expansion is:

$$\theta(s) = \frac{1+\mathrm{i}}{s\sqrt{2}} \left(1 - \frac{1}{4}\mathrm{i}Ps^2 - \frac{1}{32}P^2s^4 - \frac{1}{128}\mathrm{i}P^3s^6 + O\left(s^8\right) \right) \,.$$

The other eigenvalues are $\overline{\theta(s)}$, $-\theta(s)$, $-\overline{\theta(s)}$. The eigenvector associated with $\theta(s)$ is :

$$\mathbf{v}(s) = s \begin{pmatrix} -\frac{1}{s^4\theta} \\ \theta \\ 1 \\ \theta^2 \end{pmatrix} \,.$$

A Taylor expansion of this eigenvector is:

$$\mathbf{v}(s) = s\mathbf{v}_1 + \mathrm{i}s\mathbf{v}_2 + O\left(s^6\right) \,.$$

with

$$\mathbf{v}_1(s) = \begin{pmatrix} -\left(1/2\,\sqrt{2} + \frac{1}{8}\,\sqrt{2}Ps^2 - \frac{1}{64}\,\sqrt{2}P^2s^4 + \frac{1}{256}\,\sqrt{2}P^3s^6\right)s^{-3} \\ \frac{1}{256}\,\sqrt{2}P^3s^5 - \frac{1}{64}\,\sqrt{2}P^2s^3 + \frac{1}{8}\,\sqrt{2}Ps + \frac{\sqrt{2}}{2s} \\ 1 \\ \frac{1}{2}P \end{pmatrix}$$

and

$$\mathbf{v}_2(s) = \begin{pmatrix} -\left(-1/2\,\sqrt{2} + \frac{1}{8}\,\sqrt{2}Ps^2 + \frac{1}{64}\,\sqrt{2}P^2s^4 + \frac{1}{256}\,\sqrt{2}P^3s^6\right)s^{-3} \\ -\frac{1}{256}\,\sqrt{2}P^3s^5 - \frac{1}{64}\sqrt{2}P^2s^3 - \frac{1}{8}\sqrt{2}Ps + \frac{\sqrt{2}}{2s} \\ 0 \\ s^{-2} - \frac{1}{8}s^2P^2 \end{pmatrix}.$$

$(\operatorname{Re} v(s), \operatorname{Im} v(s))$ is a basis of the unstable space. Let V_{unst} be the matrix whose columns are $\operatorname{Re} v(s)$ and $\operatorname{Im} v(s)$).

The eigenvector associated to $-\theta(s)$ is:

$$\mathbf{w}(s) = s \begin{pmatrix} \frac{1}{s^4\theta} \\ -\theta \\ 1 \\ \theta^2 \end{pmatrix}$$

$(\operatorname{Re} \mathbf{w}(s), \operatorname{Im} \mathbf{w}(s))$ is a basis of the unstable space. Let U_{st} the matrix whose columns are $\operatorname{Re} \mathbf{w}(s)$ and $\operatorname{Im} \mathbf{w}(s)$).

The matrix $\left(V_{unst}|U_{st}\right)$ is not a symplectic matrix but $V(s) = \left(V_{unst}|V_{st}\right)$, with $V_{st} = -U_{st}(V_{unst}^T J U_{st})^{-1}$, is. Besides, we have:

$$V_{st} = \begin{pmatrix} \frac{1}{2s} & \frac{-\frac{1}{4}s^2P - \frac{1}{32}P^3s^6}{s} \\ 0 & \frac{\frac{1}{2}s^2 + \frac{1}{16}s^6P^2}{s} \\ \frac{\frac{1}{4}\sqrt{2}s^3 - \frac{1}{16}\sqrt{2}Ps^5}{s} & \frac{-\frac{1}{4}\sqrt{2}s^3 - \frac{1}{16}\sqrt{2}Ps^5}{s} \\ \frac{-\frac{1}{4}\sqrt{2}s + \frac{1}{16}\sqrt{2}Ps^3 - \frac{3}{128}\sqrt{2}P^2s^5}{s} & \frac{-\frac{1}{4}\sqrt{2}s - \frac{1}{16}\sqrt{2}Ps^3 - \frac{3}{128}\sqrt{2}P^2s^5}{s} \end{pmatrix} + O(s^6)$$

We also have $V^{-1} = -J({}^T V)J$ since V is a symplectic matrix.

Let

$$\mathbf{T} = \begin{pmatrix} 0 & 0 & 1 & 0 \\ 0 & 0 & 0 & 0 \\ 0 & 0 & 0 & 0 \\ 0 & 0 & 0 & 0 \end{pmatrix}.$$

We are now able to evaluate: $V^{-1}BV$: $V^{-1}BV = O\left(s^2\right)$ but also

$$V^{-1}BV \begin{pmatrix} 1 & 0 \\ 0 & 1 \\ 0 & 0 \\ 0 & 0 \end{pmatrix} = VBV_{unst} = O\left(s^2\right).$$

Therefore, $(V^{-1}BV)^{(n)}e_1 = O\left(s^2\right)$. Therefore, as $R(x, \lambda) = A(x, \lambda) - A_\infty(\lambda) = (1 - a(x))B$ and as $|1 - a(x)| \le C_1 e^{-C_2|x|}$, this proves that Hypothesis 4 of Proposition 20 is satisfied.

Appendix G

Approximating single eigenvalues for regular Sturm-Liouville problems with separated Hermitian boundary conditions

The 1D Sturm-Liouville equation arises in various fields like Quantum Mechanics or the integrable Korteweg-de Vries equation. The natural generalization of this well-known problem is:

Find λ and $u : [a,b] \to \mathbb{R}^{2n}$ such that:

- $E_1 u(a) + E_2 u(b) = 0$ with $(E_2|E_2)$ of full rank and $E_1 J E_1^* = E_2 J E_2^*$.

- $\forall x \in [a,b] \quad u_x = \begin{pmatrix} 0 & B(x) \\ -D(x) + \lambda C(x) & 0 \end{pmatrix} u$ with B and C symmetric definite positive and D symmetric. We also suppose that B,C,D are continuous functions.

This class of boundary conditions are called Hermitian. We can see that one cannot always choose $u(a)$ and $u(b)$ independently. However we will only study the 'separated' case where $u(a)$ and $u(b)$ can be chosen independently:

Find λ and $u : [a,b] \to \mathbb{R}^{2n}$ such that:

- $u(a) \in U$ and $u(b) \in V$, where U and V are Lagrangian planes.

- $\forall x \in [a,b] \quad u_x = \begin{pmatrix} 0 & B(x) \\ -D(x) + \lambda C(x) & 0 \end{pmatrix} u$ with B and C symmetric definite positive and D symmetric. We also suppose that B,C,D are continuous function.

In any case, all Hermitian boundary conditions can be reduced to separated ones (see [60]).

Dwyer & Zettl [61] have described a method which enables an exact count of the eigenvalues. However, they have to use the bisection method to locate precisely the eigenvalues.

We use an n-form approach instead.

Let $\mathbf{U}$ and $\mathbf{V}$ be two n-forms which map the Lagrangian spaces.

Suppose that $\mathbf{W}(x, \lambda)$ satisfies $\mathbf{W}_x(x, \lambda) = A(x, \lambda)\mathbf{W}(x, \lambda)$ and $\mathbf{W}(a, \lambda) = \mathbf{U}$.

Let $E(\lambda) = \mathbf{W}(b, \lambda) \wedge \mathbf{V}$.

E is a C^1 function and its zeros are the eigenvalues of the Sturm-Liouville problem. The zeros E can be computed by using the secant method. For single zeros, the difference between the eigenvalue and the n-th iterate is known to be below $C(\frac{1+\sqrt{5}}{2})^{-n}$. For multiple ones, convergence is worse, though geometric.

We try these ideas on the system presented in [61]:

$$A(x, \lambda) = \begin{pmatrix} 0 & 0 & 0 & \frac{1}{2} & 0 & -\frac{3}{2} \\ 0 & 0 & 0 & 0 & \frac{1}{8} & -\frac{1}{4} \\ 0 & 0 & 0 & -\frac{3}{2} & -\frac{1}{4} & 6 \\ -38\lambda & -24\lambda & -12\lambda & 0 & 0 & 0 \\ -24\lambda & -18\lambda & -8\lambda & 0 & 0 & 0 \\ -12\lambda & -8\lambda & -4\lambda & 0 & 0 & 0 \end{pmatrix} \text{ and } U = V = \left\{ \begin{pmatrix} 0 \\ 0 \\ 0 \\ u_4 \\ u_5 \\ u_6 \end{pmatrix}, \begin{pmatrix} u_4 \\ u_5 \\ u_6 \end{pmatrix} \in \mathbb{R}^3 \right\}.$$

We performed the integration over 100 time steps and got the following results:

Exact eigenvalue	Zeros of the approximation of E
0.25	0.2500002973
2.25	2.2502709926
6.25	6.2528890688

About eight iterations were required to reach machine precision for these single eigenvalues.

We also tried to reach multiple eigenvalues but it required more iterations than the method used in [61].

Appendix H

Index of definitions and notations

- $T_a M$ is defined as the tangent space of the manifold M at the point a.

- $\#S$ is the number of elements in the set S.

- Let U and V two subspaces of a space E and S be a bilinear form over E.

  $$\forall u \in U, v \in V \quad S(u,v) = 0 \quad \Leftrightarrow_{def} \quad U \perp_S V$$

  In that case, U and V are said to be S-orthogonal.

- $\mathbb{U}$ is the set of complex numbers of modulus one.

- $\Lambda(n)$ is the set of Lagrangian planes in $\mathbb{R}^{2n}$.

- $S_n(\mathbb{R})$ is the set of symmetric $n \times n$-matrices

- Let $S \in S_n(\mathbb{R})$, r^- the number of strictly negative eigenvalues of S and r^+ the number of strictly positive eigenvalues of S.

  The signature of S is defined as (r^-, r^+).

- Let U be a Lagrangian plane. $\Lambda(U)$ is the set of Lagrangian planes which are not transverse to U.

- The k-th Grassmannian of E denoted by $G_k(E)$ is the set of k-dimensional subspaces of E.

- $Sp(2n)$ is the set of symplectic matrices, e.g. $2n \times 2n$-matrices such that $A^T \mathcal{J} A = \mathcal{J}$.

- A is said to be an Hamiltonian matrix if and only if $\mathcal{J} A = (\mathcal{J} A)^T$.

- $O(n)$ is the set of orthogonal matrices, e.g. real matrices A such that $AA^t = I_n$.

- $SO(n)$ is the set orthogonal matrices with a determinant equal to 1.

- $U(n)$ is the set of unitary matrices, e.g. complex matrices A such that $AA^* = I_n$.

- Range : $M_{k,r}(\mathbb{K}) \to \{$Subspaces of $\mathbb{K}^k\}$ is the mapping that associates a matrix to the space spanned by its columns.

- $X_n = \left\{ \begin{pmatrix} X \\ Y \end{pmatrix} \in M_{2n,n}(\mathbb{R}) \mid X^T Y = Y^T X \text{ and } \begin{pmatrix} X \\ Y \end{pmatrix} \text{ has rank } n \right\}$

- $\theta : \begin{cases} U(n) \to \Lambda(n) \\ X + iY \to \text{Range}\left(\begin{pmatrix} X \\ Y \end{pmatrix}\right) \end{cases}$

- $\psi : \begin{cases} (X_n)^2 \to GL_n(\mathbb{C}) \\ \left(\begin{pmatrix} W \\ Z \end{pmatrix}, \begin{pmatrix} X \\ Y \end{pmatrix}\right) \mapsto (X - iY)^{-1}(W - iZ)(W + iZ)^{-1}(X + iY) \end{cases}$

- $s : \Lambda(n) \to \mathbf{U}$ is defined by $s\left(\text{Range}\begin{pmatrix} X \\ Y \end{pmatrix}\right) = \det((X - iY)^{-1}(X + iY))$.

- $K_{\text{Range}(B)} : \begin{cases} \Lambda(n) \to \mathbb{U}^n/\sim \\ \text{Range}(A) \to \text{Eigenvalues of } \psi(A, B) \end{cases}$ where $\sim$ is the relation of equivalence defined by:

  $(x_1, x_2, \ldots, x_n) \sim (y_1, y_2, \ldots, y_n) \Leftrightarrow \exists \sigma \text{ one-to-one } (x_1, x_2, \ldots, x_n) = (y_{\sigma(1)}, y_{\sigma(2)}, \ldots, y_{\sigma(n)})$.

- $\widetilde{\Lambda(n)}$ is the universal covering of $\Lambda(n)$.

  There is a smooth diffeomorphism between $\widetilde{\Lambda(n)}$ and the following closed subset of $\mathbb{R} \times \Lambda(n)$:

  $\{(\kappa, U) \text{ s.t. } e^{is(U)} = e^{i\kappa}\}$

- Let $(\alpha, A), (\beta, B) \in \widetilde{\Lambda(n)}$, $C \in \Lambda(n)$, and $r_A = \dim(A \cap C)$, $r_B = \dim(B \cap C)$. Let $\alpha_1, \alpha_2, \ldots, \alpha_{n-r_A} \in]0, 2\pi[$, $\beta_1, \beta_2, \ldots, \beta_{n-r_B} \in]0, 2\pi[$ such that

  $K_C(A) = (e^{i\alpha_1}, e^{i\alpha_2}, \ldots, e^{i\alpha_{n-r_A}}, 1, \ldots, 1)$ and $K_C(B) = (e^{i\beta_1}, e^{i\beta_2}, \ldots, e^{i\beta_{n-r_B}}, 1, \ldots, 1)$.

  Define

  $$m_C((\alpha, A), (\beta, B)) = \frac{\beta - \sum_{i=0}^{n-r_B} \beta_i}{2\pi} - \frac{\alpha - \sum_{i=0}^{n-r_A} \alpha_i}{2\pi} + \frac{1}{2}(r_B - r_A)$$

- Let W be a Lagrangian space and $\gamma : [0, 1] \to \Lambda(n)$ be a continuous path and let $\kappa : [0, 1] \to \mathbb{R}$ be a continuous function such that $e^{i\kappa(x)} = s(\gamma(x))$. The Maslov index of γ with respect to W is

  $$m_W(\gamma) = m_W((\kappa(0), \gamma(0)), (\kappa(1), \gamma(1))).$$

  If $\gamma(0) = \gamma(1)$, $m(\gamma) = m_W(\gamma) = \frac{\kappa(1) - \kappa(0)}{2\pi}$.

- $E_\lambda(A)$ is defined as the generalized eigenspace of A associated to λ, the set of x such that $\exists k \in \mathbb{N}^* \quad (A - \lambda)^k x = 0$.

- $\mathrm{E}^u(A) = \{x : \lim_{t \to -\infty} e^{tA} x = 0\}$ and $\mathrm{E}^s(A) = \{x : \lim_{t \to +\infty} e^{tA} x = 0\}$.

- Let $\mathbf{U}$ be a k-form. $\rho_{\mathbf{U}} : \begin{cases} \bigwedge^k E \to \bigwedge^{k+1} E \\ x \to \mathbf{U} \wedge x \end{cases}$

- $\bigwedge^k E$ denotes the k-th exterior product of the vector space E. $\wedge$ denotes the exterior product.

- $A^{(k)} : \bigwedge^k E \to \bigwedge^k E$ is the k-th compound matrix of A. It is defined as the matrix such that: $A^{(k)} a_1 \wedge \ldots \wedge a_k = \sum_{j=1}^{k} a_1 \wedge \ldots A a_j \wedge \ldots a_k$.

- $A^{[k]} : \bigwedge^k E \to \bigwedge^k E$ is the k-th exterior power of A. It is defined as the matrix such that: $A^{[k]} a_1 \wedge \ldots \wedge a_k = A a_1 \wedge \ldots \wedge A a_k$.

- $G : \bigwedge^n \mathbb{R}^{2n} \to \mathbb{C}$ is the linear form over $\bigwedge^n \mathbb{R}^{2n}$ such that $G\left(\begin{pmatrix} \mathbf{X} \\ \mathbf{Y} \end{pmatrix}^{[n]} \right) = \det(\mathbf{X} - i\mathbf{Y}) = K_E(\text{Range}(\begin{pmatrix} \mathbf{X} \\ \mathbf{Y} \end{pmatrix}))$, with $E = \text{Range}(\begin{pmatrix} I \\ 0 \end{pmatrix}))$.

Appendix I

Computer programs

In this section, we give describe the programs we used to make numerical simulations.

I.1   Spectral method to compute the periodic orbits

Main program used to compute periodic solutions:

```
% differential equation: y'''' - P y'' + c*y - y^(p+1) = 0
%
% at P = -2, the 1:1 resonance occurs
% at P = +2, one has double real eigenvalues
%
% we are interested in the branch of solitary waves
% extending from P = -2 to P = infty
%
% for P = (p^2+4*p+8)/(2(p+2)), this solitary wave can be computed
% explicitly
%
% we use periodic boundary conditions
%eta=10;
c=1;
p=1;
%p=5;
N=2^10
h=2*pi/N;
x=(-pi:h:pi-h)';
%P=-1

% we now vary the parameter P and etas
Pvalue=[(3:-.1:-1.9)];
etas=(100:-.01:0)'
```

```
%compute exact solution for
P = (p^2+4*p+8)/(2*(p+2));
sol=((p+4)*(3*p+4)/(8*(p+2)))^(1/p)*sech((x*etas(1))*p./sqrt(8*(p+2))).^(4/p);

s=size(etas,1);
t=size(Pvalue,2);
u=sol;
E=zeros(size(sol,1),s);
Energy=zeros(s,t);
ErrE=zeros(s,t);
for jj=1:t,
%    u=sol;
for ii=1:s,
   [u,err,energy,errE]=solfourier3_KdV(N, etas(ii,1), Pvalue(1,jj), u, p,c);
   if (ii==1), sol=u;end;
   plot(u)
   drawnow
   E(:,ii)=u;
   Energy(ii,jj)=energy;
   ErrE(ii,jj)=errE;
   ii
   jj
end
end

norm(ErrE,inf)
% waterfall(eta*x, Pvalue, E),
% axis([eta*min(x) eta*max(x) min(Pvalue) max(Pvalue) -1 1.5]);
```

   The auxiliary routine **solfourier3_KdV.m** is:

```
function [u,err,energy,errE]=solfourier3_KdV(N, eta, P, u, p,c)

%It finds a periodic solution to the following ODE:
%y'''' - P y'' + c*y - y^(p+1)
%
%The solver does all the inversions in the Fourier domain.
%N is the number of points used by the discretization.


Dfourier=i*[0:(N/2-1),0,(-N/2+1):-1]'*(1/eta);
Dfourier2=-[0:(N/2),(-N/2+1):-1]'.^2*(1/eta^2);
Dfourier3=Dfourier.*Dfourier2;
```

```
Dfourier4=[0:(N/2),(-N/2+1):-1]'.^4*(1/eta^4);


LL=(Dfourier4-P*Dfourier2+c);
Lf=@(x)(x.*LL);                  %Operator L:y->y'''' - P y'' + c*y in the
                                 %Fourier domain.


Lfinv=@(x)(x./LL);               %Inverse of operator L in the Fourier domain.


F=@(u)[real(ifft(Lf(fft(u))))-u.^(p+1)]; %Functional whose zeros
                                          %are the solutions of the ODE.


max_it=20;
h=2*pi/N; x=(-pi:h:pi-h)';



change=1; it=0;
while change>1e-12*norm(u) & it<max_it
    %This loop tries to find the zeros of the functional F.
    y=F(u);

    Dff=@(x)(Lf(x)-real(fft((p+1)*(u.^p).*ifft(x))));
    %Jacobian in Fourier Domain.

    unew=u-real(ifft(symmlq(Dff,real(fft(y)),10^(-9),N,Lfinv)));
    % Newton iteration. Inversion of the Jacobian
    %in the Fourier Domain using Lfinv as a preconditionner.

    change = norm(unew-u, inf);
    u=unew; it=it+1;
end
err=norm(ifft(Lf(fft(u)))-u.^(p+1));

 foD=@(x)(real(ifft(fft(x).*Dfourier)));    %1st order derivative.
 foD2=@(x)(real(ifft(fft(x).*Dfourier2))); %2nd order derivative.
 foD3=@(x)(real(ifft(fft(x).*Dfourier3))); %3rd order derivative.
 foD4=@(x)(real(ifft(fft(x).*Dfourier4))); %4th order derivative.



W=foD3(u).*foD(u) ...
-(1/2)*foD2(u).^2 ...
-(1/2)*P*foD(u).^2 ...
+(1/2)*u.^2-(1/(p+2))*u.^(p+2);          %Evaluation of the energy.
```

```
energy=sum(W)/N;                    %Evaluation of the average energy.
errE=norm(W-energy,2)/sqrt(N); %Control of the conservation of the energy.
```

I.2 Shooting algorithm to obtain symmetric homoclinic solutions

I.2.1 The shooting method

Reversible problems

Let V be an $2n$-dimensional system.

Let $\mathcal{R}$ be an endomorphism of V such that $\ker(\mathcal{R} + Id)$ is n-dimensional and $\mathcal{R}^2 = Id$.

Let $F : V \to V$ be such that:

- $\mathcal{R} \circ F = F \circ \mathcal{R}$. (Reversibility)

- $F(0) = 0$ and dF_0 has no imaginary eigenvalue. (0 is a hyperbolic equilibrium point.)

We would like to find a symmetric homoclinic solution, i.e. a solution x such that $x(0) = \mathcal{R}x(0)$ and $\lim_{t \to -\infty} x(t) = 0$

The shooting algorithm

Let $\Phi : \mathbb{R} \times V \to V$ such that $\frac{\partial \Phi}{\partial t}(t, x) = F(t, \Phi(t, x))$ and $\Phi(0, x) = x$.

The unstable space U and the stable space S of dF_0 are n-dimensional (because $S \oplus U = V$, $\mathcal{R}U = S$ and $\mathcal{R}S = U$).

Let T be a large enough positive number.

Let $\Phi_{\Delta t}(t, x)$ be an approximation of the flow $\Phi_{\Delta t}(t, x)$ obtained by using a numerical integrator like the fourth-order Runge-Kutta method.

Then, by using Newton's method, it is possible to find a zero x_0 of the differentiable function $(\mathcal{R} - Id) \circ U_{T,n} : U \to \ker(\mathcal{R})$.

Once x_0 is obtained, the homoclinic orbit is approximated by

$$
\begin{cases}
e^{dF_0(t+T)}x_0 & \text{if } t < -T \\
\Phi_{\Delta t}(t+T, x_0)x_0 & \text{if } -T \le t \le 0 \\
\mathcal{R}\Phi_{\Delta t}(t+T, x_0)x_0 & \text{if } -T \le t \le 0 \\
\mathcal{R}e^{-dF_0(t-T)}x_0 & \text{if } t > T
\end{cases}
$$

I.2.2 Computer routine

The following program implements the previous algorithm in the case of the stationary part of the Kawahara equation

$$
\begin{pmatrix} u_1 \\ u_2 \\ u_3 \\ u_4 \end{pmatrix}_t = \begin{pmatrix} u_2 \\ u_3 \\ u_4 \\ Pu_3 - u_1 + u_1^{p+1} \end{pmatrix}.
$$

The function called `homoclinic` finds a point u close to $xe^{-\text{back } dF_0}$ such that $\Phi(Ndt, u) = \begin{pmatrix} q_1 \\ q_2 \\ 0 \\ 0 \end{pmatrix}$ and $u \in E^u(dF_0)$. Φ is computed by using the fourth-order Runge-Kutta scheme. u is found by using a Newton iteration.

$\Phi(t, u)$ for $t \in [0, 4Ndt]$ is an approximation of a symmetric homoclinic orbit $\phi(t - 4Ndt)$ for $t \in [0, 4Ndt]$.

```
function[u,dP]=homoclinic(x,back,dt,N)
global P;
A=jac([0,0,0,0]');

[vn,vp]=eig(A);

if P<2
for i=1:4
        if real(vp(i,i)>0)
            vec=[real(vn(:,i)),imag(vn(:,i))];
        end;
end;


[vn,vp]=eig(A');
for i=1:4
        if real(vp(i,i)>0)
            proj=[real(vn(:,i)),imag(vn(:,i))]';
        end;
end;


else
j=1;k=1;
for i=1:4
        if real(vp(i,i)>0)
            vec(:,j)=vn(:,i);j=j+1;
        end;
end;
%x=-x*10^(-2);
[vn,vp]=eig(A');
j=1;
for i=1:4
        if real(vp(i,i)>0)
            proj(j,:)=vn(:,i)';j=j+1;
        end;
end;
```

```
end;
A=proj*vec;
vec=vec/A;
B=jac(0)*vec*proj;
x=expm(-B*back)*x;
ret=vec*proj;
x=proj*x;
%x=rot(2.5673859-3.0137255)*x;
err=10;
while abs(err)>10^(-10)
[y,A,dP]=calcul(vec*x,vec,N);
err=[y(2,:);y(4,:)];
dP=[dP(2,1);dP(4,1)];
A=[A(2,:);A(4,:)];
x=x-A\err;dP=A\dP;  %Newton iteration
end
u=vec*x;dP=vec*dP;


function[y,A,dP]=calcul(x,A,N)
y=x;
dt=1/1000;
dP=zeros(4,1);
for i=1:N
    f1=f(x);
    f2=f(x+f1*dt/2);
    f3=f(x+f2*dt/2);
    f4=f(x+f3*dt);
    d1=jac(x)*A;
    d2=jac(x+f1*dt/2)*(A+d1*dt/2);
    d3=jac(x+f2*dt/2)*(A+d2*dt/2);
    d4=jac(x+f3*dt)*(A+d3*dt);

    dP1=jac(x)*dP+dfdP(x);
    dP2=jac(x+f1*dt/2)*(dP+(dt/2)*dP1)+dfdP(x+f1*dt/2);
    dP3=jac(x+f2*dt/2)*(dP+(dt/2)*dP2)+dfdP(x+f2*dt/2);
    dP4=jac(x+f3*dt)*(dP+dt*dP3)+dfdP(x+f3*dt);

x=x+(dt/6)*(f1+2*f2+2*f3+f4);
A=A+(dt/6)*(d1+2*d2+2*d3+d4);
dP=dP+(dt/6)*(dP1+2*dP2+2*dP3+dP4);
y=x;
end
```

```
function[y]=f(x)
global P;
global p;
y=[x(2,1),x(3,1),x(4,1),P*x(3,1)-x(1,1)+x(1,1)^(p+1)]';
end


function[y]=jac(x)
global P;
global p;
a=x(1,1)^p;
y=[[0,1,0,0];...
   [0,0,1,0];...
   [0,0,0,1];...
   [(p+1)*a-1,0,P,0]];
end
```

I.3 Program to compute the Maslov index of periodic waves

The following routine is the implementation of the algorithm described in section 2.3, applied to the case of the Kawahara equation.

This routine takes the following inputs:

- `h` is the λ parameter at which $I_{hom}(\phi, \lambda)$ is evaluated.

- `P` is the parameter in Kawahara equation.

- `T` is the period of the periodic orbit.

- `a` is a vector containing $a(x) = 1 - (q+1)\phi(x)^p$ evaluated at equidistant points over one period.

The routine returns the following outputs:

- `mas` is the Maslov index $I_{hom}(\phi, \lambda)$,

- `jj` the number of iterations that were necessary to reach the unstable space.

```
function[mas,jj]=maslov_periodic(h,P,T,a)
%This function computes the Maslov index at h for the operator
%Lu=u_xxxx - P*u_xx + a(x)*u in the periodic case.
%The vector gives the values of a on equidistant points over a period.
%The matrix used to compute A2(x,lambda) was
%[[0,0,0,1];[0,0,1,P];[-a+h,0,0,0];[0,1,0,0]].
```

```
f=rand(6,1);
e=rand(6,1);
s=0;
jj=0;
AA=mmatA2_4(P,a(1,1)-h);
while ((jj<200) & ~iscolinear(e,f))
  f=e/norm(e);
  e=f;
  eka=(e(1,1)+i*e(3,1)-i*e(4,1)-e(6,1));
  kappa0=angle(eka);
  kappa=kappa0;


n=size(a,1);
dx=T/n;
    for ii=1:2:(n-1)

        ah=a(ii,1)-h;
        AA(4,1)=-(-ah);
        AA(6,3)=-ah;
        f1=AA*e-s*e;

        ah=a(ii,1)-h;
        AA(4,1)=-(-ah);
        AA(6,3)=-ah;
        aux=e+dx*f1;
        f2=AA*aux-s*aux;

        ah=a(ii,1)-h;
        AA(4,1)=-(-ah);
        AA(6,3)=-ah;
        aux=e+dx*f2;
        f3=AA*aux-s*aux;

        ah=a(mod(ii+2,n),1)-h;
        AA(4,1)=-(-ah);
        AA(6,3)=-ah;
        aux=e+2*dx*f3;
        f4=AA*aux-s*aux;

        e=e+(2*dx/6)*(f1+2*f2+2*f3+f4);

        ekb=(e(1,1)+i*e(3,1)-i*e(4,1)-e(6,1));
```

```
        kappa=kappa+angle(ekb/eka);
        eka=ekb;
    end
    mas=(kappa-kappa0)/(pi);
s=s+log(norm(e)/norm(f))/T;
jj=jj+1;
end;
```

```
function[y]=mmatA2_4(P,ah)
y=zeros(6,6);
y(1,2)=1;
y(1,3)=P;
y(1,5)=-1;

y(2,6)=-1;

y(3,1)=1;

y(4,1)=-(-ah);
y(4,6)=-P;

y(5,6)=1;

y(6,3)=-ah;
y(6,4)=-1;
end
```

```
function[t]=iscolinear(x,y)
n=size(x,1);
z=x(2:n,1).*y(1:n-1,1)-x(1:n-1,1).*y(2:n,1);
t=(1==0);
if (norm(z)<10^(-14)*norm(x)*norm(y))
t=(0==0);
end;
end
```

I.4   Program to compute the Maslov index of solitary waves

The following routine is the implementation of the algorithm described in section 2.4.4, applied to the case of the Kawahara equation.

This routine takes the following inputs:

- `h` is the λ parameter at which $I_{hom}(\phi, \lambda)$ is evaluated.

- `P` is the parameter in Kawahara equation.

- `a` is a line matrix containing $a(x) = 1 - (q+1)\phi(x)^p$ evaluated every `dx`.

- `ainf` is the limit of $a(x)$ when $x \to \pm\infty$.

- `dx` is the step size between each value of $a(x)$.

The routine returns the following outputs:

- `ek1,ek2` are the complex numbers $(e^{i\kappa_1}, e^{i\kappa_2})$ associated to $\mathbf{R}^{[2]}(\lambda)^{-1}\mathbf{U}$,

- `mas` is the Maslov index $I_{hom}(\phi, \lambda)$,

- `ev` is the Evans function.

```
function[ek1,ek2,mas,ev]=maslov_8(h,P,a,ainf,dx)
%This function computes the Maslov index in h for the operator
%Lu=u_xxxx - P*u_xx + a(x)*u.
%The vector gives the value of a on the interval ]-pi*eta, pi*eta].
%The matrix used to compute A2(x,lambda) was
%[[0,0,0,1];[0,0,1,P];[-a+h,0,0,0];[0,1,0,0]].
%
%mas gives the Maslov index at h.
%ev gives the Evans funtion at h.
%ek1(i) and ek2(i) gives the K function associated to the unstable space at
%x(i).

J=[0,0,1,0;0,0,0,1;-1,0,0,0;0,-1,0,0];
skip=1;
if ((ainf-(P^2/4))>h | (ainf>h & P>0))
    [vc,vn]=eig([[0,0,0,1];[0,0,1,P];[-ainf+h,0,0,0];[0,1,0,0]]);

    n=size(a,1)-1;
    dx=skip*dx;
    Ainf=mmatA2_4(P,ainf-h);
    [vc,vn]=eig(Ainf);
    jj=1;

    sigma=zeros(6,6);
    sigma(6,1)=1;
    sigma(5,2)=-1;
    sigma(4,3)=1;
```

```
    sigma(3,4)=1;
    sigma(2,5)=-1;
    sigma(1,6)=1;


    %   Computation of the eignevectors of the system at infinity   //


    for ii=1:6
        if real(vn(ii,ii))<real(vn(jj,jj));
            jj=ii;
        end
    end


    d=vc(:,jj);
    jj=1;


    for ii=1:6
        if real(vn(ii,ii))>real(vn(jj,jj));
            jj=ii;
        end
    end
    e=vc(:,jj);
    e=e/(transpose(e)*(sigma*d));
    s=vn(jj,jj);
    AA=Ainf;
    stable=d;

CC0=symbase(h,P)^(-1);
CC=eye(6,6)
ek1=(n/2+1:2*skip:(n-1))'*0;
ek2=(n/2:2*skip:(n-1))'*0;

inter1=0;
inter2=0;
        f=CC*e;
        Delta=sqrt(4*f(1,1)*f(6,1)+2*f(3,1)*f(4,1)-f(3,1)^2-f(4,1)^2);
        ek1a=(f(1,1)+f(6,1)+Delta)/(f(1,1)+i*f(3,1)-i*f(4,1)-f(6,1));
        ek2a=(f(1,1)+f(6,1)-Delta)/(f(1,1)+i*f(3,1)-i*f(4,1)-f(6,1));
        ek1b=ek1a;
        ek2b=ek2a;




r=0;
```

```
for ii=1:2*skip:(n-1)
    ep=e;
    inter=transpose(e)*sigma*stable;
    ah=a(ii,1)-h;
    AA(4,1)=-(-ah);
    AA(6,3)=-ah;
    f1=AA*e-s*e;

    ah=a(ii+skip,1)-h;
    AA(4,1)=-(-ah);
    AA(6,3)=-ah;
    aux=e+dx*f1;
    f2=AA*aux-s*aux;

    ah=a(ii+skip,1)-h;
    AA(4,1)=-(-ah);
    AA(6,3)=-ah;
    aux=e+dx*f2;
    f3=AA*aux-s*aux;

    ah=a(ii+2*skip,1)-h;
    AA(4,1)=-(-ah);
    AA(6,3)=-ah;
    aux=e+2*dx*f3;
    f4=AA*aux-s*aux;

    e=e+(2*dx/6)*(f1+2*f2+2*f3+f4);

    r=r+1;
    f=CC*e;
    Delta=sqrt(4*f(1,1)*f(6,1)+2*f(3,1)*f(4,1)-f(3,1)^2-f(4,1)^2);
    ek1b=(f(1,1)+f(6,1)+Delta)/(f(1,1)+i*f(3,1)-i*f(4,1)-f(6,1));
    ek2b=(f(1,1)+f(6,1)-Delta)/(f(1,1)+i*f(3,1)-i*f(4,1)-f(6,1));


    ek1(r,1)=ek1b;
    ek2(r,1)=ek2b;

    if (angle(ek1a)*angle(ek1b)<0) & (abs(angle(ek1a))<1)
      inter1=inter1+sign(angle(ek1b));  %Intersections associated
                                        %to the first angle.
    end
    if (angle(ek2a)*angle(ek2b)<0) & (abs(angle(ek2a))<1)
```

```
            inter2=inter2+sign(angle(ek2b));  %Intersections associated
                                              %to the second angle.
        end
        ek1a=ek1b;
        ek2a=ek2b;
    end
    mas=inter1+inter2;
    ev=(transpose(e)*(sigma*d));
else
    mas=NaN;
    ev=NaN;
end


function[y]=mmatA2_4(P,ah)
y=zeros(6,6);
y(1,2)=1;
y(1,3)=P;
y(1,5)=-1;

y(2,6)=-1;

y(3,1)=1;

y(4,1)=-(-ah);
y(4,6)=-P;

y(5,6)=1;

y(6,3)=-ah;
y(6,4)=-1;
end

%Computation of a basis adpated to the stable and the unstable space.
function[y]=symbase(h,P)
J=[0,0,1,0;0,0,0,1;-1,0,0,0;0,-1,0,0];
ainf=1
h=0;
AINF=[[0,0,0,1];[0,0,1,P];[-ainf+h,0,0,0];[0,1,0,0]];
[vn,vp]=eig(AINF);
U=[real(vn(:,1)),imag(vn(:,1))];
S=[real(vn(:,3)),imag(vn(:,3))];
No=(U'*J*S)^(-1);
```

```
V=[U*No,S];
y=zeros(6,6)
r=1;s=1;
for ii=1:4
  for j=ii+1:4
    for k=1:4
      for l=k+1:4
        y(r,s)=det(V([ii,j],[k,l]));
        s=s+1;
      end
    end
  s=1;r=r+1;
  end
end
end


end
```

Bibliography

[1]   J. Alexander, R. Gardner & C. K. R. T. Jones, *A topological invariant arising in the stability analysis of traveling waves*, J. Reine Angew. Math. **410** (1990), 167–272.

[2]   J. C. Alexander & C. K. R. T. Jones, *Existence and stability of asymptotically oscillatory triple pulses*, Z. Angew. Math. Phys. **44** (1993), no. 2, 189–200.

[3]   J. C. Alexander & C. K. R. T. Jones, *Existence and stability of asymptotically oscillatory double pulses*, J. Reine Angew. Math. **446** (1994), 49–79.

[4]   L. Allen & T. J. Bridges, *Numerical exterior algebra and the compound matrix method*, Numerische Mathematik **92** (2002), 197–232.

[5]   L. Allen & T. J. Bridges, *Hydrodynamic stability of the Ekman boundary layer including interaction with a compliant surface: a numerical framework*, Eur. J. Mech. B Fluids **22** (2003), no. 3, 239–258.

[6]   V. I. Arnol'd, *Characteristic class entering in quantization conditions*, Funktsional'nyi Analiz i Ego Prilozheniya **1,1** (1967), 1–14.

[7]   V. I. Arnol'd, *The Sturm theorems and symplectic geometry*, Funktsional'nyi Analiz i Ego Prilozheniya **19,4** (1985), 11–22.

[8]   V. I. Arnol'd, *Mathematical methods of classical mechanics*, 2nd ed., Graduate Texts in Mathematics, vol. 60, Springer Verlag, New York, 1989, 508 pages.

[9]   P. G. Baines, *Topographic effects in stratified flows*, Cambridge Monographs on Mechanics, Cambridge University Press, Cambridge, 1995.

[10]   H. Baumgärtel, *Analytic perturbation theory for matrices and operators*, Birkhaüser, 1985.

[11]   D. Bekiranov, T. Ogawa & G. Ponce, *Weak solvability and well-posedness of a coupled Schrödinger-Korteweg de Vries equation for capillarity-gravity wave interactions*, Proceedings of the American Mathematical Society **125** (1997), 2907–2919.

[12]   E. S. Benilov & S. P. Burtsev, *To the integrability of the equations describing the Langmuir-wave ion-acoustic wave interaction*, Phys. Lett., A **98** (1983), 256–258.

[13] B. J. BINDER, F. DIAS & J.-M. VANDEN-BROECK, *Influence of rapid changes in a channel bottom on free-surface flows*, IMA J. Appl. Math. **73** (2008), no. 1, 254–273.

[14] B. J. BINDER, J.-M. VANDEN-BROECK & F. DIAS, *Forced solitary waves and fronts past submerged obstacles*, Chaos **15** (2005), no. 3, 037106, 13.

[15] J. L. BONA, P. E. SOUGANIDIS & W. A. STRAUSS, *Stability and instability of solitary waves of Korteweg-de Vries type*, Proc. R. Soc. Lond. A **411** (1987), 395–412.

[16] A. BOSE & C. K. R. T. JONES, *Stability of the in-phase travelling wave solution in a pair of coupled nerve fibers*, Indiana University Mathematics Journal **44** (1995), no. 1, 189–220.

[17] R. BOTT, *On the iterations of closed geodesics and the Sturm intersection theory*, Communications on Pure and Applied Mathematics **9** (1956), 171–206.

[18] J. BOUSSINESQ, *Théorie de l'intumenscence liquide appelée onde solitaire ou de translation, se propageant dans un canal rectangulaire*, C. R. Acad. Sci. Paris **72** (1871), 755–759.

[19] J. P. BOYD, *Chebyshev and Fourier spectral methods*, 2nd ed., Dover Publication Inc., 2000.

[20] T. J. BRIDGES & G. DERKS, *Linear instability of solitary-wave solutions of the Kawahara equation and its generalizations*, SIAM J. Math. Anal. **33** (2002), 1356–1378.

[21] T. J. BRIDGES, G. DERKS & G. GOTTWALD, *Stability and instability of solitary waves of the fifth-order KdV equation: a numerical framework*, Physica D **172** (2002), 190–216.

[22] T. J. BRIDGES & G. DERKS, *Unstable eigenvalues and the linearization about solitary waves and fronts with symmetry*, R. Soc. Lond. Proc. Ser. A Math. Phys. Eng. Sci. **455** (1999), no. 1987, 2427–2469.

[23] T. J. BRIDGES & G. DERKS, *Constructing the symplectic Evans matrix using maximally analytic individual vectors*, Proc. Roy. Soc. Edinburgh Sect. A **133** (2003), no. 3, 505–526.

[24] T. J. BRIDGES & N. M. DONALDSON, *Degenerate periodic orbits and homoclinic torus bifurcation*, Phys. Rev. Lett. **95** (2005), 104301.

[25] T. J. BRIDGES & S. REICH, *Computing Lyapunov exponents on a Stiefel manifold*, Physica D **156** (2001), no. 3-4, 219–238.

[26] J. C. BRONSKI & Z. RAPTI, *Modulationnal instability for nonlinear Schrödinger equations with a periodic potential*, Dynamics of PDE **2** (2004), no. 4, 335–356.

[27] B. BUFFONI, A. R. CHAMPNEYS & J. F. TOLAND, *Bifurcation and coalescence of a plethora of homoclinic orbits for a Hamiltonian system*, J. Dyn. Differ. Equations **8** (1996), no. 2, 221–279.

[28] B. Buffoni & E. Séré, *A global condition for quasi-random behavior in a class of conservative systems*, Communications on Pure and Applied Mathematics **49** (1996), no. 3, 285–305.

[29] J. Burke & E. Knobloch, *Homoclinic snaking: structure and stability*, Chaos **17** (2007), no. 3, 037102, 15.

[30] A. V. Buryak & A. R. Champneys, *On the stability of solitary waves of the fifth-order KdV equation*, Physics Letters A **233** (1997), 58–62.

[31] R. Camassa & T. Y.-t. Wu, *Stability of forced steady solitary waves*, Philos. Trans. Roy. Soc. London Ser. A **337** (1991), no. 1648, 429–466.

[32] R. Camassa & T. Y.-t. Wu, *Stability of some stationary solutions for the forced KdV equation*, Phys. D **51** (1991), no. 1-3, 295–307, Nonlinear science: the next decade (Los Alamos, NM, 1990).

[33] S. E. Cappell, R. Lee & E. Y. Miller, *On the Maslov index.*, Commun. Pure Appl. Math. **47** (1994), no. 2, 121–186.

[34] A. R. Champneys, *Homoclinic orbits in reversible systems and their applications in mechanics, fluids and optics*, Physica D **112** (1999), 158–186.

[35] F. Chardard, *Maslov index for solitary waves obtained as a limit of the Maslov index for periodic waves*, C. R. Acad. Sci. Paris, Ser. I **345/12** (2007), 689–694.

[36] F. Chardard, F. Dias & T. Bridges, *Computational aspects of the Maslov index of solitary waves*, Preprint hal-00383888, `http://hal.archives-ouvertes.fr/hal-00383888/en/`, 59 pages MSC: 53D12 (37J45,37K40,35Q51).

[37] F. Chardard, F. Dias & T. J. Bridges, *Fast computation of the Maslov Index for hyperbolic linear systems with periodic coefficients*, Journal of Physics A : Mathematical and General **39** (2006), no. 47, 14545–14557.

[38] F. Chardard, F. Dias & T. J. Bridges, *Computing the Maslov index of solitary waves. part 1: Hamiltonian systems on a 4-dimensional phase space*, Physica D **238** (2009), no. 18, 1841–1867.

[39] F. Chardard, F. Dias & T. J. Bridges, *On the Maslov index of multi-pulse orbits*, R. Soc. Lond. Proc. Ser. A (in press) **465** (2009), no. 2109, 2897–2910.

[40] C.-N. Chen & X. Hu, *Maslov index for homoclinic orbits of Hamiltonian systems*, Ann. Inst. H. Poincaré Anal. Non Linéaire **24** (2007), no. 4, 589–603.

[41] M. Chugunova & D. Pelinovsky, *Count of eigenvalues in the generalized eigenvalue problem*, accepted in Journal of Mathematical Physics, `http://arxiv.org/abs/math.DS/0602386` (2009).

[42] M. CHUGUNOVA & D. PELINOVSKY, *Two-pulse solutions in the fifth-order KdV equation: rigorous theory and numerical approximations*, Discrete Contin. Dyn. Syst. Ser. B **8** (2007), no. 4, 773–800.

[43] C. CONLEY, *An oscillation theorem for linear systems with more than one degree of freedom*, IBM technical report 18004, IBM Watson Research Center, Yorktown Heights, New York, 1982.

[44] G. CONTRERAS, J.-M. GAMBAUDO, R. ITURRIAGA & G. P. PATERNAIN, *The asymptotic Maslov index and its applications*, Ergodic Theory and Dynamical Systems **23** (2003), 1415–1443.

[45] G. J. COOPER, *Stability of Runge-Kutta methods for trajectory problems*, IMA J. Num. Anal. **7** (1987), 1–13.

[46] S. C. CREAGH, J. M. ROBBINS & R. G. LITTLEJOHN, *Geometrical properties of maslov indices in the semiclassical trace formula for the density of states*, Phys. Rev. A **42** (1990), no. 4, 1907–1922.

[47] J. DENG, *Instability of waves and patterns in Hamiltonian systems and the Maslov index*, Ph.D. thesis, Brown University Providence, RI 02912, 2002.

[48] J. DENG & S. NII, *Infinite-dimensional Evans function theory for elliptic eigenvalue problems in a channel*, J. Differ. Equations **225** (2006), no. 1, 57–89.

[49] J. DENG & S. NII, *An infinite-dimensional Evans function theory for elliptic boundary value problems*, J. Differ. Equations **244** (2008), no. 4, 753–765.

[50] R. L. DEVANEY, *Homoclinic orbits in Hamiltonian systems*, J. Differ. Equations **21** (1976), 431–438.

[51] B. DEY, A. KHARE & G. N. KUMAR, *Stationary solutions of the fifth order KdV-type equation and their stabilization*, Physics Letters A **223** (1996), 449–452.

[52] F. DIAS & G. IOOSS, *Water-Waves as a Spatial Dynamical System*, Handbook of mathematical fluid dynamics, vol. 2, Elsevier Science B.V., 2003.

[53] F. DIAS & E. A. KUZNETSOV, *On the non-linear stability of solitary wave solutions of the fifth-order Korteweg-de Vries equation*, Physics Letters A **263** (1999), 98–104.

[54] F. DIAS & J.-M. VANDEN-BROECK, *Trapped waves between submerged obstacles*, J. Fluid Mech. **509** (2004), 93–102.

[55] F. DIAS, D. MENASCE & J.-M. VANDEN-BROECK, *Numerical study of capillary-gravity solitary waves*, Eur. J. Mech. B/Fluids **15** (1996), 17–36.

[56] F. DIAS & J.-M. VANDEN-BROECK, *Steady two-layer flows over an obstacle*, R. Soc. Lond. Philos. Trans. Ser. A Math. Phys. Eng. Sci. **360** (2002), no. 1799, 2137–2154, Recent developments in the mathematical theory of water waves (Oberwolfach, 2001).

[57] F. Dias & J.-M. Vanden-Broeck, *Two-layer hydraulic falls over an obstacle*, Eur. J. Mech. B Fluids **23** (2004), no. 6, 879–898.

[58] D. Dong & Y. Long, *The iteration formula of the Maslov-type index theory with applications to nonlinear Hamiltonian systems*, Trans. Am. Math. Soc. **349** (1997), no. 7, 2619–2661.

[59] J. J. Duistermaat, *On the Morse index in variational calculus*, Adv. in Math. **21** (1976), 173–195.

[60] H. I. Dwyer & A. Zettl, *Computing Eigenvalues of Regular Sturm-Liouville Problems*, Electronic Journal of Differential Equations **1994** (1994), no. 6, 1–10.

[61] H. I. Dwyer & A. Zettl, *Eigenvalue Computations for Regular Matrix Sturm-Liouville Problems*, Electronic Journal of Differential Equations **1995** (1995), no. 5, 1–13.

[62] J. W. Evans, *Nerve axon equations IV. The stable and the unstable impulse*, Indiana University Mathematics Journal **24** (1975), 1169–1190.

[63] L. K. Forbes & L. W. Schwartz, *Free-surface flow over a semicircular obstruction*, J. Fluid Mech. **114** (1982), 299–314.

[64] R. A. Gardner, *Spectral analysis of long wavelength periodic waves and applications*, Journal für die reine und angewandte Mathematik **491** (1997), 149–181.

[65] R. A. Gardner & K. Zumbrun, *The gap lemma and geometric criteria for instability of viscous shock profiles*, Comm. Pure Appl. Math. **51** (1998), no. 7, 797–855.

[66] A. B. Givental', *Global properties of the Maslov index and Morse theory*, Funct. Anal. Appl. **22** (1988), no. 2, 141–142.

[67] K. Gorshkov & L. Ostrovsky, *Interactions of solitons in nonintegrable systems: Direct perturbation method and applications*, Physica D: Nonlinear Phenomena **3** (1981), no. 1-2, 428 – 438.

[68] P. Griffiths & J. Harris, *Principles of algebraic geometry*, pp. 193–209, John Wiley and Sons, 1978.

[69] R. Grimshaw & N. Smyth, *Resonant flow of a stratified fluid over topography*, J. Fluid Mech. **169** (1986), 429–464.

[70] M. D. Groves, *Solitary-wave solutions to a class of fifth-order model equations*, Nonlinearity **11** (1998), no. 2, 341–353.

[71] M. C. Gutzwiller, *Chaos in classical and quantum mechanics*, Springer, 1990.

[72] M. Hărăguş, *Model equations for water waves in the presence of surface tension*, European J. Mech. B Fluids **15** (1996), no. 4, 471–492.

[73] P. Hartman, *Ordinary differential equations*, Wiley, 1964.

[74] U. Helmke & J. B. Moore, *Optimization and dynamical systems*, Communications and Control Engineering Series. London: Springer-Verlag. xiii, 403 p., 1994 (English).

[75] M. Hărăguş & T. Kapitula, *On the spectra of periodic waves for infinite-dimensional Hamiltonian systems*, Physica D **237** (2008), no. 20, 2649–2671.

[76] G. Iooss & M. Pérouème, *Perturbed homoclinic solution in reversible 1:1 resonance vector field*, Journal of Differential Equations **102** (1993), no. 1, 62–88.

[77] C. K. R. T. Jones, *Instability of standing waves for non-linear Schrödinger-type equations*, Ergodic Theory and Dynamical Systems **8*** (1988), 119–138.

[78] T. Kapitula, P. G. Kevrekidis & B. Sandstede, *Counting eigenvalues via the Krein signature in infinite-dimensional Hamiltonian systems*, Physica D **195** (2004), no. 3-4, 263–282.

[79] T. Kato, *Perturbation theory for linear operators*, 2nd ed., pp. 99–101, Springer, Heidelberg, 1984.

[80] T. Kawahara, *Oscillatory solitary waves in dispersive media*, Journal of the physical society of Japan **33** (1972), 260–264.

[81] T. Kawahara, N. Sugimoto & T. Kakutani, *Nonlinear interaction between short and long capillarity-gravity waves*, J. Phys. Soc. Japan **39** (1975), 1379–1386.

[82] Y. Kodama & D. Pelinovsky, *Spectral stability and time evolution of N-solitons in the KdV hierarchy*, Journal of Physics A: Mathematical and General **38** (2005), 6129–6140.

[83] D. J. Korteweg & G. De Vries, *On the change of form of long waves advancing in a rectangular canal and on a new type of long stationary wave*, Phil. Mag. **39** (1895), 422–443.

[84] A. Kushner, V. Lychagin & V. Rubtsov, *Contact geometry and non-linear differential equations*, Encyclopedia of Mathematics and its Applications, vol. 101, Cambridge University Press, Cambridge, 2007.

[85] Y. A. Kuznetsov, *Elements of applied bifurcation theory*, 3rd ed., Springer, 2004.

[86] A. Lafiti & L. Leon, *On the interaction of Langmuir waves with acoustic waves in plasmas*, Phys. Lett., A **152** (1991), 171–177.

[87] J. D. Lambert, *Computational methods in ordinary differential equations*, p. 153, John Wiley and Sons, 1973.

[88] B. J. Leimkuhler & E. S. Van Vleck, *Orthosymplectic integration of linear Hamiltonian systems*, Numerische Mathematik **77** (1997), no. 2, 269–282.

[89] S. Lewandosky, *Stability of solitary waves of a fifth-order water wave model*, Physica D **227** (2007), no. 2, 162–172.

[90] R. G. Littlejohn & J. M. Robbins, *New way to compute maslov indices*, Phys. Rev. A **36** (1987), no. 6, 2953–2961.

[91] Y. C. MA, *On the multi-soliton solutions of some nonlinear evolution equations*, Stud. Appl. Math. **60** (1979), 73–82.

[92] A. MARCHENKO, *Long waves in shallow liquid under ice cover*, J. Appl. Math. Mech. **52** (1988), no. 2, 180–183.

[93] D. MCDUFF & D. SALAMON, *Introduction to symplectic topology*, pp. 35–78, Oxford Science Publications, 1995.

[94] K. R. MEYER & G. R. HALL, *Introduction to Hamiltonian dynamical systems and the N-body problem*, Applied Mathematical Sciences, vol. 90, Springer-Verlag, New York, 1992.

[95] P. A. MILEWSKI & J.-M. VANDEN-BROECK, *Time dependent gravity-capillary flows past an obstacle*, Wave Motion **29** (1999), no. 1, 63–79.

[96] J. MONTALDI, *A note on the geometry of linear hamiltonian systems of signature 0 in $\mathbb{R}^4$*, Diff. Geom. Appl. **25** (2007), 344–350.

[97] M. MORSE, *The critical points of functions and the calculus of variations in the large*, Bull. Amer. Math. Soc. **35** (1929), no. 1, 38–54.

[98] P. MURATORE-GINANNESCHI, *Path integration over closed loops and Gutzwiller's trace formula*, Phys. Rep. **383** (2003), no. 5-6, 299–397.

[99] H. Oertel (ed.), *Prandtl's essentials of fluid mechanics*, 2nd ed., Springer, 2003.

[100] D. C. OFFIN, *Variational structure of the zones of instability*, Differ. Integral Equ. **14** (2001), no. 9, 1111–1127.

[101] M. OH & K. ZUMBRUN, *Stability of Periodic Solutions of Conservation Laws with Viscosity:Analysis of the Evans Function*, Archive for Rational Mechanics and Analysis **166** (2003), 99–166.

[102] A. PATOINE & T. WARN, *The interaction of long, quasi-stationary baroclinic waves with topography*, Journal of the Atmospheric Sciences **39** (1982), no. 5, 1018–1025.

[103] R. L. PEGO & M. I. WEINSTEIN, *Eigenvalues, and Instabilities of Solitary Waves*, Philos. Trans. R. Soc. Lond., Ser. A **340** (1992), no. 1656, 47–94.

[104] M. PLETYUKHOV & M. BRACK, *On the canonically invariant calculation of Maslov indices*, J. Phys. A, Math. Gen. **36** (2003), no. 36, 9449–9469.

[105] A. PORTALURI, *Maslov index for Hamiltonian systems*, Electron. J. Diff. Eqns. **2008** (2008), no. 09, 1–10.

[106] L. J. PRATT, *On nonlinear flow with multiple obstructions*, Journal of the Atmospheric Sciences **41** (1984), no. 7, 1214–1225.

[107] A. QUARTERONI, R. SACCO & F. SALERI, *Numerical Mathematics*, Springer, 2000.

[108] J. Robbin & D. Salamon, *The Maslov index for paths*, Topology **32** (1993), no. 4, 827–844.

[109] J. Robbin & D. Salamon, *The spectral flow and the Maslov index*, Bull. Lond. Math. Soc. **27** (1995), no. 1, 1–33.

[110] J. Robbins, *Winding number formula for Maslov indices*, Chaos **2** (1992), no. 1, 145–147.

[111] J. M. Robbins, *Maslov indices in the Gutzwiller trace formula*, Nonlinearity **4** (1991), no. 2, 343–363.

[112] B. Sandstede & A. Scheel, *Absolute and convective instability of waves on unbounded and large bounded domain*, Physica D **145** (2000), 233–277.

[113] B. Sandstede & A. Scheel, *On the Stability of Periodic Travelling Waves with Large Spatial Period*, Journal of Differential Equations **172** (2001), 134–188.

[114] J. C. Saut & N. Tzvetkov, *The Cauchy problem for the fifth order KP equations*, J. Math. Pures Appl. (9) **79** (2000), no. 4, 307–338.

[115] C. Stéphanos, *Sur une extension du calcul des substitutions linéaires*, C. R. Acad. Sci. **128** (1899), 593–596.

[116] J. Stoer & S. Bulirsch, *Introduction to numerical analysis*, Springer-Verlag, 1992.

[117] M. Stratmann, T. Pagel & F. Mitscke, *Experimental Observation of Temporal Soliton Molecules*, Physical Review Letters **95** (2005), 143902.

[118] A. Sugita, *Geometrical properties of Maslov indices in periodic-orbit theory*, Phys. Lett., A **266** (2000), no. 4-6, 321–330.

[119] L. N. Trefethen, *Spectral methods in Matlab*, Society for Industrial and Applied Mathematics, 2000.

[120] A. Vanderbauwhede & B. Fiedler, *Homoclinic period blow-up in reversible and conservative systems*, Z. Angew. Math. Phys. **43** (1992), no. 2, 292–318.

[121] M. G. Vavilov & A. I. Larkin, *Quantum disorder and quantum chaos in Andreev billiards*, Physical Review B **67** (2003), 115335.

[122] F. Verhulst, *Nonlinear differential equations and dynamical systems*, Springer, 1996.

[123] G. B. Whitham, *Linear and nonlinear waves. Paperback ed.*, Wiley-Interscience, 1999 (English).

[124] Y.-C. Wong, *Differential geometry of Grassmann manifolds*, Proc. Nat. Acad. Sci. U.S.A. **57** (1967), 589–594.

[125] P. D. Woods & A. R. Champneys, *Heteroclinic tangles and homoclinic snaking in the unfolding of a degenerate reversible Hamiltonian-Hopf bifurcation*, Phys. D **129** (1999), no. 3-4, 147–170.

[126] J. D. WRIGHT & A. SCHEEL, *Solitary waves and their linear stability in weakly coupled KdV equations*, Z. Angew. Math. Phys. **58** (2007), no. 4, 535–570.

[127] T. Y.-T. WU, *Generation of upstream advancing solitons by moving disturbances*, J. Fluid Mech. **184** (1987), 75–99.

[128] V. A. YAKUBOVICH & V. M. STARZHINSKIJ, *Linear differential equations with periodic coefficients. Vol. 1, 2. Translated from Russian by D. Louvish.*, New York - Toronto: John Wiley & Sons; Jerusalem - London: Israel Program for Scientific Translations, a Halsted Press Book. XII, 839 p. 20.60 , 1975 (English).

[129] Y. YING & I. N. KATZ, *A reliable argument principle algorithm to find the number of zeros of an analytic function in a bounded domain*, Numerische Mathematik **53** (1988), 143–163.

[130] N. J. ZABUSKY & M. D. KRUSKAL, *Interaction of "solitons" in a collisionless plasma and the recurrence of initial states*, Phys. Rev. Lett. **15** (1965), no. 6, 240–243.

[131] V. ZAKHAROV & L. FADDEEV, *Korteweg-de Vries equation: A completely integrable Hamiltonian system*, Funct. Anal. Appl. **5** (1971), 280–287.